Nuclear structure studies (via excited state spectroscopy)

Lectures at the
Joint ICTP-IAEA Workshop on Nuclear Data : Experiment, Theory and Evaluation

Miramare, Trieste, Italy, October 2018

Paddy Regan
Department of Physics, University of Surrey
Guildford, GU2 7XH
&
National Physical Laboratory, Teddington, UK
p.regan@surrey.ac.uk ; paddy.regan@npl.co.uk

What is nuclear data?

- Measured values of a range of nuclear energy & time parameters, including:
  - Nuclear ground state masses, decay modes (α, β, fission,,..) and decay energies (Q values).
  - Nuclear decay lifetimes and partial decay modes; branching ratios.
    - Competing internal decays verses beta/alpha decay modes.
    - Beta-delayed neutron probabilities, P_n(%) values, in fission.
  - Nuclear reaction 'cross-sections' as a function of energy, (n,f), (p,f) reactions etc., e.g., thermal neutron capture cross-sections.
  - Reaction product distributions from thermal and fast-neutron fission.
  - Excited state properties of nuclei, characteristic gamma-ray energies, relative P_γ(%) values, transition rates from nuclear excited states (lifetimes range from ~10^{-15} s to 10^{10} secs) internal conversion coefficients and gamma-ray decay multipolarities.
  - Magnetic and quadrupole moments of nuclear excited and ground states.
  - …lots more.

The Chart of the Nuclides

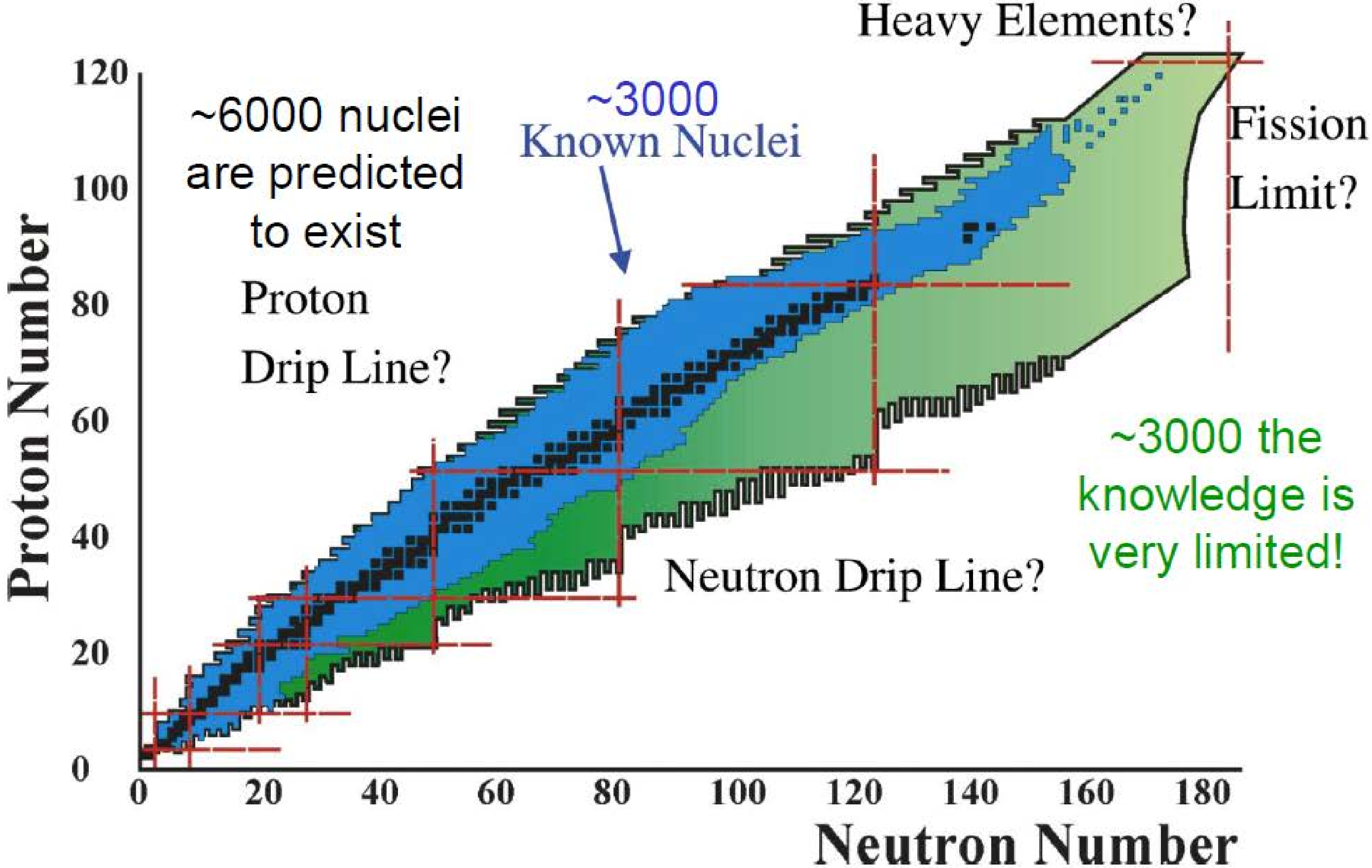

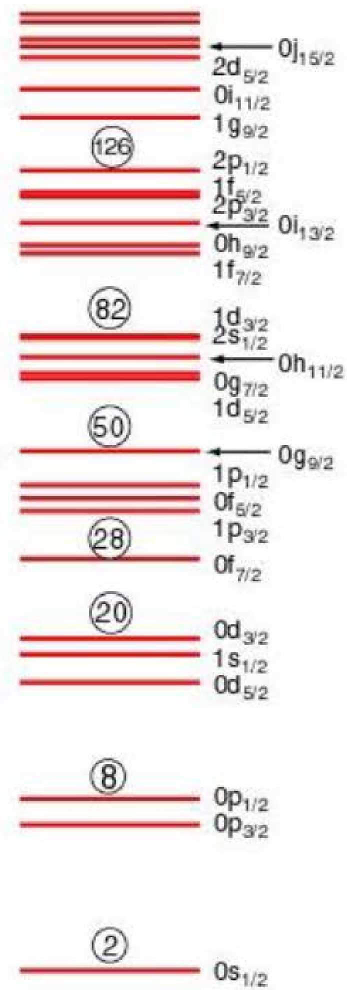

Fundamental Rules in Nuclear Structure Research

- The nuclei and final excited states populated depend on the reaction / decay mechanism used.
- All of these are **SELECTIVE** in one way or another.
  - **Fusion-evaporation**: higher spins; near-yrast states; (usually) neutron-deficient residual nuclei.
  - **(Prompt) Fission**: Medium spins, ~8-16 ħ per fragment; near-yrast states; wide spread of neutron-rich nuclei centred around A~95 & ~135.
  - **Radioactive decay (α, β)** usually lower-spin states due to selection rules; ΔI=0,1 'allowed'.
  - **Populated excited states below particle separation energies decay via EM selection rules and transition rates dependency.**

Some nuclear observables.

1) Masses and energy differences
2) Energy levels
3) Level spins and parities
4) EM transition rates between states
5) Magnetic properties (g-factors)
6) Electric quadrupole moments?

This is the essence of nuclear structure physics.

How do these change as functions of N, Z, I, Ex ?

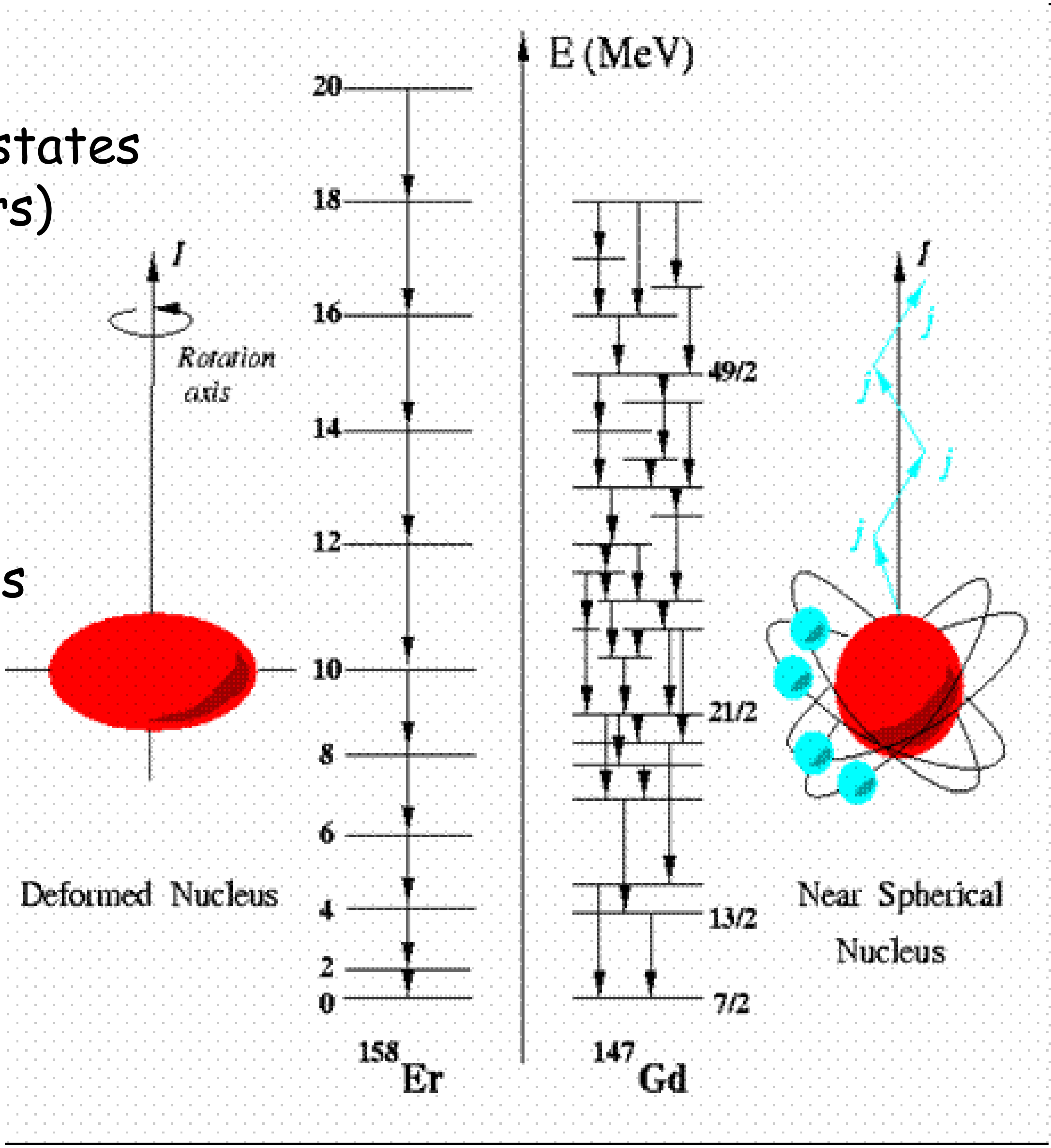

Measuring Excited Excited States – Nuclear Spectroscopy & Nuclear (Shell) Structure

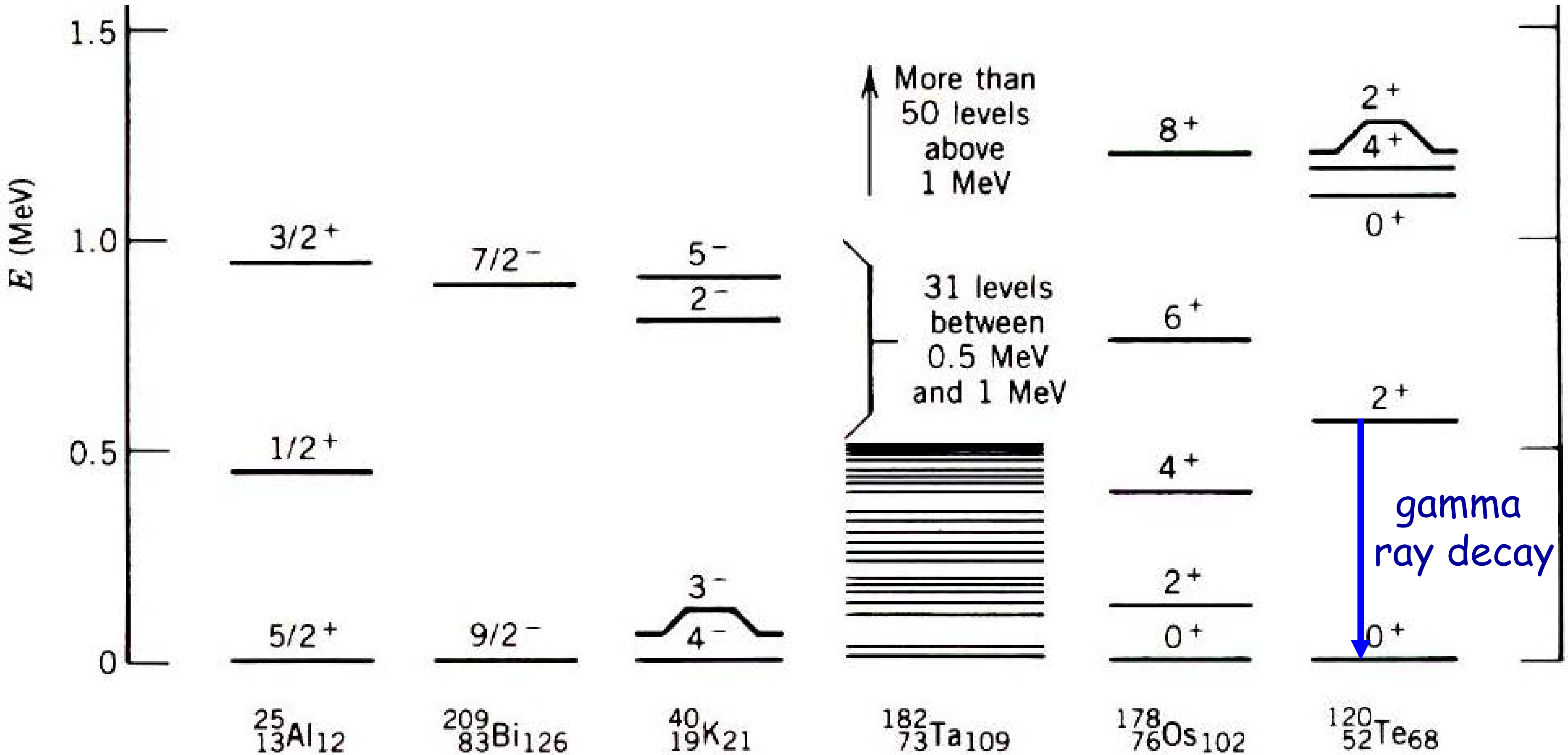

- Nuclear states labelled by spin and parity quantum numbers and energy.
- Excited states (usually) decay by gamma rays (non-visible, high energy light).
- Measuring gamma rays gives the energy differences between quantum states.

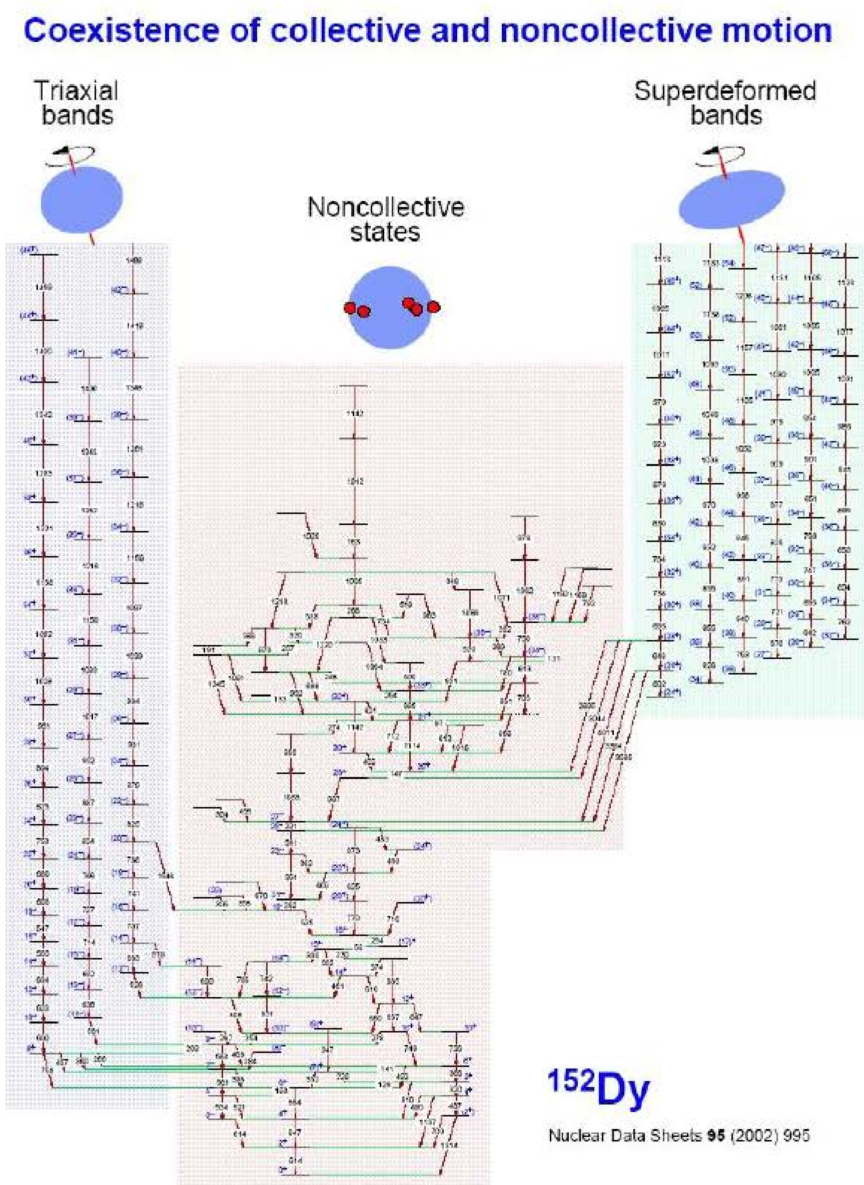

Energy levels are determined by measuring gamma-rays decaying from excited states.

Many, many possible states can be populated…many different gamma-ray energies need to be measured at the same time (in coincidence).

(LN_2 cooled) germanium detectors have the combination of good energy resolution (ΔE~2 keV @ $E\gamma$=1 MeV) and acceptable detection efficiency.

Various multi-detector 'arrays' of germanium detectors around the World. e.g., GAMMASPHERE, MINIBALL, GaSp
JUROGAM, RISING, INGA,
EXOGAM, AGATA, GRETINA,
NuBALL, EXILL+FATIMA, RoSPHERE

Fusion-evaporation reactions best way to make the highest spins. Nuclear EM decay usually decay via 'near yrast' sequence (since decay prob ~ $E\gamma^{2L+1}$)

Compton Suppression

Gammasphere

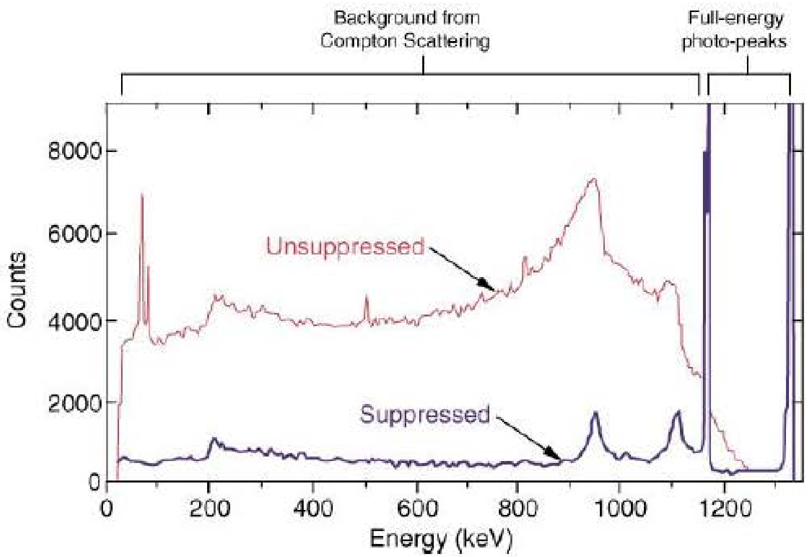

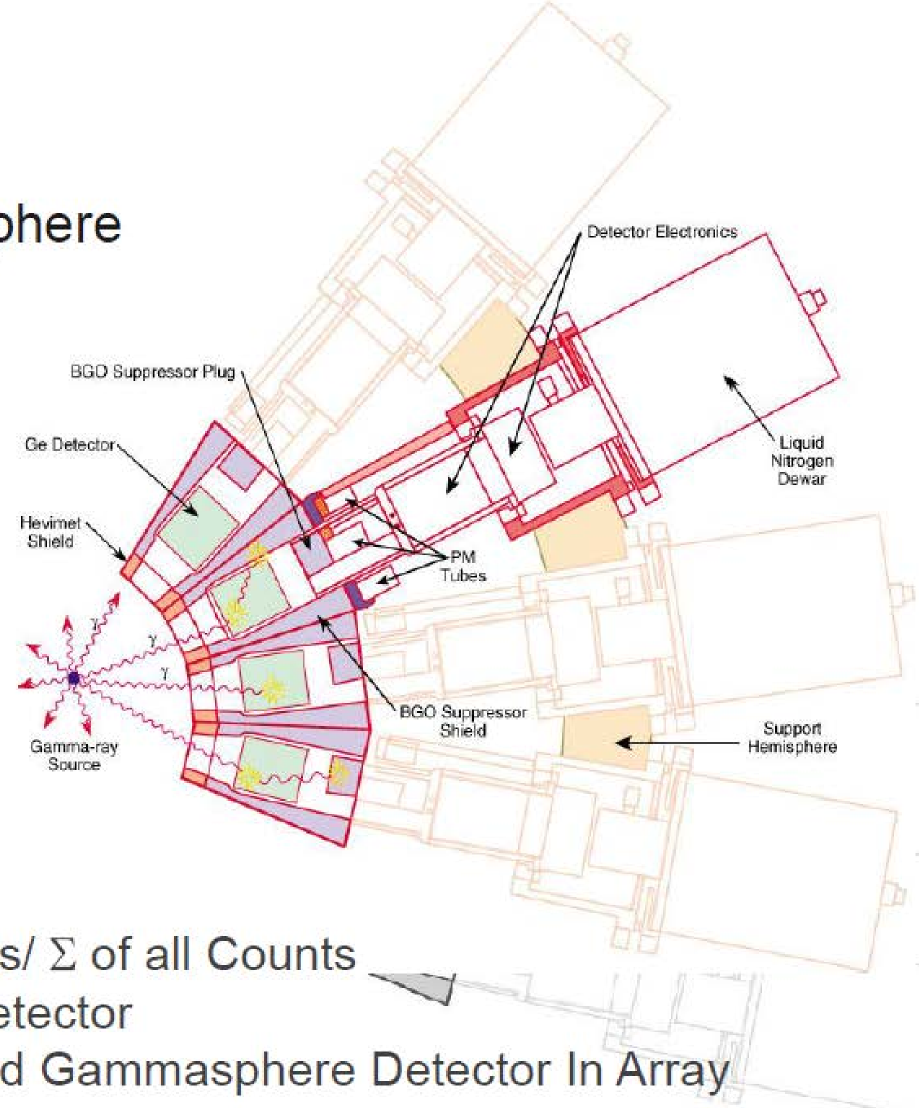

- Peak to Total (P/T) = Σ Photo Peaks/ Σ of all Counts
- P/T ~ 0.20 for 70% Co-axial Ge Detector
- P/T ~ 0.55 for Compton Suppressed Gammasphere Detector In Array
- Photopeak efficiency is ~10% for 1 MeV γ ray (110 Detectors)
- δE = 2.5 keV at 1MeV

Compton Suppressed Arrays

For the last ~ 15 - 20 years, large arrays of Compton-suppressed Ge detectors such as EuroBall, JUROBALL , GASP, EXOGAM, TIGRESS, INGA, Gammasphere and others have been the tools of choice for nuclear spectroscopy.

EUROBALL

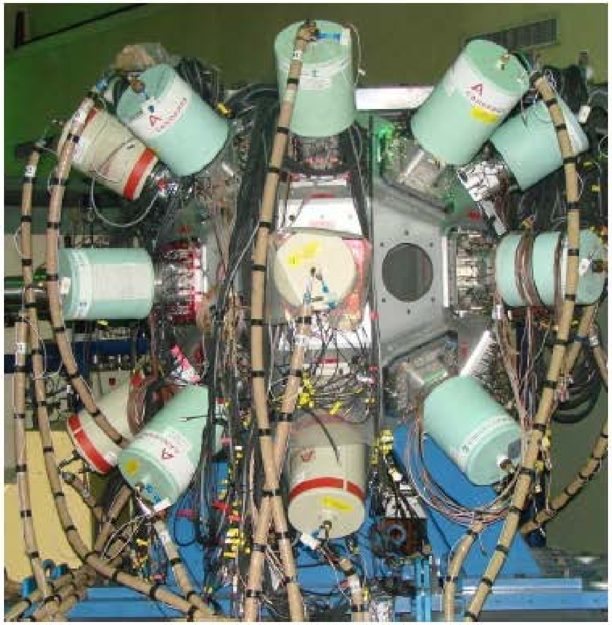

INGA

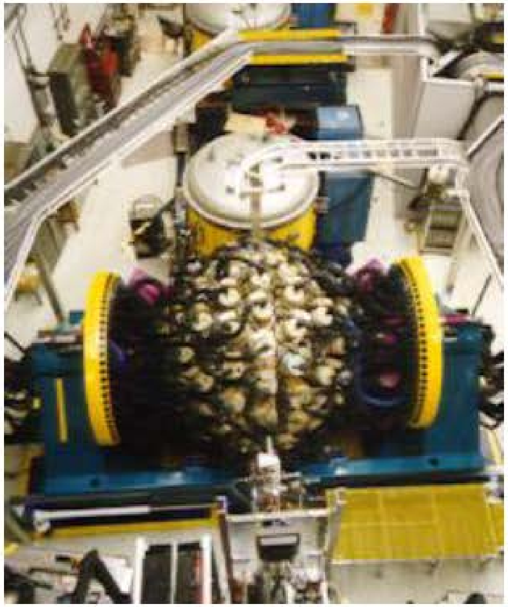

Gammasphere

More recent development include TRACKING arrays (e.g., GRETINA & AGATA) ; and 'Hybrid' arrays (e.g., EXILL+FATIMA, RoSPHERE, NuBALL etc.)

Compton Suppressed Arrays: Recent Example: NuBall at IPN-Orsay.

- **20 $LaBr_3$ detectors** with from FATIMA collaboration -time resolution ~250 ps
- **24 HPGe clover detectors** with BGO shielding for Compton Suppression
- **10 coaxial HPGe detectors** with BGO shielding
- **FASTER Digital DAQ;** 500 MHz sampling for the $LaBr_3$ detectors; 125 MHz sampling for the HPGe and BGO detectors
- Internal **pulse shape analysis**

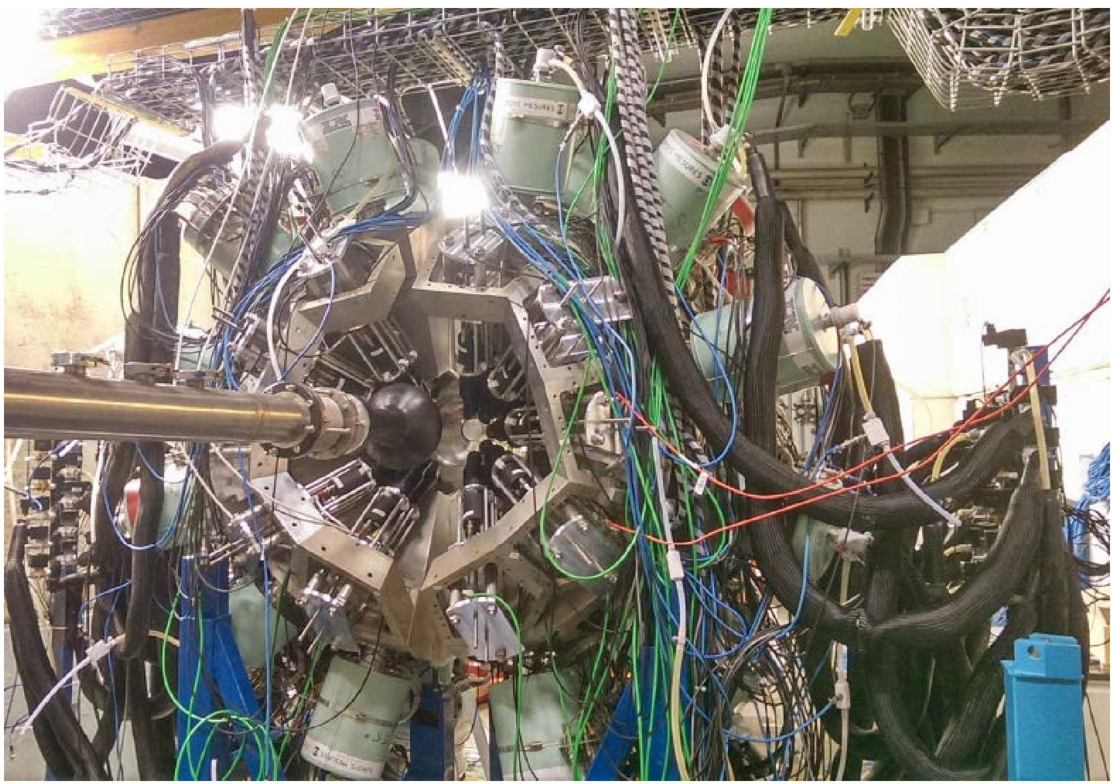

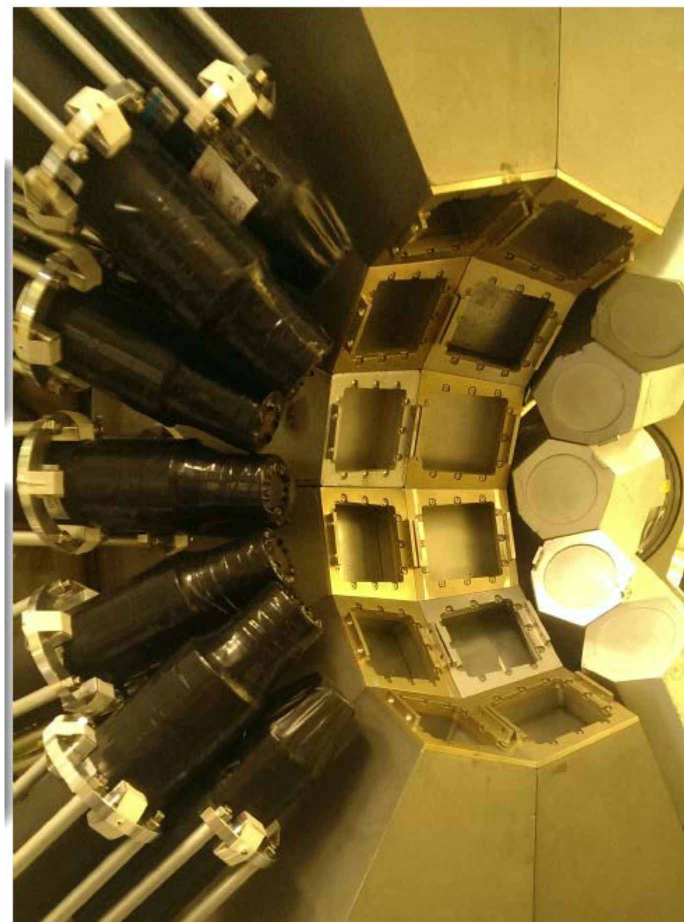

Basic EM Selection Rules?

$$|I_i + I_f| \geq L \geq |I_i - I_f|$$

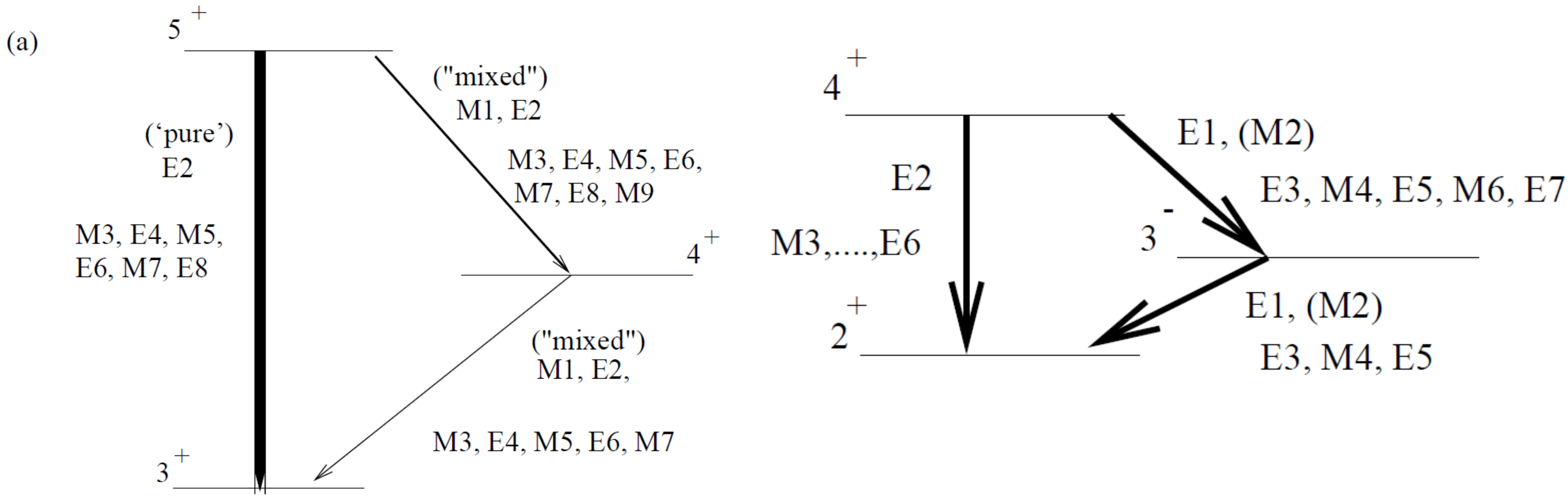

The transition probability for a state decaying from state J_i to state J_f, separated by energy E_γ, by a transition of multipole order L is given by [1, 7]

$$T_{fi}(\lambda L) = \frac{8\pi(L+1)}{\hbar L\,((2L+1)!!)^2}\left(\frac{E_\gamma}{\hbar c}\right)^{2L+1} B(\lambda L : J_i \rightarrow J_f) \qquad (1.1.2)$$

where $B(\lambda L : J_i \rightarrow J_f)$ is called the *reduced matrix element*.

EM decay selection rules reminder.

Suppose we are concerned with a transition between the states i and f of characters (spin, parity) (J_i, π_i) and (J_f, π_f) respectively; defining a quantity p, which is 0 for even parity and $+1$ for odd parity, we see that the multipoles that can contribute are delimited by

$$J_i + J_f \geqq L \geqq |J_i - J_f|,$$

and by the further conditions:

$$p_i + p_f + L = \text{odd for magnetic multipoles}$$
$$p_i + p_f + L = \text{even for electric multipoles.}$$

TABLE I

OBSERVED MULTIPOLE TRANSITIONS

Multipole L		1	2	3	4	5
Parity change	Yes	$E1$	$M2$	$E3$	$M4$	$E5$
	No	$M1$	$E2$	$M3$	$E4$	

Since the quantity that enters in the vector potential of the L-multipole is:

$$j_L(kr) \cong \frac{(kr)^L}{(2L+1)!!}, \qquad 9.$$

we see that the lowest possible multipole transition is greatly favored for $kr \ll 1$. The range of energies for which $(kr) \ll 1$ is frequently called the "long wave-length" region. In fact, usually only the lowest possible multipole contributes, but sometimes also the next order will appear. It is this fact that makes the measurement of multipole order so useful a tool in the assignment of characters to levels. The most important examples of mixed multipoles are found for $M1+E2$ and $E1+M2$ transitions; these are indicated in the above table by connecting lines.

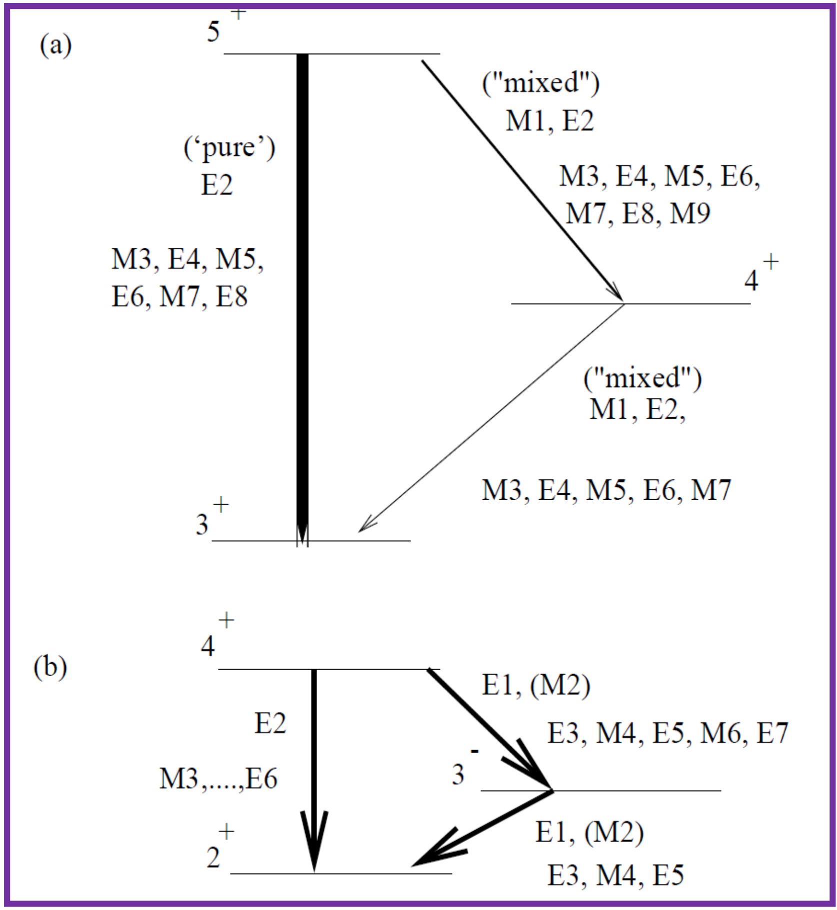

From M.Goldhaber & J.Weneser, Ann. Rev. Nucl. Sci. 5 (1955) p1-24

Nuclear level schemes can be constructed using gamma-gamma coincidence techniques.

‘Gating’ on a particular discrete gamma-ray energy in one detector and observing which transitions are in temporal coincidence with this particular transition.

NANA – the NAtional Nuclear Array

- Up to 12 LaBr3 scintillator gamma-ray detectors.
- Digitised signal output performed by CAEN V1751C module.
- 2.6 % energy resolution @661 keV.
- < 300 ps timing resolution.
- Developed using a validated GEANT4 Monte Carlo simulation.

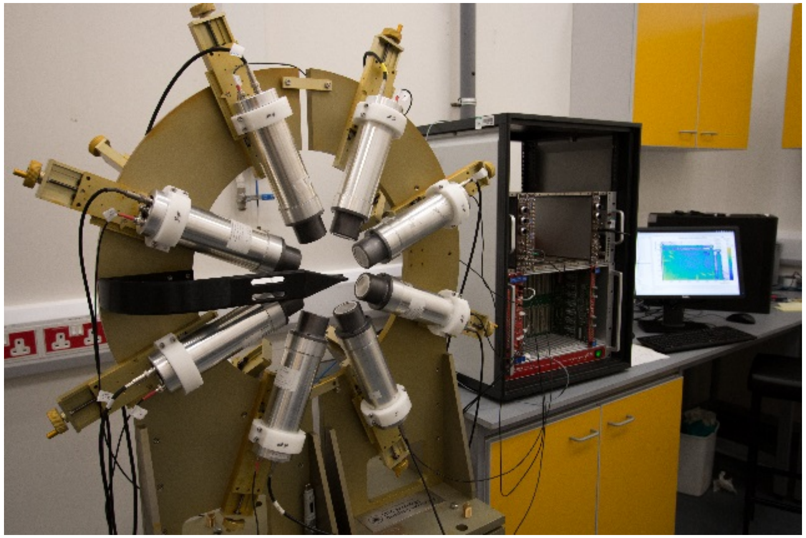

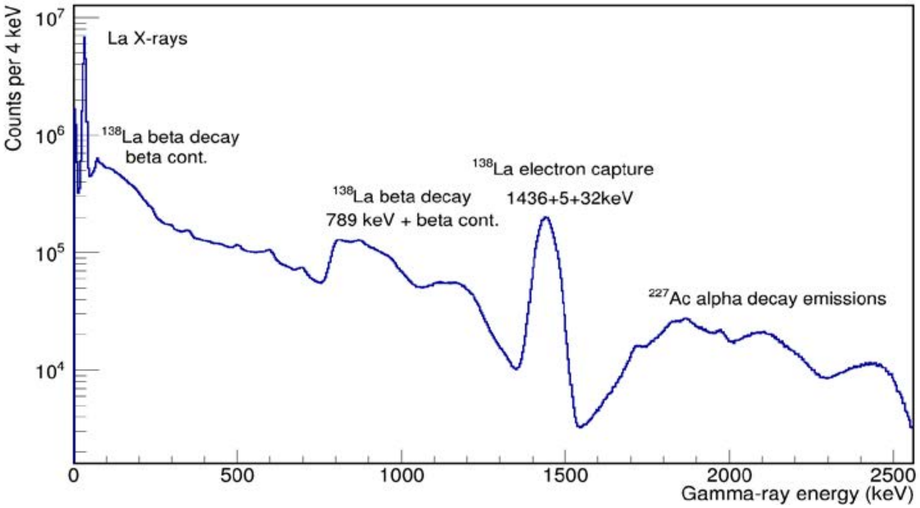

^{134}Cs source decay in γ–γ coincidence.

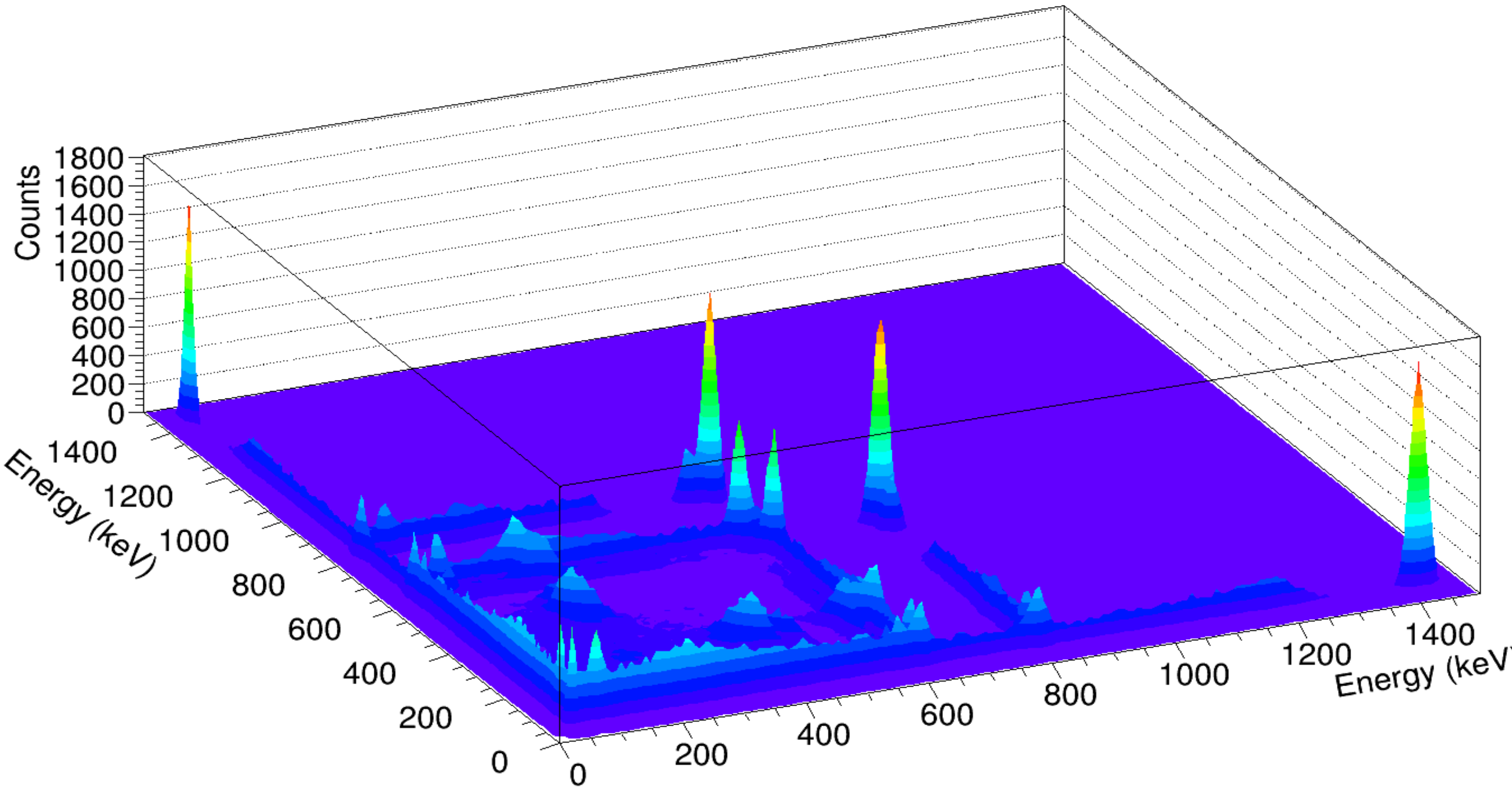

Resolving and selection of weakly populated decay channels

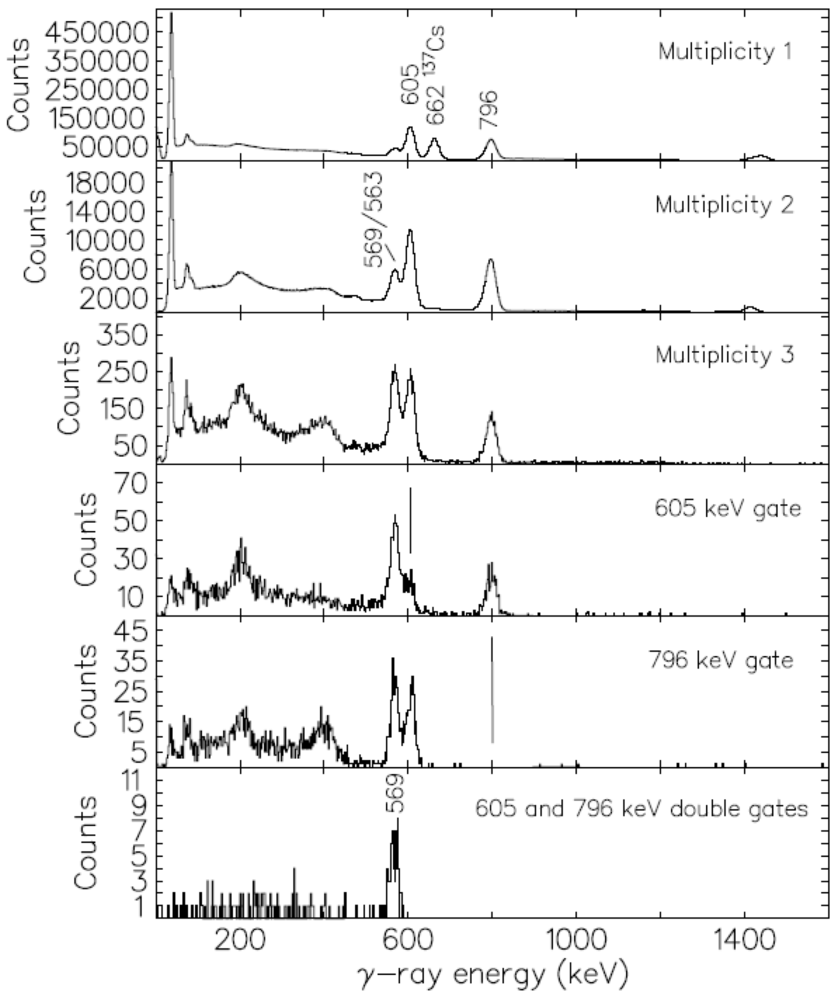

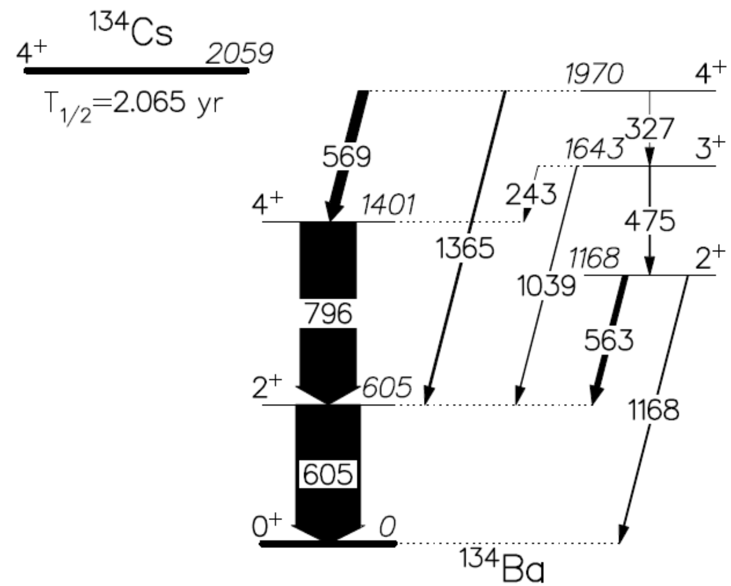

For 605 keV and 796 keV double gate, the peak-to-total of the 569 keV is 40 %! Loss of statistics but much improved signal cleanliness.

How is measuring the lifetime useful?

<u>Nuclear structure information.</u>
The '**reduced matrix element**', **B(λL)** tells us the overlap between the initial and final nuclear single-particle wavefunctions.

$$T_{fi}(\lambda L) = \frac{8\pi(L+1)}{\hbar L\left((2L+1)!!\right)^2}\left(\frac{E_\gamma}{\hbar c}\right)^{2L+1} B(\lambda L : J_i \rightarrow J_f)$$

Transition probability (i.e., 1/mean lifetime as measured for state which decays by EM radiation)

(trivial) gamma-ray energy dependence of transition rate, goes as. *E_γ^{2L+1} e.g., E_γ^{5} for E2s for example.*

EM Transition Rates

Classically, the average power radiated by an EM multipole field is given by

$$P(\sigma L) = \frac{2(L+1)c}{\varepsilon_0 L[(2L+1)!!]^2}\left(\frac{\omega}{c}\right)^{2L+2}[m(\sigma L)]^2$$

$m(\sigma L)$ is the time-varying electric or magnetic multipole moment.
ω is the (circular) frequency of the EM field

For a quantized (nuclear) system, the decay probability is determined by the MATRIX ELEMENT of the EM MULTIPOLE OPERATOR, where

$$m_{fi}(\sigma L) = \int \psi_f^* m(\sigma L)\psi_i dv$$ i..e, integrated over the nuclear volume.

We can then get the general expression for the probability per unit time for gamma-ray emission, $\lambda(\sigma L)$, from:

$$\lambda(\sigma L) = \frac{1}{\tau} = \frac{P(\sigma L)}{\hbar\omega} = \frac{2(L+1)}{\varepsilon_0 \hbar L[(2L+1)!!]^2}\left(\frac{\omega}{c}\right)^{2L+1}[m_{fi}(\sigma l)]^2$$

(see Introductory Nuclear Physics, K.S. Krane (1988) p330).

The lifetime of an isomeric state is related to the total decay width, Γ, a linear sum of all partial decay widths (γ ray, conversion electrons, α decay, β decay, fission, etc.), through the uncertainty relationship (in convenient units):

$$\Gamma \times \tau = \hbar = 0.6582 \times 10^{-15}\ [\mathrm{eV} \cdot \mathrm{s}], \tag{3}$$

where τ is the level mean life, which is related to the half-life as $T_{1/2} = \ln 2 \times \tau$.

For an isomeric state with N branches, predominantly γ rays and internal conversion in the present cases, the partial γ-ray mean life of an individual transition j, τ_γ^j, is given by:

$$\tau_\gamma^j = \tau^{exp} \times \frac{\sum_{k=1}^{N} I_\gamma^k \times (1 + \alpha_T^k)}{I_\gamma^j}, \tag{4}$$

EM Selection Rules and their Effects on Decays

- Allowed decays have:

$$\left|I_i - I_f\right| \le \lambda \le \left|I_i - I_f\right|$$

e.g., decays from $I^{\pi} = 6^{+}$ to $I^{\pi} = 4^{+}$ are allowed to proceed with photons carrying angular momentum of $\lambda = 2,3,4,5,6,7,8,9$ and $10\,\hbar$.

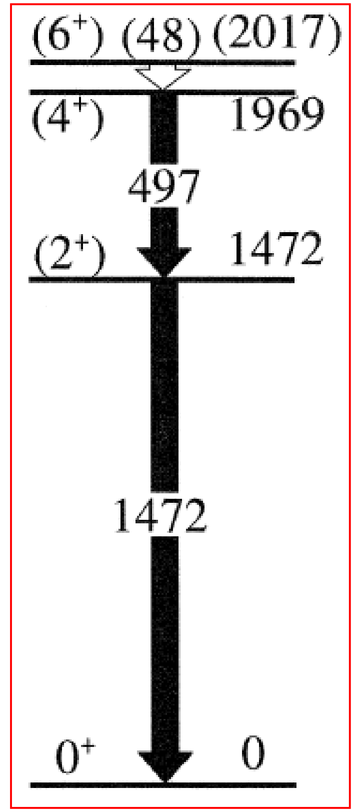

e.g., $^{102}Sn_{52}$

Why do we only observe the E2 decays ?

Are the other multipolarity decays allowed / present ?

Need also to conserve parity between intial and final states, thus, here the transition can not change the parity.

This adds a further restriction : Allowed decays now restricted to E2, E4, E6, E8 and E10 ; and M3, M5, M7, M9

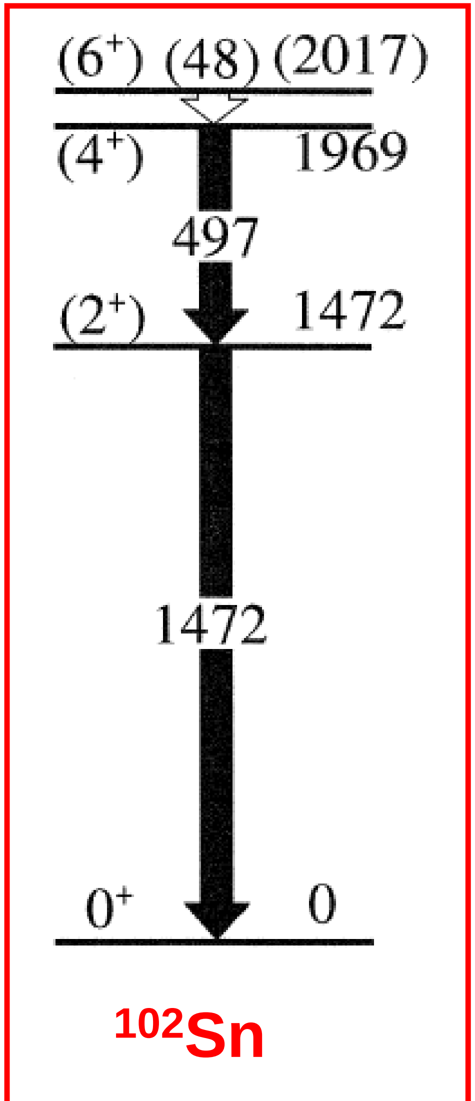

E_γ	E2 (1Wu)	M3 (1Wu)	E4 (1Wu)
48 $(6^+\rightarrow 4^+)$	112μs	782,822 s	2.5E+14s
555 $(6^+\rightarrow 2^+)$			66,912s

497 $(4^+\rightarrow 2^+)$	0.9ns	61ms	180,692s
1969 $(4^+\rightarrow 0^+)$			751ms

Conclusion, in general see a cascade of (stretched) E2 decays in near-magic even-even nuclei.

Weisskopf single-particle estimates

τ_{sp} *for 1 Wu at A~100 and* E_γ *= 200 keV*

M1 2.2 ps	M2 4.1 ms	M3 36 s
E1 5.8 fs	E2 92 ns	E3 0.2 s

The lowest order multipole decays are highly favoured.

BUT need to conserve angular momentum so need at minimum $\lambda = I_i - I_f$ *is needed for the transition to take place.*

Note, for low E_γ *and high -* λ*, internal conversion also competes/dominates.*

The EM transition rate depends on $E_\gamma^{2\lambda+1}$; the highest energy transitions for the lowest λ are (usually) favoured.
This results in the preferential population of yrast and near-yrast states.

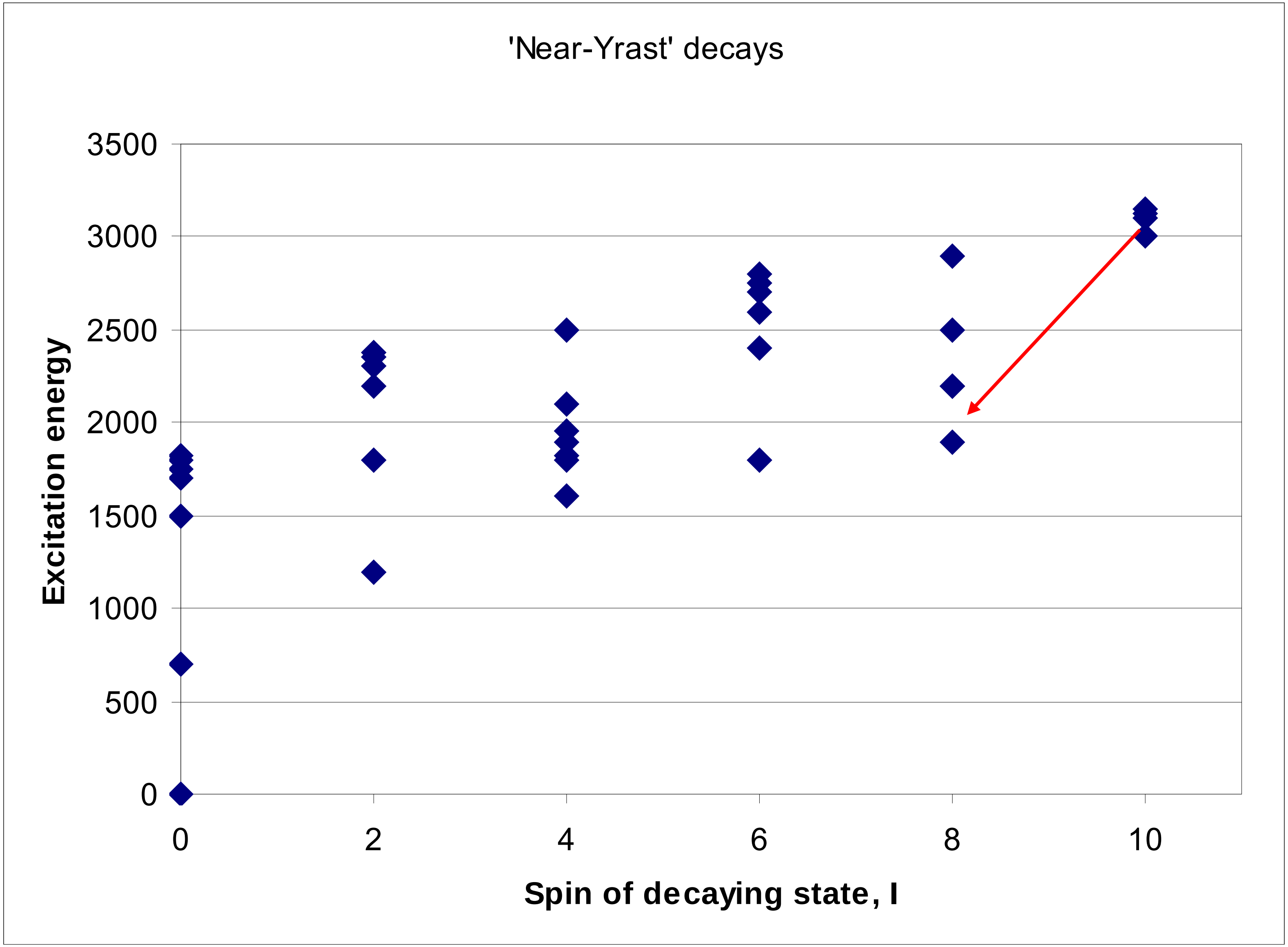

The EM transition rate depends on $E\gamma^{2\lambda+1}$,, the highest energy transitions for the lowest λ are (generally) favoured.
This results in the preferential population of yrast and near-yrast states.

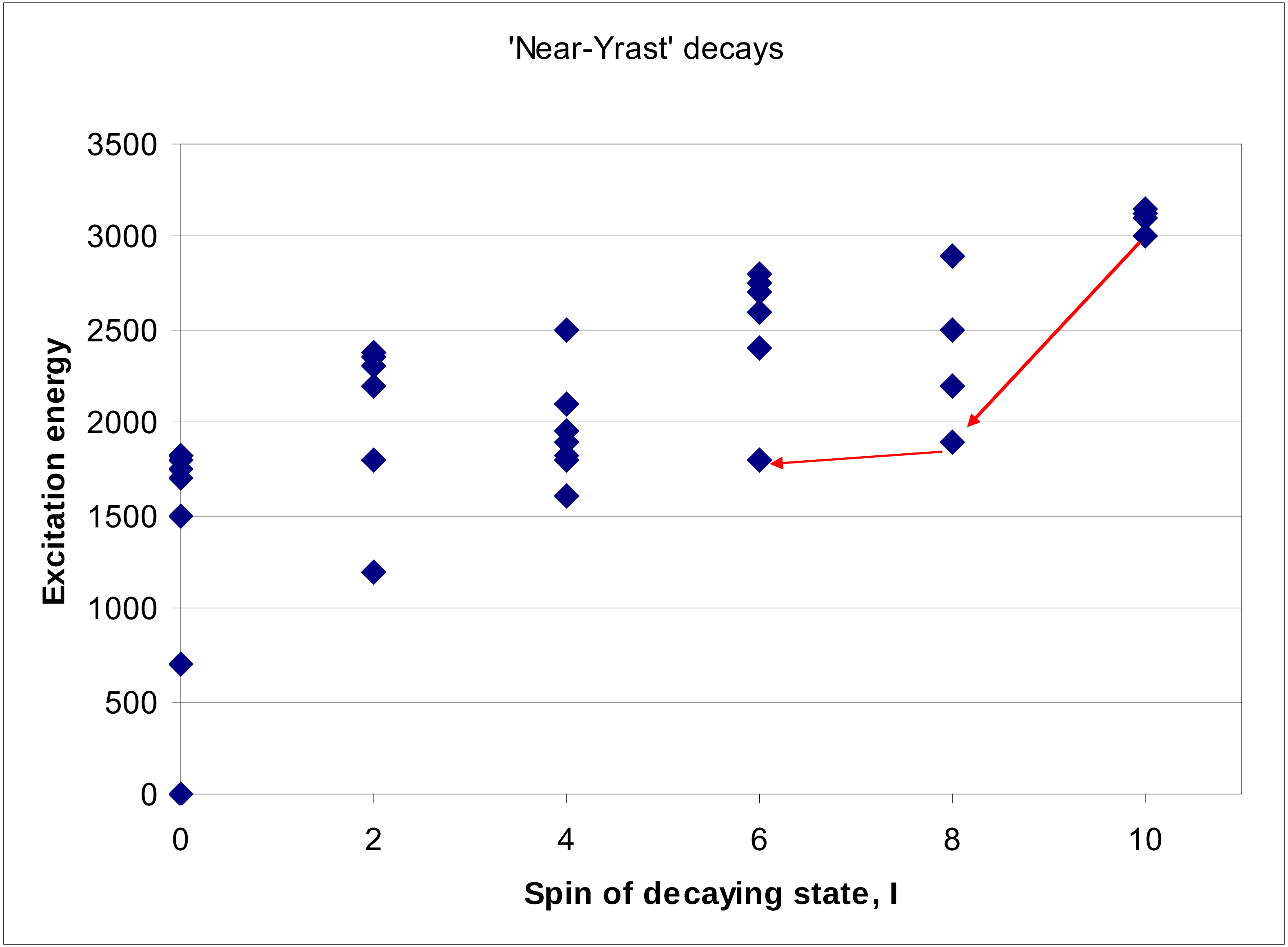

The EM transition rate depends on $E\gamma^{2\lambda+1}$,, the highest energy transitions for the lowest λ are (generally) favoured.
This results in the preferential population of yrast and near-yrast states.

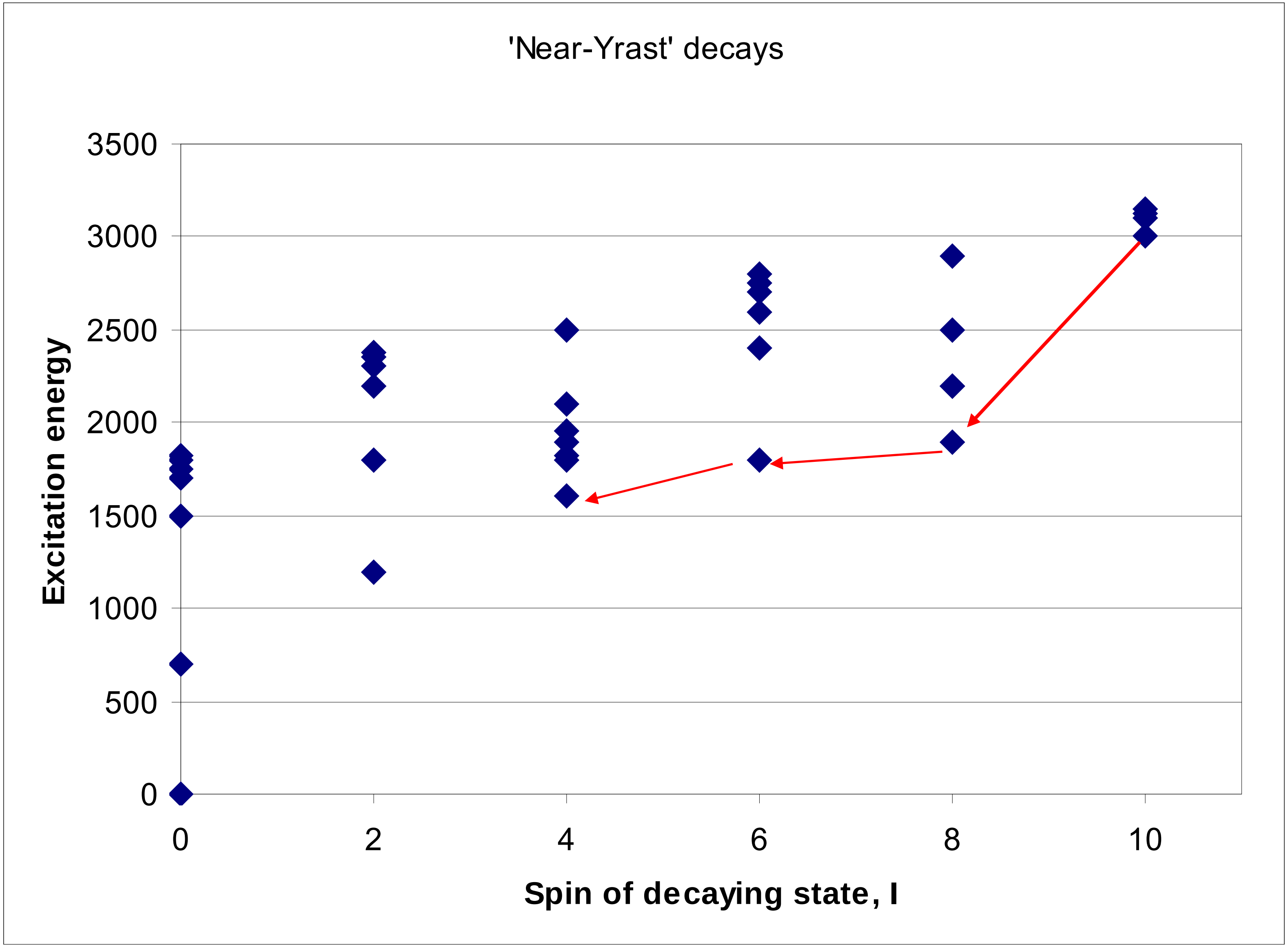

The EM transition rate depends on $E\gamma^{2\lambda+1}$,, the highest energy transitions for the lowest λ are (generally) favoured.

This results in the preferential population of yrast and near-yrast states.

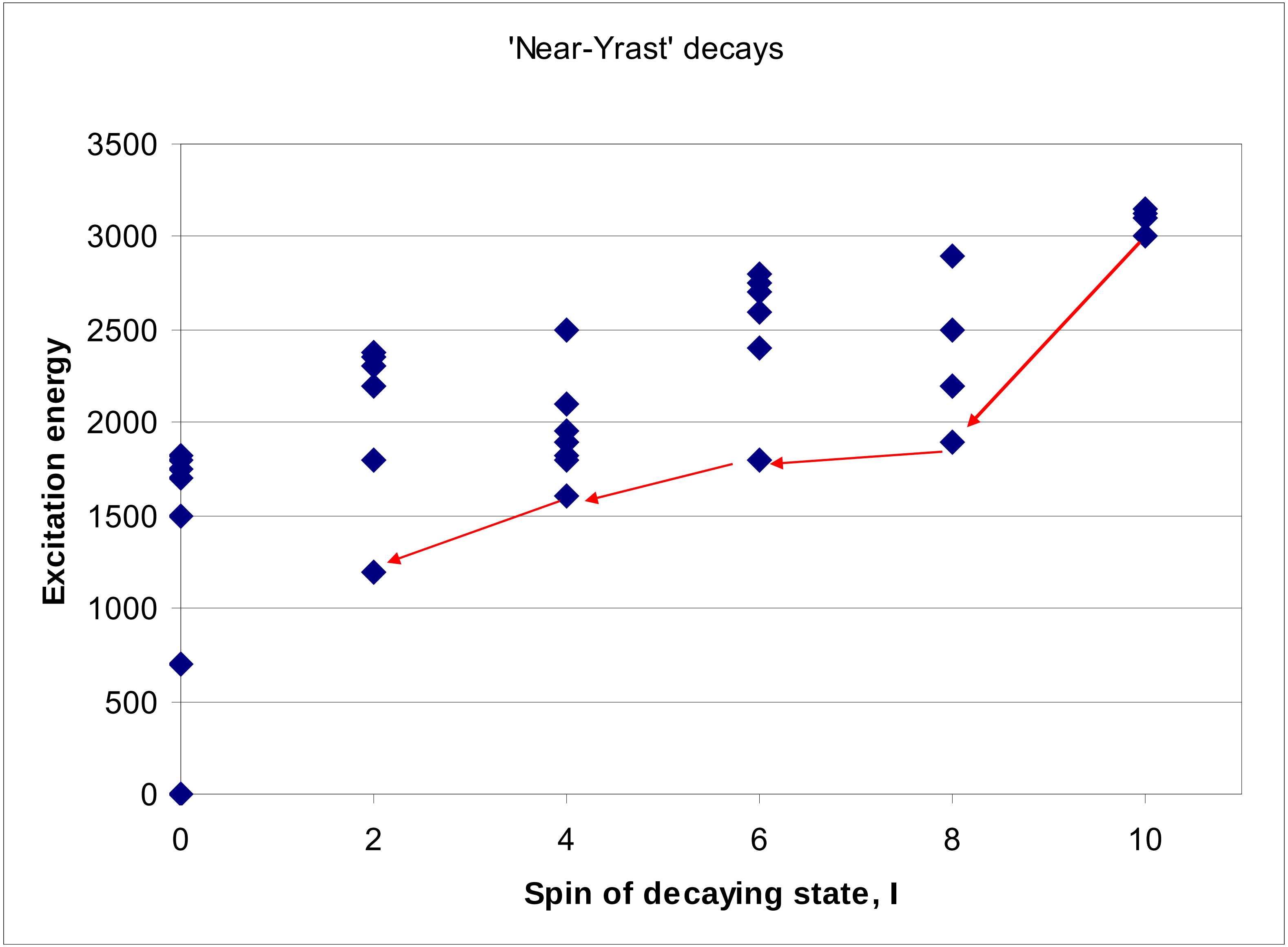

The EM transition rate depends on $E\gamma^{2\lambda+1}$,, the highest energy transitions for the lowest λ are (generally) favoured.

This results in the preferential population of yrast and near-yrast states.

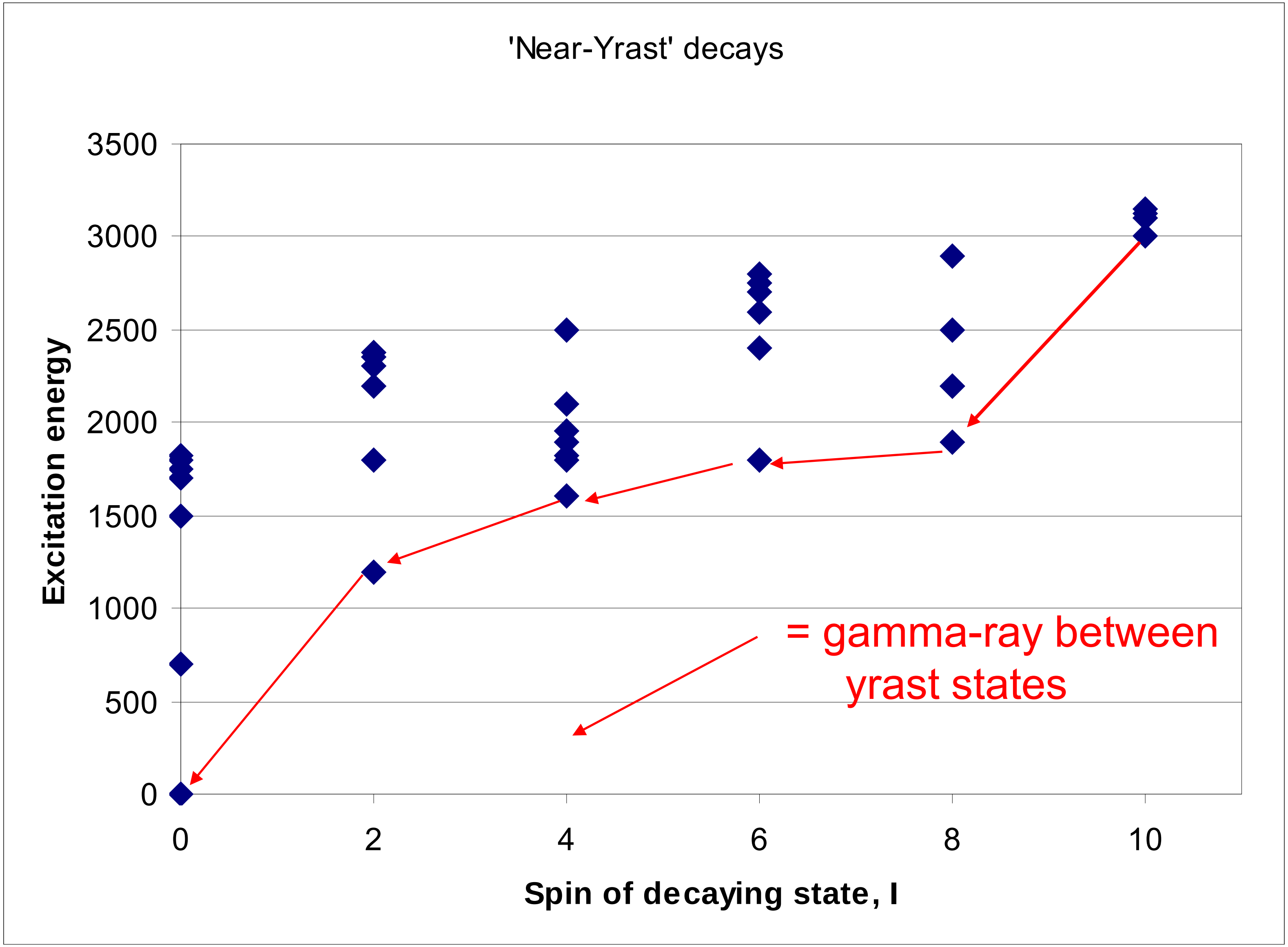

The EM transition rate depends on $E\gamma^{2\lambda+1}$, (for E2 decays E_γ^5)
Thus, the highest energy transitions for the lowest λ are usually favoured.
Non-yrast states decay to yrast ones (unless very different ϕ, K-isomers)

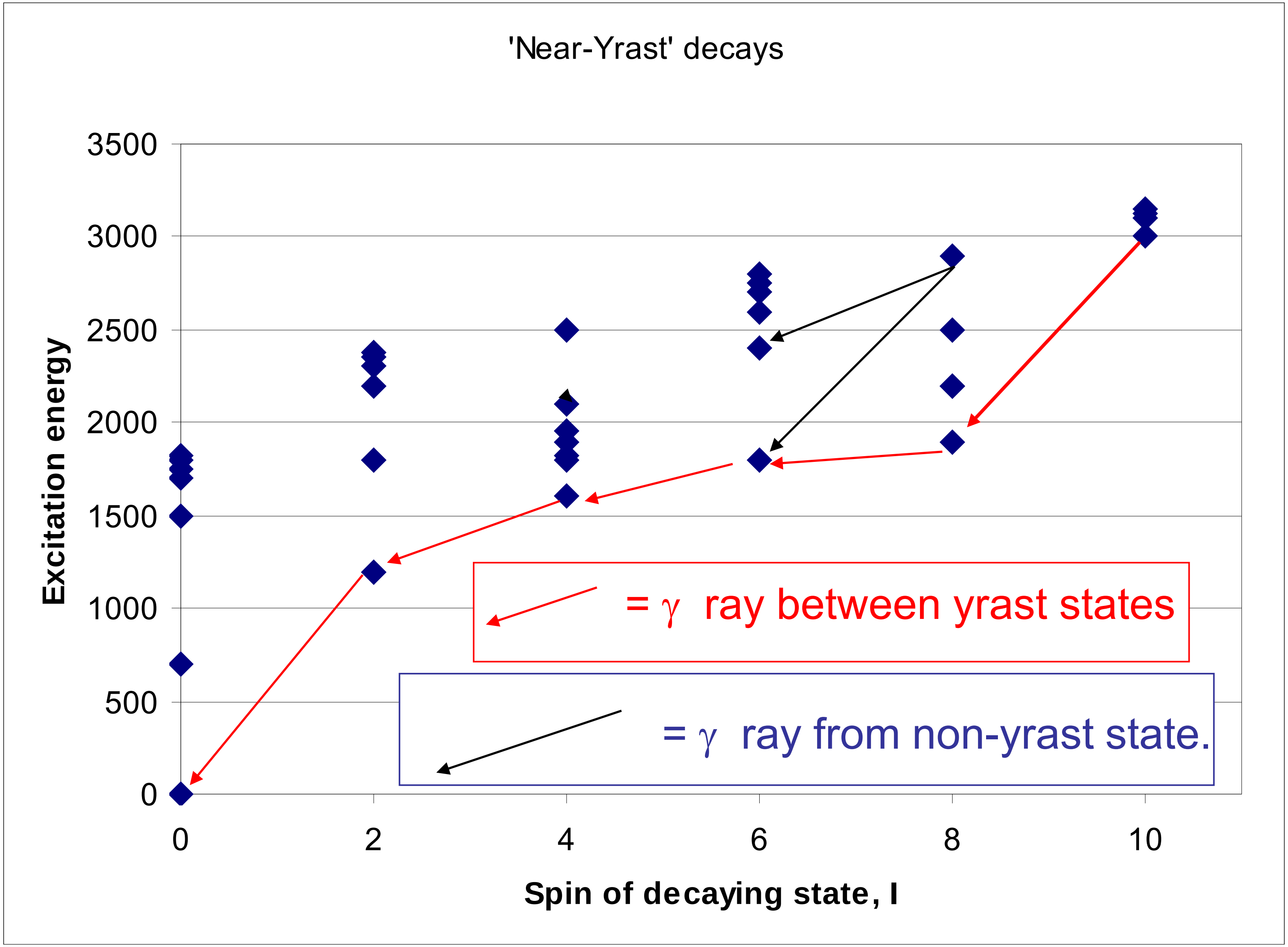

The EM transition rate depends on $E\gamma^{2\lambda+1}$, (for E2 decays E_γ^{5})
Thus, the highest energy transitions for the lowest λ are usually favoured.
Non-yrast states decay to yrast ones (unless very different ϕ, K-isomers etc.)

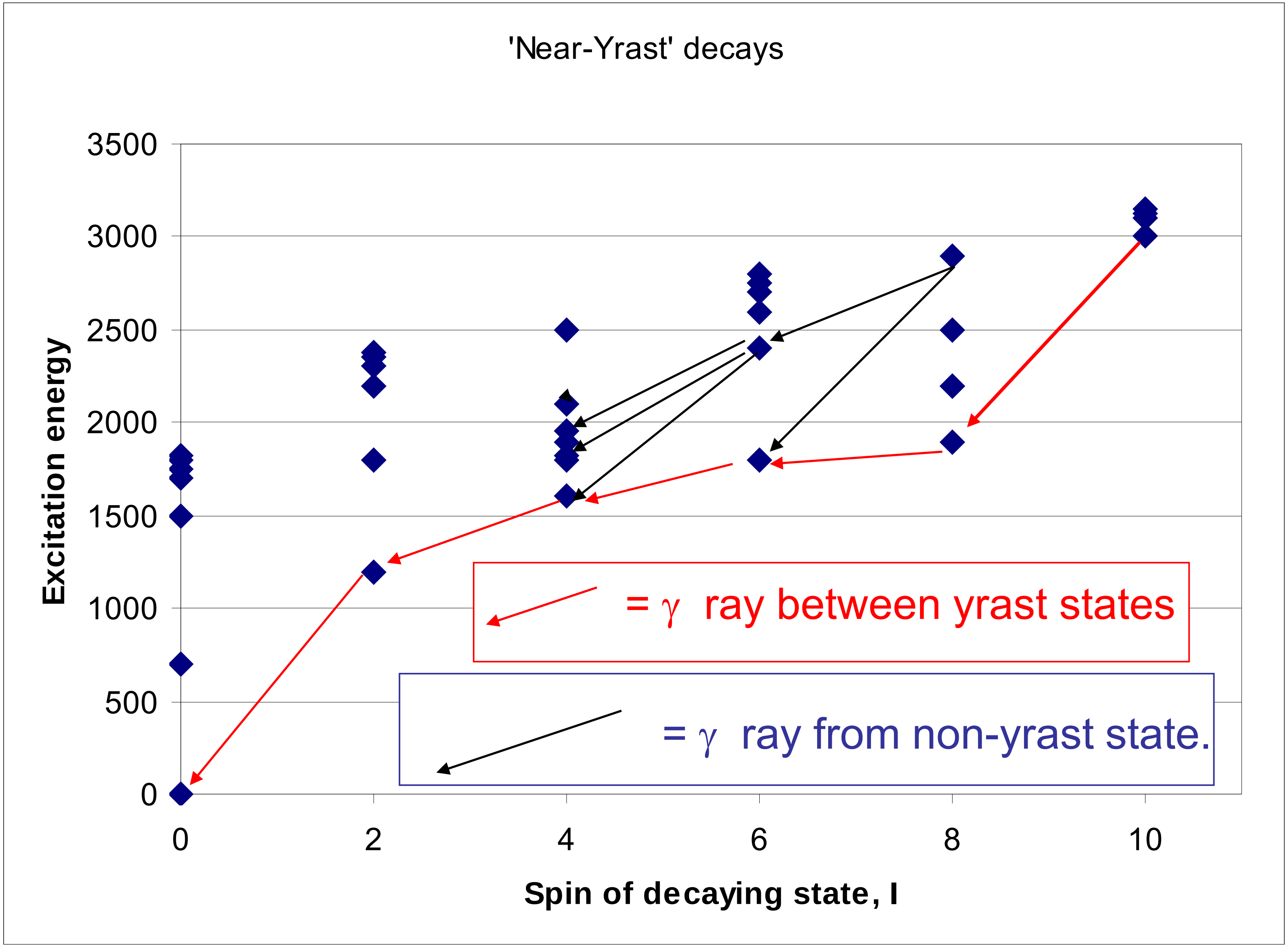

The EM transition rate depends on $E\gamma^{2\lambda+1}$, (for E2 decays $E_\gamma{}^5$)
Thus, the highest energy transitions for the lowest λ are usually favoured.
Non-yrast states decay to yrast ones (unless very different ϕ , K-isomers)

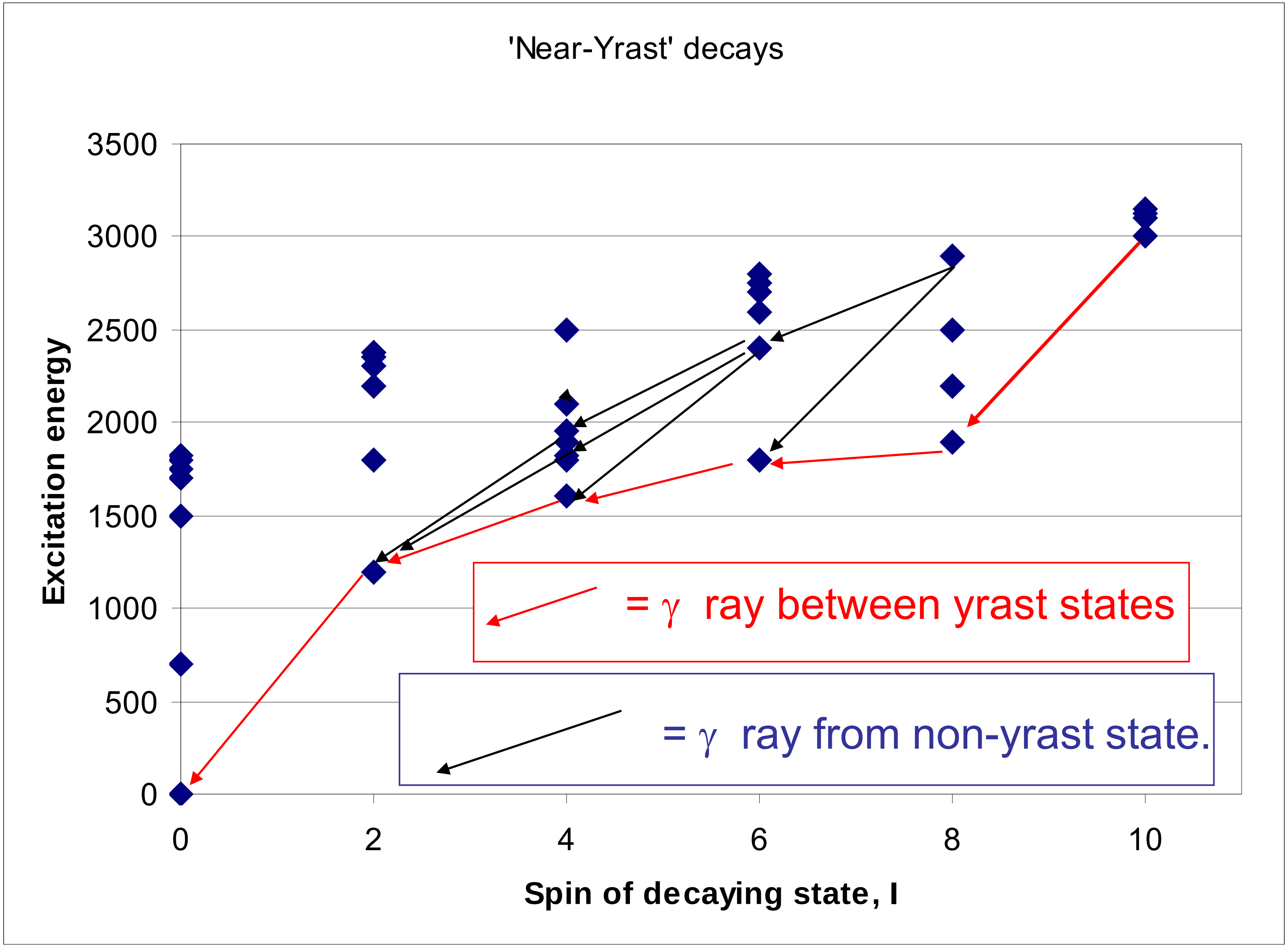

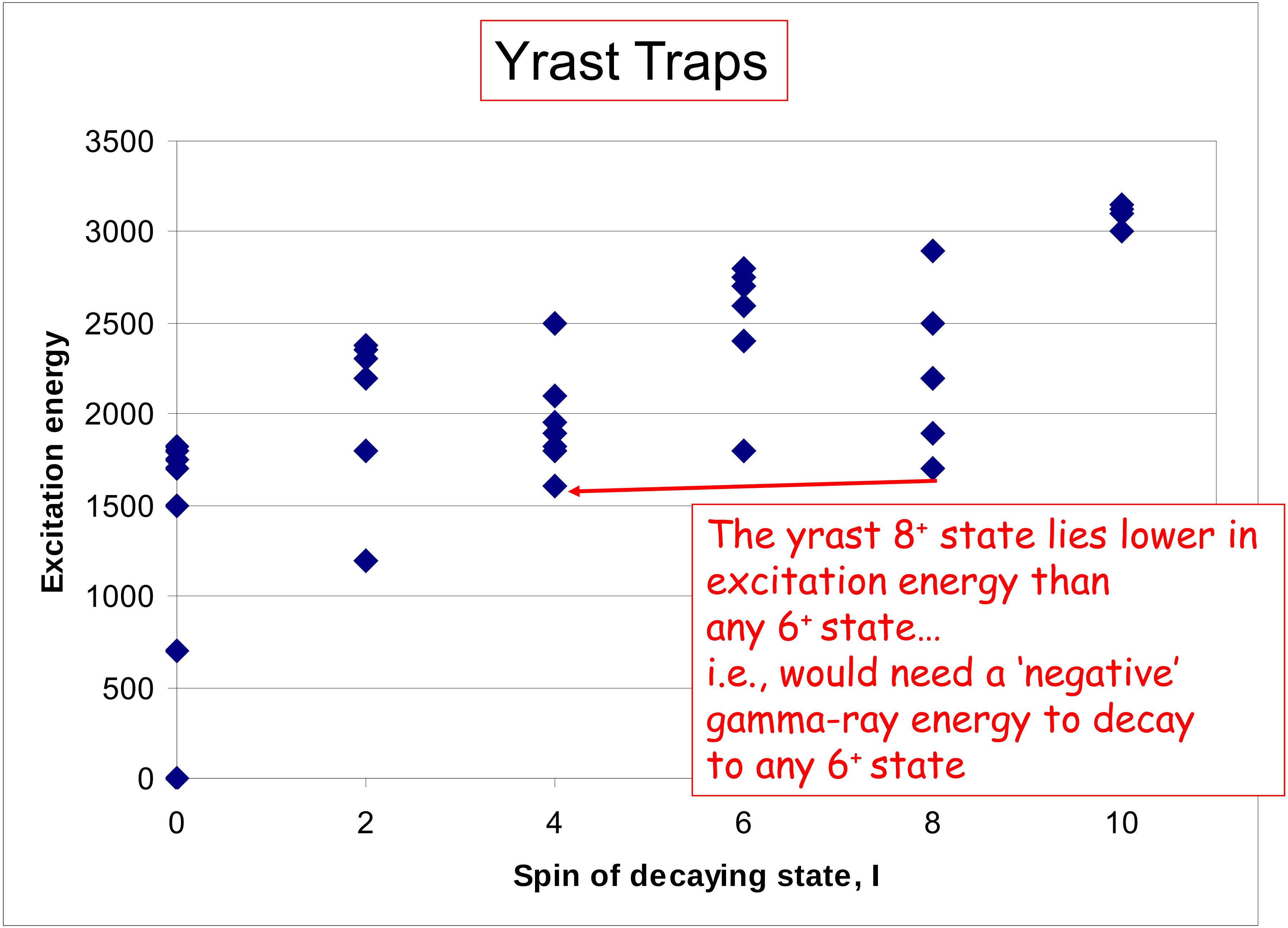
Yrast Traps
3500
3000
2500
2000
1500
1000
500
0
Excitation energy
0
2
4
6
8
10
Spin of decaying state, I
The yrast 8+ state lies lower in
excitation energy than
any 6+ state…
i.e., would need a 'negative'
gamma-ray energy to decay
to any 6+ state

Yrast Traps

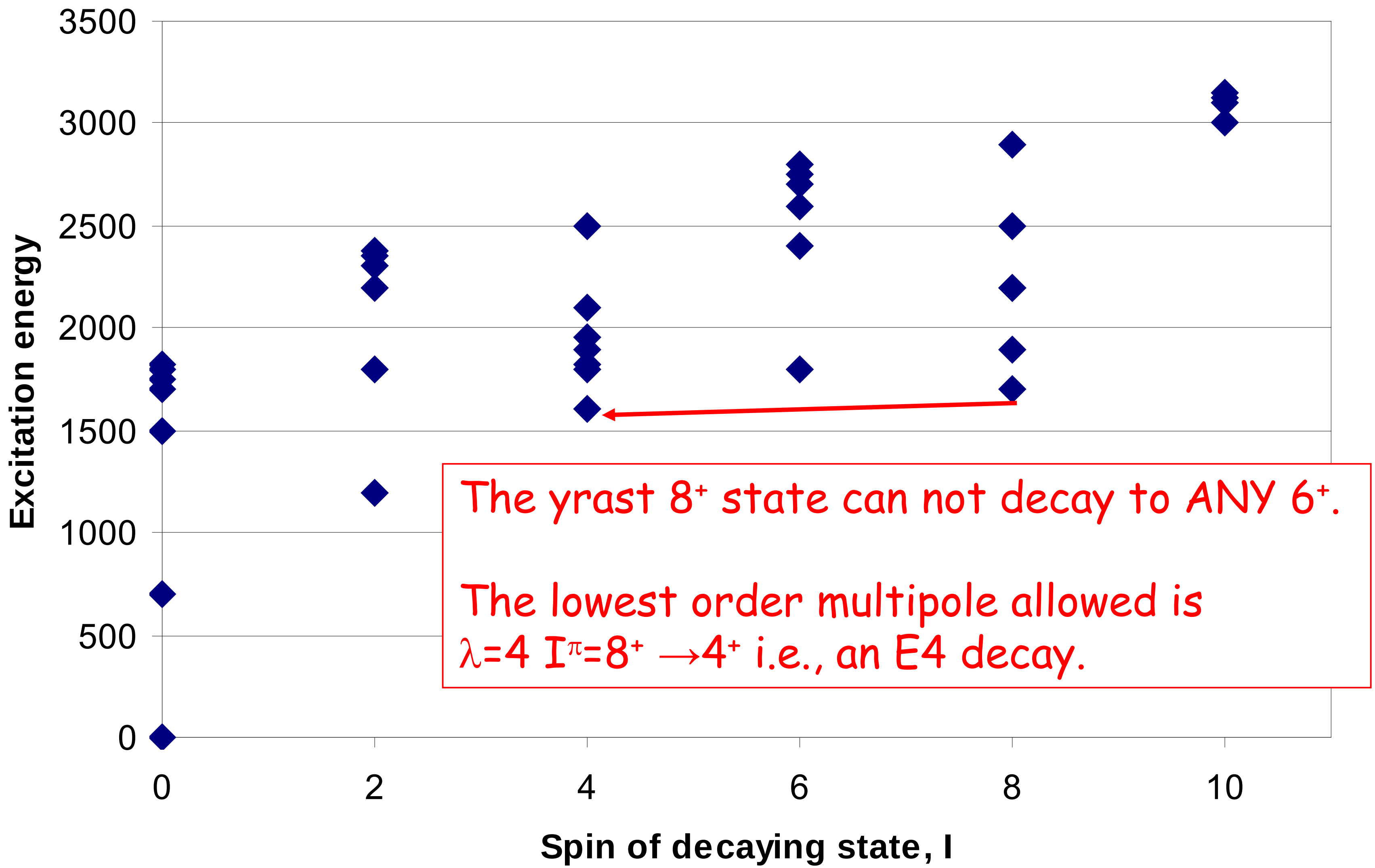

The yrast 8^+ state can not decay to ANY 6^+.

The lowest order multipole allowed is
$\lambda=4$ $I^\pi=8^+ \rightarrow 4^+$ i.e., an E4 decay.

e.g. ^{223}Ra decay.

Characteristic signatures of decay include:

i) Alpha decay (and rare ^{14}C cluster emission)

ii) Fine structure in alpha decay to ^{219}Rn excited states.

iii) Gamma ray emission from excited states in the ^{219}Rn daughter.

Iv) Internal electron conversion emission in competition with gamma ray emission.

v) Daughter (^{219}Rn), granddaughter (^{215}Po) and subsequent decays….

Very complex alpha decay fine structure, many alpha lines to excited states in ^{219}Rn. (from ENSDF nuclear data based from 2001 evaluation in Nuclear Data Sheets).

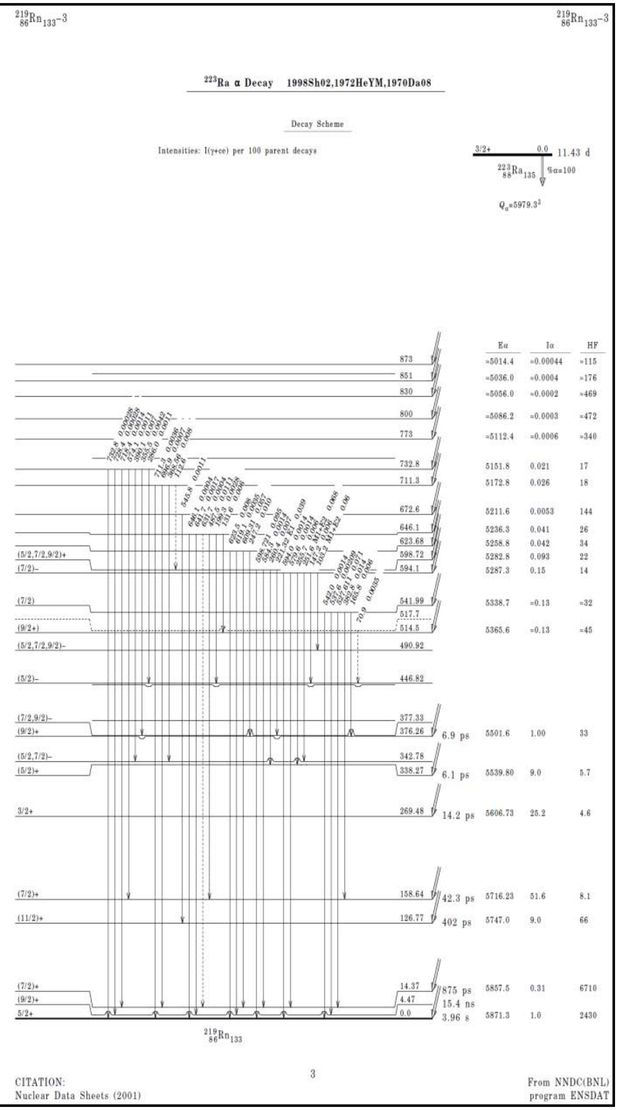

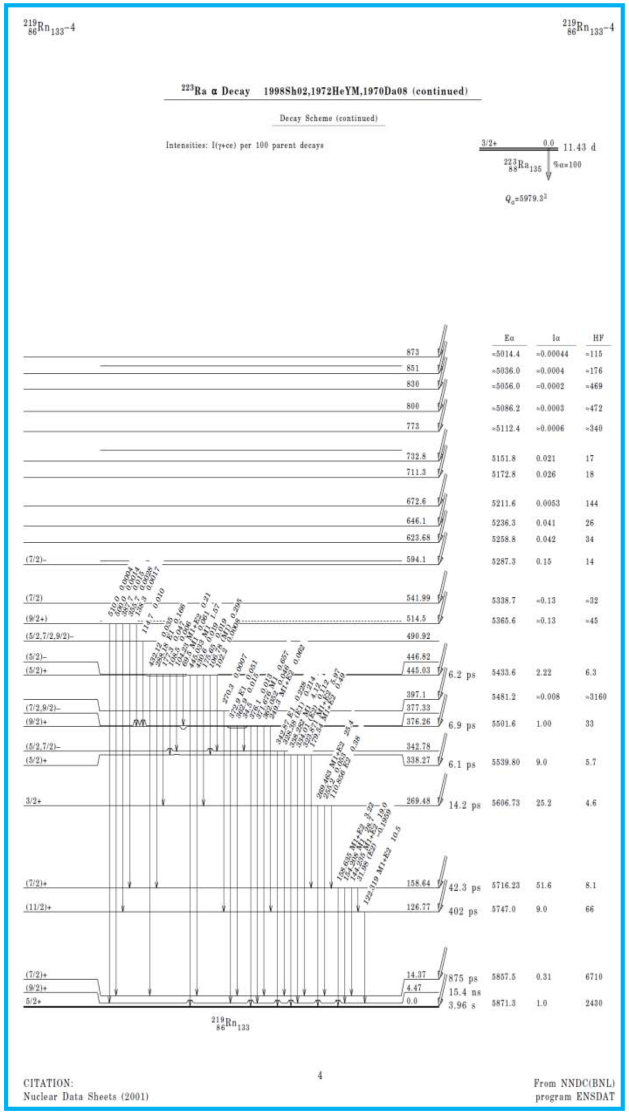

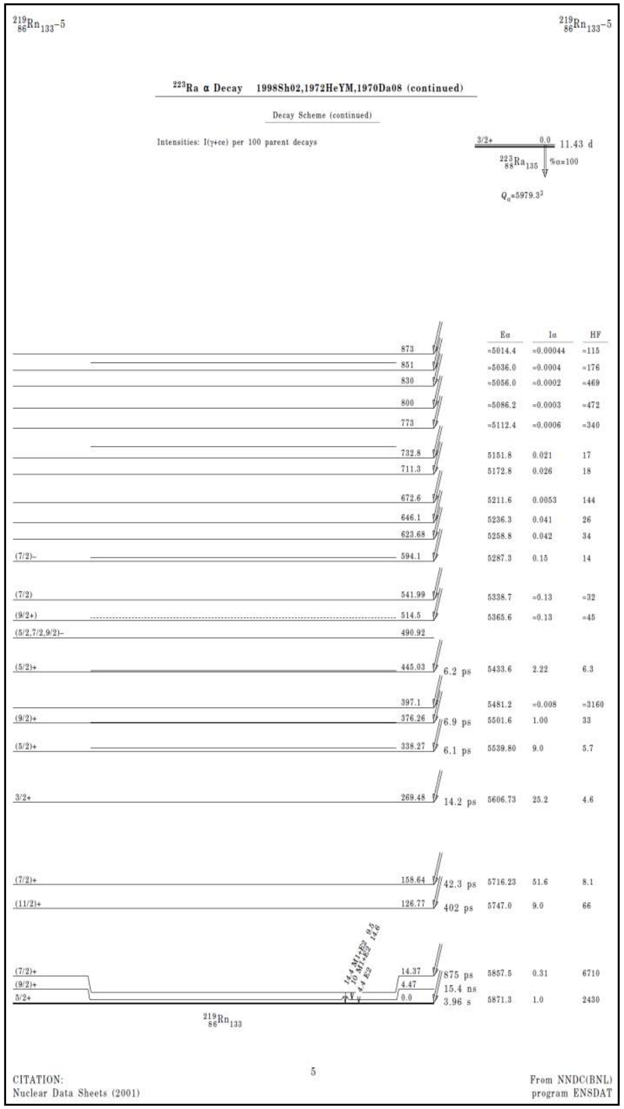

Initial decay energetics of ^{223}Ra

Basic modes of decay for heavy nuclei are beta decay to lighter nucleus with the same A (=N+Z) value (e.g., $^{227}Ac \rightarrow {}^{227}Th + \beta^- + \nu$) until minimum energy isobar is reached for a given A value.

This is usually then followed by α decay (i.e., emission of a ^4He nucleus) to create a daughter nucleus with A-4, e.g., $^{227}Th \rightarrow {}^{223}Ra + \alpha$.

- Some decays of odd-A nuclei populate excited nuclear states in the daughter - leads to **fine structure** in α decay

.

- mass parabolas for A= constant from the semi-empirical mass equation

- ^{223}**Ra** (Z=88) is lowest energy isobar for A=223; it must decay by α emission.

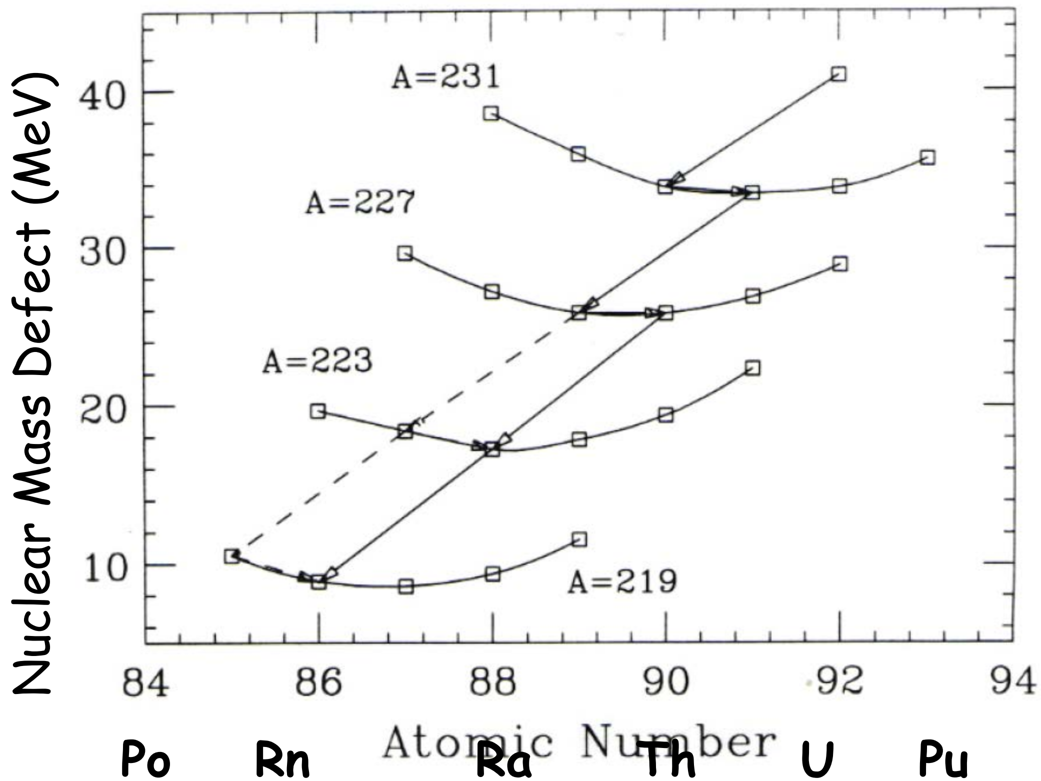

Alpha Decay Selection Rules.

- Alpha decay to excited states in nuclei is observed empirically.
- Alpha particle spectra from odd-A and odd-odd nuclei can become (very) complex, with a number of characteristic alpha decay energies up to the the ground state to ground state decay E_α value.
- In order to conserve angular momentum, alpha particles can be emitted with some additional ***orbital angular momentum*** value, *l*, relative to the daughter nucleus.
- This also gives rise to an effective increase in the potential energy barrier height for that decay (called the **centrifugal barrier**).
- Any orbital angular momentum adds $l(l+1)\hbar^2/2\mu r^2$ to potential barrier for that decay.
- Angular momentum selection rule $|I_i - I_f| \leq l_\alpha \leq |I_i + I_f|$ in α decay required that the spins of the state populated by direct decay must be equal to the vector sum of the spin of the emitting state in the mother, plus any relative orbital angular momentum carried away from the a particle, l_α.
- $l = 0$ alpha decays would be favored. (i.e., same spin/parity for mother decaying state and daughter state populated directly in alpha decay).
- Excited energy states in daughter can have different spin (and parity) values which affect the relative population in α decay.

PHYSICAL REVIEW C VOLUME 57, NUMBER 1 JANUARY 1998

Configurations and level structure of ^{219}Rn

R. K. Sheline*
Departments of Chemistry and Physics, Florida State University, Tallahassee, Florida 32306

C. F. Liang and P. Paris
Centre de Spectrométrie Nucléaire et de Spectrométrie de Masse, Bâtiment 104, 91405 Campus Orsay, France

(Received 6 May 1997)

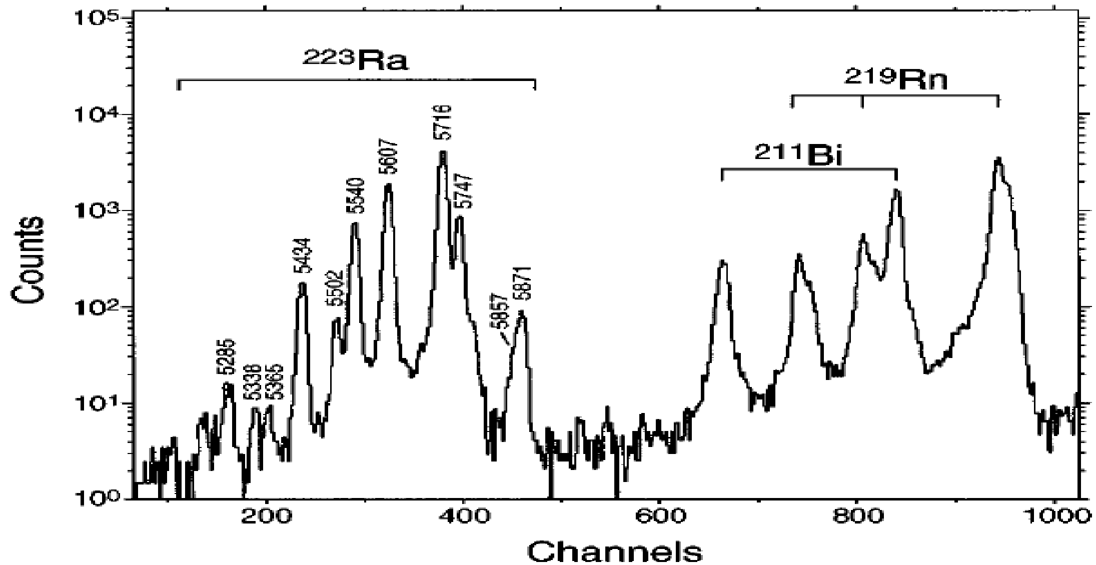

FIG. 1. The alpha spectra of ^{223}Ra, ^{219}Rn, and ^{211}Bi. Alphas from the various activities are bracketed. Alphas from ^{223}Ra leading to levels in ^{219}Rn are labeled with their energies in keV.

Most intense α decay energies associated with ^{223}Ra decay have E_α=5176(4) and 5607(4) keV.
These correspond to the **direct population** from spin/parity 3/2+ ground state of ^{223}Ra
to (a) the 7/2+ excited state at E_x=(5871-5716) = 155(5) keV (Δl=2) and
(b) the 3/2+ excited state at E_x=(5871-5607) = 264(5) keV (Δl=0) above the ^{219}Rn g.s..

Note a large observed hindrance (~2800) for the decay to the ground state (5871 keV).

Excited states populated in ^{219}Rn following ^{223}Ra decay.

Applied Radiation and Isotopes 102 (2015) 15–28

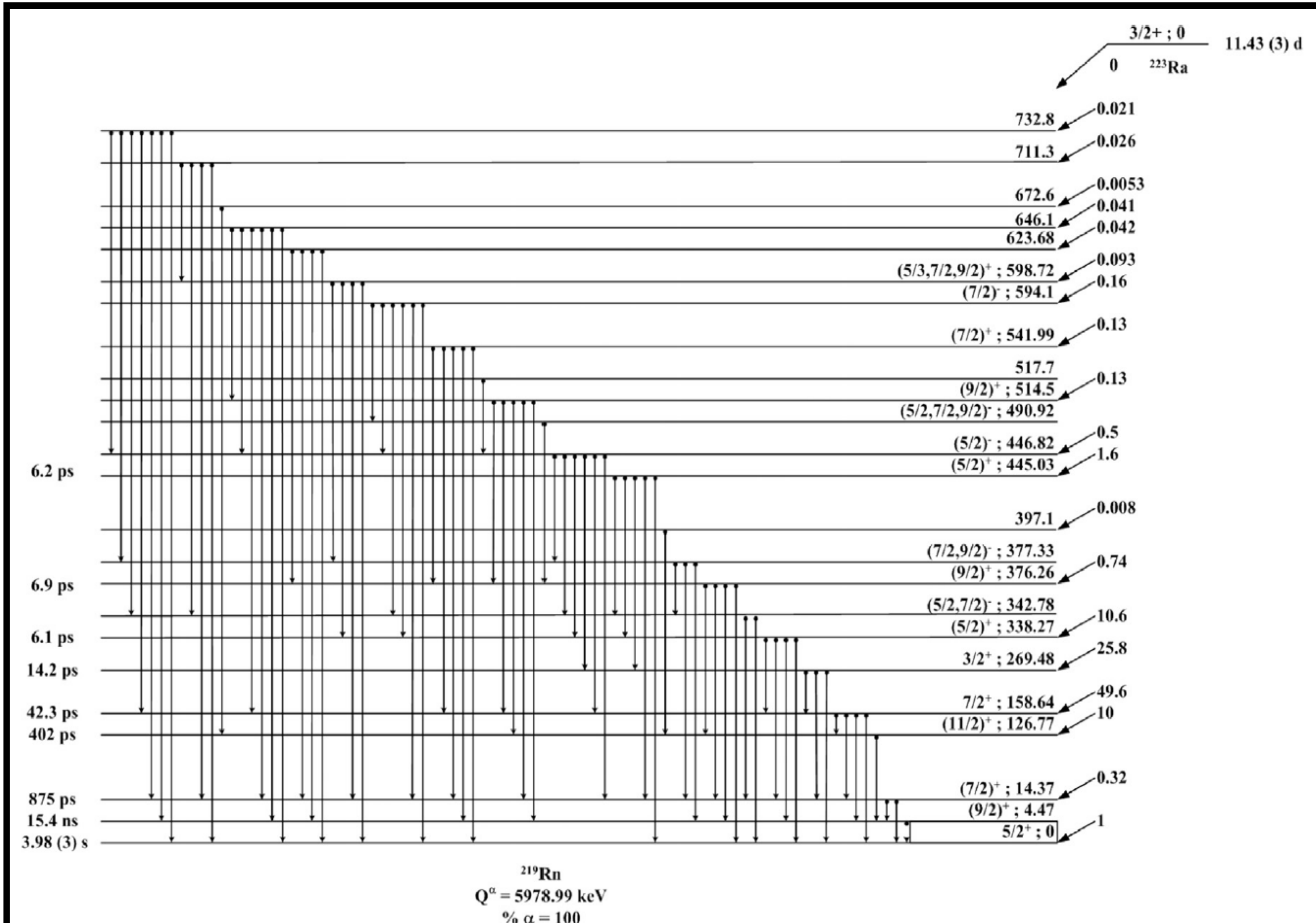

Selection rules in α decay (of ^{223}Ra) mean that different excited states are populated in the daughter nucleus.
These can then subsequently decay to the ground state of the daughter (^{219}Rn) by characteristic **gamma-ray emission**.

$$E_i = E_f + E_\gamma + E_R$$

or

$$\Delta E = E_i - E_f = E_\gamma + E_R = E_\gamma + \frac{E_\gamma}{2\mathrm{m}_{nuc}c^2}$$

where $E_\gamma \sim 1\ MeV$, $Mc^2_{nuc} \sim A \times GeV$, thus recoil the term

$$\frac{E_\gamma}{2\mathrm{m}_{nuc}c^2} \ll\sim E_\gamma$$

Gamma-ray multipoles determine the angular momentum (spin) & parity differences between the initial & final nuclear states linked by gamma-ray emission.

E1 = one unit change in spin ; change parity
M1 = 1 change in spin ; no change in parity
E2 = 2 unit change in spin ; no parity change

Nuclear states are labelled by angular momentum (or 'spin') and parity (+ or -) quantum numbers.
The angular momentum removed by the emitted gamma-ray (ΔL) from the nucleus is related to the spin difference between the initial and final nuclear states (usually the lowest order decay $\Delta L = |I_i - I_f|$ dominates).

Different nuclear reaction mechanisms?

- Heavy-ion fusion-evaporation reactions: makes mostly neutron-deficient residual nuclei.
- Spontaneous fission sources such as ^{252}Cf: makes mostly neutron-rich residual nuclei).
- Deep-inelastic/multi-nucleon transfer and heavy-ion fusion-fission reactions: makes near-stable/slightly neutron-rich residual nuclei).
- High-energy Projectile fragmentation / projectile fission at e.g., GSI, RIKEN, GANIL, MSU, makes all types of nuclei.
- Coulomb excitation, EM excitations via E2 (usually).
- Single particle transfer reactions (p,d)
- Radioactivity, β decay ; α decay ; proton radioactivity
- Other probes (e,e'γ), (γ,γ'), (n,γ), (p,γ), (n,n'γ) etc.

First four generally populate <u>'near-yrast'</u> states
– most useful to see 'higher' spins states and excitations.

Heavy-ion induced nuclear reactions on fixed targets can result in a range of different nuclear reactions taking place.

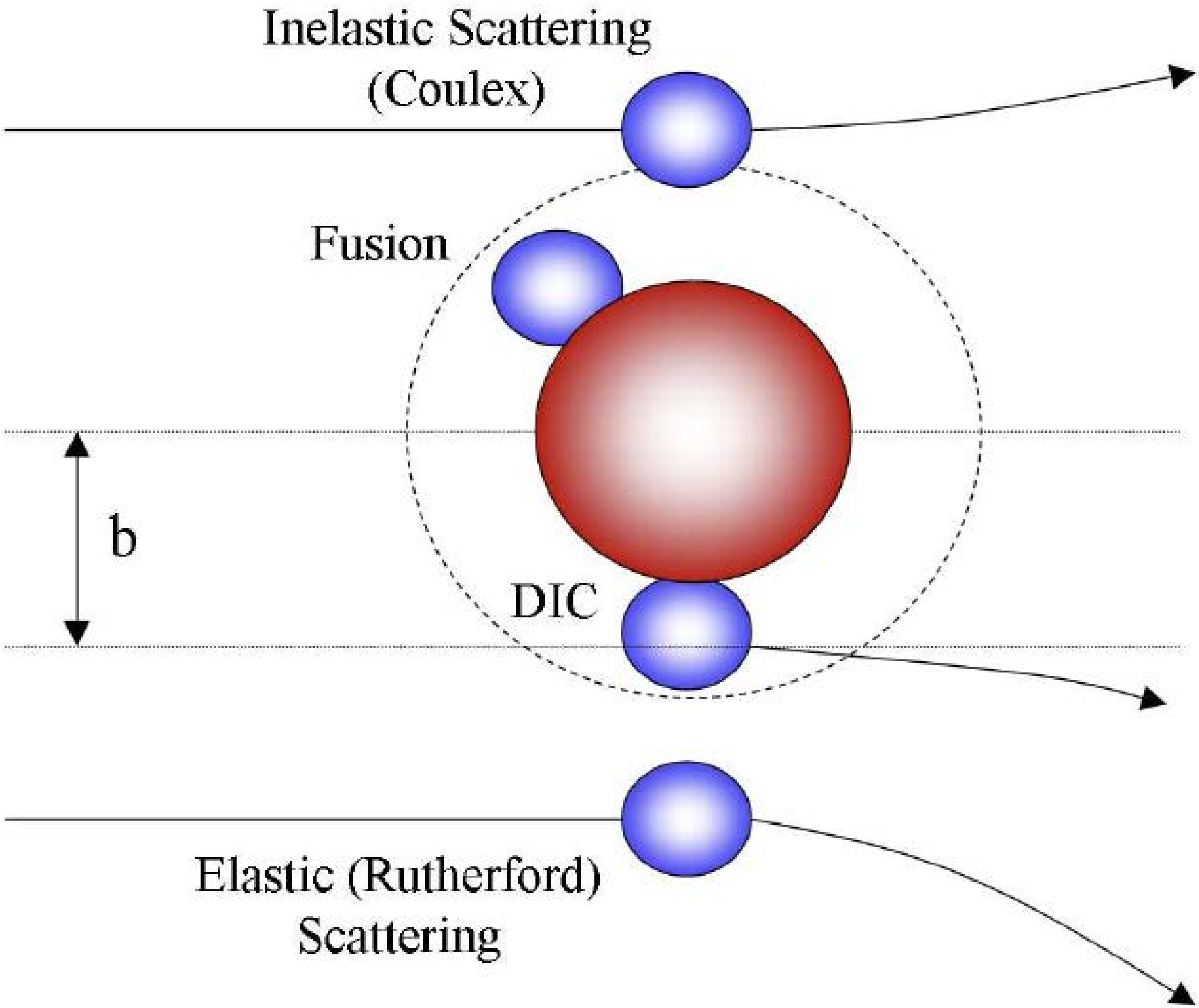

The specifics depends on the (1) beam and target nuclei (A,Z,I);
(2) the beam energy (higher or lower than the Coulomb repulsion between the two nuclei), and (3) the impact parameter, b.

Selection and identification of high-spins states.

- Need a top quality gamma-ray spectrometer to measure full-energies of emitted gamma rays from (high-spin) excited nuclear states.

- Helpful to have some sort of channel selection device (e.g., recoil separator; fragment detector).

- Timing between reaction and detection of gamma ray(s) and also the time differences between individual gamma rays in a decay sequences can also be helpful in channel selection and decay scheme building.

- Use EM selection rules, transition rates and DCO/W(θ) etc. to assign spin and parities to excited states.

$$E^*_R = E_{Beam} + Q_{reaction} - KE_{recoil}$$

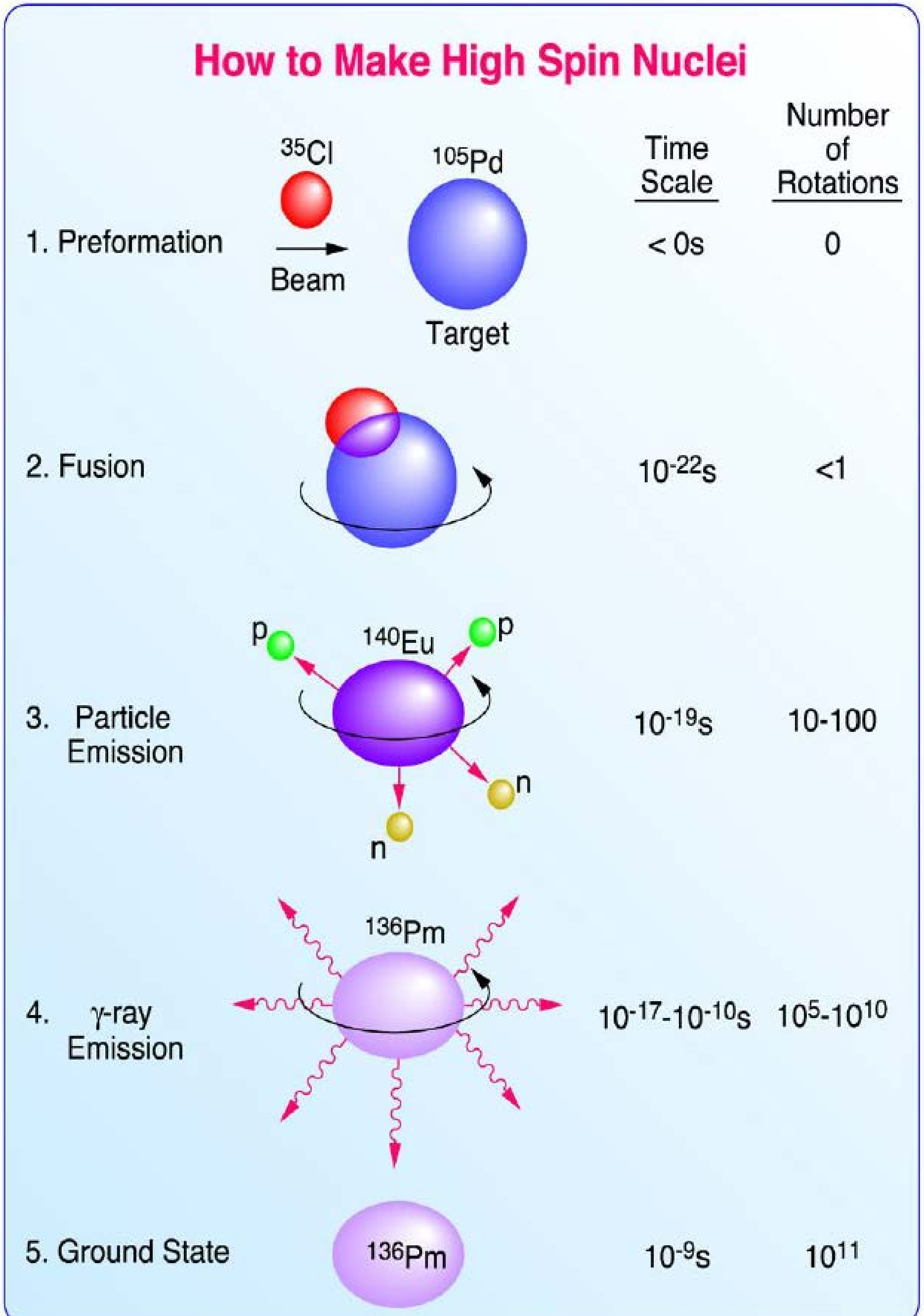

Less particle evaporation corresponds to higher spins states for a particular bombarding energy.

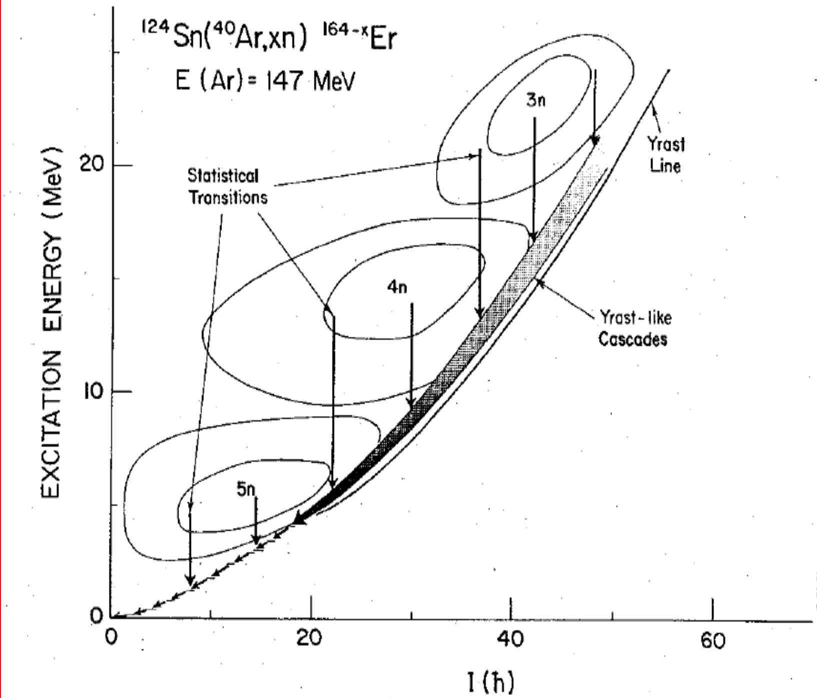

Fusion evaporation reactions fuse heavy-ion beams of stable nuclei onto stationary, metallic foils of other stable nuclei.

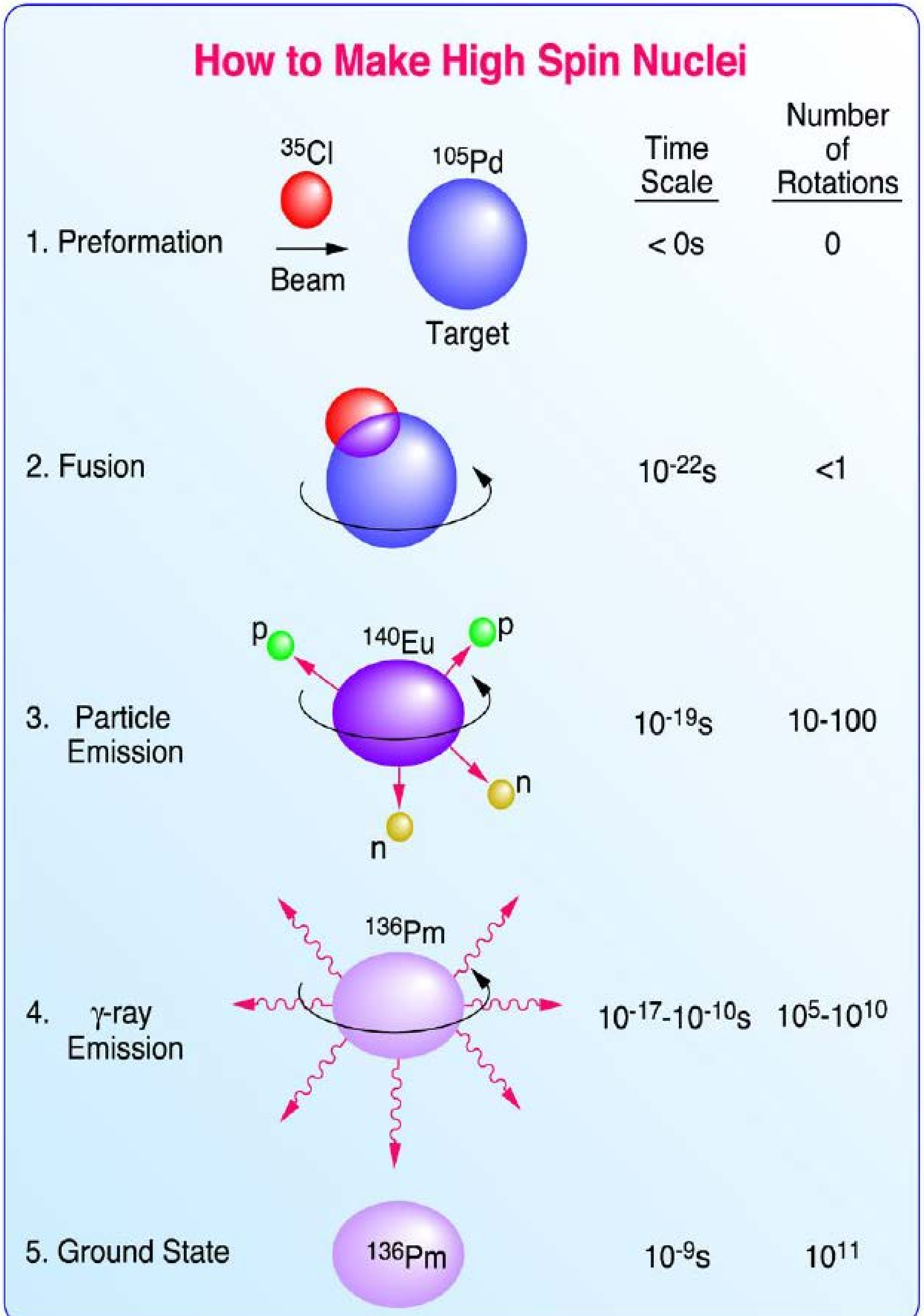

$$E^*_R = E_{Beam} + Q_{reaction} - KE_{recoil}$$

Less particle evaporation corresponds to higher spins states for a particular bombarding energy.

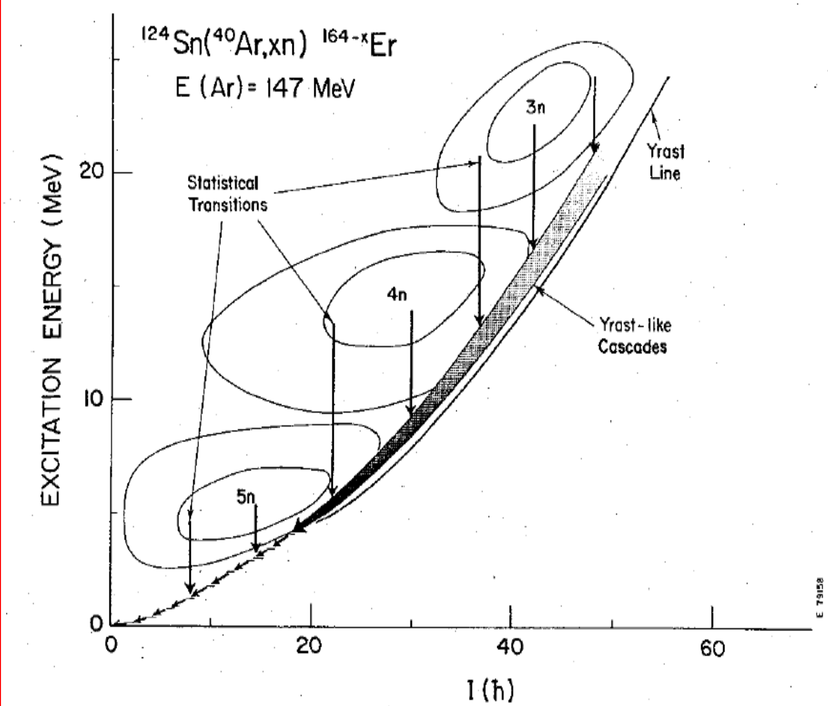

Maximum angular momentum input to compound system (l_{max}) depends on

$\underline{\mathbf{l}} = \underline{\mathbf{r}} \times \underline{\mathbf{p}}$

i.e. beam energy (linked to **p**) and maximum overlap of nuclear radii (**r**)

Example: $^{96}Ru(^{40}Ca,xpyn)^{136}Gd$-xp-yn

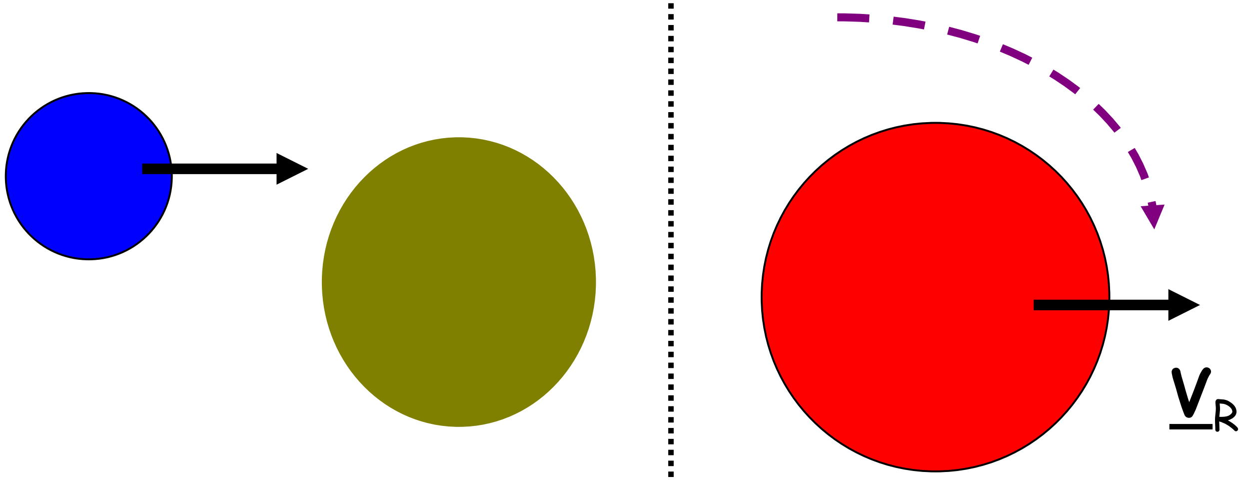

^{40}Ca
Z=20
N=20

^{96}Ru
Z=44
N=52

^{136}Gd (Z=64 N=72).

Hot, compound system recoils backwards at 0^{o} in the lab frame.

Example: $^{96}Ru(^{40}Ca,xpyn)^{136}Gd$-xp-yn

$m_B\underline{\mathbf{V}}_B$

$m_T\underline{\mathbf{V}}_T=0$

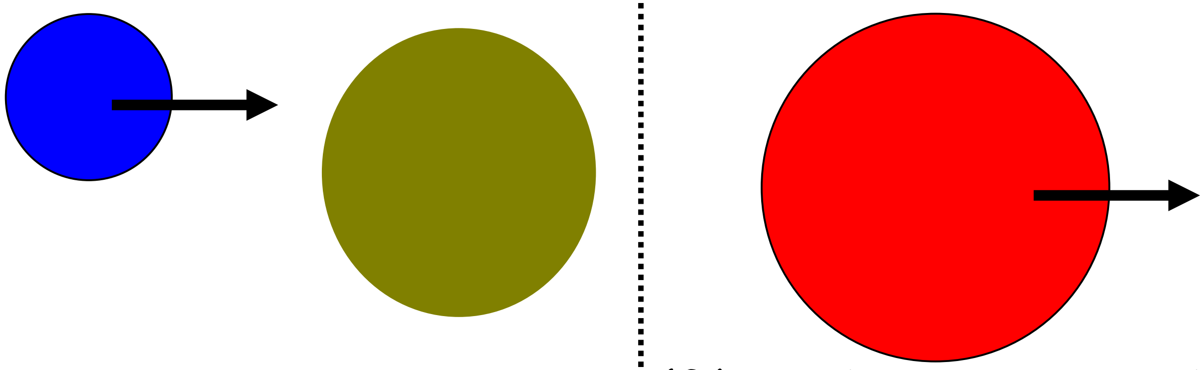

^{40}Ca
Z=20
N=20

^{96}Ru
Z=44
N=52

KE of beam = $\frac{1}{2}\, m_B V_B^{\,2}$

^{136}Gd (Z=64 N=72).
Hot, compound nucleus recoils backwards at 0^o in the lab frame with velocity, $\underline{\mathbf{V}}_R$.

Example: $^{96}Ru(^{40}Ca,xpyn)^{136}Gd$-xp-yn

$m_B\underline{\mathbf{V}}_B$

$m_T\underline{\mathbf{V}}_T=0$

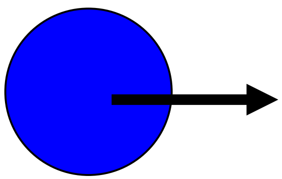

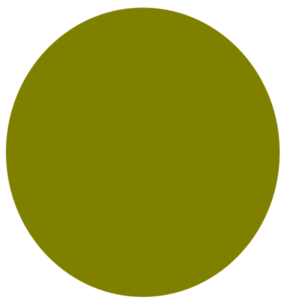

^{40}Ca
Z=20
N=20

^{96}Ru
Z=44
N=52

KE of beam = $\frac{1}{2}\, m_B V_B^2$

$m_R\underline{\mathbf{V}}_R = (m_B+m_T)\underline{\mathbf{V}}_R = m_B\underline{\mathbf{V}}_B$. Therefore,

$\underline{\mathbf{V}}_R=(m_B)\underline{\mathbf{V}}_B/(m_B+m_T)$

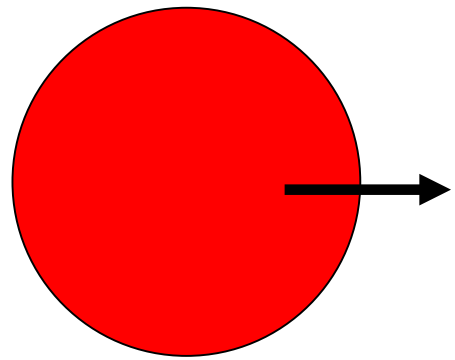

$\underline{\mathbf{V}}_R$

^{136}Gd (Z=64 N=72).
Hot, compound nucleus recoils backwards at 0° in the lab frame with velocity, $\underline{\mathbf{V}}_R$.

Example: $^{96}Ru(^{40}Ca,xpyn)^{136}Gd$-xp-yn

$m_B \underline{\mathbf{V}}_B$

$m_T \underline{\mathbf{V}}_T = 0$

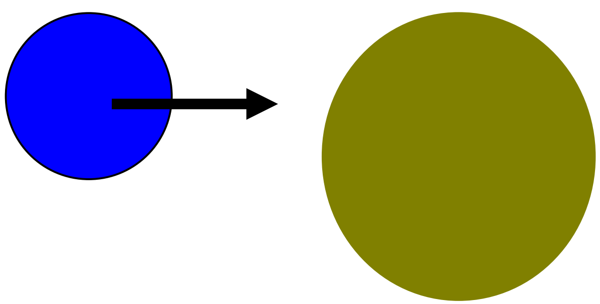

^{40}Ca
Z=20
N=20

^{96}Ru
Z=44
N=52

KE of beam = $\frac{1}{2} m_B V_B^2$

$m_R \underline{\mathbf{V}}_R = (m_B + m_T)\underline{\mathbf{V}}_R = m_B \underline{\mathbf{V}}_B$. Therefore,

$\underline{\mathbf{V}}_R = (m_B)\underline{\mathbf{V}}_B / (m_B + m_T)$

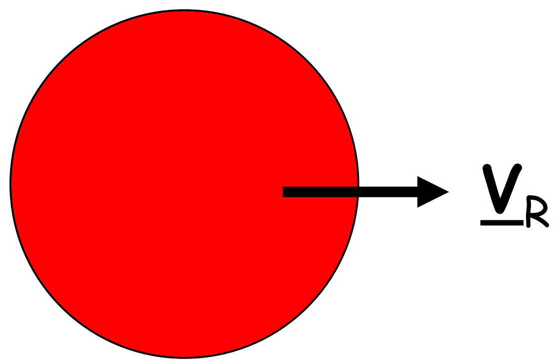

^{136}Gd (Z=64 N=72).
Hot, compound nucleus recoils backwards at 0° in the lab frame with velocity, v_R.

KE of recoiling nucleus $= \frac{1}{2}(M_B + M_T)V^2_R$

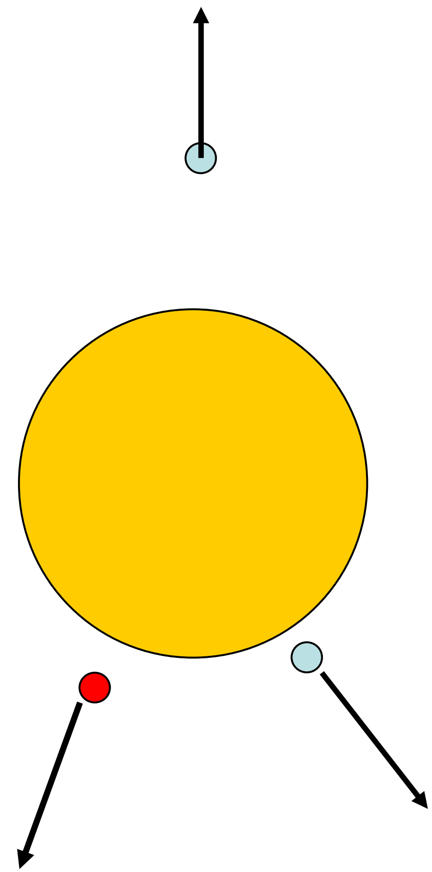

Light particles p,n,α evaporated.
Sn,Sp ~ 1-15 MeV.

Example: $^{96}Ru(^{40}Ca,xpyn)^{136}Gd$-xp-yn

$m_B\underline{\mathbf{V}}_B$

$m_T\underline{\mathbf{V}}_T=0$

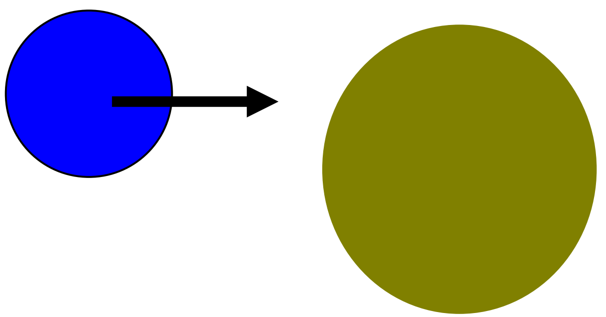

^{40}Ca
Z=20
N=20

^{96}Ru
Z=44
N=52

KE of beam = $\frac{1}{2}\, m_B v_B^2$

$m_R\underline{\mathbf{V}}_R = (m_B+m_T)\underline{\mathbf{V}}_R = m_B\underline{\mathbf{V}}_B$. Therefore,
$\underline{\mathbf{V}}_R=(m_B)\underline{\mathbf{V}}_B/(m_B+m_T)$

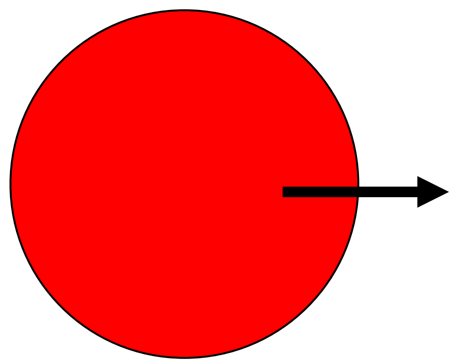

^{136}Gd (Z=64 N=72).
Hot, compound nucleus recoils backwards at 0° in the lab frame with velocity, v_R.
KE of recoiling nucleis = $\frac{1}{2}\,(M_B+M_T)V^2_R$

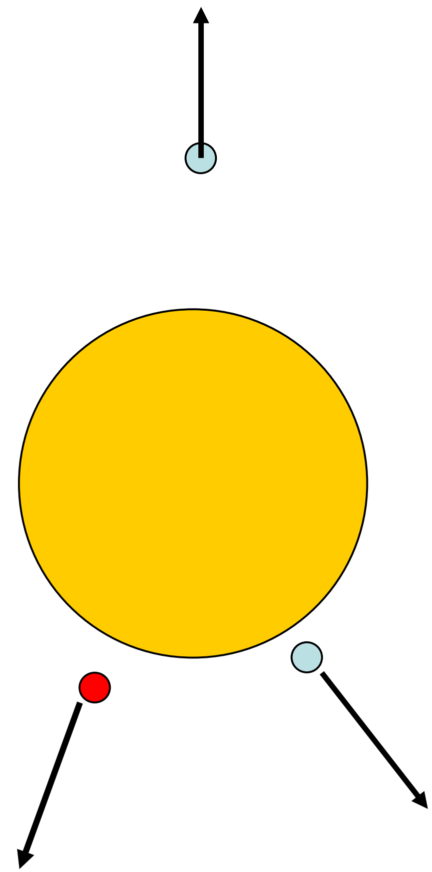

$^{136}Gd+3p = {}^{133}Pm$
$^{136}Gd+2pn={}^{133}Sm$
$^{136}Gd+3pn={}^{134}Pm$
$^{136}Gd+2p2n={}^{132}Sm$

Production of High-Spin States

$$E_{ex} = E_{cm} + Q_{fus} \tag{2.1.1}$$

E_{cm} is the kinetic energy of the collision which is transfered to the compound system. It can be calculated by taking the kinetic energy of the beam, E_B and subtracting the kinetic energy of the recoiling compound system, E_R. Thus

$$E_{cm} = E_B - E_R \tag{2.1.2}$$

By conservation of momentum, for beam and target masses of M_B and M_T respectively, the velocity of the recoiling compound, V_R can be calculated using

$$M_B V_B = (M_T + M_B)\, V_R \tag{2.1.3}$$

and by conservation of energy,

$$E_{cm} = E_B - \frac{1}{2}(M_T + M_B)\, V_R^2 \tag{2.1.4}$$

substituting in for V_R, and recalling that $E_B = \frac{1}{2} M_B V_B^2$, we obtain

$$E_{cm} = E_B \left(1 - \frac{M_B}{M_T + M_B}\right) \tag{2.1.5}$$

Example: $^{96}Ru(^{40}Ca,xpyn)^{136}Gd$-xp-yn

$m_B\underline{\mathbf{V}}_B$

$m_T\underline{\mathbf{V}}_T=0$

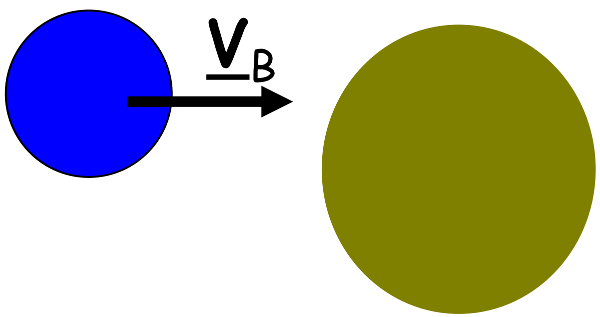

^{40}Ca
Z=20
N=20

^{96}Ru
Z=44
N=52

KE of beam = $\frac{1}{2}\, m_B v_B{}^2$

$m_R\underline{\mathbf{V}}_R = (m_B+m_T)\underline{\mathbf{V}}_R = m_B\underline{\mathbf{V}}_B$. Therefore,
$\underline{\mathbf{V}}_R=(m_B)\underline{\mathbf{V}}_B/(m_B+m_T)$

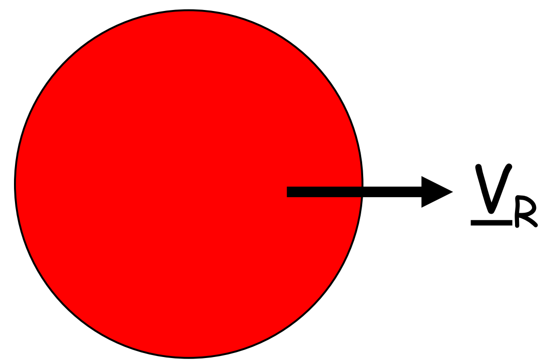

^{136}Gd (Z=64 N=72).
Hot, compound nucleus recoils backwards at 0° in the lab frame with velocity, $\underline{\mathbf{V}}_R$.
KE of recoiling nucleis
$= \frac{1}{2}\,(M_B+M_T)V^2{}_R$

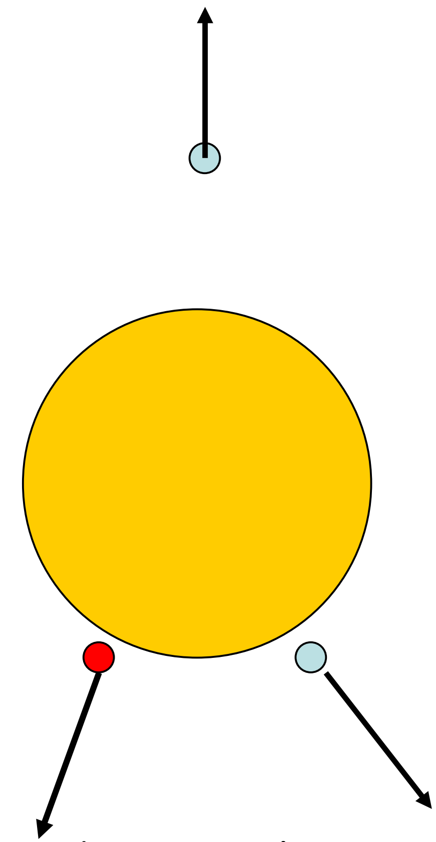

Light particle emission causes small recoil cone in lab frame due to cons. of linear momentum.

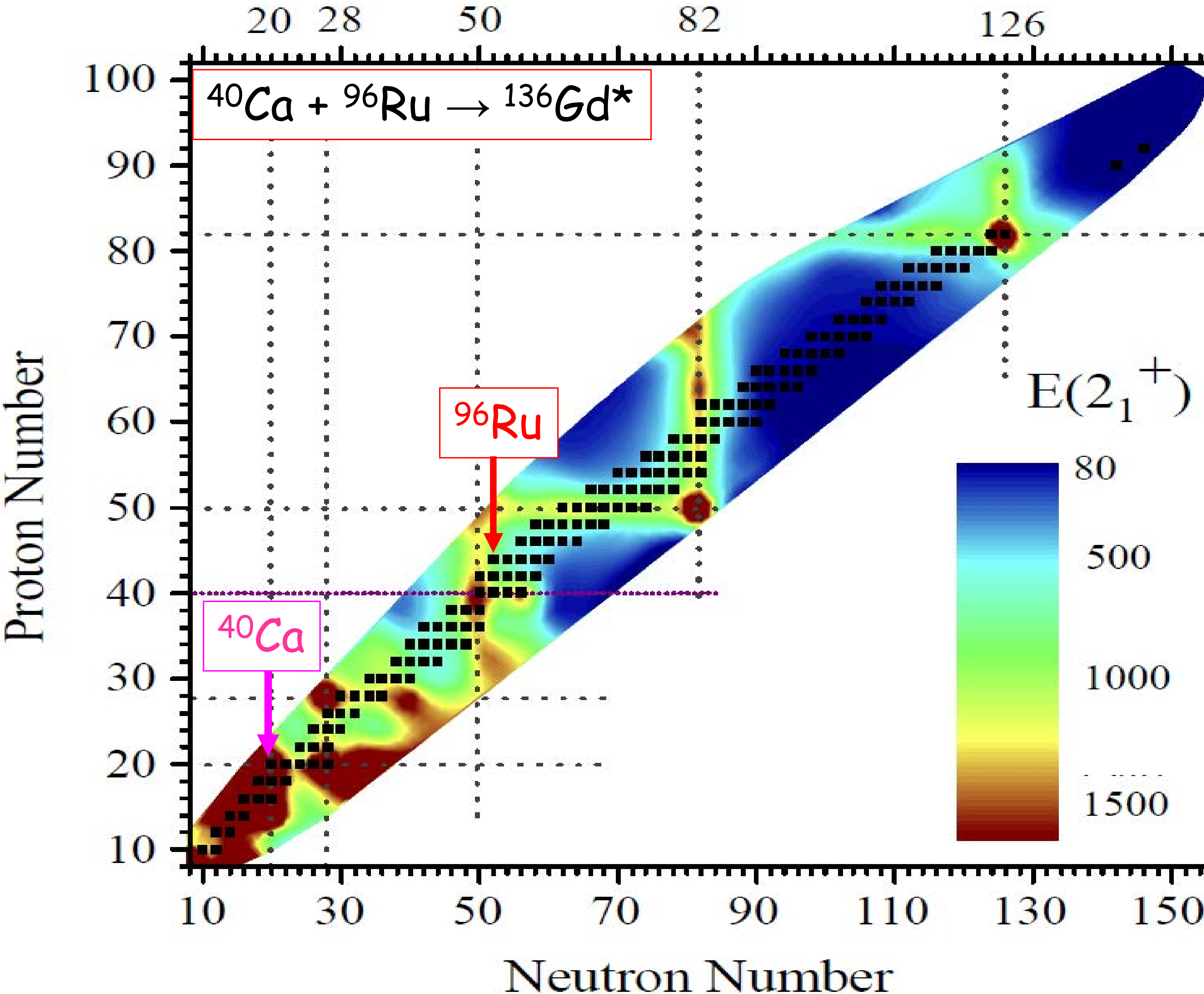

$^{40}Ca + ^{96}Ru \rightarrow ^{136}Gd^*$
^{96}Ru
^{40}Ca
$E(2_1^+)$
80
500
1000
1500
20 28 50 82 126
Proton Number
Neutron Number

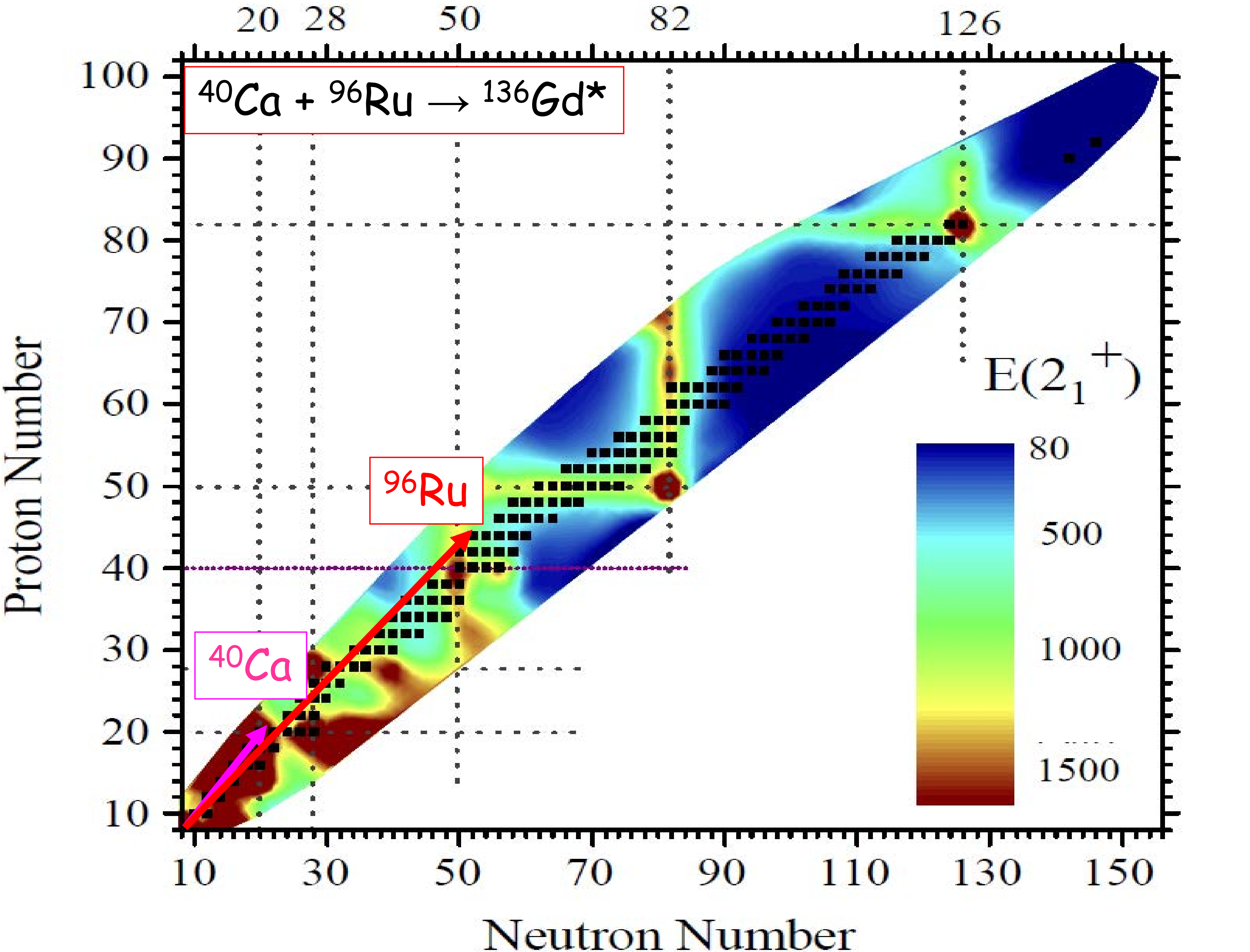

^{40}Ca + ^{96}Ru → ^{136}Gd*
^{96}Ru
^{40}Ca
E(2$_1^+$)
80
500
1000
1500
20 28 50 82 126
Proton Number
Neutron Number

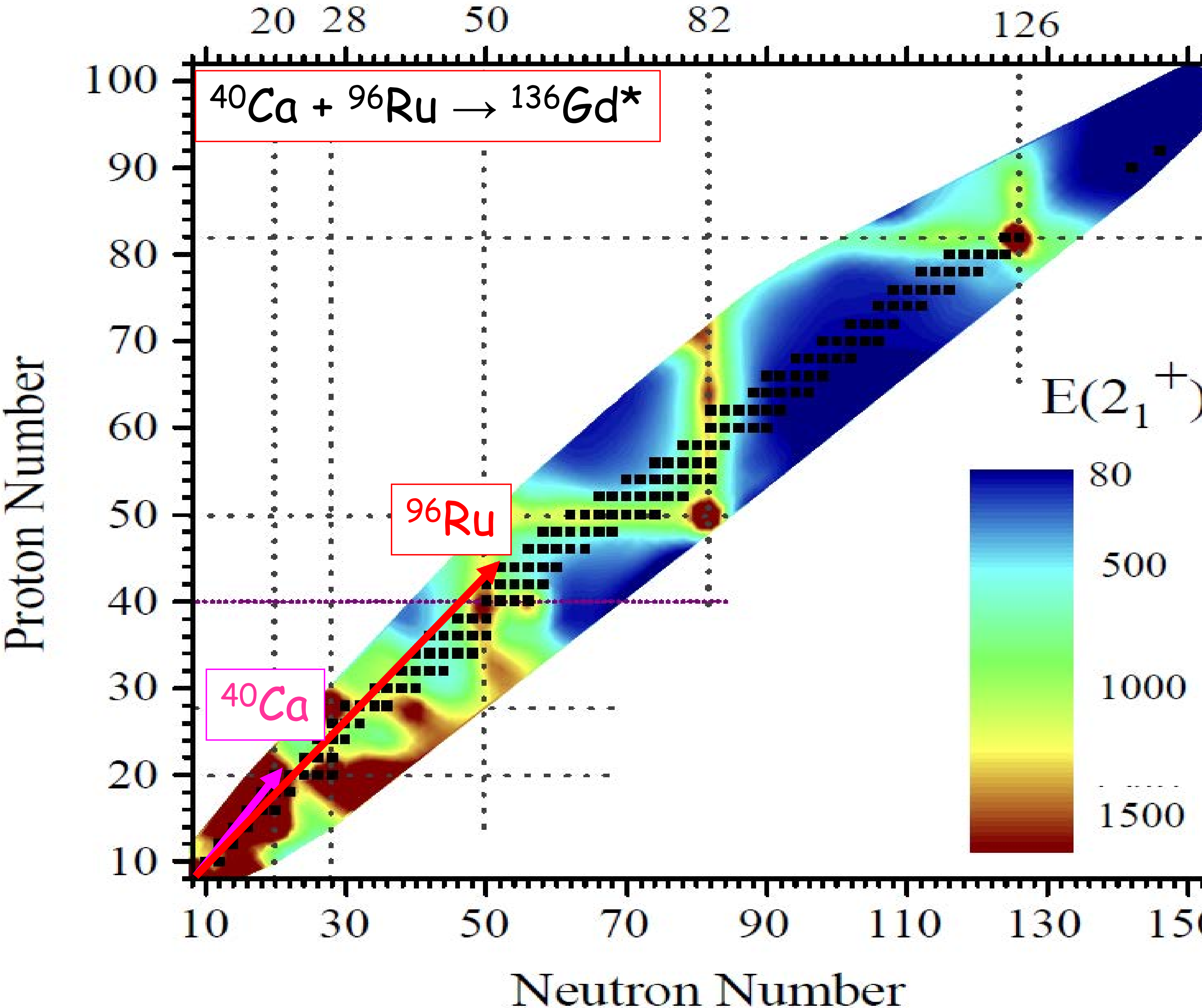

40Ca + 96Ru → 136Gd*
96Ru
40Ca
E(2₁⁺)
80
500
1000
1500
20 28 50 82 126
Proton Number
Neutron Number

$^{40}Ca + ^{96}Ru \rightarrow ^{136}Gd^*$
Heavy-ion fusion-evaporation reactions usually make neutron deficient compound nuclei.

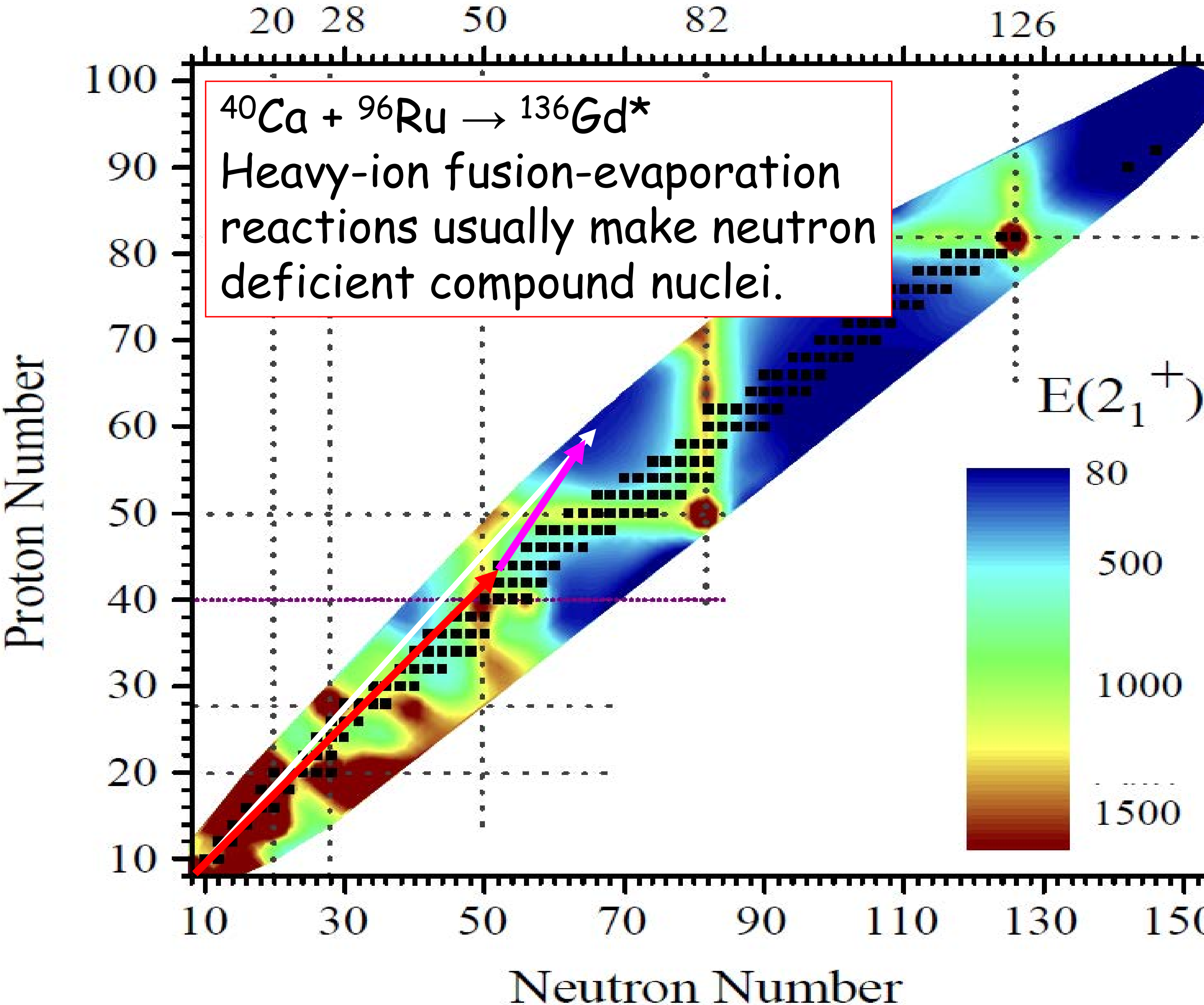

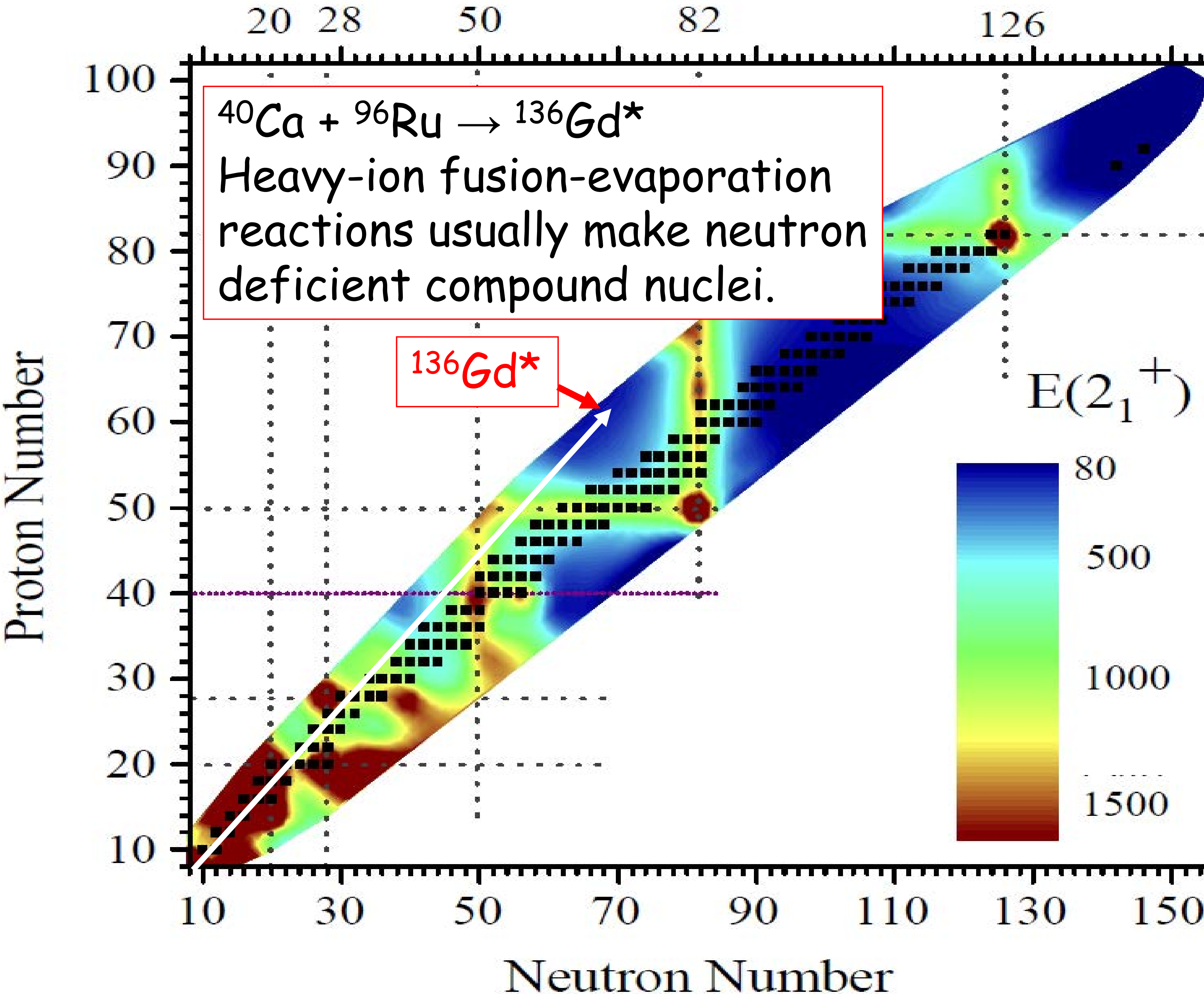
$^{40}Ca + ^{96}Ru \rightarrow ^{136}Gd^*$
Heavy-ion fusion-evaporation reactions usually make neutron deficient compound nuclei.
$^{136}Gd^*$
$E(2_1^+)$
80
500
1000
1500
20
28
50
82
126
Proton Number
Neutron Number
10
30
50
70
90
110
130
150
10
20
30
40
50
60
70
80
90
100

Do you evaporate protons or neutrons?

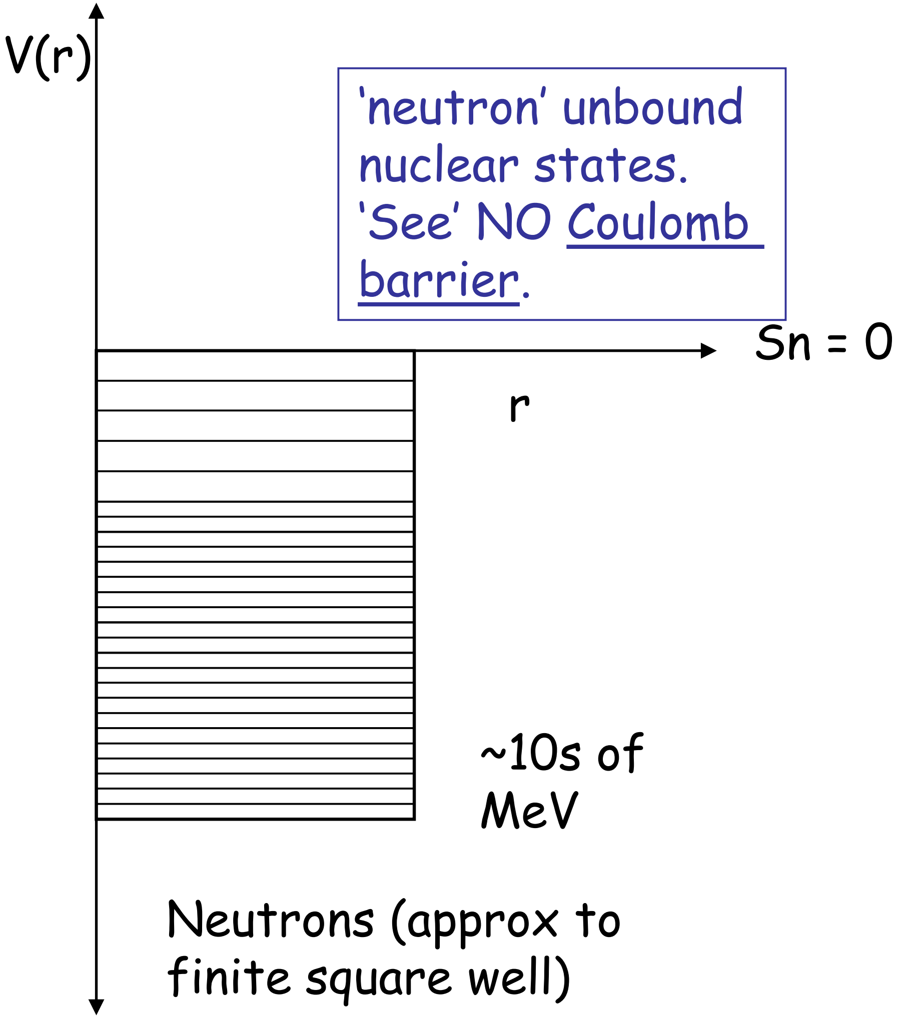

Do you evaporate protons or neutrons?

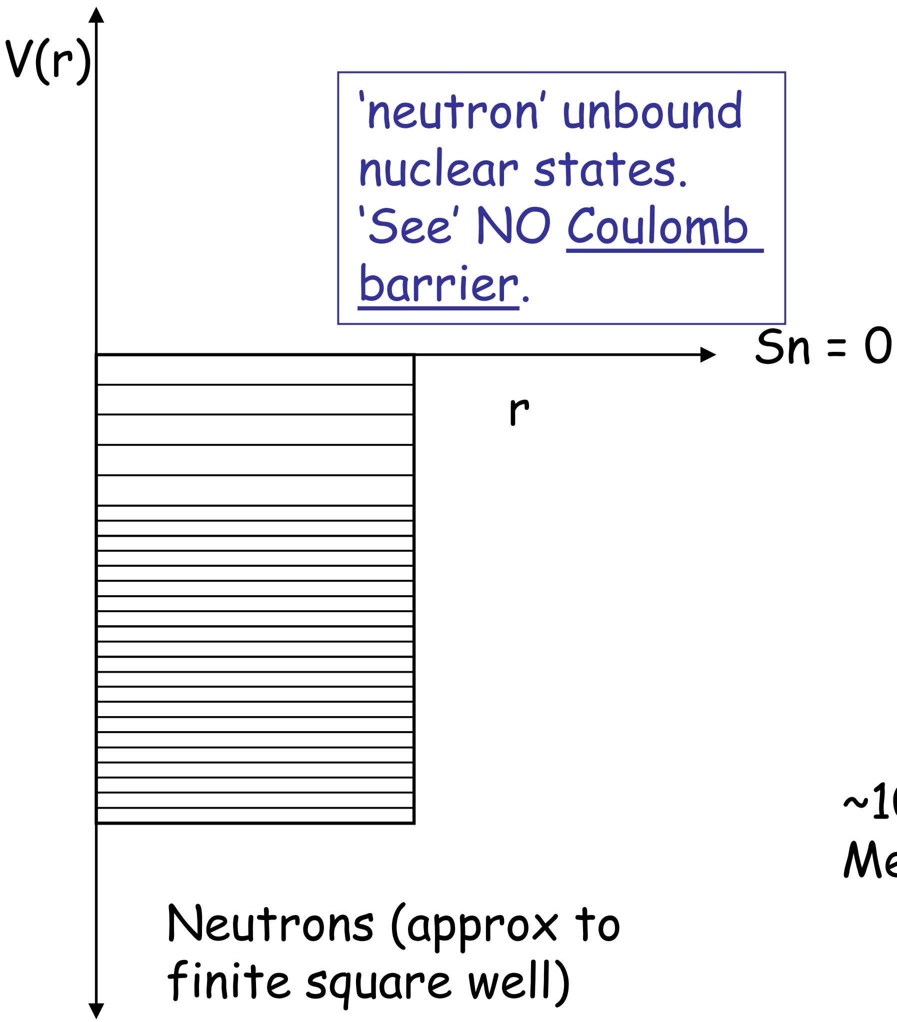

Neutrons (approx to finite square well)

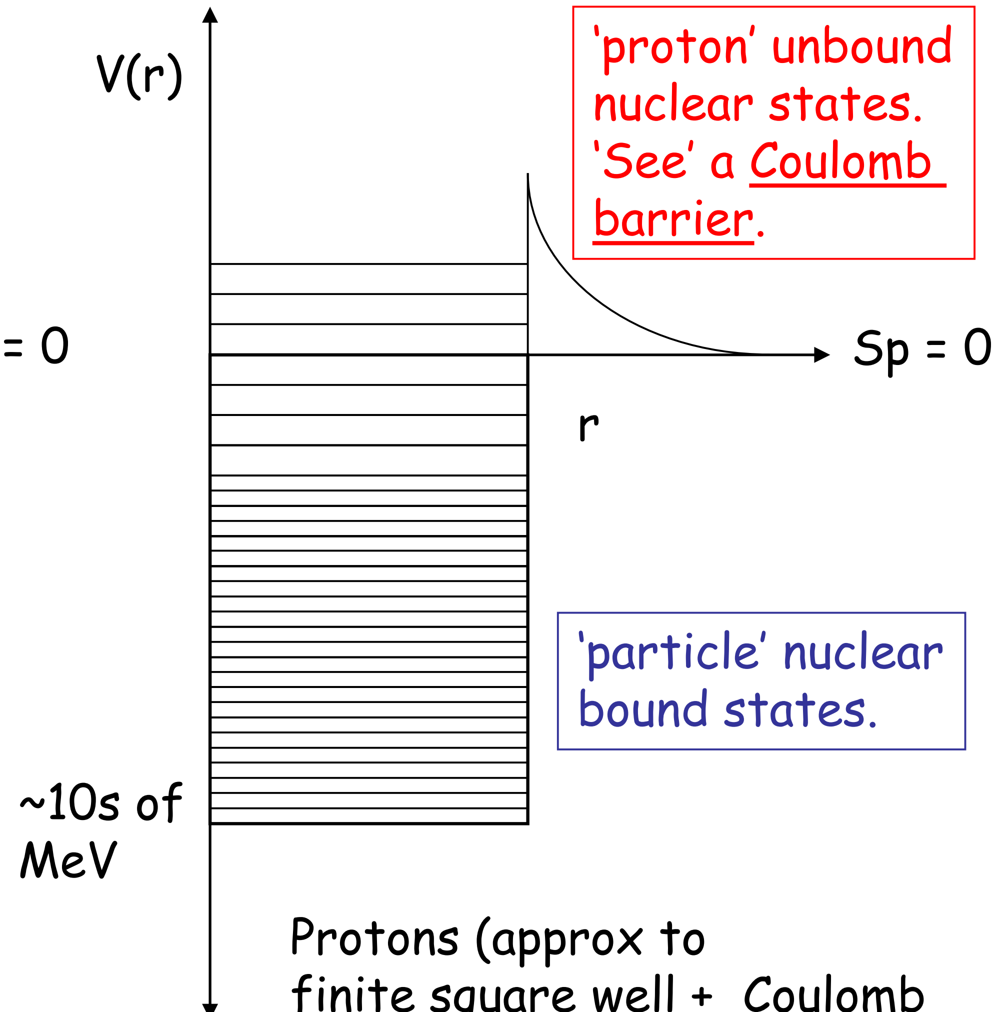

Protons (approx to finite square well + Coulomb Barrier above Sp=0)

Near stable (compound) nuclei, Sp ~ Sn ~ 5-8 MeV.

Coulomb barrier means (HI,xn) favoured over (HI,xp)

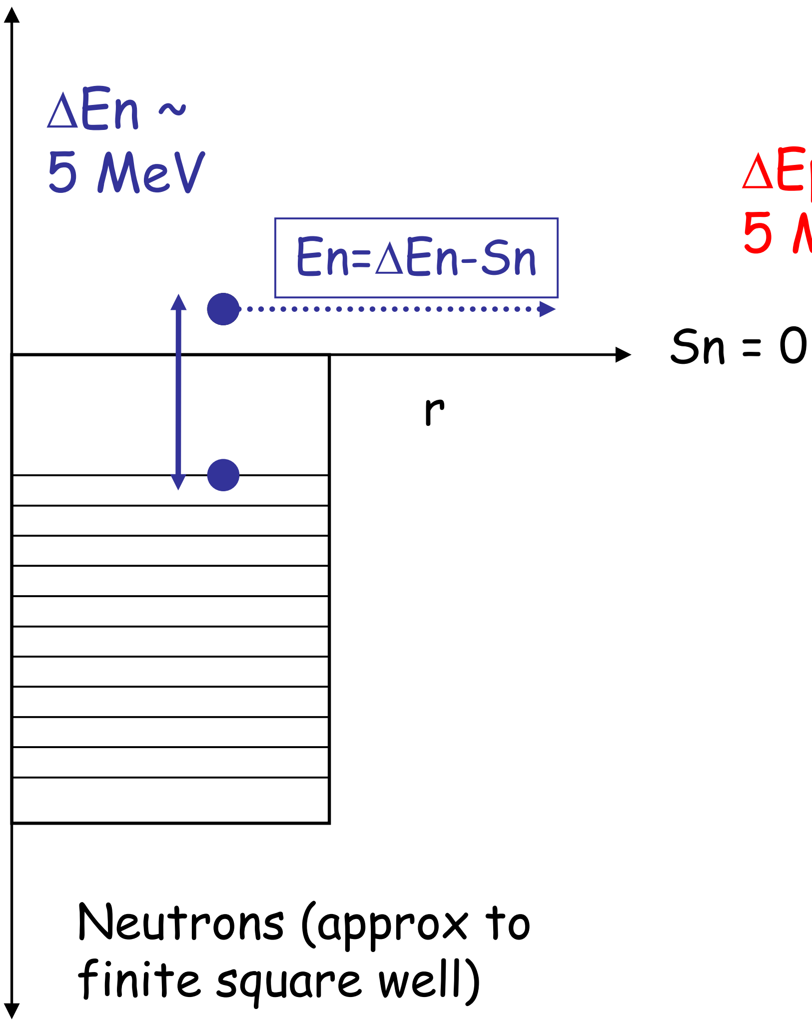

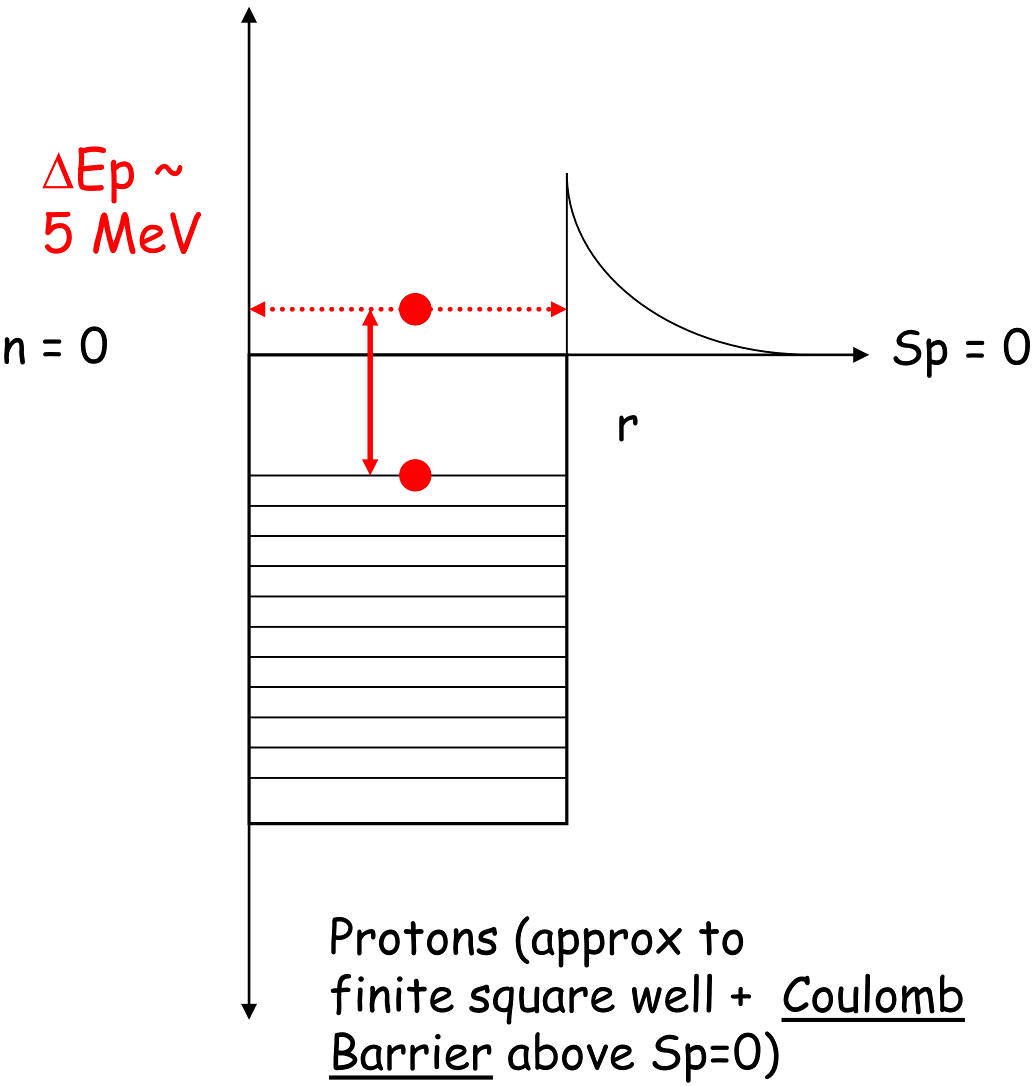

Angular Momentum Input in HIFE Reactions?

$$\hbar l_{max} = \mu v R$$

Reduced mass of system,

$\mu = m_b.m_T / (m_B+m_T)$

$$\frac{1}{2}\mu v^2 = E_{cm} - V_c$$

$$l_{max}^2 = \frac{2\mu R^2}{\hbar^2}(E_{cm} - V_c)$$

$^{98}Mo + ^{12}C \rightarrow ^{110}Cd$ fusion evaporation calculations using PACE4 S.F. Ashley, PhD thesis, University of Surrey (2007)

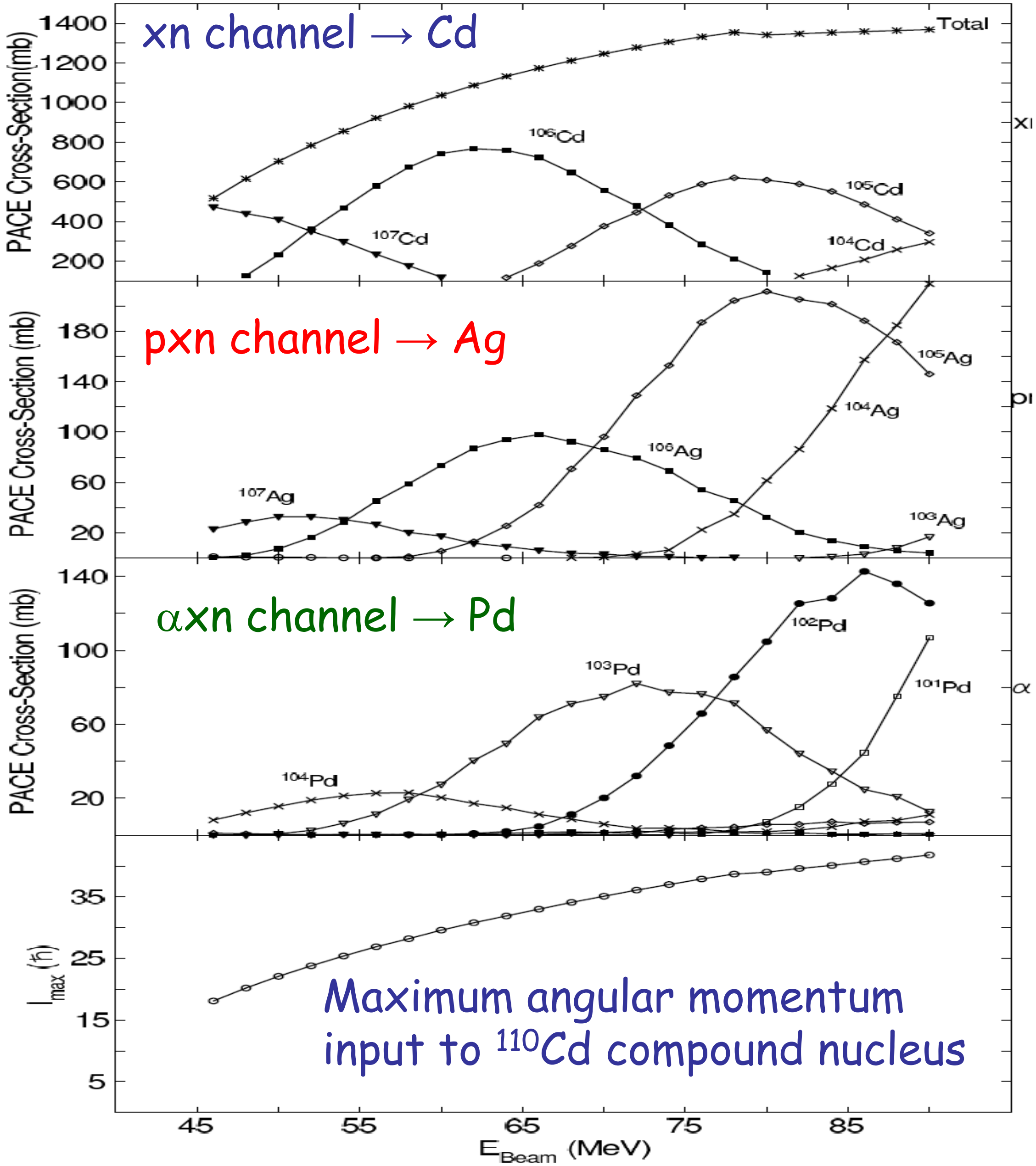

Increasing the beam energy increases the maximum input angular momentum,

but

Causes more nucleons to be evaporated (on average).

Also, increasing the beam energy increases the recoil velocity.

For the ^{110}Cd compound nucleus:
S_n = 9.9 MeV
S_p = 8.9 MeV

Coulomb barrier means neutron evaporation is much favoured.

Very neutron-deficient (compound) nuclei, e.g. ^{136}Gd, S_p= 2.15 MeV, S_n=12.94 MeV

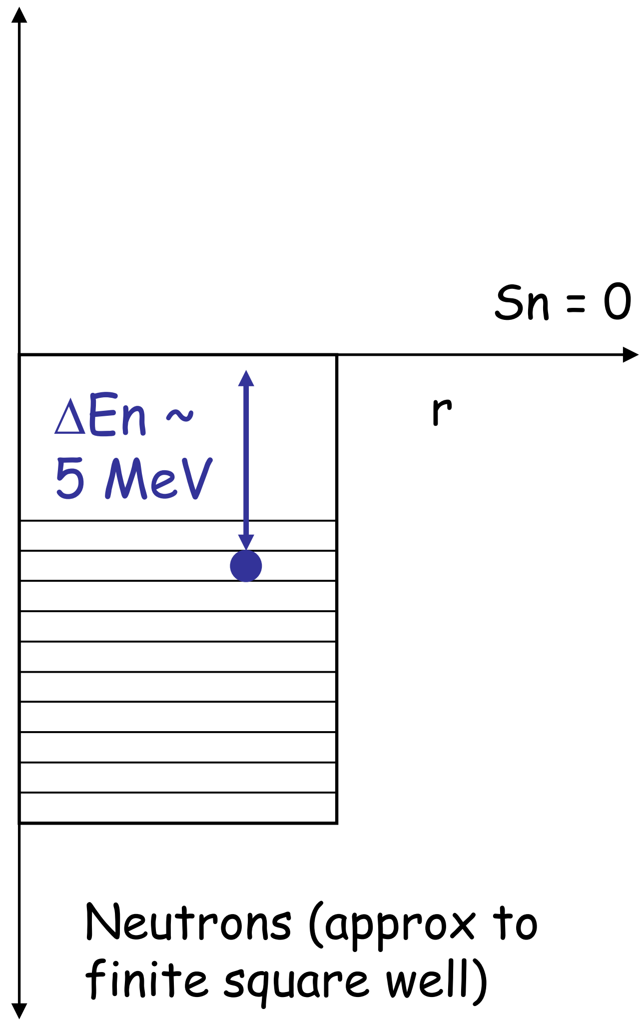

Neutrons (approx to finite square well)

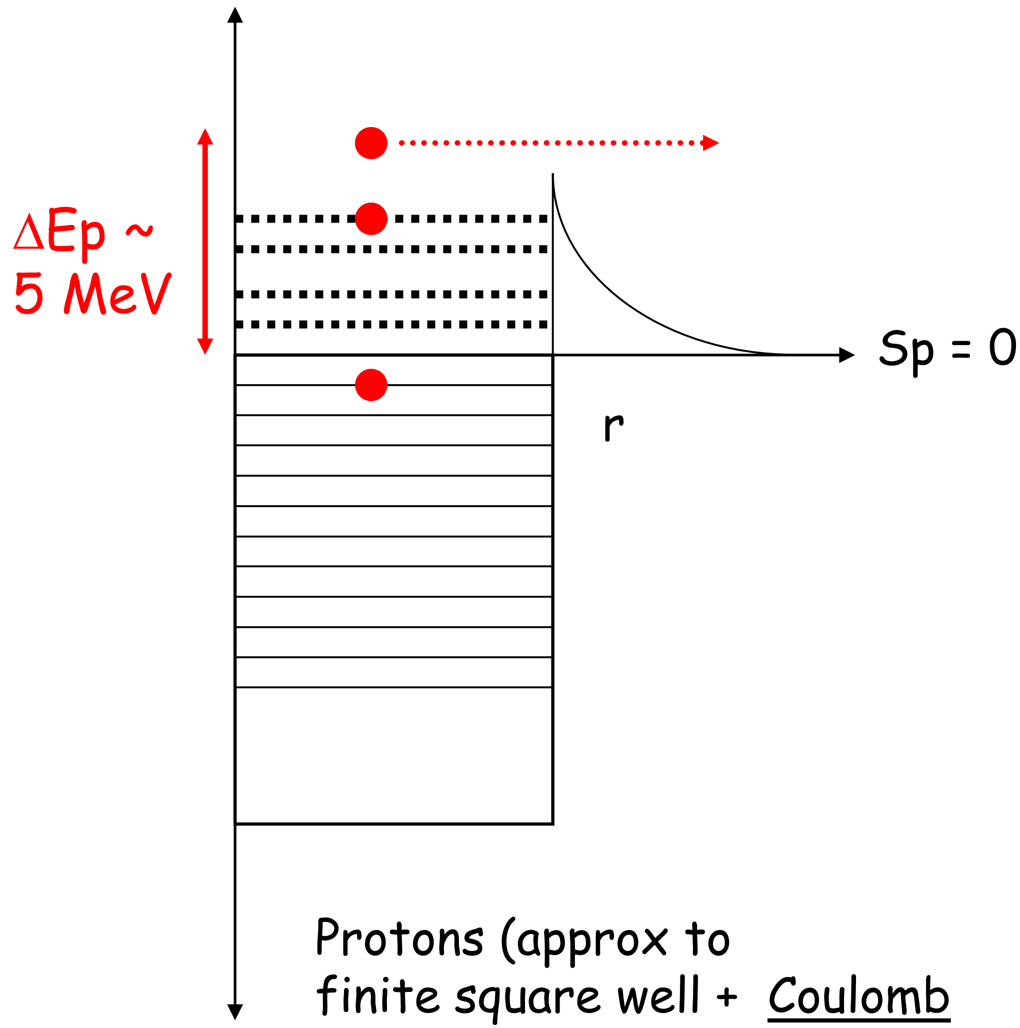

Protons (approx to finite square well + Coulomb Barrier above Sp=0)

Excitation Functions?

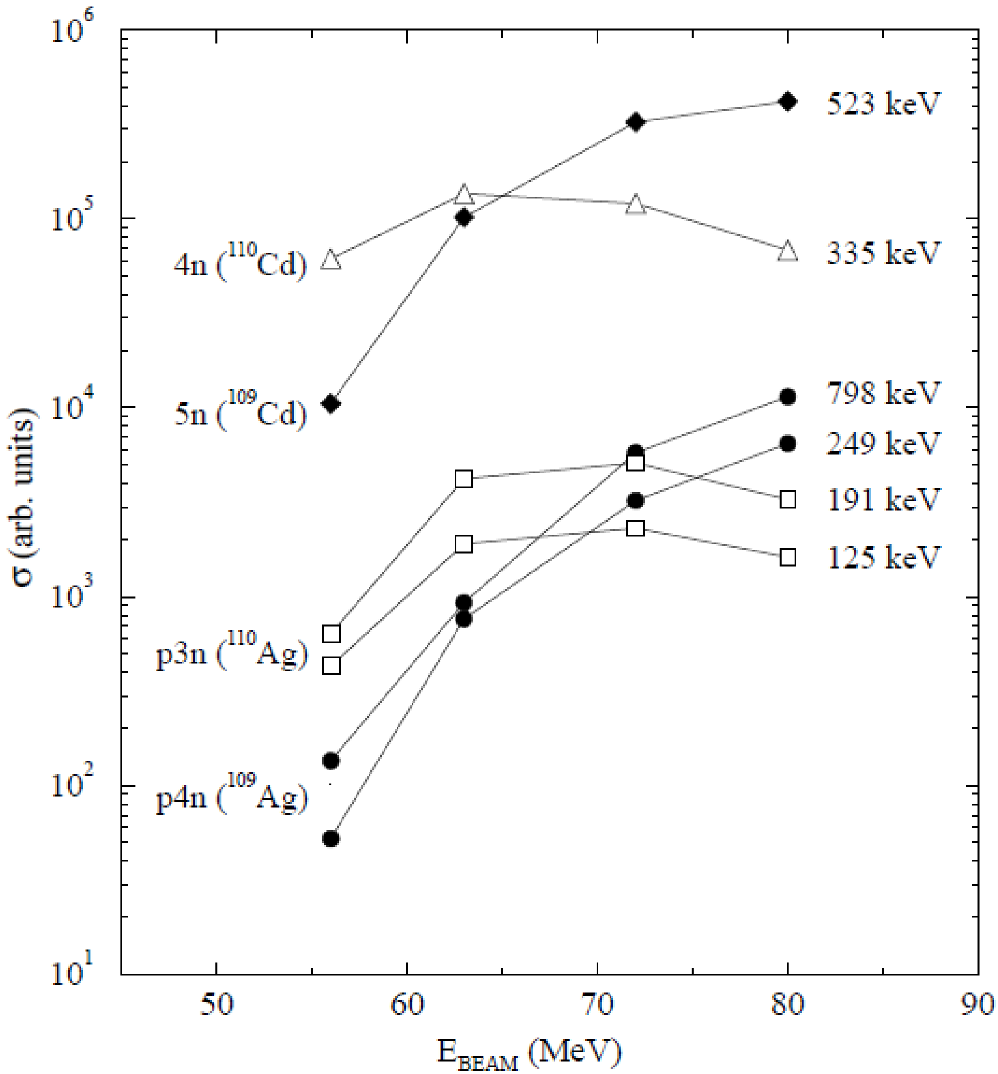

Excitation function for various products of the reaction $^{18}O+^{96}Zr$

P.H. Regan et al., Phys. Rev. **C49** (1994) 1885

Doppler Shifts

Moving source – nucleus which emits gamma-ray ;
Stationary observer - Ge detector.

$$E_S = E_0 \frac{\sqrt{1-\beta^2}}{1-\beta\cos\theta} \approx E_0(1+\beta\cos\theta)$$

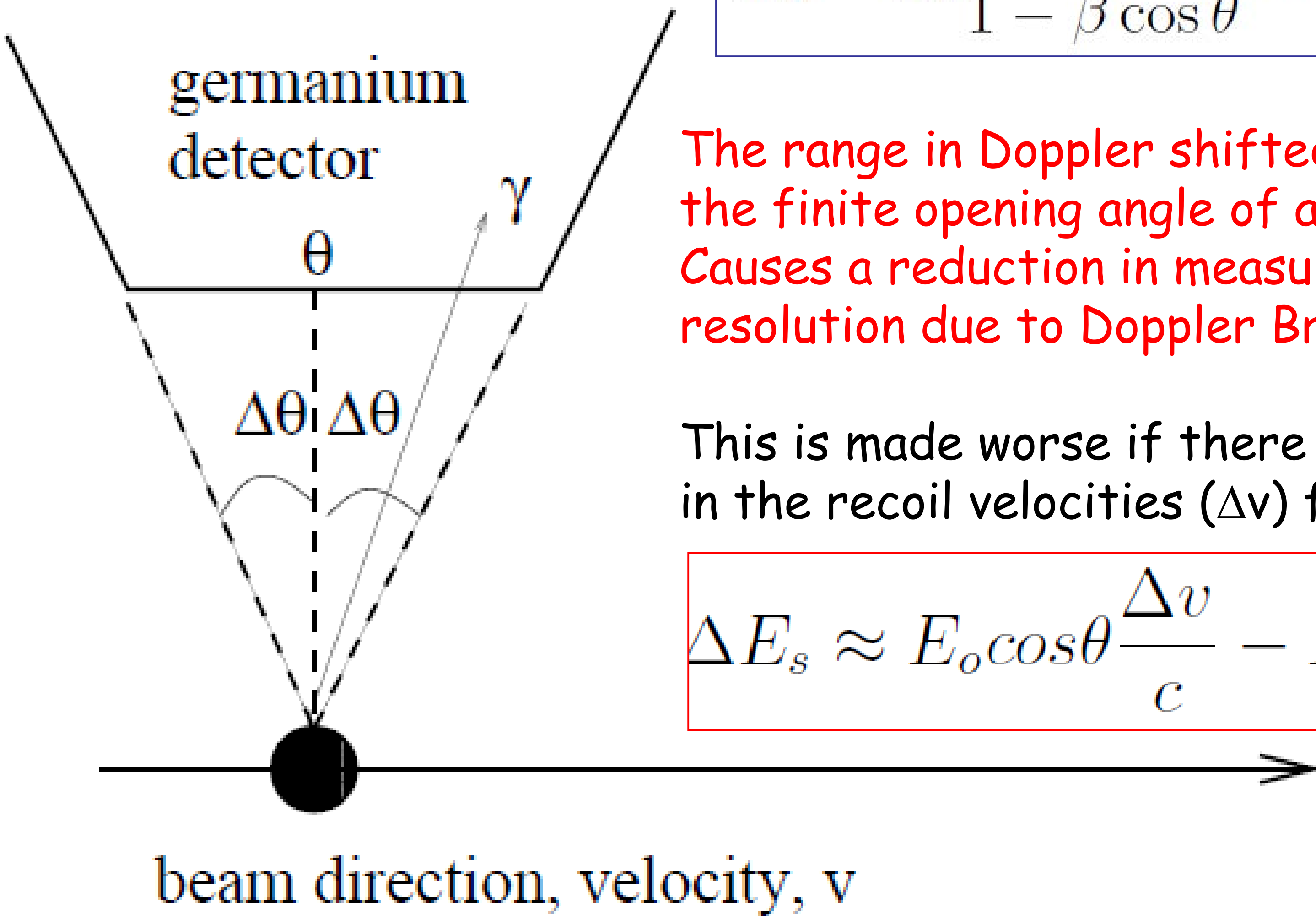

The range in Doppler shifted energy across the finite opening angle of a detector (Δθ) Causes a reduction in measured energy resolution due to Doppler Broadening.

This is made worse if there is also a spread in the recoil velocities (Δv) for the recoils.

$$\Delta E_s \approx E_o cos\theta \frac{\Delta v}{c} - E_o \frac{v}{c} sin\theta \Delta\theta$$

Experimental channel selection in HIFEs?

- Could use gamma-ray gates themselves if some initial discrete energies are established. γ–γ($-\gamma$) coincidence method.
- Use coincident timing; beam-pulsing to establish ordering or decay transitions across/below isomers.
- (Fold , sum energy) can be use to select (Spin , E_x) following compound system evaporation.
- Measure coincident evaporated charged particles protons , α etc. (e.g., microball) and/or neutrons (e.g. NEDA) – to select / remove specific evap-channels.
- Use recoil separators (e.g., FMA) to detector fusion products; can be vacuum (like FMA) or gas-filled (e.g. BGS ; RITU).

Recoil (Mass) Separators

Gas Filled

- Pros: High Efficiency
- Cons: No Mass Resolution
- Examples: RITU (Jyvaskyla), BGS (Berkeley)

Vacuum

- Pros: Mass Resolution
- Conn: Low Efficiency
- Examples: FMA (Argonne), RMS (Oak Ridge)

Using Fragment Mass Analyzer (FMA) for High Spin Studies

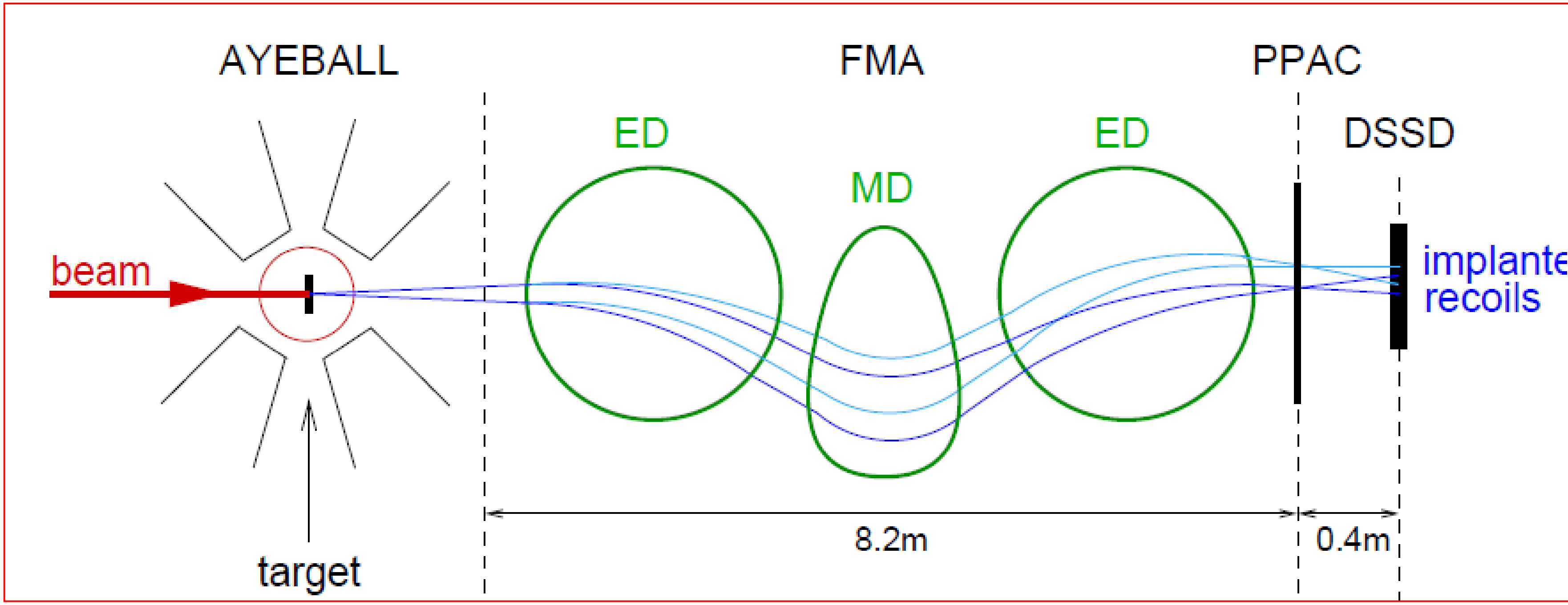

- Separates ions produced at the target position as a function of M/q at the focal plane.
- 8.9 meters long with a +/- 20% energy acceptance.
- Mass resolution is ~ 350:1.
- Multiple detector configurations at focal plane.

PHYSICAL REVIEW C, VOLUME 60, 064308

Near yrast study of the *fpg* shell nuclei ^{58}Ni, ^{61}Cu, and ^{61}Zn

S. M. Vincent,[1,*] P. H. Regan,[1] S. Mohammadi,[1,†] D. Blumenthal,[2] M. Carpenter,[2] C. N. Davids,[2] W. Gelletly,[1] S. S. Ghugre,[3] D. J. Henderson,[2] R. V. F. Janssens,[2] M. Hjorth-Jensen,[4] B. Kharraja,[5] C. J. Lister,[2] C. J. Pearson,[1] D. Seweryniak,[2] J. Schwartz,[2,6] J. Simpson,[7] and D. D. Warner[7]

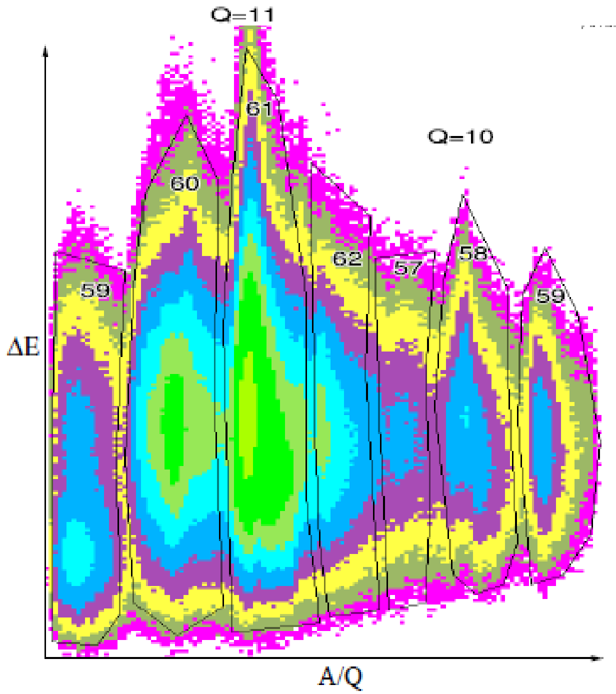

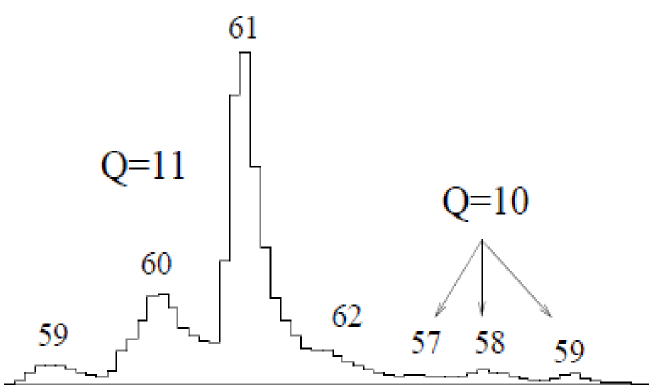

^{24}Mg beam on ^{40}Ca target @65 MeV.

Compound =^{64}Ge
Recoils focussed through Argonne FMA, separated by A/Q.

Observed recoils
2p+^{62}Zn
2pn+^{61}Zn
3p+^{61}Cu
4p+^{60}Ni
3pn+^{60}Cu
α2p+^{58}Ni

and ^{64}Zn ?? (from ^{44}Ca in target).

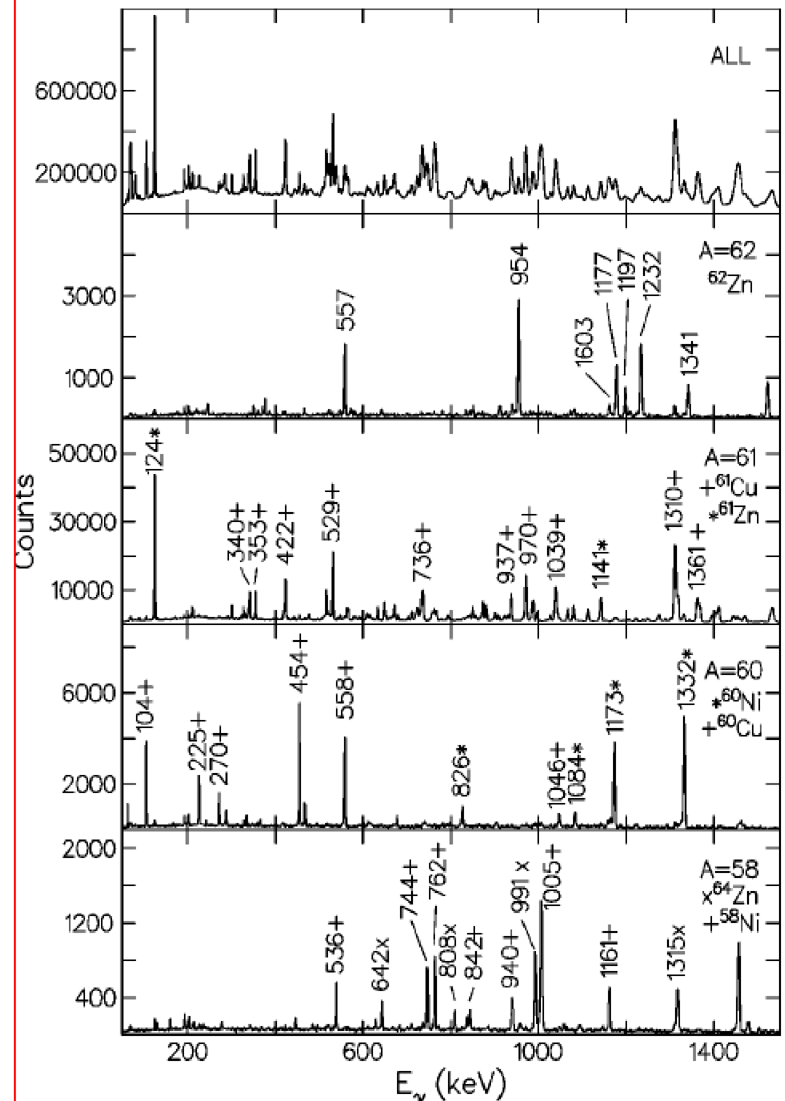

Can be used to select very weak channels (1 part in 10^6 or less);
Good example is SHE studies where most compound nuclei fission.

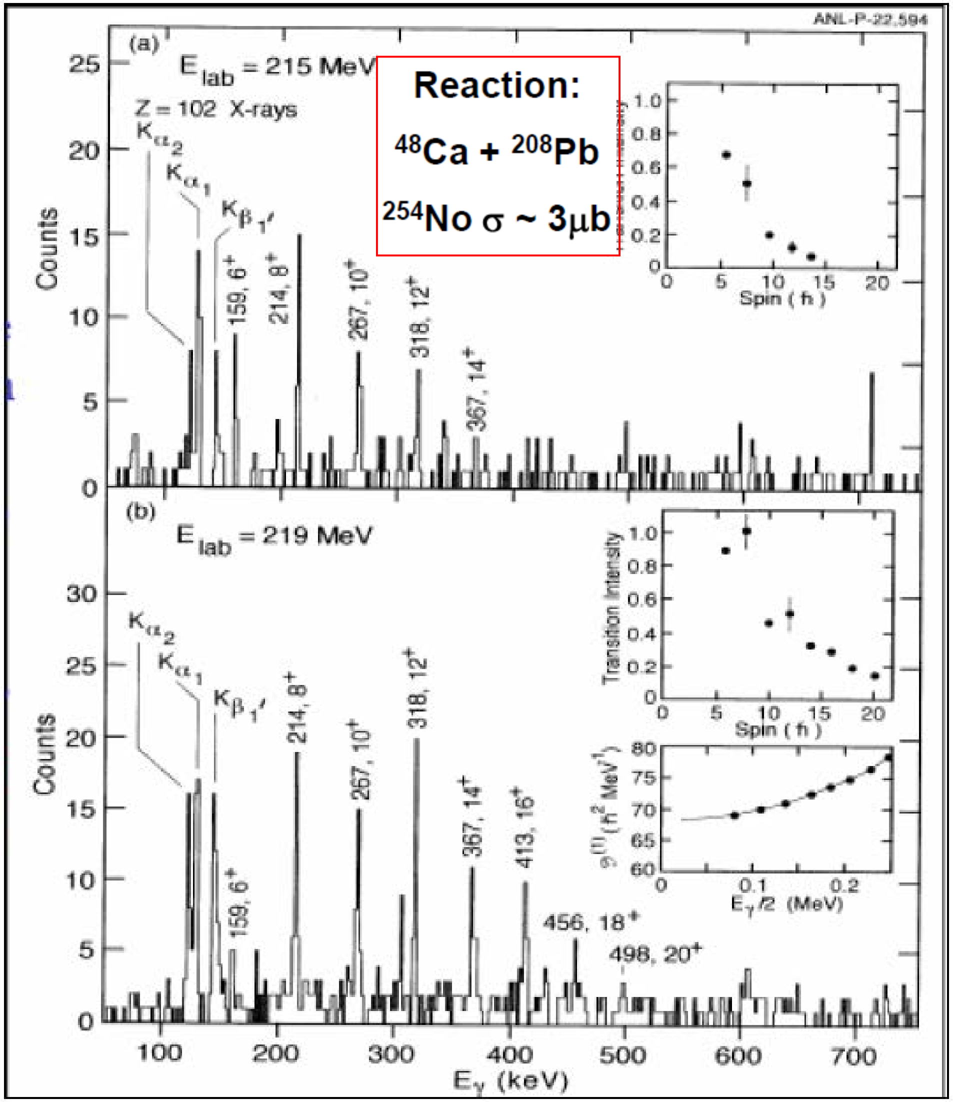

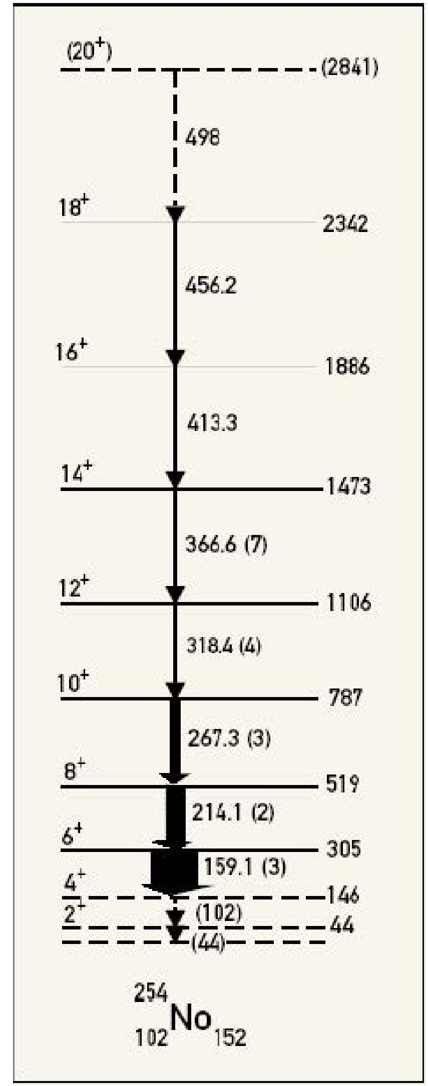

. Reiter *et al.*, Phys. Rev. Lett. 82 (1999) 509

Recoil Decay Tagging (Isotopic Identification)

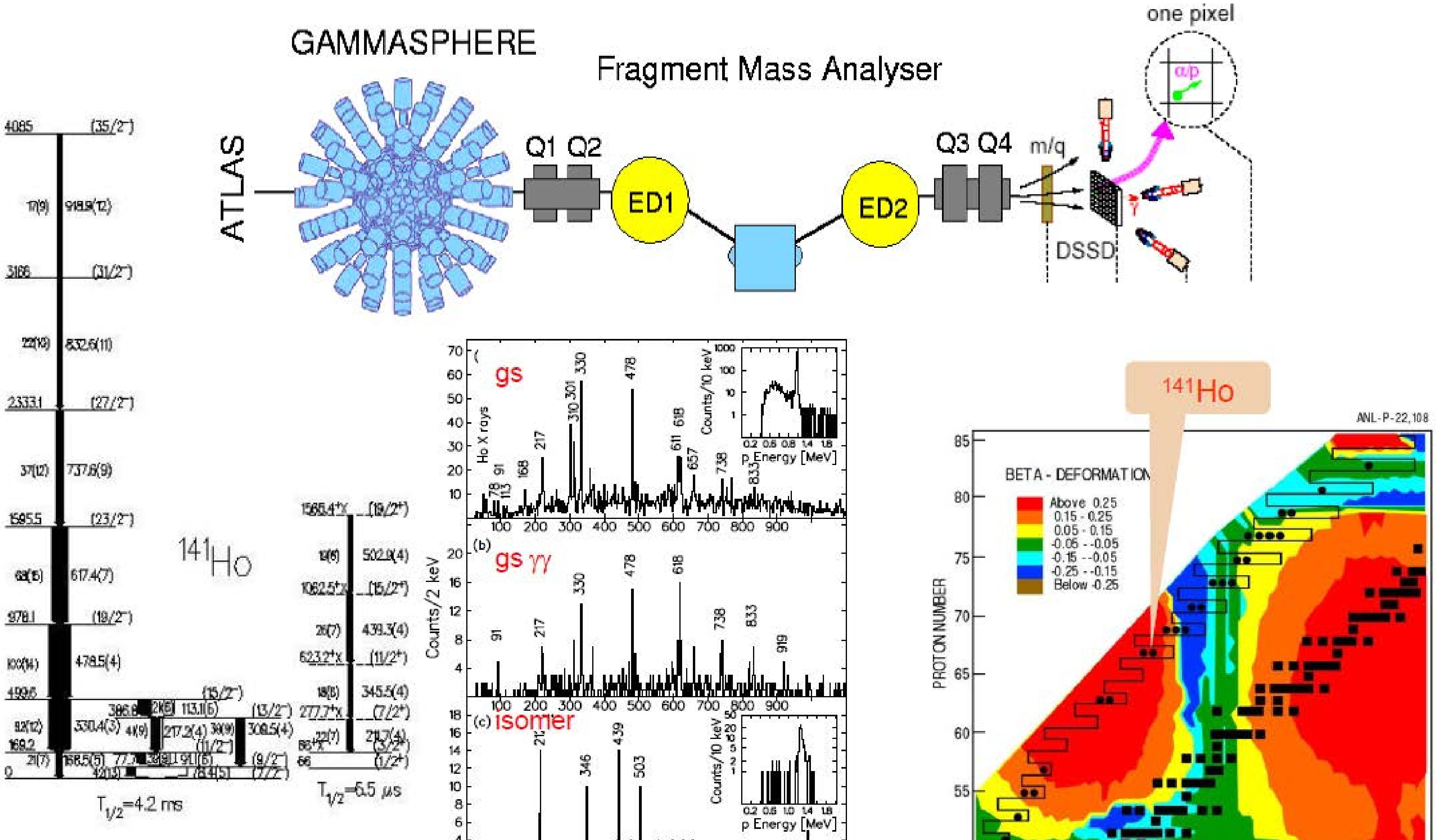

σ=300nb σ=50nb

D. Seweryniak *et al.*, PRL 86 (2001) 1458.

Can use 'fine structure' in radioactivity to select decays to specific states (i.e., different single particle configurations).

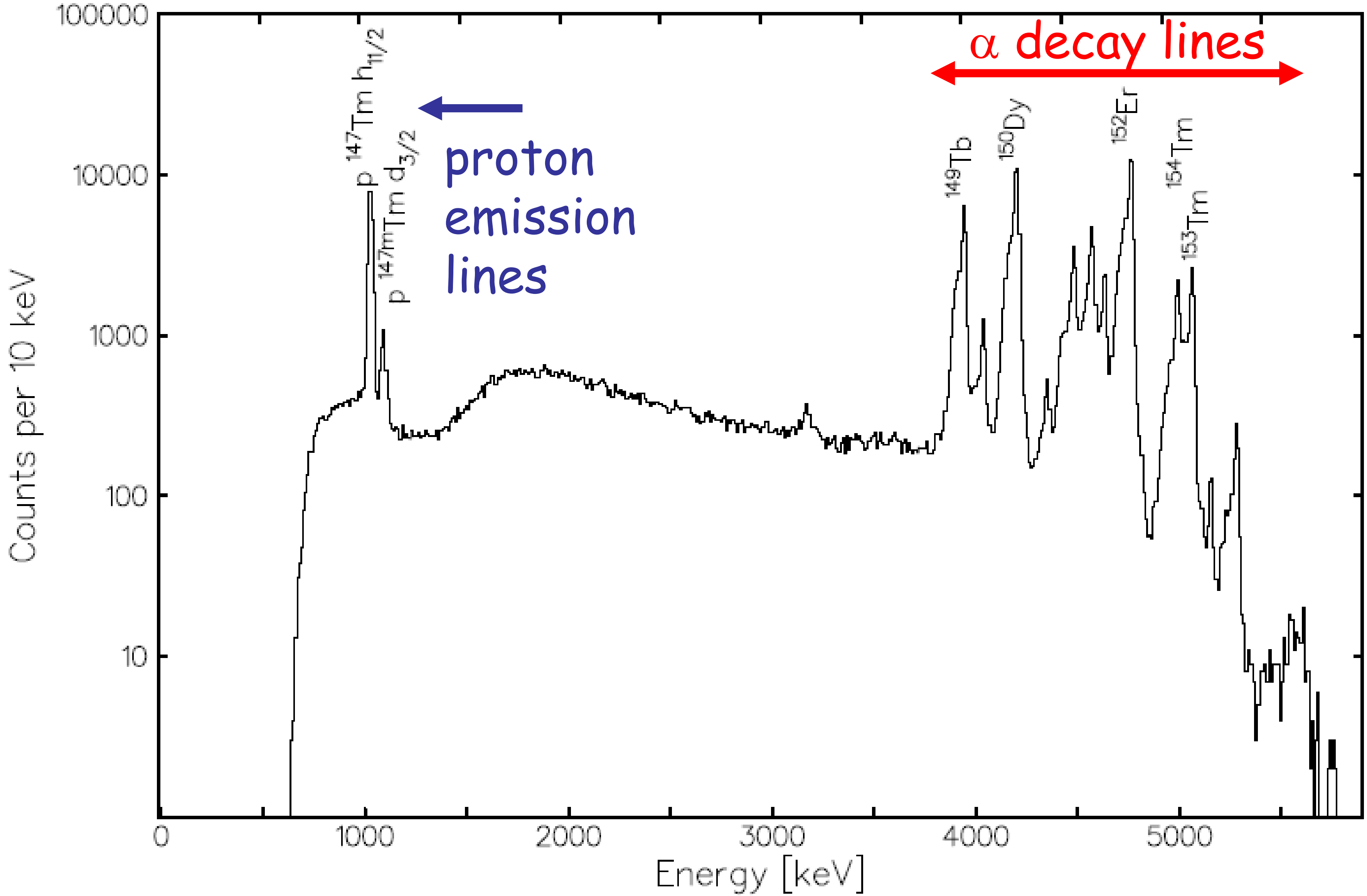

D. Seweyniak *et al. Phys. Rev.* **C55** (1997) R2137

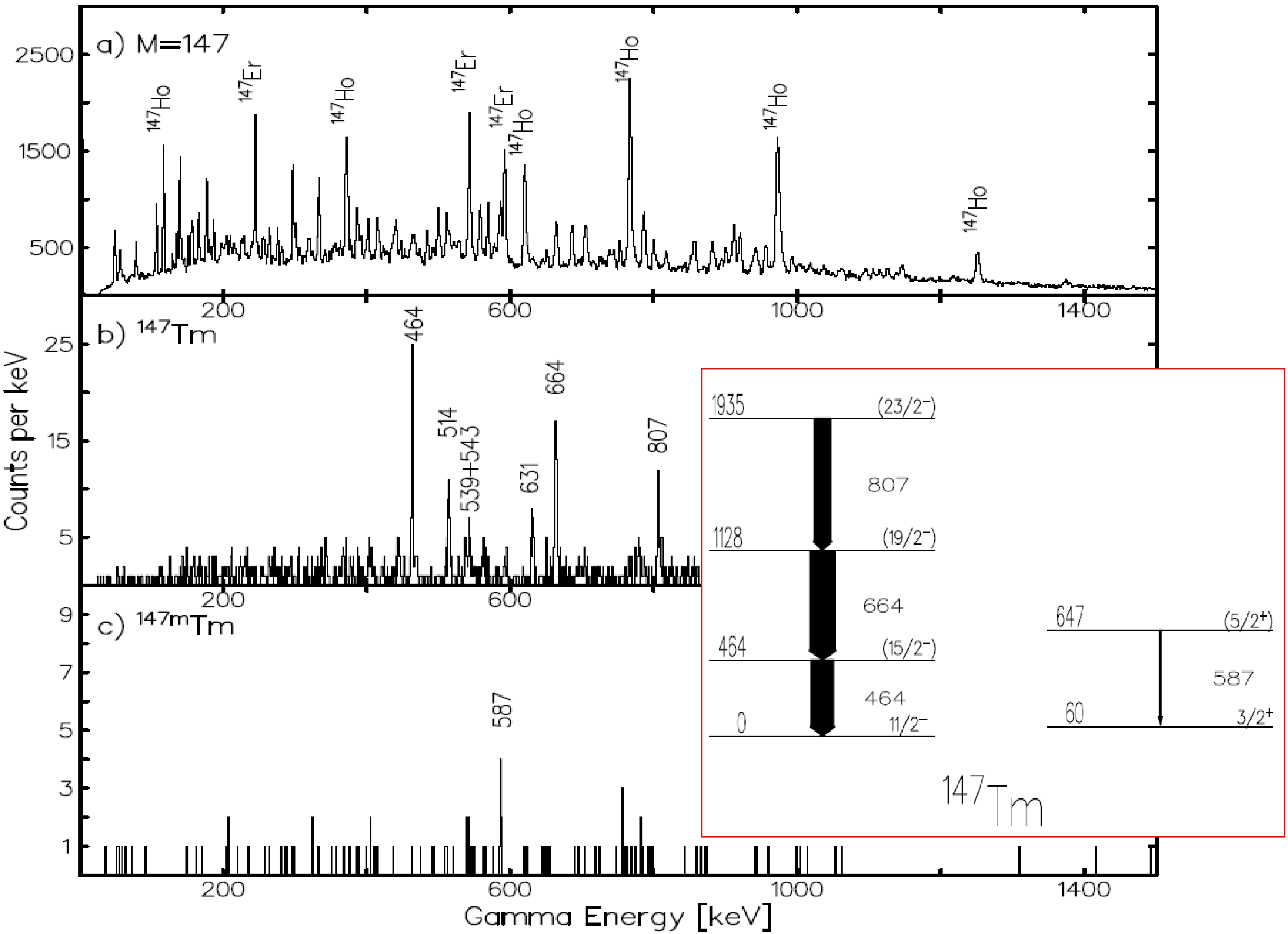

D. Seweyniak *et al.* *Phys. Rev.* **C55** (1997) R2137

Neutron-Rich Nuclei?

How do you make and study neutron-rich nuclei ?

- (low-cross-section) fusion evap. reactions, e.g., $^{18}O + ^{48}Ca \rightarrow 2p + ^{64}Fe$
  - Limited compound systems using stable / beam target combinations.
  - Highly selective reactions (if good channel selection applied).

- Spontaneous fission sources (e.g., ^{244}Cm)
  - Good for some regions of the nuclear chart, but little/no selectivity in the 'reaction' mechanism.
  - Can make quite high spins in each fragment ($10 \rightarrow 20\hbar$)

- Fusion fission reactions
  - e.g., $^{18}O + ^{208}Pb \rightarrow ^{226}Th^* \rightarrow f_1 + f_2 + xn$ (e.g., $^{112}_{44}Ru + ^{112}_{46}Pd + 2n$)
  - Doesn't make very neutron-rich, little selectivity.
  - Medium spins (~10 $\hbar$ in each fragment) populated

- Heavy-ion deep-inelastic / multi-nucleon transfer reactions (e.g.,
  - e.g. $^{136}Xe + ^{198}Pt \rightarrow ^{136}Ba + ^{194}Os + 2n$.
  - Populations Q-value dependent; medium spins accessed in products, make nuclei 'close' to the original (stable) beam and target species.
  - Selectivity can be a problem, large Doppler effects.

- Projectile fragmentation (or Projectile Fission)
  - (v. different energy regime)
  - Need a fragment separator.

Nuclei produced in ^{252}Cf fission ; GAMMASPHERE + FATIMA; Argonne National Lan, Dec. 2015 -Jan . 2016

- 1 Ci ^{252}Cf source
- about 20% of total activity extracted as ions
- works for all species
- large improvement over existing ISOL based facilities

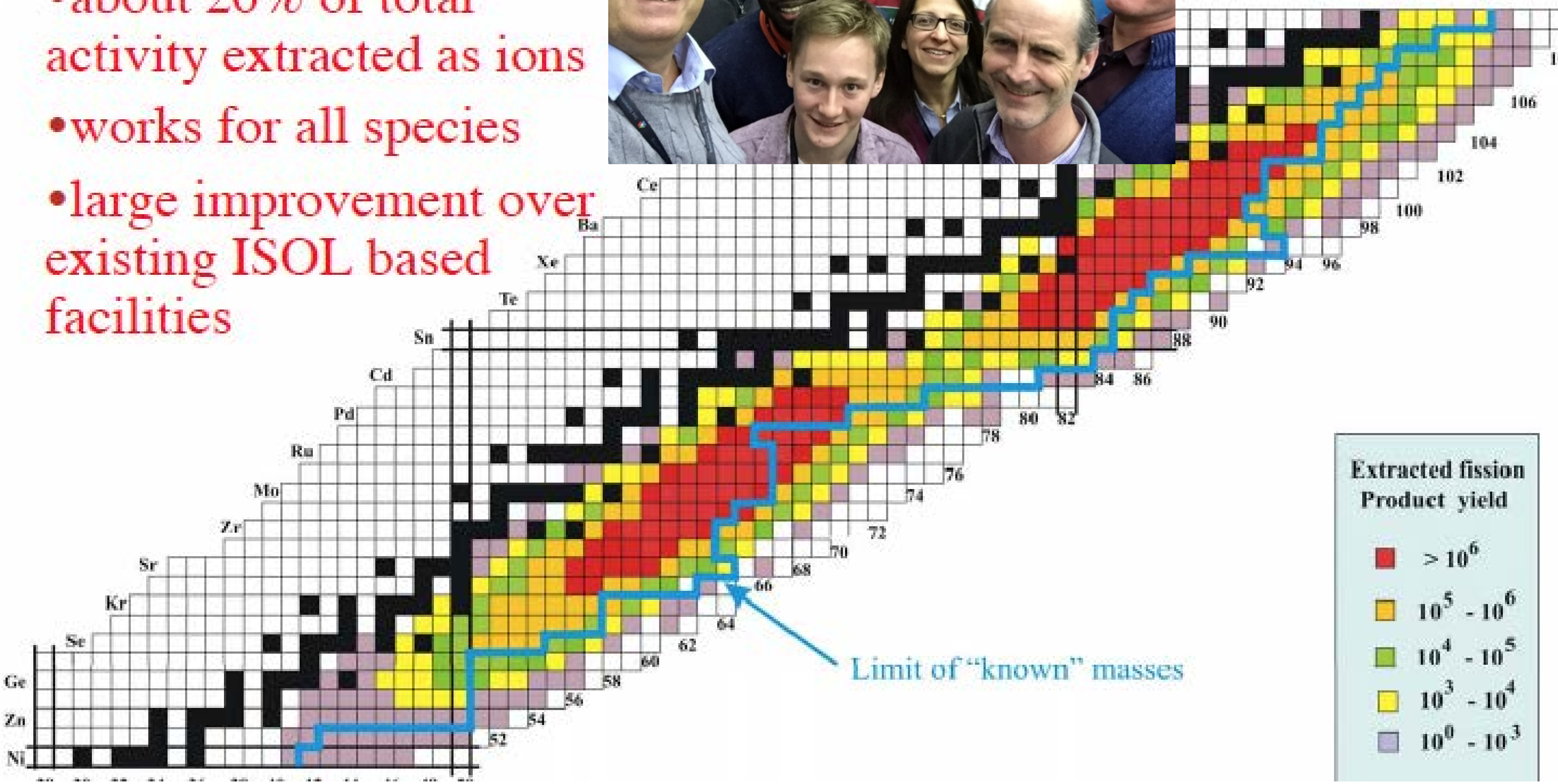

Aim: Investigation of the deformed regions of the nuclear chart around mass $A \sim 100$ and $A \sim 150$

- A 34.4 μCi ^{252}Cf source at the focus of the 2 hemispheres ($t_{1/2}$ = 2.645 y, Z = 98 N = 154)
- A scintillator array made of 25 $LaBr_3$(Ce) detectors (FATIMA)
- One hemisphere of Gammasphere made of 51 Compton-suppressed HPGe detectors
- First time Gammasphere was coupled with 25 $LaBr_3$(Ce) detectors
- Digital acquisition for the entire $LaBr_3$(Ce) array for the first time

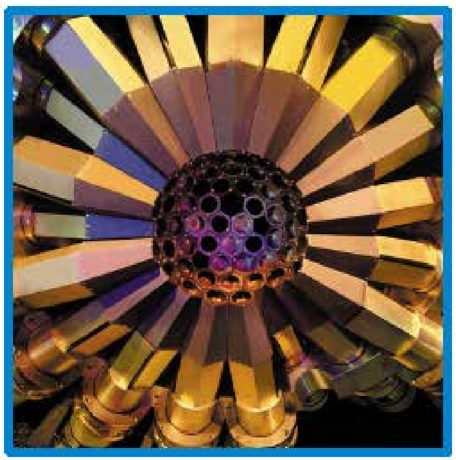

+

INSTITUTE OF PHYSICS PUBLISHING JOURNAL OF PHYSICS G: NUCLEAR AND PARTICLE PHYSICS

J. Phys. G: Nucl. Part. Phys. **32** (2006) R151–R192 doi:10.1088/0954-3899/32/6/R01

TOPICAL REVIEW

Spectroscopic studies with the use of deep-inelastic heavy-ion reactions

R Broda

Niewodniczański Institute of Nuclear Physics PAN, Kraków, Poland

$$L = \mu R^2\omega + \Im_p\omega_p + \Im_t\omega_t,$$

$$\mu = \frac{A_p A_t}{A_p + A_t}.$$

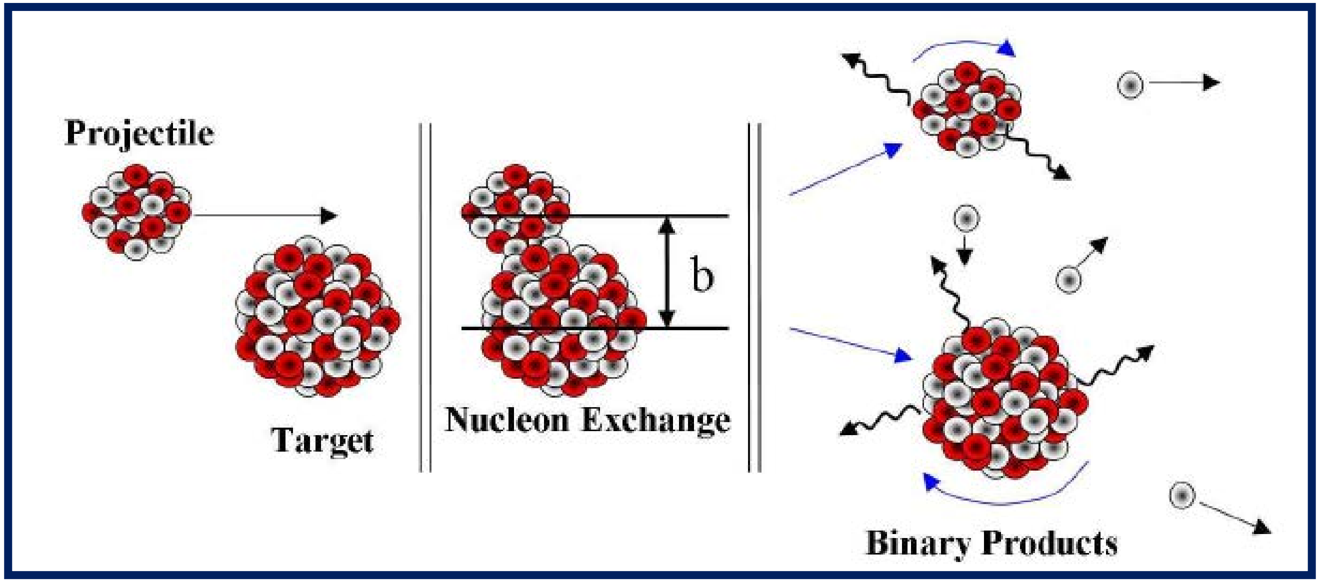

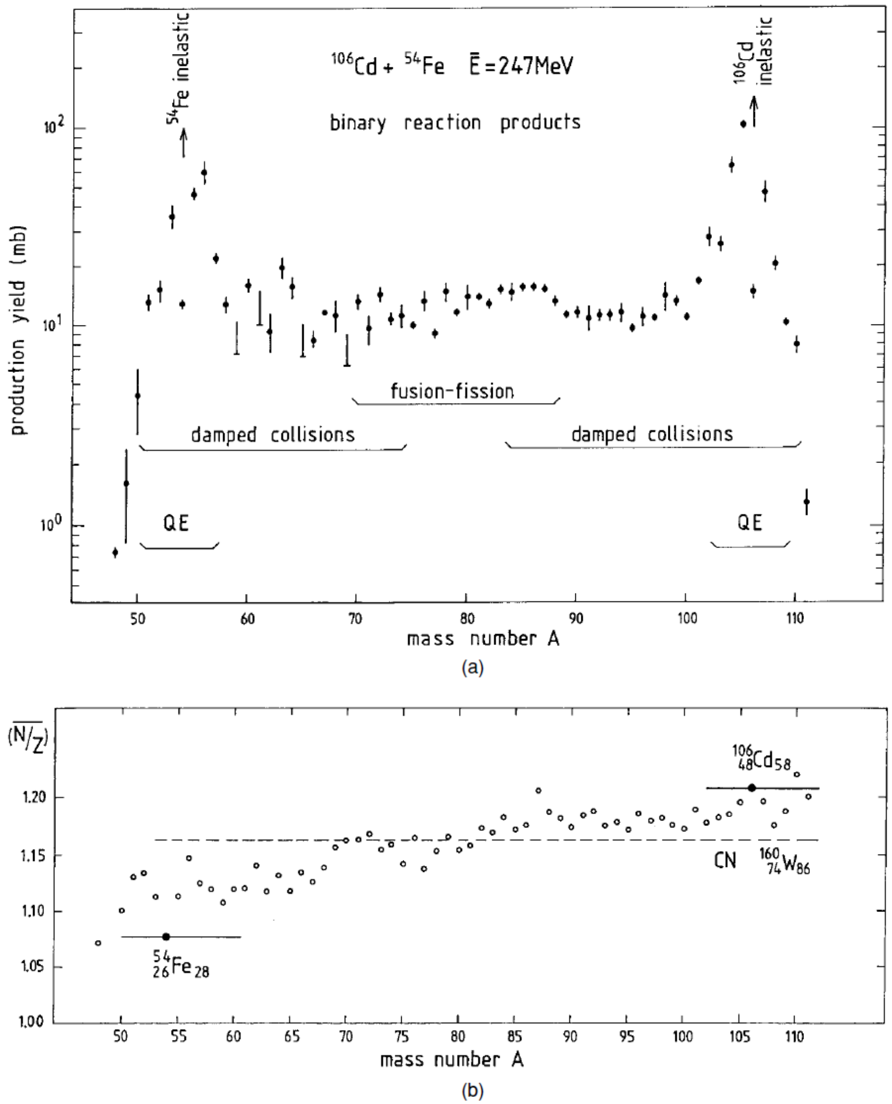

Figure 3. Isobar-integrated production cross sections (a) and the average N/Z ratios (b) as a function of binary reaction product mass in ^{106}Cd + ^{54}Fe collisions. Reprinted with permission from [11] © 1994 American Physical Society.

Both the target-like and beam-like fragments and the intermediated fusion-fission residues are usually **stopped** in a thick/backed target.

For discrete gamma rays decaying from states with effective lifetimes of a few picoseconds, there is **no Doppler shift** effect as the sources are stopped in the target and have v/c=0.

Prompt decays from higher-spin / faster lifetime states (< 1ps) will be 'smeared' out by the Doppler broadening effect.

Backed/thick target experiments can not correct for Doppler shifts as the direction and velocity of the emitting fragment is not known.

e.g., ^{82}Se + ^{192}Os at INFN-Legnaro.

Discrete gamma rays detected using GASP array.

Triples gamma-ray coincidences measured within ~ 50 ns timing window.

Discrete states to ~ 12ħ observed in BLF.

More like ~ 20 ħ in some of the TLFs.

PHYSICAL REVIEW C 76, 054317 (2007)

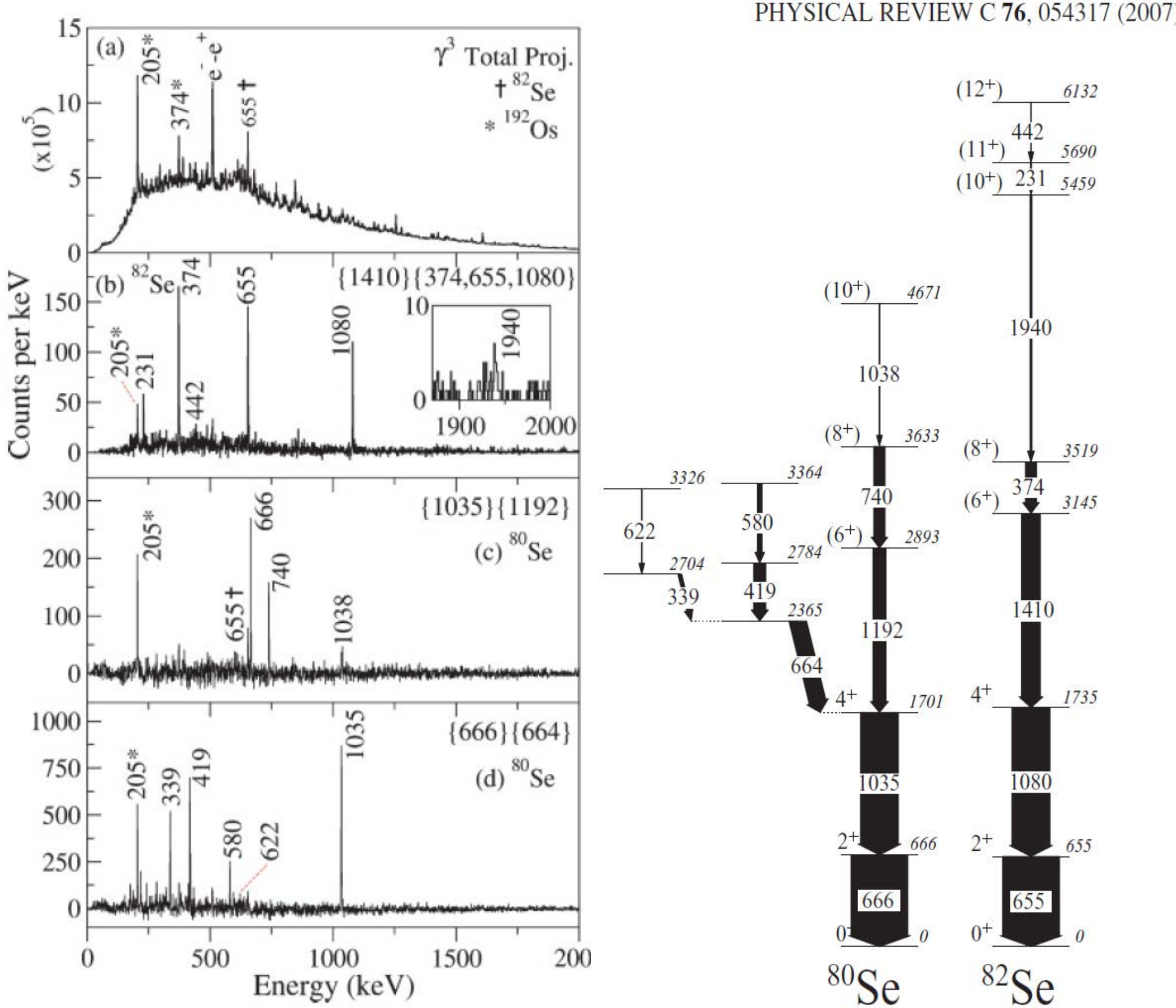

PHYSICAL REVIEW C 76, 054317 (2007)

Yrast studies of ^{80,82}Se using deep-inelastic reactions

G. A. Jones,[1] P. H. Regan,[1] Zs. Podolyák,[1] N. Yoshinaga,[2] K. Higashiyama,[3] G. de Angelis,[4] Y. H. Zhang,[5] A. Gadea,[4] C. A. Ur,[6] M. Axiotis,[4] D. Bazzacco,[6] D. Bucurescu,[7] E. Farnea,[6] W. Gelletly,[1] M. Ionescu-Bujor,[7] A. Iordachescu,[7] Th. Kröll,[4] S. D. Langdown,[1] S. Lenzi,[6] S. Lunardi,[6] N. Marginean,[4] T. Martinez,[4] N. H. Medina,[8] R. Menegazzo,[6] D. R. Napoli,[4] B. Quintana,[9] B. Rubio,[10] C. Rusu,[11] R. Schwenger,[12] D. Tonev,[4] J. J. Valiente Dobón,[1,4] and W. von Oertzen[13]

States to spins of >20 ħ can be populated in DIC.

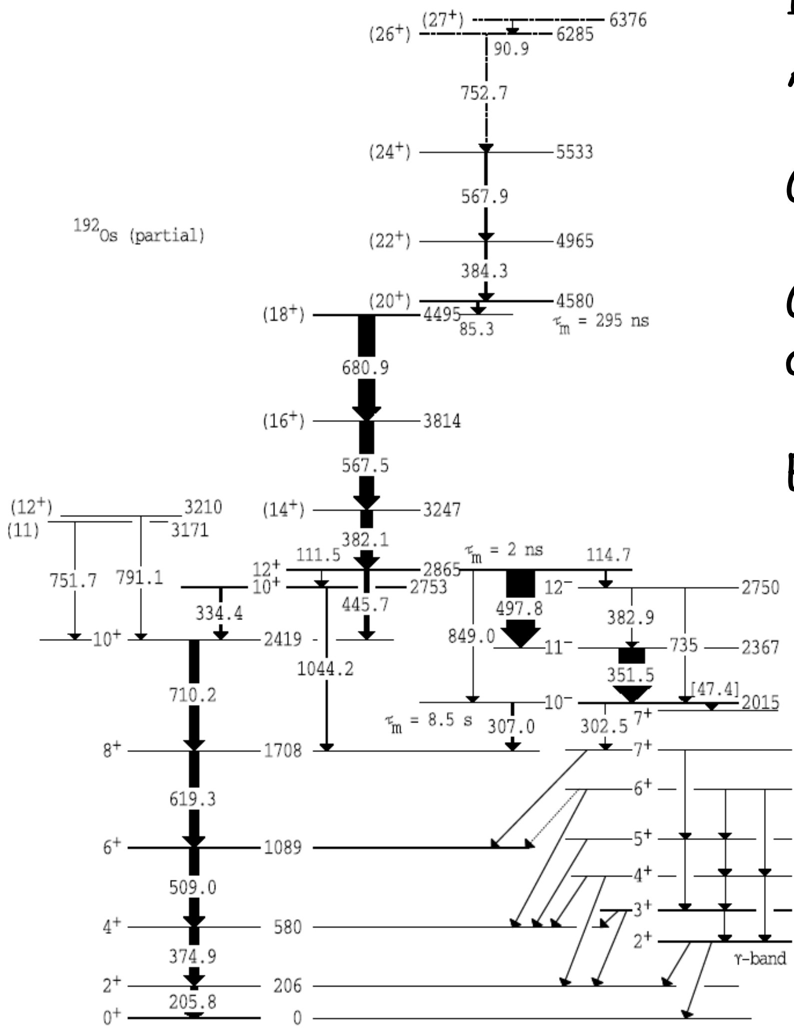

^{136}Xe beam on thick, backed ^{192}Os target at Argonne National Lab.

Gamma rays measured using GAMMASPHERE

Gamma rays decaying following isomeric states are all stopped in the target, no Doppler shifts.

Evidence for population of states with I>25 ħ.

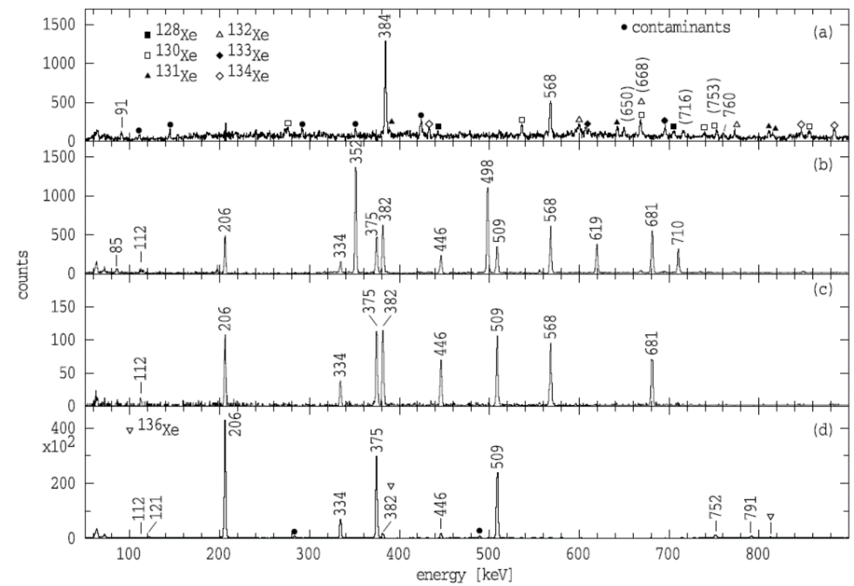

Physics Letters B 720 (2013) 330–335

Isomers and excitation modes in the gamma-soft nucleus ^{192}Os

G.D. Dracoulis [a,*], G.J. Lane [a], A.P. Byrne [a], H. Watanabe [a,b,1], R.O. Hughes [a,2], F.G. Kondev [c], M. Carpenter [d], R.V.F. Janssens [d], T. Lauritsen [d], C.J. Lister [d], D. Seweryniak [d], S. Zhu [d], P. Chowdhury [e], Y. Shi [f], F.R. Xu [f]

Conservation of linear angular momentum gives,

$$P_0 = P_p \cos\theta_p + P_t \cos\theta_t$$
$$0 = P_p \sin\theta_p - P_t \sin\theta_t$$

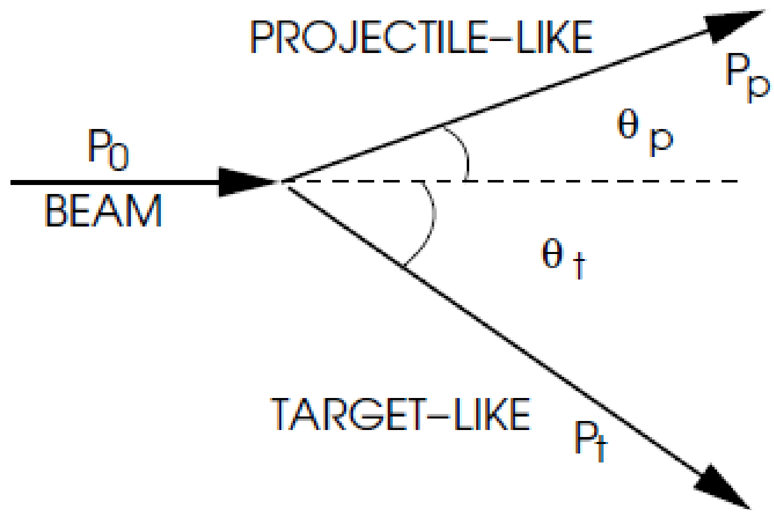

After some algebra manipulation, the relation of the recoil momenta to the initial beam momentum is given by,

$$P_{p,t} = P_0 \frac{\sin(\theta_t, \theta_p)}{\sin(\theta_p + \theta_t)} \tag{2.2}$$

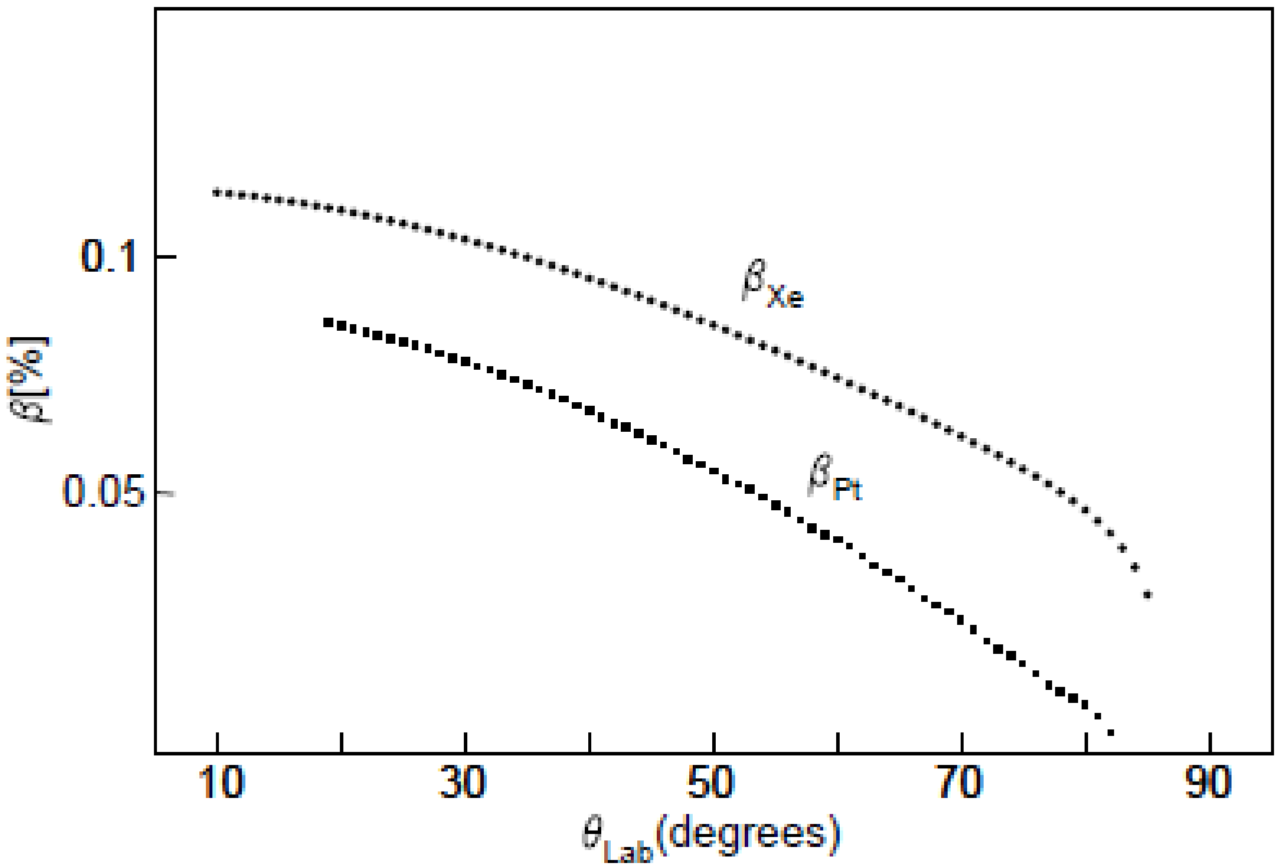

Figure 2.3: Calculated velocities of the projectile and the target recoils for the particular case of a ^{136}Xe beam at 850 MeV in the laboratory frame impinging on a ^{198}Pt target. An elastic collision and simple two-body kinematics have been assumed.

PHYSICAL REVIEW C **69**, 024316 (2004)

^{136}Ba studied via deep-inelastic collisions: Identification of the $(\nu h_{11/2})^{-2}_{10+}$ isomer

J. J. Valiente-Dobón,[1,*] P. H. Regan,[1,2] C. Wheldon,[1,3] C. Y. Wu,[4] N. Yoshinaga,[5] K. Higashiyama,[5] J. F. Smith,[6] D. Cline,[4] R. S. Chakrawarthy,[6] R. Chapman,[7] M. Cromaz,[8] P. Fallon,[8] S. J. Freeman,[6] A. Görgen,[8] W. Gelletly,[1] A. Hayes,[4] H. Hua,[4] S. D. Langdown,[1,2] I. Y. Lee,[8] X. Liang,[7] A. O. Macchiavelli,[8] C. J. Pearson,[1] Zs. Podolyák,[1] G. Sletten,[9] R. Teng,[4] D. Ward,[8] D. D. Warner,[10] and A. D. Yamamoto[1,2]

^{136}Xe beam on a thin ^{198}Pt target.

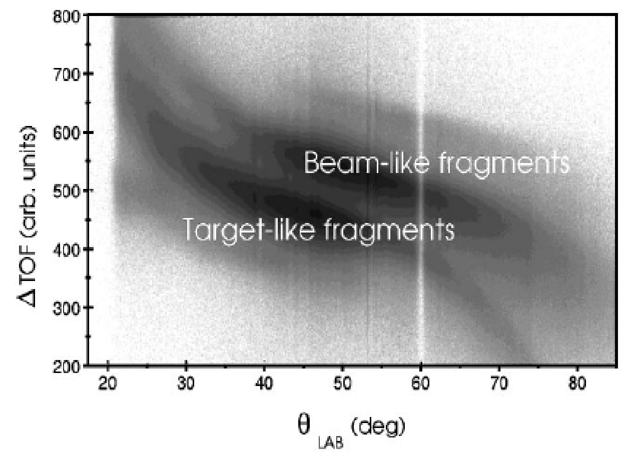

Residual reaction nuclei measured in 'binary' pairs using CHICO, a position sensitive gas detector.

Gamma rays from beam and target-like fragments measured in GAMMASPHERE.

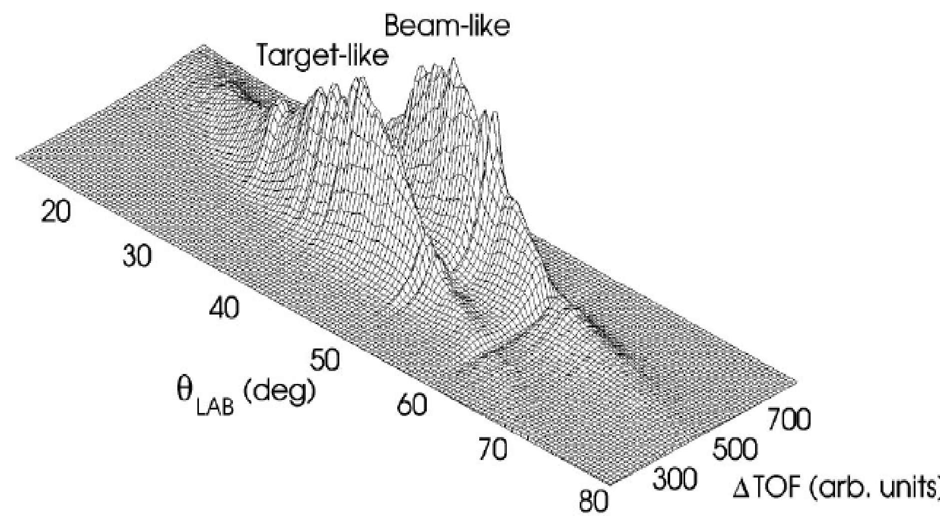

Difference in time of flight between BLF and TLF hitting CHICO can be used to deduce which fragments is which (heavier one usually moved more slowly due to COLM).

Angle differences between CHICO and GAMMASPHERE can be used for Doppler Corrections.

Use spectrometer to 'tag' on one of the reaction fragments for Doppler Correction.
e.g., ^{82}Se (Z=34) beam on thin ^{170}Er (Z=68) target at INFN-Legnaro.

PHYSICAL REVIEW C **81**, 034310 (2010)

Spectroscopy of neutron-rich ^{168,170}Dy: Yrast band evolution close to the N_pN_n valence maximum

P.-A. Söderström,[1] J. Nyberg,[1] P. H. Regan,[2] A. Algora,[3] G. de Angelis,[4] S. F. Ashley,[2] S. Aydin,[5] D. Bazzacco,[5] R. J. Casperson,[6] W. N. Catford,[2] J. Cederkäll,[7,8] R. Chapman,[9] L. Corradi,[4] C. Fahlander,[8] E. Farnea,[5] E. Fioretto,[4] S. J. Freeman,[10] A. Gadea,[3,4] W. Gelletly,[2] A. Gottardo,[4] E. Grodner,[4] C. Y. He,[4] G. A. Jones,[2] K. Keyes,[9] M. Labiche,[9] X. Liang,[9] Z. Liu,[2] S. Lunardi,[5] N. Mărginean,[4,11] P. Mason,[5] R. Menegazzo,[5] D. Mengoni,[5] G. Montagnoli,[5] D. Napoli,[4] J. Ollier,[12] S. Pietri,[2] Zs. Podolyák,[2] G. Pollarolo,[13] F. Recchia,[4] E. Şahin,[4] F. Scarlassara,[5] R. Silvestri,[4] J. F. Smith,[9] K.-M. Spohr,[9] S. J. Steer,[2] A. M. Stefanini,[4] S. Szilner,[14] N. J. Thompson,[2] G. M. Tveten,[7,15] C. A. Ur,[5] J. J. Valiente-Dobón,[4] V. Werner,[6] S. J. Williams,[2] F. R. Xu,[16] and J. Y. Zhu[16]

Measure BLFs directly in PRISMA spectrometer and gammas in CLARA gamma-ray array.
Reverse correct for heavier TLF using 2-body kinematics.

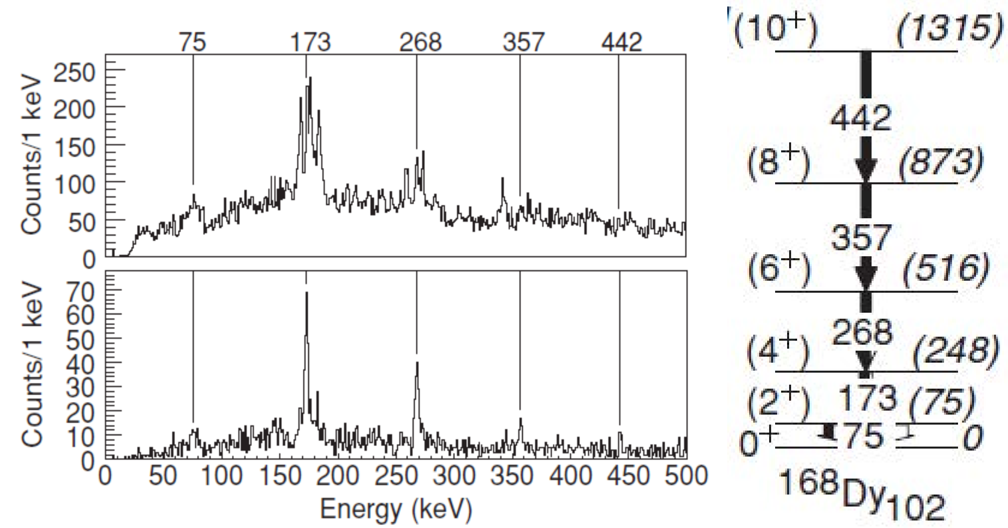

FIG. 3. Spectrum of γ-ray energies from targetlike fragments gated on the beamlike fragments ^{84}Kr (top) and on beamlike fragments ^{84}Kr plus a short time of flight (bottom). The transitions identified as the rotational band in ^{168}Dy are marked with solid lines.

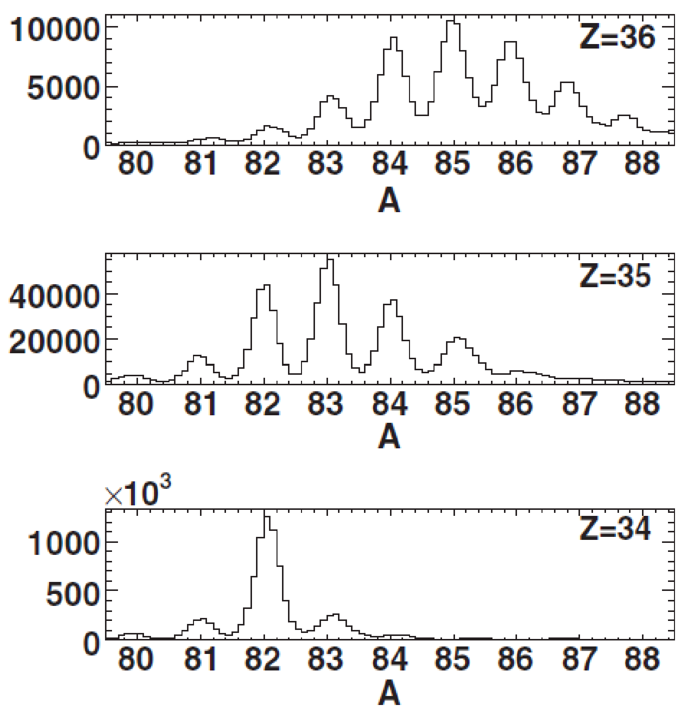

Gate on ^{84}Kr (Z=36) fragment in PRISMA.
Complementary fragment (assuming no neutron evaporation) for ^{82}Se+^{170}Er reaction for ^{84}Kr is ^{168}Dy (Z=66) (+2p transfer channel).
Shortest time of flight in PRISMA associated with least neutron evaporation.

Determining spins from gamma-ray multipolarities

DCO and DCO Ratios

JULY 15, 1940 PHYSICAL REVIEW VOLUME 58

On Directional Correlation of Successive Quanta

DONALD R. HAMILTON*
Harvard University, Cambridge, Massachusetts

(Received May 6, 1940)

A theoretical investigation shows that there should be a correlation between the directions of propagation of the quanta emitted in two successive transitions of a single radiating system. This correlation is described by a function $W(\theta)$ which gives the relative probability that the second quantum will be emitted at an angle θ with the first; W is determined by the angular momenta of the three levels involved in the two transitions and by the multipole order of the radiation emitted in these transitions. The explicit forms of W for all angular momenta and for dipole and quadrupole radiation are given; experimental determination of W in any given case should limit these factors to a small number of possibilities. This has particular interest as a means of investigating the nuclear energy levels involved in γ-radiation; here W should be observable by measuring the variation with θ of gamma-gamma coincidence counting rates.

First real 'evidence' of angular correlations between successive gamma rays;

Radioactive decays of

^{60}Co ($I^{\pi}=5^{+}$, $T_{1/2}$=5.27 yrs to ^{60}Ni)
^{46}Sc ($I^{\pi}=4^{+}$, $T_{1/2}$=84 days to 46Ti)
^{88}Y ($I^{\pi}=4-$, $T^{1/2}$=107 days to ^{88}Sr)
^{134}Cs ($I^{\pi}=4^{+}$, $T_{1/2}$=2.1 yrs to ^{134}Ba).

(note, says ^{86}Y in paper, means ^{88}Y)

Angular Correlation of Successive Gamma-Ray Quanta

EDWARD L. BRADY AND MARTIN DEUTSCH
Massachusetts Institute of Technology, Cambridge, Massachusetts
September 10, 1947

THEORETICAL considerations[1,2] predict a directional correlation of successive quanta of the form

$$W(\theta)=1+\sum_{i=1}^{l} A_i \cos^{2i}\theta$$

if $2l$ is the highest multipole order occurring. Attempts to demonstrate this effect experimentally have heretofore been inconclusive.[3] We have studied coincidences between successive gamma-rays of Co^{60}, Sc^{46}, Y^{86} (106 day), and Cs^{134} at angles 180° and 90° between the counters, and found a pronounced anisotropy in the first two named and no correlation within the experimental error in the last two. Our results, together with the gamma-ray energies concerned, are shown in Table I. The quantity $(W(\pi)$

TABLE I. Anisotropy of gamma-ray coincidences.

Source	Co^{60}	Sc^{46}	Y^{86}	Cs^{134}
ϵ	0.21 ± 0.025	0.20 ± 0.035	-0.05 ± 0.03	0.01 ± 0.04
Gamma-rays Mev	1.1, 1.3	0.89, 1.12	0.91, 1.89	0.58, 0.78
Reference	4	5	6	7

$-W(\pi/2))/W(\pi/2)$ should be equal to ΣA_i. Our results

The probability, per unit solid angle, that two successive gamma-rays are emitted at an angle θ is proportional to

$$W(\theta)=1+\sum_{1}^{l} a_i \cos^{2i}\theta$$

where $2l$ is the order of the lowest multipole in the cascade. Thus, if both gamma-rays are quadrupoles $W(\theta)=1+a_1\cos^2\theta+a_2\cos^4\theta$. If one is a dipole $W(\theta)=1+a_1\cos^2\theta$, etc. A further restriction on the number of terms in $W(\theta)$ is $a_i=0$ for $i>J_2$. J_2 is the spin of the intermediate state in the cascade. Thus if J_2 is zero or $\frac{1}{2}$, the angular correlation will always be isotropic; if J_2 is 1 or $\frac{3}{2}$, the correlation will at most contain terms in $\cos^2\theta$. The coefficients a_1 and a_2 have been given by Hamilton[2] for all possible combinations of angular momenta. In Table I we have listed the values of these coefficients from Hamilton's paper for the values of J which are of interest in connection with our experiments. Coefficients for octupole radiation should be very useful, but have not yet been published. If the transition involves mixed multipoles, e.g., electric quadrupole and magnetic dipole components, the situation becomes very complicated and the coefficients depend not only on the relative intensities of the two components but also on their relative phases.[5]

PHYSICAL REVIEW VOLUME 78, NUMBER 5 JUNE 1, 1950

Angular Correlation of Successive Gamma-Rays*

E. L. Brady† and M. Deutsch
Laboratory for Nuclear Science and Engineering, Department of Physics and Chemistry Department, Massachusetts Institute of Technology, Cambridge, Massachusetts

(Received February 6, 1950)

The angular correlation of successive gamma-rays emitted by six even-even nuclei has been investigated and found to be anisotropic in every case, and of the magnitude expected theoretically. Effects of external magnetic fields and of chemical binding on the correlations are found to be smaller than the experimental uncertainty for some exploratory experiments. Interpretation of the results in terms of the nuclear states involved is in general possible by use of additional evidence such as relative transition probabilities.

TABLE I. Coefficients for the angular correlation with the spin of the ground state $J_1=0$.

J_2	J_3	Multipoles	a_1	a_2
1	0	Dipole–Dipole	1	0
1	1	Dipole–Dipole	−1/3	0
1	2	Dipole–Dipole	−1/3	0
1	1	Quadrupole–Dipole	−1/3	0
1	2	Quadrupole–Dipole	3/7	0
1	3	Quadrupole–Dipole	−3/29	0
2	3	Dipole–Quadrupole	−3/29	0
2	2	Dipole–Quadrupole	3/7	0
2	1	Dipole–Quadrupole	−1/3	0
2	0	Quadrupole–Quadrupole	−3	4
2	1	Quadrupole–Quadrupole	5	−16/3
2	2	Quadrupole–Quadrupole	−15/13	16/13
2	3	Quadrupole–Quadrupole	0	−1/3
2	4	Quadrupole–Quadrupole	1/8	1/24

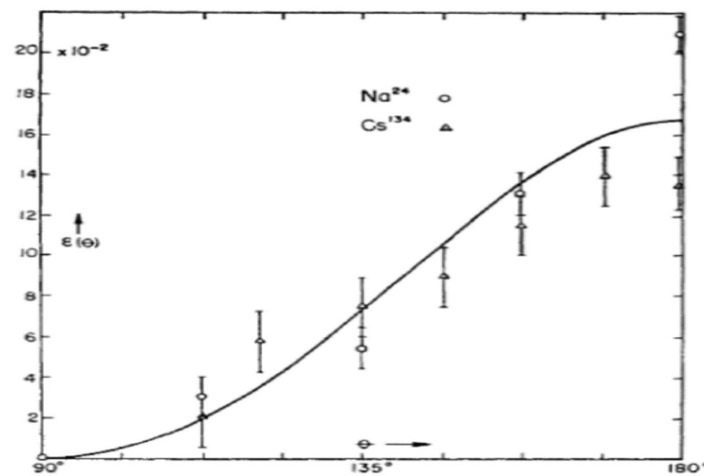

FIG. 4. Correlation of gamma-rays from Cs^{134} and Na^{24}.

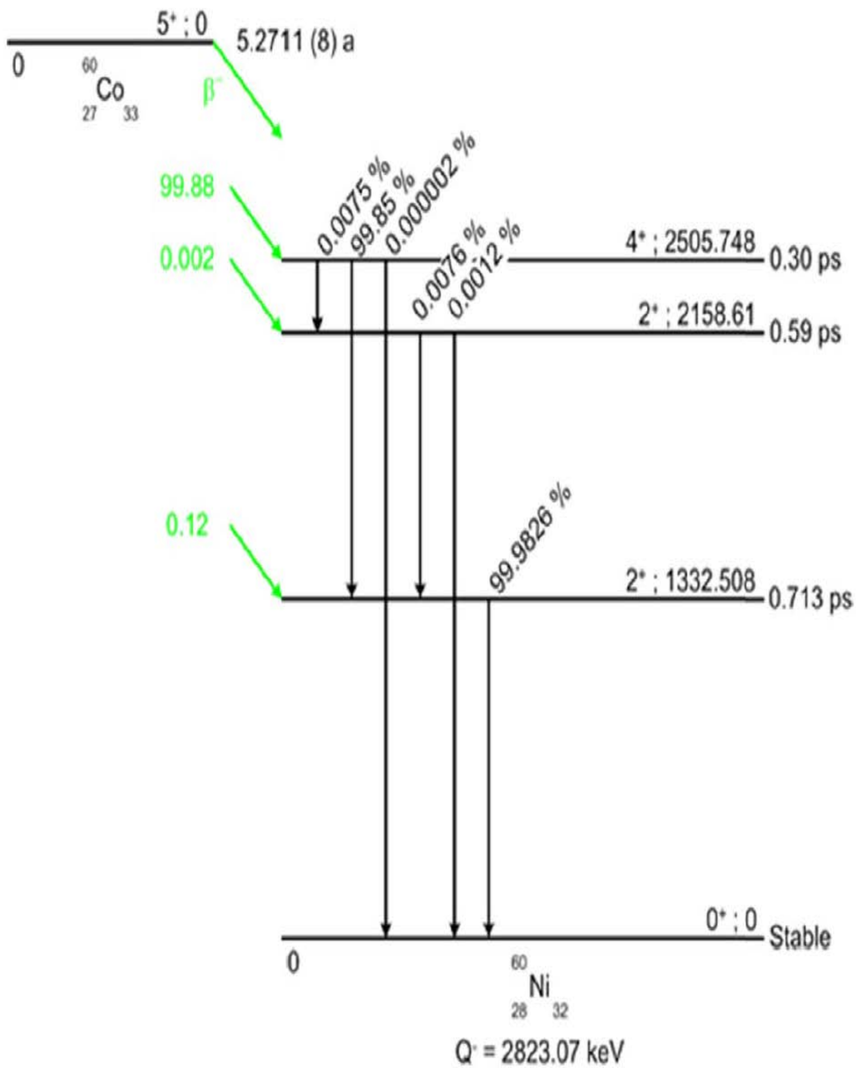

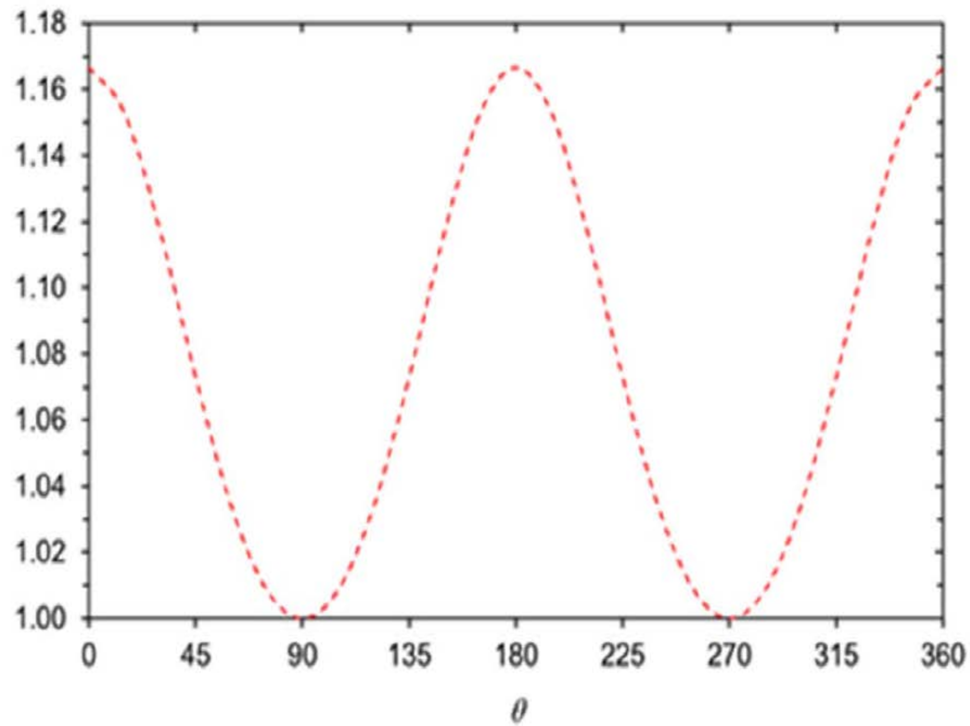

3. The angular correlation of the $4^+ \rightarrow 2^+ \rightarrow 0$ decay of ^{60}Co as a function of θ, nalised to the angular correlation at 90°.

$$\overline{W}(\theta) = \sum_{even\ k}^{k_{\max}} a_{kk} P_k(\cos\theta) Q_k(1) Q_k(2)$$

Angular correlations using the NAtional Nuclear Array

- Multi-detector NANA used for ^{60}Co primary standard expt.
- Effect of angular correlations on the activity clear.

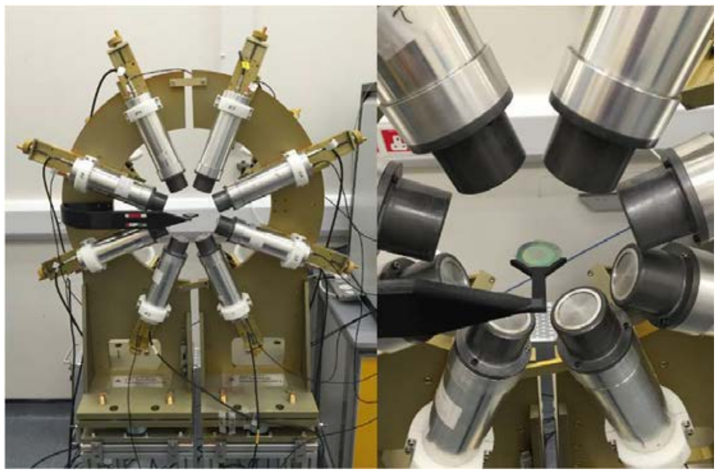

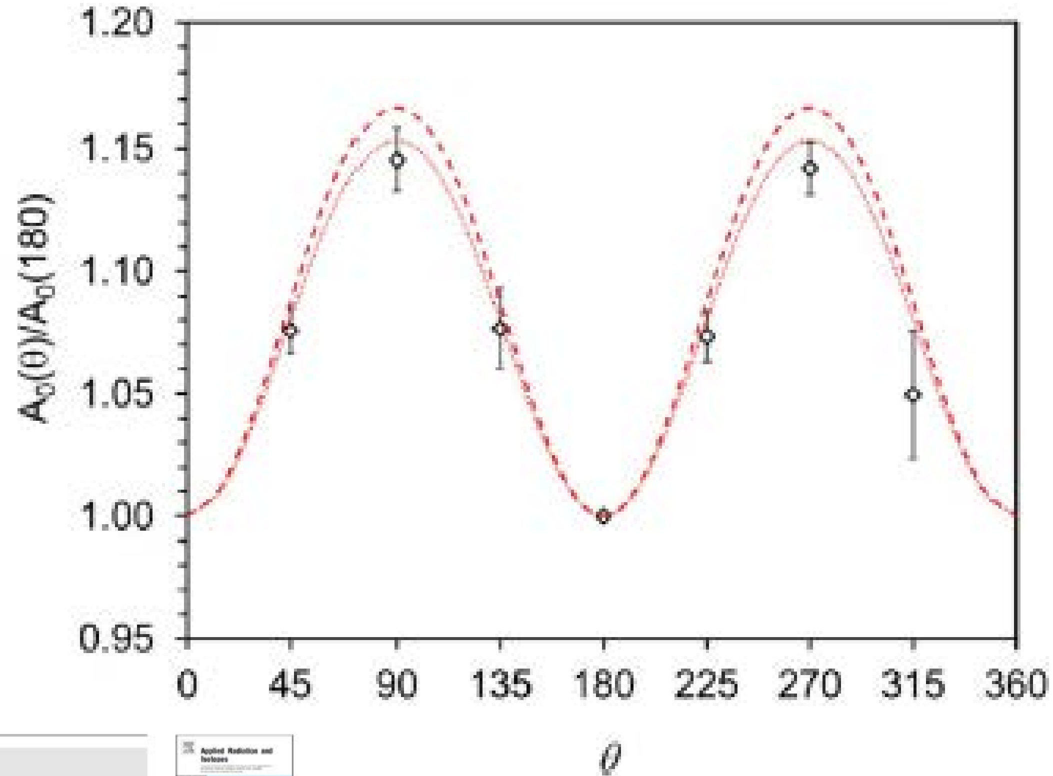

Contents lists available at ScienceDirect

Applied Radiation and Isotopes

journal homepage: www.elsevier.com/locate/apradiso

Investigation of γ-γ coincidence counting using the National Nuclear Array (NANA) as a primary standard

S.M. Collins[a,b,*], R. Shearman[a,b], J.D. Keightley[a], P.H. Regan[a,b]

[a] National Physical Laboratory, Hampton Road, Teddington, Middlesex TW11 0LW, United Kingdom
[b] Department of Physics, University of Surrey, Guildford GU2 7XH, United Kingdom

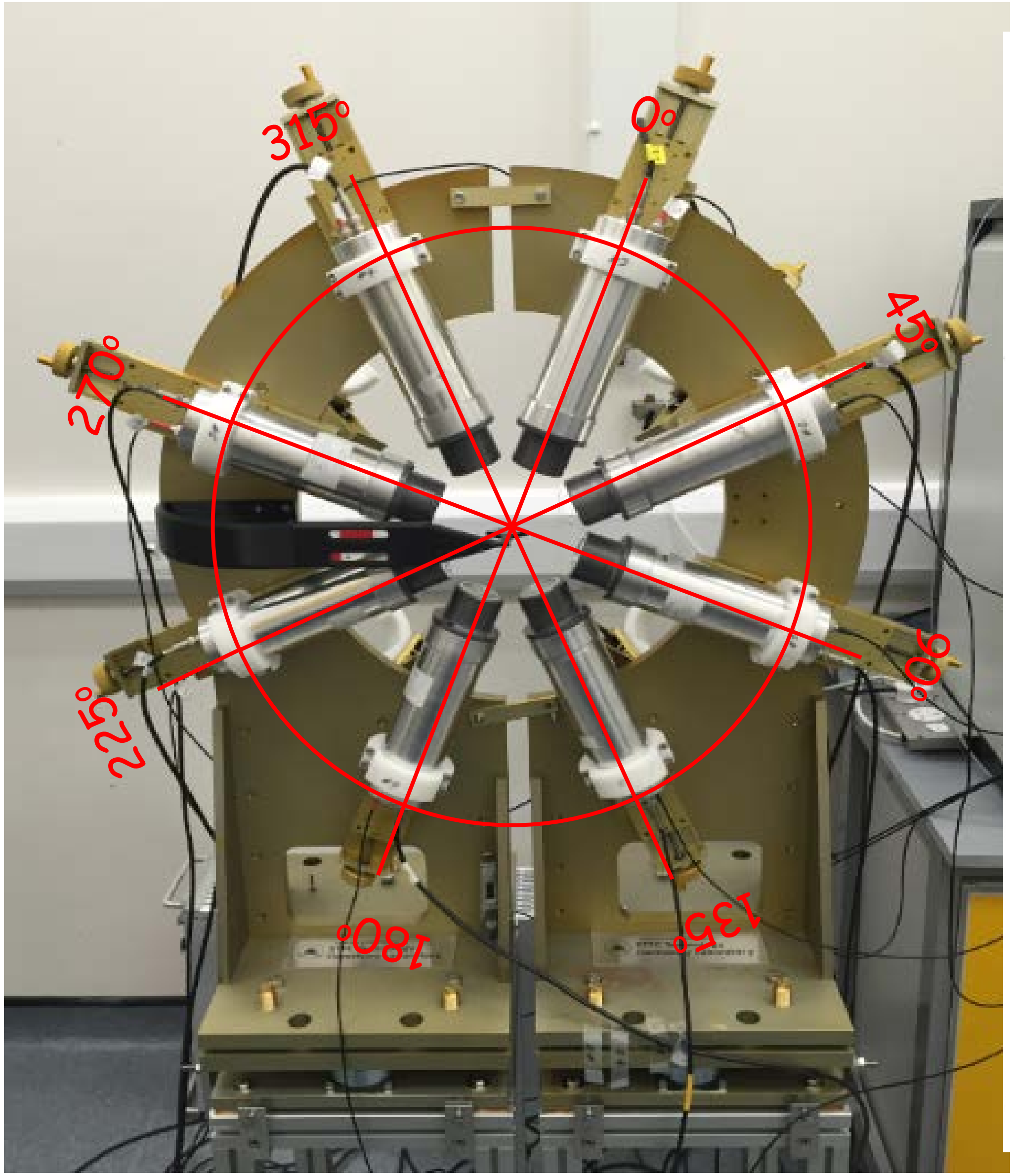

Angular Correlation of Successive Gamma-Ray Quanta

EDWARD L. BRADY AND MARTIN DEUTSCH
Massachusetts Institute of Technology, Cambridge, Massachusetts
September 10, 1947

THEORETICAL considerations[1,2] predict a directional correlation of successive quanta of the form

$$W(\theta)=1+\sum_{i=1}^{l} A_i \cos^{2i}\theta$$

if $2l$ is the highest multipole order occurring. Attempts to demonstrate this effect experimentally have heretofore been inconclusive.[3] We have studied coincidences between successive gamma-rays of Co^{60}, Sc^{46}, Y^{86} (106 day), and Cs^{134} at angles 180° and 90° between the counters, and found a pronounced anisotropy in the first two named and no correlation within the experimental error in the last two. Our results, together with the gamma-ray energies concerned, are shown in Table I. The quantity $(W(\pi)$

TABLE I. Anisotropy of gamma-ray coincidences.

Source	Co^{60}	Sc^{46}	Y^{88}	Cs^{134}
ϵ	0.21 ± 0.025	0.20 ± 0.035	-0.05 ± 0.03	0.01 ± 0.04
Gamma-rays Mev	1.1, 1.3	0.89, 1.12	0.91, 1.89	0.58, 0.78
Reference	4	5	6	7

$-W(\pi/2))/W(\pi/2)$ should be equal to $\sum A_i$. Our results

Dropping a constant factor, our correlation function for calculation is

$$\mathbf{W}(\theta)=1+(\mathbf{R}/\mathbf{Q})\cos^2\theta+(\mathbf{S}/\mathbf{Q})\cos^4\theta.$$

TABLE I. *R/Q, for both transitions dipole.*

	$\Delta J=-1$	$\Delta J=0$	$\Delta J=1$
$\Delta j=-1$	$\frac{1}{13}$	$\frac{-(2J-1)}{(14J+13)}$	$\frac{J(2J-1)}{(26J^2+67J+40)}$
$\Delta j=0$	$\frac{-(2J+3)}{(14J+1)}$	$\frac{(2J-1)(2J+3)}{(12J^2+12J+1)}$	
$\Delta j=1$	$\frac{(J+1)(2J+3)}{(26J^2-15J-1)}$		

TABLE II. *R/Q, for first transition quadrupole, second dipole.*

	$\Delta J=1$	$\Delta J=0$	$\Delta J=-1$
$\Delta j=2$	$\frac{-3}{29}$	$\frac{3(2J+3)}{(26J-3)}$	$\frac{-3(J+1)(2J+3)}{(58J^2-23J+3)}$
$\Delta j=1$	$\frac{3(J-5)}{(55J+61)}$	$\frac{-3(2J+3)(J-5)}{(58J^2+49J-15)}$	$\frac{3(2J+3)(J-5)}{(110J^2-49J+15)}$
$\Delta j=0$	$\frac{(2J-3)(2J+5)}{(36J^2+92J+61)}$	$\frac{-(2J-3)(2J+5)}{5(4J^2+4J-1)}$	$\frac{(2J-3)(2J+5)}{(36J^2-20J+5)}$
$\Delta j=-1$	$\frac{3(2J-1)(J+6)}{(110J^2+269J+174)}$	$\frac{-3(2J-1)(J+6)}{(58J^2+67J-6)}$	$\frac{3(J+6)}{(55J-6)}$
$\Delta j=-2$	$\frac{-3J(2J-1)}{(58J^2+139J+84)}$	$\frac{3(2J-1)}{(26J+29)}$	$\frac{-3}{29}$

Dropping a constant factor, our correlation function for calculation is

$$\mathbf{W}(\theta)=1+(\mathbf{R}/\mathbf{Q})\cos^2\theta+(\mathbf{S}/\mathbf{Q})\cos^4\theta.$$

TABLE III. *R/Q, for both transitions quadrupole.*

	$\Delta J=0$	$\Delta J=-1$	$\Delta J=-2$
$\Delta j=-2$	$\frac{-(2J-3)(2J+1)}{(2J+3)(6J+5)}$	$\frac{(J+3)}{(17J+15)}$	$\frac{1}{8}$
$\Delta j=-1$	$\frac{(5J-2)(2J-3)(2J+5)}{(20J^3+52J^2+41J+6)}$	$\frac{-(17J^2+17J-30)}{(35J^2+35J+6)}$	$\frac{(J-2)}{(17J+2)}$
$\Delta j=0$	$\frac{-(2J-3)(4J^2+4J-7)(2J+5)}{(2J-1)(2J+3)(4J^2+4J-1)}$	$\frac{(5J+7)(2J-3)(2J+5)}{(20J^3+8J^2-3J+3)}$	$\frac{-(2J+1)(2J+5)}{(2J-1)(6J+1)}$
$\Delta j=1$		$\frac{-(2J+3)(17J^3+69J^2-77J-105)}{(70J^4-9J^3-73J^2-27J-9)}$	$\frac{(2J+3)(J^2+18J+5)}{(34J^3-57J^2+8J+3)}$
$\Delta j=2$			$\frac{(J+1)(2J+3)(2J^2-9J+1)}{(2J-1)(16J^3-42J^2+29J+3)}$

	$\Delta J=2$	$\Delta J=1$
$\Delta j=-2$	$\frac{J(2J-1)(2J^2+13J+12)}{(2J+3)(16J^3+90J^2+161J+84)}$	$\frac{(2J-1)(J^2-16J-12)}{(34J^3+159J^2+224J+96)}$
$\Delta j=-1$		$\frac{-(2J-1)(17J^3-18J^2-164J-24)}{(70J^4+289J^3+374J^2+188J+24)}$

TABLE IV. *S/Q, for both transitions quadrupole.*

	$\Delta J=0$	$\Delta J=-1$	$\Delta J=-2$
$\Delta j=-2$	$\frac{4(J-1)(2J-3)}{3(2J+3)(6J+5)}$	$\frac{-4(2J-3)}{3(17J+15)}$	$\frac{1}{24}$
$\Delta j=-1$	$\frac{-16(J-1)(2J-3)(2J+5)}{3(20J^3+52J^2+41J+6)}$	$\frac{16(2J-3)(2J+5)}{3(35J^2+35J+6)}$	$\frac{-4(2J+5)}{3(17J+2)}$
$\Delta j=0$	$\frac{16(J-1)(J+2)(2J-3)(2J+5)}{3(2J-1)(2J+3)(4J^2+4J-1)}$	$\frac{-16(J+2)(2J-3)(2J+5)}{3(20J^3+8J^2-3J+3)}$	$\frac{4(J+2)(2J+5)}{3(2J-1)(6J+1)}$
$\Delta j=1$		$\frac{16(2J-3)(2J+3)(J+2)(2J+5)}{3(70J^4-9J^3-73J^2-27J-9)}$	$\frac{-4(2J+3)(J+2)(2J+5)}{3(34J^3-57J^2+8J+3)}$
$\Delta j=2$			$\frac{(J+1)(2J+3)(J+2)(2J+5)}{3(2J-1)(16J^3-42J^2+29J+3)}$

	$\Delta J=2$	$\Delta J=1$
$\Delta j=-2$	$\frac{J(2J-1)(J-1)(2J-3)}{3(2J+3)(16J^3+90J^2+161J+84)}$	$\frac{-4(2J-1)(J-1)(2J-3)}{3(34J^3+159J^2+224J+96)}$
$\Delta j=-1$		$\frac{16(2J-1)(J-1)(2J-3)(2.}{3(70J^4+289J^3+374J^2+188.}$

JULY 15, 1940 PHYSICAL REVIEW VOLUME 58

On Directional Correlation of Successive Quanta

DONALD R. HAMILTON*
Harvard University, Cambridge, Massachusetts

(Received May 6, 1940)

PHYSICAL REVIEW C **93**, 024301 (2016)

High-precision γ-ray spectroscopy of the cardiac PET imaging isotope ^{82}Rb and its impact on dosimetry

M. N. Nino,[1] E. A. McCutchan,[2] S. V. Smith,[3] C. J. Lister,[4] J. P. Greene,[5] M. P. Carpenter,[5] L. Muench,[3] A. A. Sonzogni,[2] and S. Zhu[5]

[1]*Department of Physics and Astronomy, Hofstra University, Hempstead, New York 11549, USA*
[2]*National Nuclear Data Center, Brookhaven National Laboratory, Upton, New York 11973, USA*
[3]*Collider Accelerator Department, Brookhaven National Laboratory, Upton, New York 11973, USA*
[4]*Department of Physics and Applied Physics, University of Massachusetts Lowell, Lowell, Massachusetts 01854, USA*
[5]*Physics Division, Argonne National Laboratory, Argonne, Illinois 60439, USA*

(Received 2 October 2015; revised manuscript received 21 December 2015; published 1 February 2016)

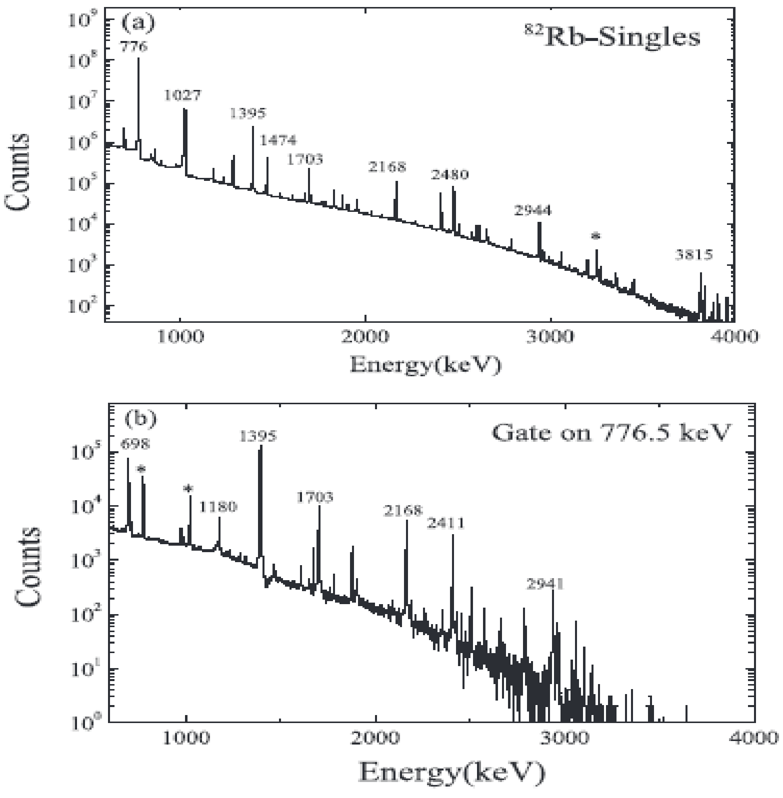

FIG. 1. (a) Singles spectrum from the decay of ^{82}Rb. (b) Spectrum obtained by gating on the 776-keV transition in ^{82}Kr. In both panels, strong transitions belonging to the decay of ^{82}Rb are labeled by their energy in keV, while background lines are indicated with a *.

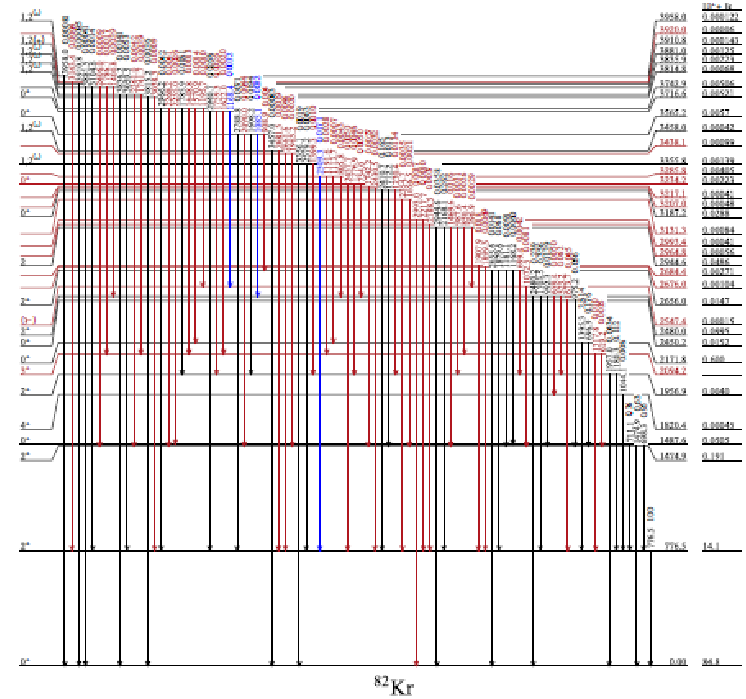

HIGH-PRECISION γ-RAY SPECTROSCOPY OF THE . . . PHYSICAL REVIEW C **93**, 024301 (2016)

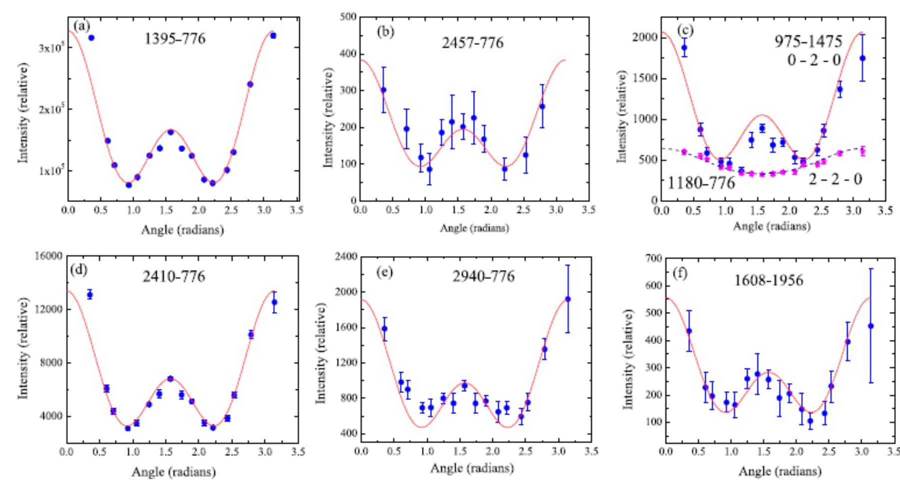

FIG. 6. Angular correlation analysis of confirmed and newly identified $0^+ \to 2^+ \to 0^+$ cascade transitions in ^{82}Kr. Solid circles give the measured intensity as a function of angle between detectors while solid lines are the theoretical predictions for a 0-2-0 sequence. Numbers in each panel give the cascade energies, in keV. In panel (c), the angular correlation of the 1180-776.5 cascade (stars) is given along with the theoretical predictions for a 2-2-0 sequence with $\delta = -0.52$ (dotted line).

Reaction mechanism itself can provide alignment of angular Momentum sub-states.

Should see angular DISTRIBUTIONS following Fusion-evaporation reactions.

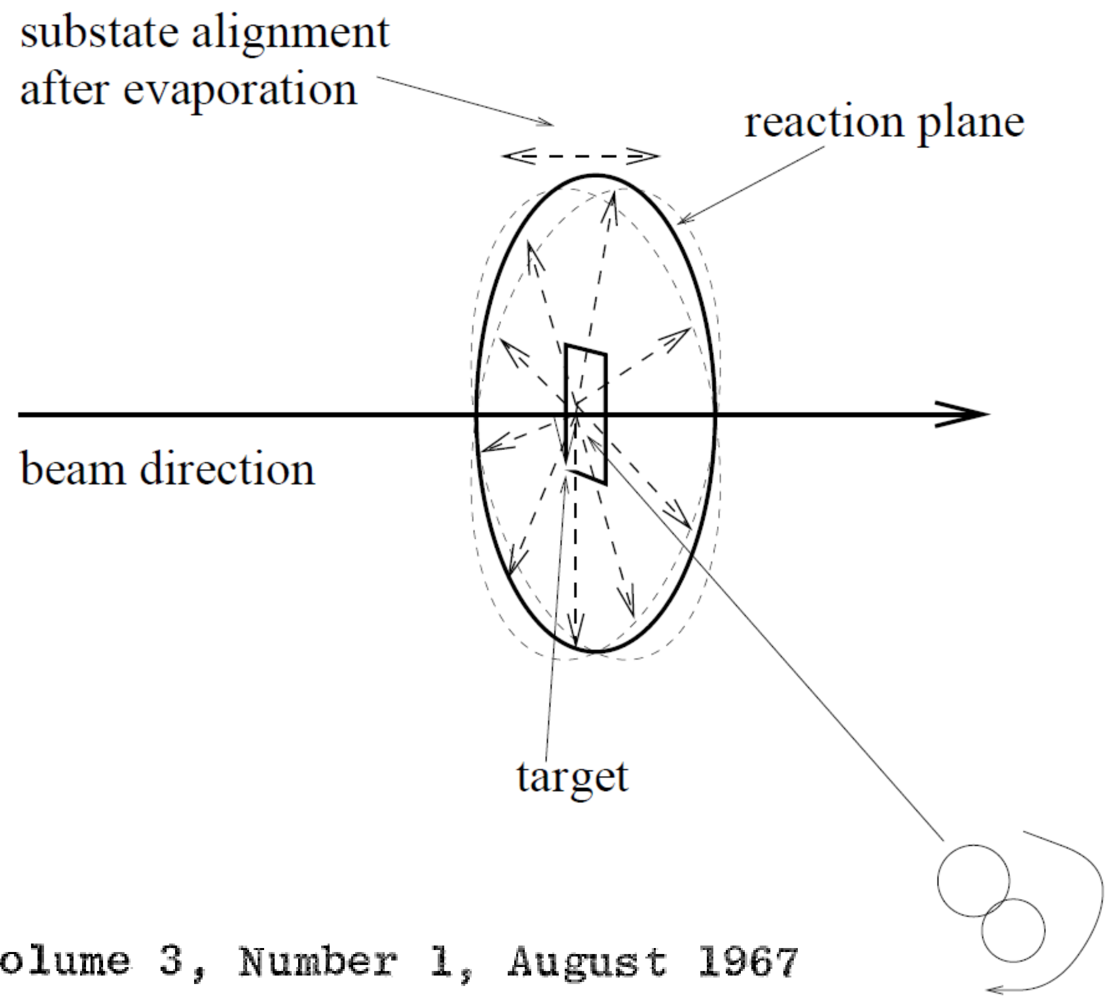

NUCLEAR DATA, Section A, Volume 3, Number 1, August 1967

TABLES OF COEFFICIENTS FOR ANGULAR DISTRIBUTION OF GAMMA RAYS FROM ALIGNED NUCLEI *

T. YAMAZAKI

Lawrence Radiation Laboratory,
University of California, Berkeley, California

$$W(\theta) = \sum_k A_k P_k(\cos\theta)$$

For ΔI=2 EM transitions, the singles angular distribution is of the form:

$$W(\theta) = A_0 \{1 + A_2 P_2(\cos\theta) + A_4 P_4(\cos\theta)\}$$

$$P_2(\cos\theta) = \frac{1}{2}(3\cos^2\theta - 1)$$

$$P_4(\cos\theta) = \frac{1}{8}(35\cos^4\theta - 30\cos^2\theta + 3)$$

E Der Mateosian and A.W. Sunyar, *Atomic Data and Nuclear Data Tables* **13** (1974) p407

K.S. Krane, R.M. Steffen and R.M. Wheeler, *Nuclear Data Tables* **11** (1973) p351

$$A = 2\left(\frac{W(37^\circ) - W(79^\circ)}{W(37^\circ) + W(79^\circ)}\right)$$

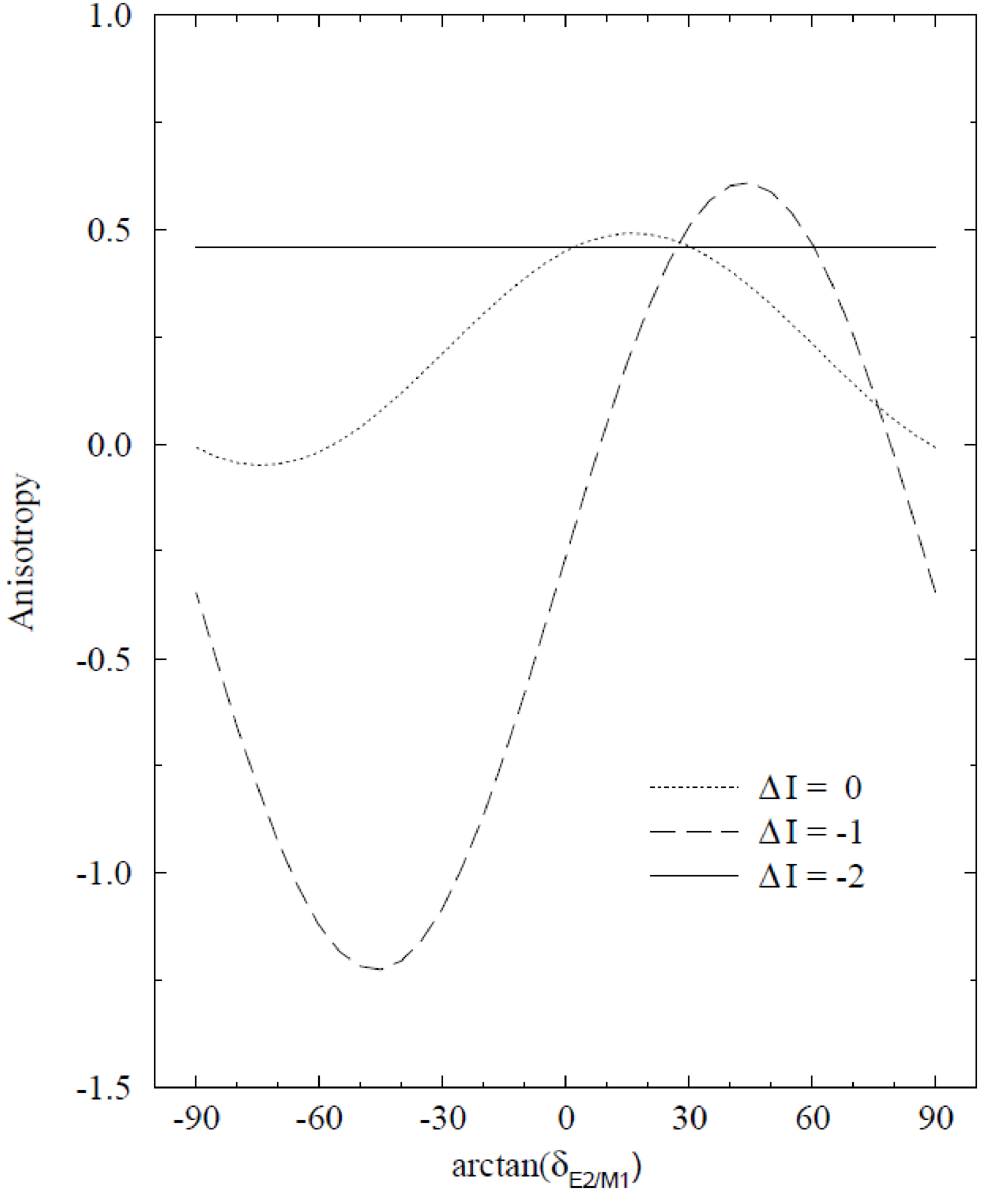

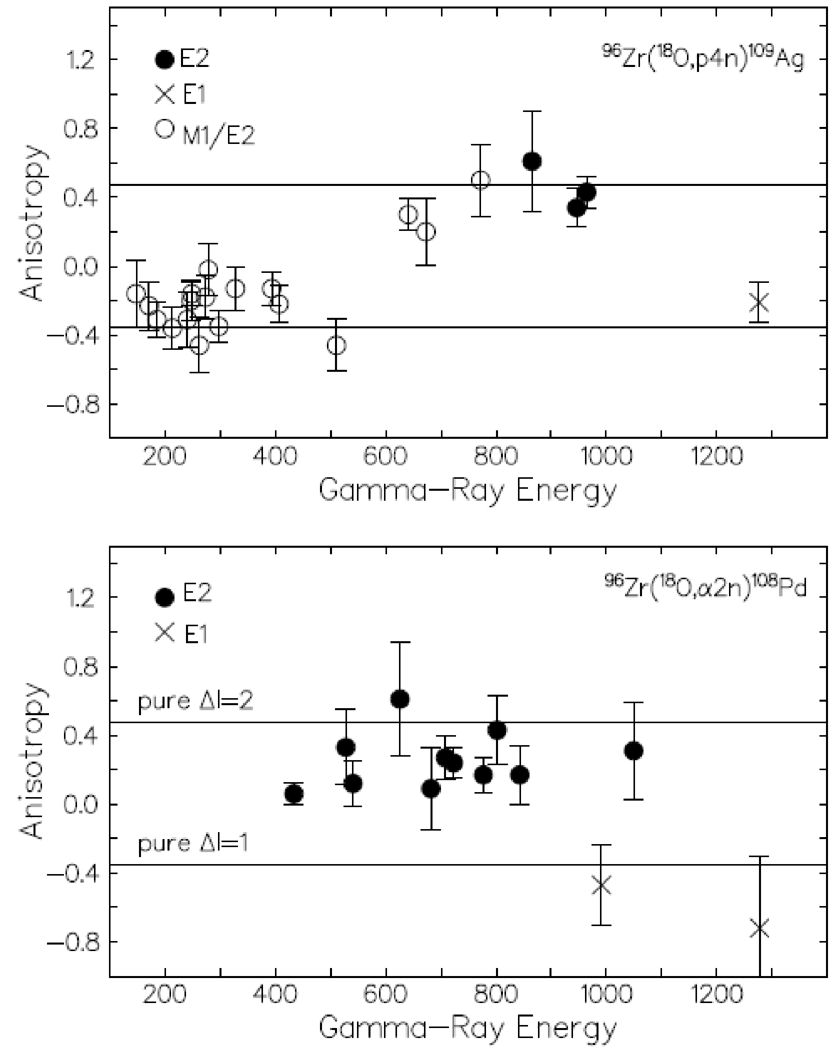

K.R. Pohl *et al.* *Phys. Rev.* **C53** (1996) p2682

EM Transition rates

Nuclear EM transition rates between excited states are <u>fundamental</u> in nuclear structure research.

$$T_{fi} = \frac{1}{\tau} = \frac{8\pi(L+1)}{\hbar\left((2L+1)!!\right)^2}\left(\frac{E_\gamma}{\hbar c}\right)^{2L+1} B\left(\lambda L: I_i \to I_f\right)$$

The extracted ***reduced matrix elements***, *B(λL)* give insights e.g.,

- Single particle / shell model-like: ~ 1 Wu (NOT for E1s)
- Deformed / collective: faster lifetimes, ~10s to 1000s of Wu (in e.g., superdeformed bands)
- Show underlying symmetries and related selection rules such as K-isomerism: MUCH slower decay rates ~ $10^{-3\to 9}$ Wu and slower).

$$T(E2) = 1.223 \times 10^9 E_\gamma^5 B(E2)$$

T(E2) = transition probability = 1/τ (secs);
E_γ = transition energy in MeV

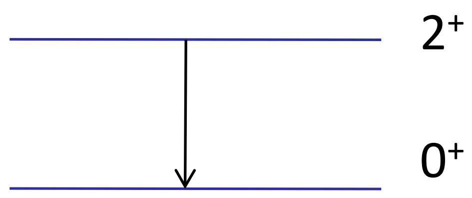

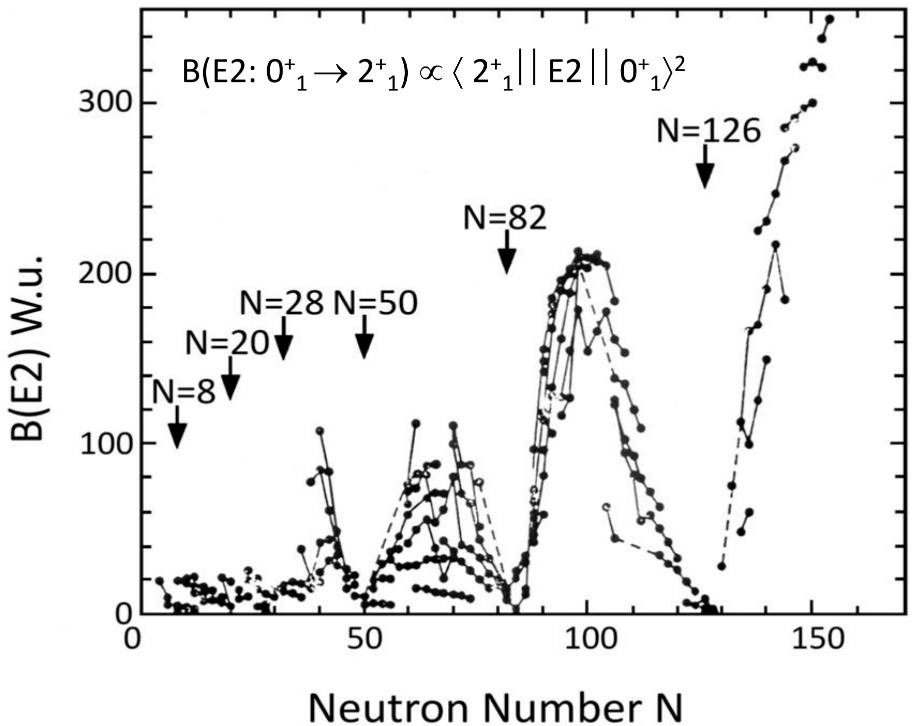

Qo = (TRANSITION) ELECTRIC QUADRUPOLE MOMENT.

This is intimately linked to the electrical charge (i.e. proton) distribution within the nucleus.

Non-zero Qo means some deviation from spherical symmetry and thus some quadrupole 'deformation'.

The nuclear rotational model: B(E2: I→I-2) gives Qo by:

$$B(E2) = \frac{5}{16\pi} Q_o^2 \frac{3(I-K)(I-K-1)(I+K)(I+K-1)}{(2J-2)(2J-1)J(2J+1)}$$

PHYSICAL REVIEW C 69, 034317 (2004)

Transition from the seniority regime to collective motion

J. J. Ressler,[1] R. F. Casten,[1] N. V. Zamfir,[1] C. W. Beausang,[1] R B. Cakirli,[1,2] H. Ai,[1] H. Amro,[1] M. A. Caprio,[1] A. A. Hecht,[1] A. Heinz,[1] S. D. Langdown,[1,3] E. A. McCutchan,[1] D. A. Meyer,[1] C. Plettner,[1] P. H. Regan,[1,3] M. J. S. Sciacchitano,[1] and A. D. Yamamoto[1,3]
[1]Wright Nuclear Structure Laboratory, Yale University, New Haven, Connecticut 06520-8124, USA
[2]Istanbul University, 34459 Vezneciler-Istanbul, Turkey
[3]University of Surrey, Guilford, Surrey GU2 7XH, United Kingdom
(Received 17 September 2003; published 15 March 2004)

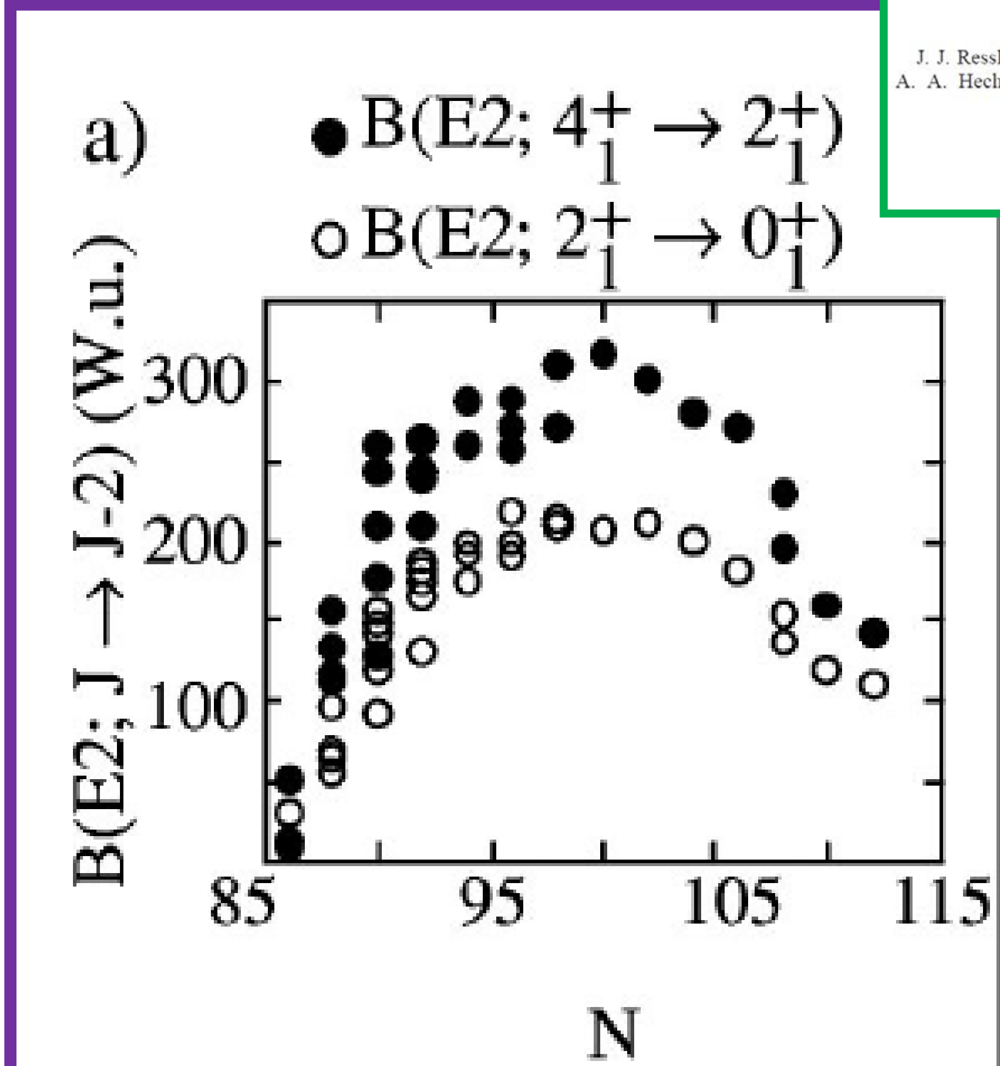

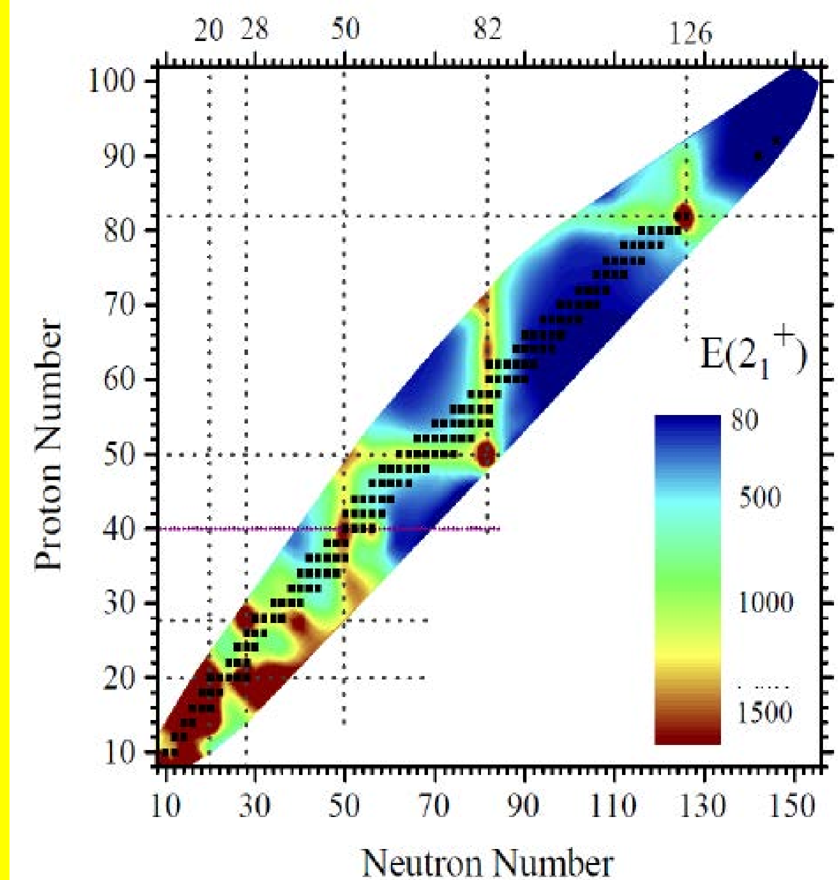

B(E2) values for low-lying even-even nuclei with Z =62 (Sm) – 74 (W).
Very 'collective' transitions (>100 Wu) with maximum B(E2) at mid-shell.
This correlates with the lowest E(2^+) excitation energy values.

Atomic Data and Nuclear Data Tables **78,** 1–128 (2001)
doi:10.1006/adnd.2001.0858, available online at http://www.idealibrary.com on IDEAL®

TRANSITION PROBABILITY FROM THE GROUND TO THE FIRST-EXCITED 2^+ STATE OF EVEN–EVEN NUCLIDES*

S. RAMAN, C. W. NESTOR, JR., and P. TIKKANEN†

Physics Division, Oak Ridge National Laboratory, Oak Ridge, Tennessee 37831

Adopted values for the reduced electric quadrupole transition probability, $B(E2)\uparrow$, from the ground state to the first-excited 2^+ state of even–even nuclides are given in Table I. Values of τ, the mean life of the 2^+ state; E, the energy; and β, the quadrupole deformation parameter, are also listed there. The ratio of β to the value expected from the single-particle model is presented. The intrinsic quadrupole moment, Q_0, is deduced from the $B(E2)\uparrow$ value. The product $E \times B(E2)\uparrow$ is expressed as a percentage of the energy-weighted total and isoscalar $E2$ sum-rule strengths.

Table II presents the data on which Table I is based, namely the experimental results for $B(E2)\uparrow$ values with quoted uncertainties. Information is also given on the quantity measured and the method used. The literature has been covered to November 2000.

The adopted $B(E2)\uparrow$ values are compared in Table III with the values given by systematics and by various theoretical models. Predictions of unmeasured $B(E2)\uparrow$ values are also given in Table III.

EXPLANATION OF TABLES

TABLE I. Adopted Values of $B(E2)\uparrow$ and Related Quantities

Throughout this table, italicized numbers refer to the uncertainties in the last digits of the quoted values.

Nuclide — The even Z, even N nuclide studied

E(level) — Energy of the first excited 2^+ state in keV either from a compilation or from current literature

$B(E2)\uparrow$ — Reduced electric quadrupole transition rate for the ground state to 2^+ state transition in units of e^2b^2

τ — Mean lifetime of the state in ps

$\tau = 40.81 \times 10^{13} E^{-5}[B(E2)\uparrow/e^2b^2]^{-1}(1+\alpha)^{-1}$ (see Table II for the α values when $\alpha > 0.001$)

β — Deformation parameter

$$\beta = (4\pi/3ZR_0^2)[B(E2)\uparrow/e^2]^{1/2}, \text{ where}$$
$$R_0^2 = (1.2 \times 10^{-13} A^{1/3} \text{ cm})^2$$
$$= 0.0144 A^{2/3} \text{ b}$$

$\beta_{(sp)}$ — β from the single-particle model

$$\beta_{(sp)} = 1.59/Z$$

Q_0 — Intrinsic quadrupole moment in b

$$Q_0 = \left[\frac{16\pi}{5}\,\frac{B(E2)\uparrow}{e^2}\right]^{1/2}$$

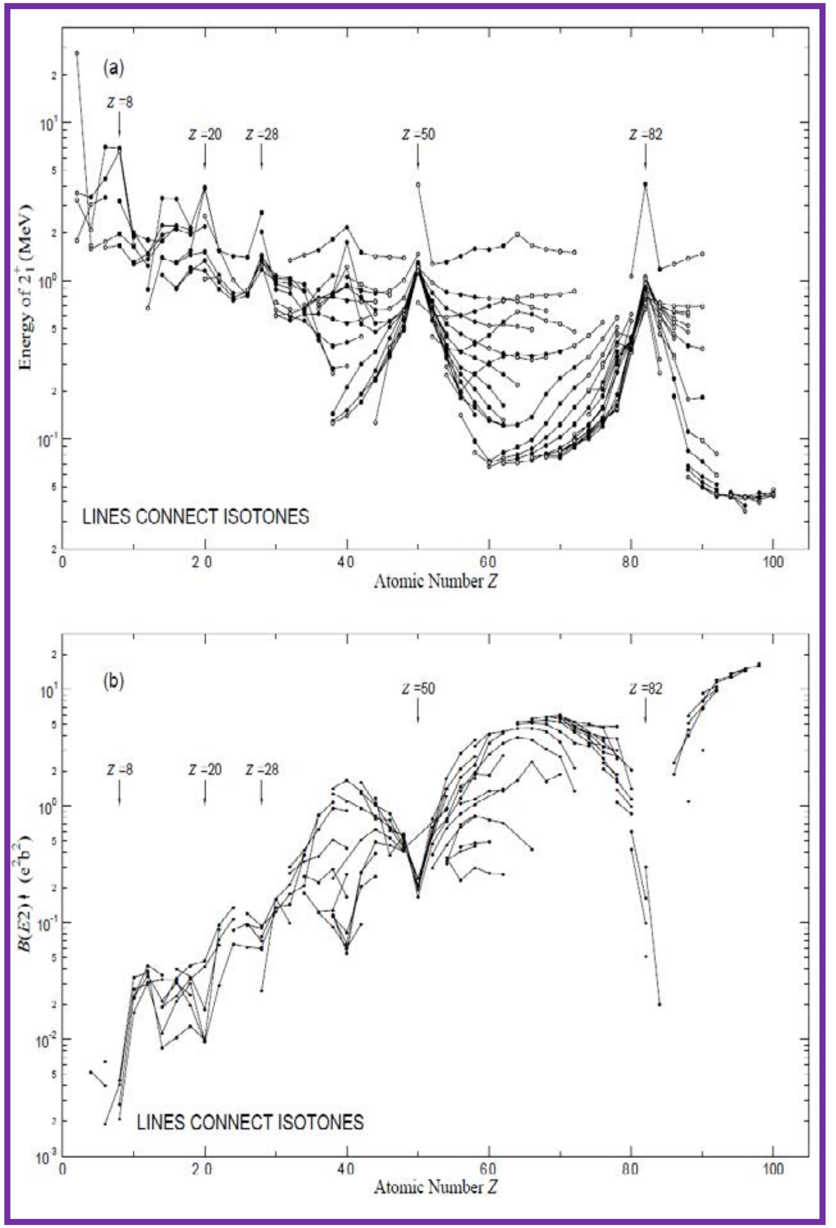

Some good recent reviews; useful references and equations..

Phys. Scr. **T152** (2013) 014015 (20pp)

Isomers, nuclear structure and spectroscopy

G D Dracoulis

Department of Nuclear Physics, RSPE Australian National University, Canberra, ACT 0200, Australia

Atomic Data and Nuclear Data Tables 103–104 (2015) 50–105

ELSEVIER

Atomic Data and Nuclear Data Tables

journal homepage: www.elsevier.com/locate/adt

Configurations and hindered decays of K isomers in deformed nuclei with A > 100

F.G. Kondev [a,*], G.D. Dracoulis [b,1], T. Kibédi [b]

[a] *Nuclear Engineering Division, Argonne National Laboratory, Argonne, IL 60439, USA*

[b] *Department of Nuclear Physics, Research School of Physics and Engineering, The Australian National University, Canberra, ACT 2601, Australia*

IOP Publishing

Reports on Progress in Physics

Rep. Prog. Phys. **79** (2016) 076301 (46pp)

doi:10.1088/0034-4885/79/7/076301

Review

Review of metastable states in heavy nuclei

G D Dracoulis[1,4], P M Walker[2] and F G Kondev[3]

[1] Department of Nuclear Physics, R.S.P.E. Australian National University, Canberra, A.C.T. 0200, Australia

[2] Department of Physics, University of Surrey, Guildford, Surrey GU2 7XH, UK

[3] Nuclear Engineering Division, Argonne National Laboratory, Argonne, IL 60439, USA

E-mail: P.Walker@Surrey.ac.uk and kondev@anl.gov

Received 13 June 2015, revised 13 April 2016
Accepted for publication 18 April 2016
Published 31 May 2016

CrossMark

Weisskopf Single Particle Estimates:

- These are 'yardstick' estimates for the speed of EM transitions for a given electromagnetic multipole order.
- They depend on the size of the nucleus (i.e., A) and the energy of the transition / gamma-ray energy (E_γ^{2L+1})
- They estimate the transition rate for spherically symmetric proton orbitals for nuclei of radius $r=r_0A^{1/3}$.

The ***half-life*** (in 10^{-9}s), equivalent to 1 Wu is given by (DWK):

$$T_{1/2}(E1) = 6.76 \times A^{-2/3}E^{-3} \times 10^{-6}$$
$$T_{1/2}(M1) = 2.20 \times E^{-3} \times 10^{-5}$$
$$T_{1/2}(E2) = 9.52 \times A^{-4/3}E^{-5}$$
$$T_{1/2}(M2) = 3.10 \times A^{-2/3}E^{-5} \times 10^{1}$$
$$T_{1/2}(E3) = 2.04 \times A^{-2}E^{-7} \times 10^{7}$$

where the transition energy E is in MeV and A is the atomic mass number

Weisskopf, V.F., 1951. *Radiative transition probabilities in nuclei.* Physical Review, **83**(5), 1073.

Transition rates can be described in terms of '**Weisskopf Estimates**'.

Classical estimates based on pure, spherical proton orbital transitions.

1 Wu is 'normal' expected (single particle) transition rate.....(sort of....)

where K is the low frequency dielectric constant, K_0 is the optical constant, ρ the density, and χ the compressibility. In Table I are listed the values of $\partial \ln K/\partial p$ calculated from (4) and (1) next to the experimental values of $\partial \ln K/\partial p$. The calculated values of $\partial \ln K/\partial p$ differ from those of Rao by the term $a(K-K_0)/K$, which arises from the difference between (1a) and (2a).

Equation (4) is derived assuming that the inner field polarizing the dielectric is independent of pressure. Since the values of $-\partial \ln K/\partial p$ obtained from (4) do not account for all the change in the dielectric constant, it seems consistent to expect that the inner field is not constant but does decrease with increasing pressure. This conclusion agrees with the one reached in my original paper using the theories of Hojendahl and Mott and Littleton.

[1] D. A. A. S. Narayana Rao, Phys. Rev. **82**, 118 (1951).
[2] S. Mayburg, Phys. Rev. **79**, 375 (1950).

Radiative Transition Probabilities in Nuclei

V. F. Weisskopf
Physics Department, Massachusetts Institute of Technology, Cambridge, Massachusetts
(Received July 20, 1951)

CONSIDER a transition from nuclear state a to nuclear state b with emission of a quantum of multipole radiation of angular momentum l (2^l-pole) and z component m. The transition probability per unit time is given by[1]

$$T(l,m)=\frac{8\pi(l+1)}{l[(2l+1)!!]^2}\frac{\kappa^{2l+1}}{\hbar}|A(l,m)+A'(l,m)|^2, \tag{1}$$

where $\kappa=2\pi\nu/c$ is the wave number of the emitted radiation, and the quantities A, A' are the multipole matrix elements caused by the electric currents and by the magnetization (spins), respectively. We find for electric radiation

$$A(l,m)=Q(l,m)=e\sum_{k=1}^{Z}\int r_k^l Y_{lm}^*(\theta_k,\phi_k)\,\varphi_b^*\varphi_a\,d\tau, \tag{2}$$

$$A'(l,m)=Q'(l,m)=-\frac{i\kappa}{l+1}\frac{e\hbar}{2Mc}\sum_{k=1}^{A}\mu_k \times\int r_k^l Y_{lm}^*(\theta_k,\phi_k)\,\mathrm{div}(\varphi_b^*\mathbf{r}_k\times\boldsymbol{\sigma}_k\varphi_a)\,d\tau, \tag{3}$$

where φ_a and φ_b are the wave functions of the nuclear states, M is the mass of each nucleon, $\mathbf{r}_k=(r_k,\theta_k,\phi_k)$ is the position vector of the kth nucleon, $\boldsymbol{\sigma}_k$ is its Pauli spin vector, and μ_k is its magnetic moment in nuclear magnetons. The sum in (2) extends over the protons, the sum in (3) over both protons and neutrons. These expressions are approximations valid for $\kappa R\ll 1$, where R is the nuclear radius.

The corresponding expressions for magnetic multipole radiation are

$$A(l,m)=M(l,m)=-\frac{1}{l+1}\frac{e\hbar}{Mc}\sum_{k=1}^{Z} \times\int r_k^l Y_{lm}^*(\theta_k,\phi_k)\,\mathrm{div}(\varphi_b^*\mathbf{L}_k\varphi_a)\,d\tau, \tag{4}$$

$$A'(l,m)=M'(l,m)=-\frac{e\hbar}{2Mc}\sum_{k=1}^{A}\mu_k \times\int r_k^l Y_{lm}^*(\theta_k,\phi_k)\,\mathrm{div}(\varphi_b^*\boldsymbol{\sigma}_k\varphi_a)\,d\tau, \tag{5}$$

where $\mathbf{L}_k=-i\mathbf{r}_k\times\nabla_k$ is the orbital angular momentum operator (in units of $\hbar$) for the kth nucleon.

We can estimate these matrix elements by the following exceedingly crude method. We assume that the radiation is caused by a transition of one single proton which moves independently within the nucleus, its wave function being given by $u(r)Y_{lm}(\theta,\phi)$. In addition we also assume that the final state of the proton is an S state.[2] We then obtain

$$Q(l,m)\sim[e/(4\pi)^{\frac{1}{2}}][3/(l+3)]R^l \tag{6}$$

where the integral $\int r^l u_b(r)u_a(r)r^2dr$ over the radial parts of the proton wave functions was set approximately equal to $3R^l/(l+3)$. The other matrix elements are estimated by replacing div by R^{-1}. We get the rough order-of-magnitude guess

$$M(l,m)\sim[e/(4\pi)^{\frac{1}{2}}][3/(l+3)][\hbar/Mc]R^{l-1}, \tag{7}$$

$$M'(l,m)\sim[e/(4\pi)^{\frac{1}{2}}][3/(l+3)]\mu_P[\hbar/Mc]R^{l-1}, \tag{8}$$

where μ_P is the magnetic moment of the proton ($=2.78$). $Q'(l,m)$ can be neglected compared to $Q(l,m)$. We therefore get a ratio of roughly

$$(1+\mu_P^2)(\hbar/McR)^2\sim 10(\hbar/McR)^2$$

between the transition probability of a magnetic multipole and an electric one of the same order. This ratio is energy-independent in contrast to widespread belief.

Inserting these estimates into (1) we get for the transition probability of an electric 2^l-pole

$$T_E(l)\cong\frac{4.4(l+1)}{l[(2l+1)!!]^2}\left(\frac{3}{l+3}\right)^2\left(\frac{\hbar\omega}{197\text{ Mev}}\right)^{2l+1} \times(R\text{ in }10^{-13}\text{ cm})^{2l}\,10^{21}\text{ sec}^{-1} \tag{9}$$

and for a magnetic 2^l-pole

$$T_M(l)\cong\frac{1.9(l+1)}{l[(2l+1)!!]^2}\left(\frac{3}{l+3}\right)^2\left(\frac{\hbar\omega}{197\text{ Mev}}\right)^{2l+1} \times(R\text{ in }10^{-13}\text{ cm})^{2l-2}\,10^{21}\text{ sec}^{-1}. \tag{10}$$

The assumptions made in deriving these estimates are extremely crude and they should be applied to actual transitions with the greatest reservations. They are based upon an extreme application of the independent-particle model of the nucleus and it was assumed that a proton is responsible for the transition. On the basis of our assumptions the electric multipole radiation with $l>1$ should be much weaker for transitions in which a single neutron changes its quantum state. No such differentiation is apparent in the data.

In spite of these difficulties it may be possible that the order of magnitude of the actual transition probabilities is correctly described by these formulas. We have published these exceedingly crude estimates only because of the rather unexpected agreement with the experimental material which was pointed out to us by many workers in this field.

The author wishes to express his appreciation especially to Dr. M. Goldhaber and Dr. J. M. Blatt for their great help in discussing the experimental material and in improving the theoretical reasoning.

[1] We use the notation $(2l+1)!!=1\cdot 3\cdot 5\cdots(2l+1)$.
[2] This latter assumption can be removed; the corrections consist in unimportant numerical factors.

Nuclear Magnetic Resonance in Metals: Temperature Effects for Na^{23}

H. S. Gutowsky
*Noyes Chemical Laboratory, Department of Chemistry, University of Illinois, Urbana, Illinois**
(Received July 2, 1951)

KNIGHT reported[1] that nuclear magnetic resonance frequencies are higher in metals than in chemical compounds. It has been proposed[2] that such frequency shifts are primarily the result of the contribution of conduction electrons to the magnetic field at the nuclei in the metal. This note gives an account of some related preliminary results including temperature and chemical effects, and also detailed line shape studies. Our experiments have been at fixed frequency using equipment and procedures outlined previously.[3,4]

The effect of temperature on the Na^{23} magnetic resonance shift in the metal, relative to a sodium chloride solution, is given in

Multipolarity	Electric Transition Rate (s^{-1})	Magnetic Transition Rate (s^{-1})
1	$1.587 \times 10^{15}\ E_\gamma^3\ B(E1)$	$1.779 \times 10^{13}\ E_\gamma^3\ B(M1)$
2	$1.223 \times 10^{9}\ E_\gamma^5\ B(E2)$	$1.371 \times 10^{7}\ E_\gamma^5\ B(M2)$
3	$5.689 \times 10^{2}\ E_\gamma^7\ B(E3)$	$6.387 \times 10^{0}\ E_\gamma^7\ B(M3)$
4	$1.649 \times 10^{-4}\ E_\gamma^9\ B(E4)$	$1.889 \times 10^{-6}\ E_\gamma^9\ B(M4)$
5	$3.451 \times 10^{-11}\ E_\gamma^{11}\ B(E5)$	$3.868 \times 10^{-13}\ E_\gamma^{11}\ B(M5)$

Table 2.2: Transition probabilities $T(s^{-1})$ expressed by $B(EL)$ in $(e^2(fm)^{2L})$ and $B(ML)$ in $(\frac{e\hbar}{2mc}(fm)^{2L-2})$. E_γ is the γ-ray energy, in MeV. (Taken from ref [69]).

Transition rates get slower (i.e., longer lifetimes associated with) higher order multipole decays

Zs. Podolyak et al., Phys. Lett. **B672** (2009) 116

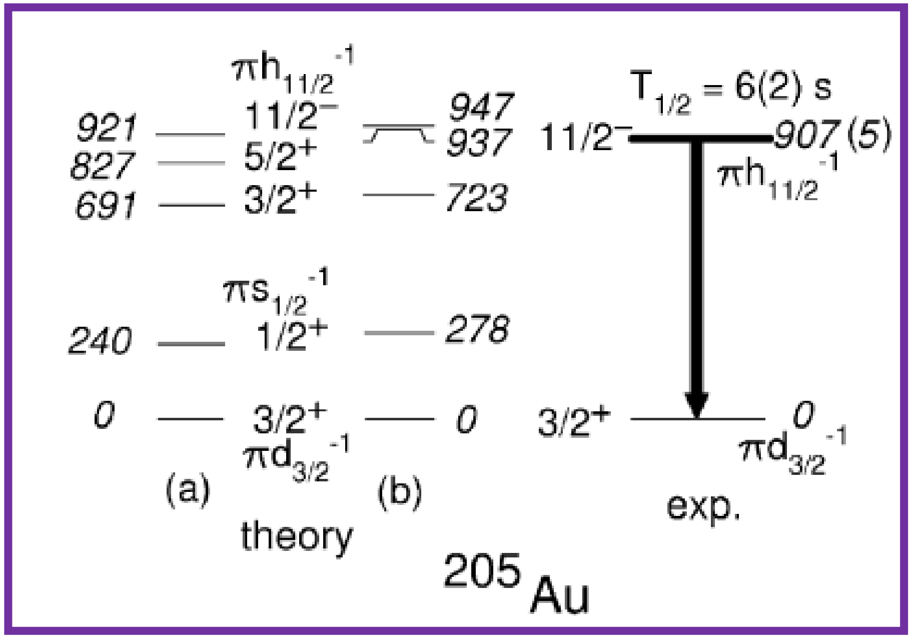

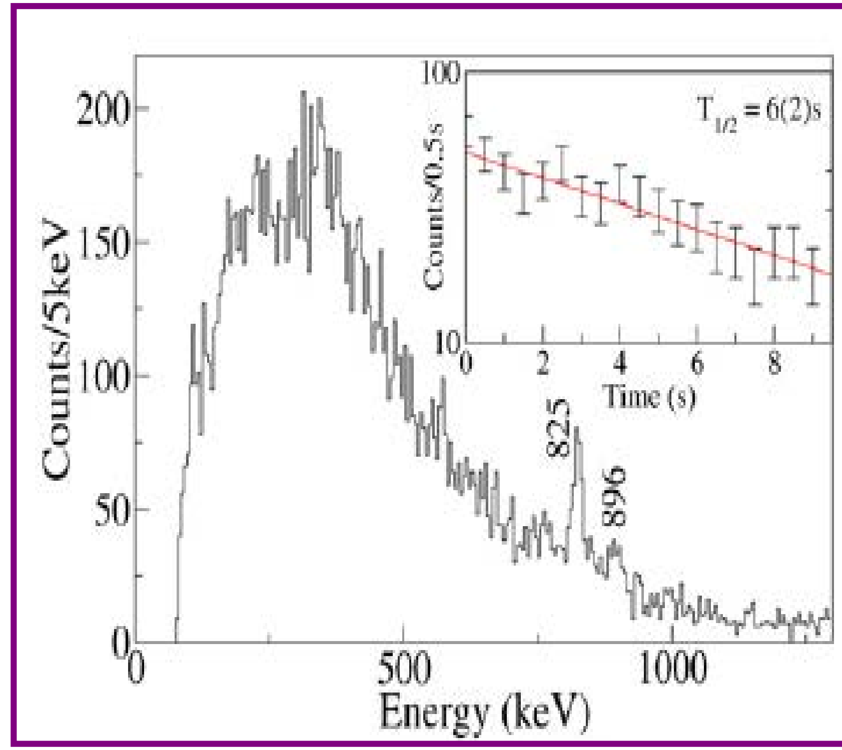

N=126 ; Z=79. Odd, single proton transition; $h_{11/2} \rightarrow d_{3/2}$ state (holes in Z=82 shell).

Angular momentum selection rule says lowest multipole decay allowed is

$\lambda = (11/2 - 3/2) = \Delta L = 4$

Change of parity means lowest must transition be M4.

1Wu 907 keV M4 in ^{205}Au has $T_{1/2}$= 8 secs; corresponding to a near 'pure' single-particle (proton) transition from ($h_{11/2}$) $11/2^-$ state to ($d_{3/2}$) $3/2^+$ state.

(Decay here is observed following INTERNAL CONVERSION).
These competing decays to gamma emission are often observed in isomeric decays

Determination of excited states lifetimes, depends on.... the lifetime ☺

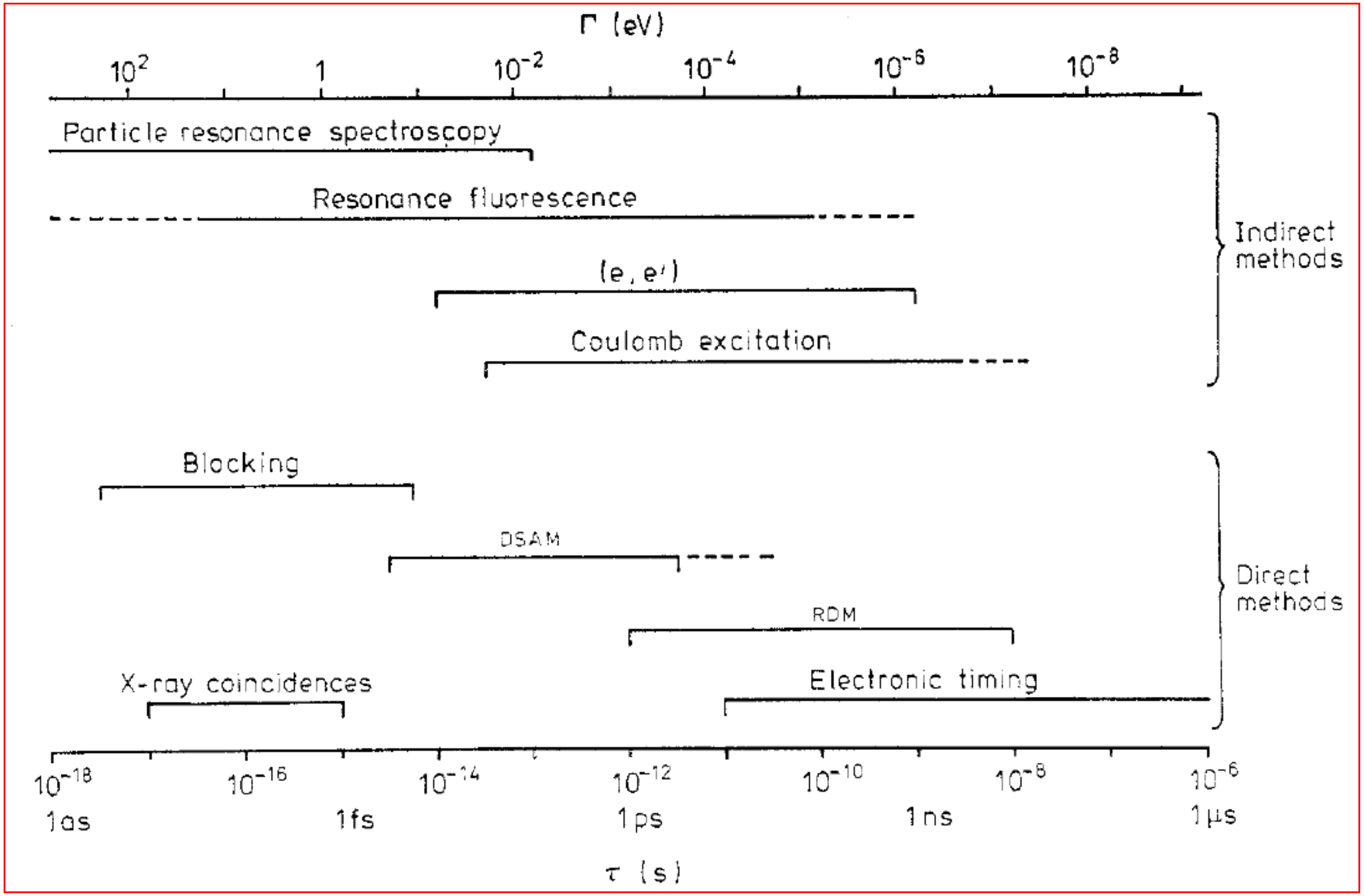

Rep. Prog. Phys., Vol. 42, 1979.

The measurement of the lifetimes of excited nuclear states

P J NOLAN† and J F SHARPEY-SCHAFER‡

$$\Gamma \propto \left|\langle \psi_f | \hat{O}_{\mathrm{decay}} | \psi_i \rangle\right|^2$$

$$\Gamma \tau = \hbar.$$

Direct extraction of excited state lifetimes.

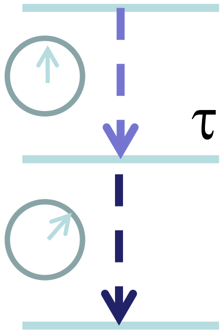

- Assuming no background contribution, the measured, 'delayed' time distribution for a E_γ–E_γ–Δt measurement is given by:

$$\boxed{D(t) = n\lambda \int_{-\infty}^{t} P(t' - t_0) e^{-\lambda(t - t')} dt' \quad \text{with} \quad \lambda = 1/\tau,}$$

$P(t'-t_0)$ is the (Gaussian) prompt response function

τ is the **mean lifetime** of the intermediate state.

See e.g., Z. Bay, Phys. Rev. **77** (1950) p419;
T.D. Newton, Phys. Rev. **78** (1950) p490;
J.M.Regis et al., EPJ Web of Conf. **93** (2015) 01014

The time distribution *D(t)* is the **convolution** of the **prompt response function** of the detector pair & the **exponential decay lifetime**.

$$D(t) = \int_{-\infty}^{t} P(x) \times e^{-\frac{t}{\tau}} \, dx$$

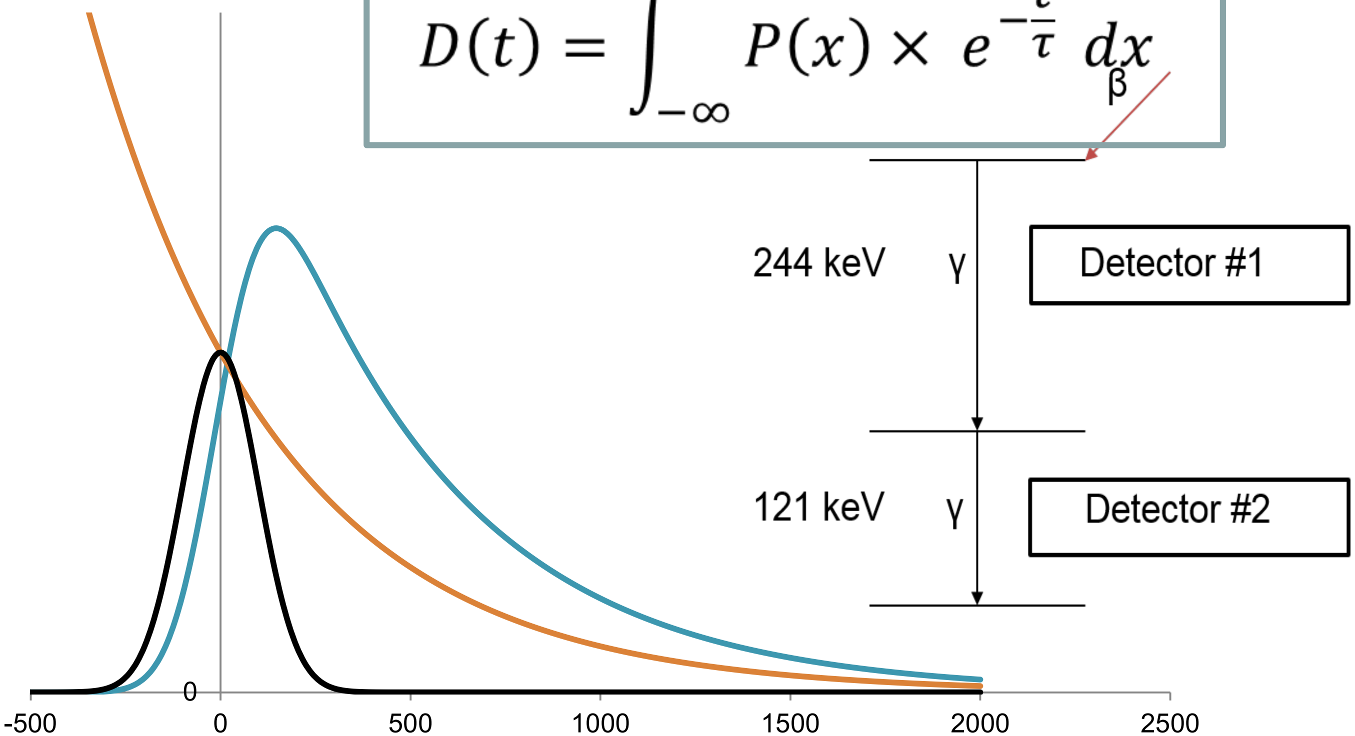

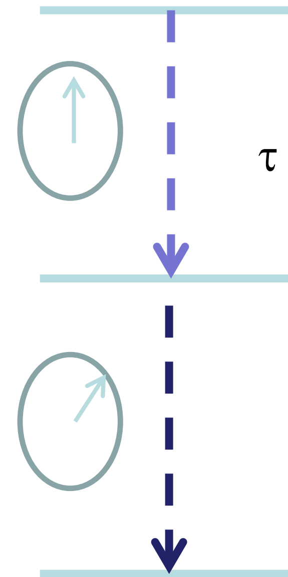

Deconvolution and (time difference function lineshapes).

If the instrument time response function R(t) is Gaussian of width σ,

$$\boxed{R(t) = A_1 \exp\left(-\frac{t^2}{2\sigma^2}\right)}$$

If the intermediate state decays with a mean lifetime τ, then

$$\boxed{S(t) = A_2 \exp\left(-\frac{t}{\tau}\right)}$$

Ignoring normalisations, the deconvolution integral is given by:

$$\boxed{I(t) = \exp\left(\frac{\sigma^2}{2\tau^2} - \frac{t}{\tau}\right)\left(1 - \operatorname{erf}\left(\frac{\sigma^2 - \tau t}{\sqrt{2}\sigma\tau}\right)\right)}$$

1-erf(x) is the complementary error function of x.

The lifetimes that can be measured depends on **σ/τ** ratio.

Timing resolution (i.e., faster responses) needed for short lifetimes.

HPGe have ~ a few ns limit using this method;

$LaBr_3(Ce)$ detectors can get down to lifetimes of <50 ps.

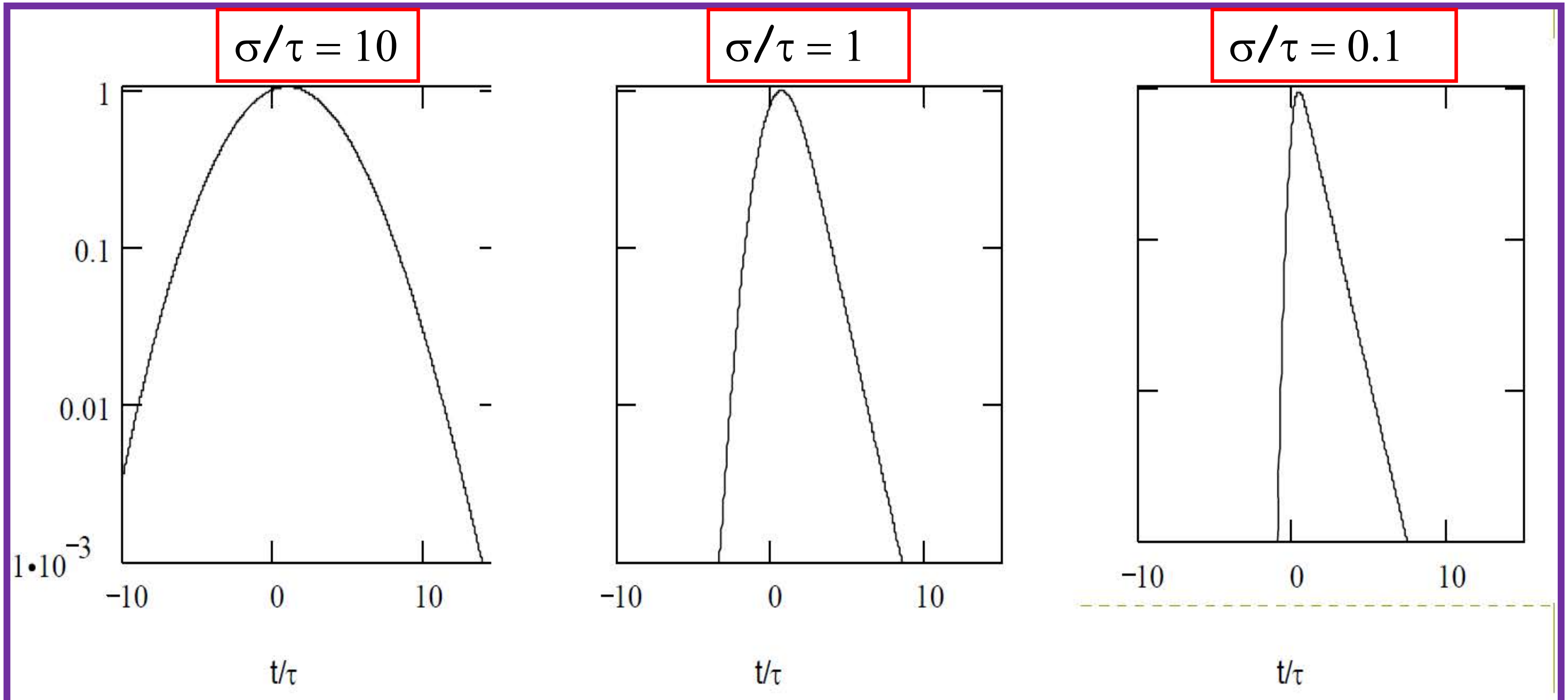

An example, 'fast-timing' and id of M2 decay in ^{34}P.

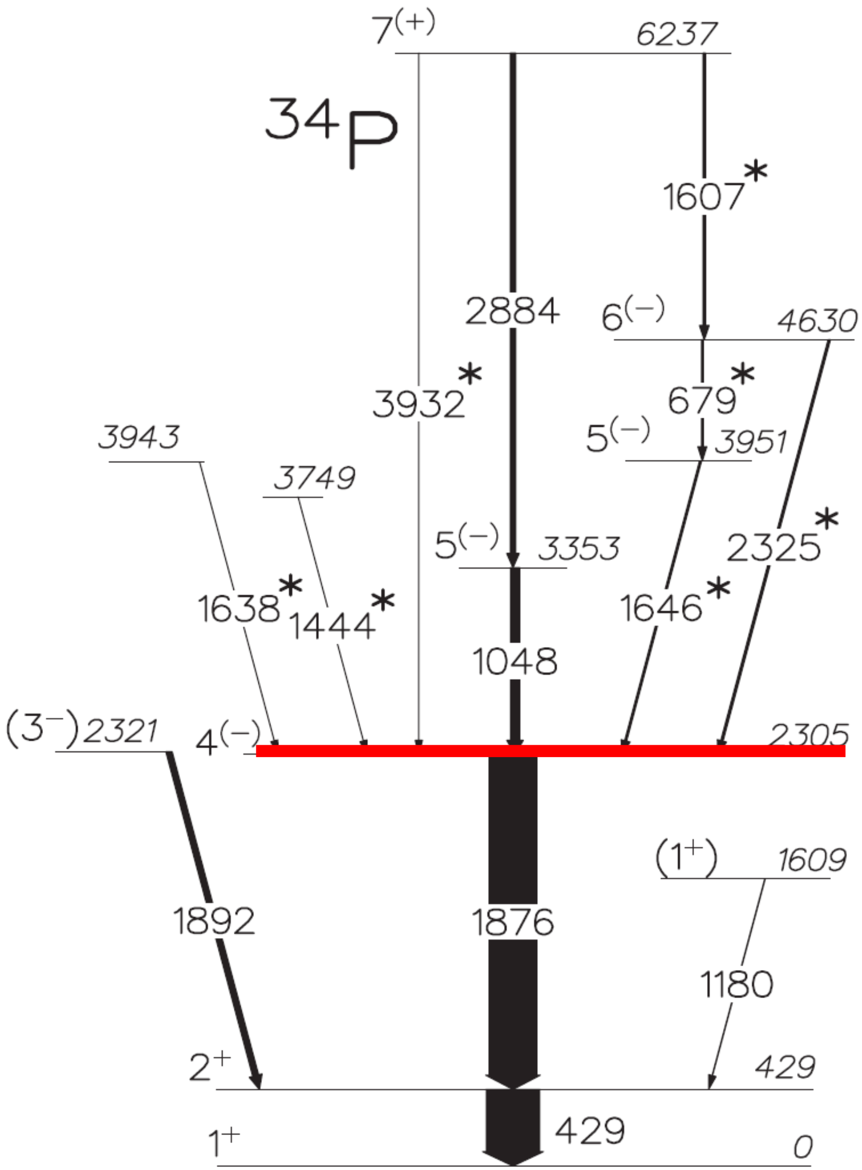

P. C. BENDER et al. PHYSICAL REVIEW C 80, 014302 (2009)

R. CHAKRABARTI et al. PHYSICAL REVIEW C 80, 034326 (2009)

- Study of ^{34}P identified low-lying $I^{\pi}=4^{-}$ state at E=2305 keV.
- $I^{\pi}=4^{-} \rightarrow 2^{+}$ transition can proceed by M2 and/or E3.
- Aim of experiment was to measure precision lifetime for 2305 keV state and obtain B(M2) and B(E3) values.
- Previous studies limit half-life to 0.3 ns < $t_{1/2}$ < 2.5ns

P.J.R.Mason et al., Phys. Rev. C85 (2012) 064303.

Ge-Gated Time differences

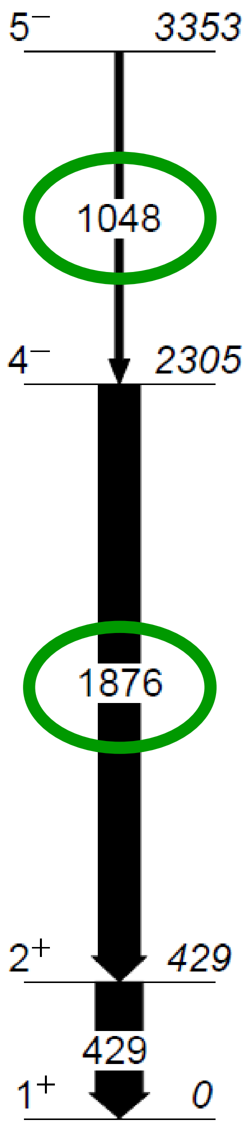

PHYSICAL REVIEW C **85**, 064303 (2012)

Half-life of the $I^{\pi} = 4^{-}$ intruder state in ^{34}P: $M2$ transition strengths approaching the island of inversion

P. J. R. Mason,[1] T. Alharbi,[1,2] P. H. Regan,[1] N. Mărginean,[3] Zs. Podolyàk,[1] E. C. Simpson,[1] N. Alkhomashi,[4] P. C. Bender,[5] M. Bowry,[1] M. Bostan,[6] D. Bucurescu,[3] A. M. Bruce,[7] G. Căta-Danil,[3] I. Căta-Danil,[3] R. Chakrabarti,[8] D. Deleanu,[3] P. Detistov,[9] M. N. Erduran,[10] D. Filipescu,[3] U. Garg,[11] T. Glodariu,[3] D. Ghiţă,[3] S. S. Ghugre,[8] A. Kusoglu,[6] R. Mărginean,[3] C. Mihai,[3] M. Nakhostin,[1] A. Negret,[3] S. Pascu,[3] C. Rodríguez Triguero,[7] T. Sava,[3] A. K. Sinha,[8] L. Stroe,[3] G. Suliman,[3] and N. V. Zamfir[3]

Gates in $LaBr_3$ detectors to observe time difference and obtain lifetime for state

Ideally, we want to measure the time difference between transitions directly feeding and depopulating the state of interest (4^{-})

Gamma-ray energy coincidences 'locate' transitions above and below the state of interest….

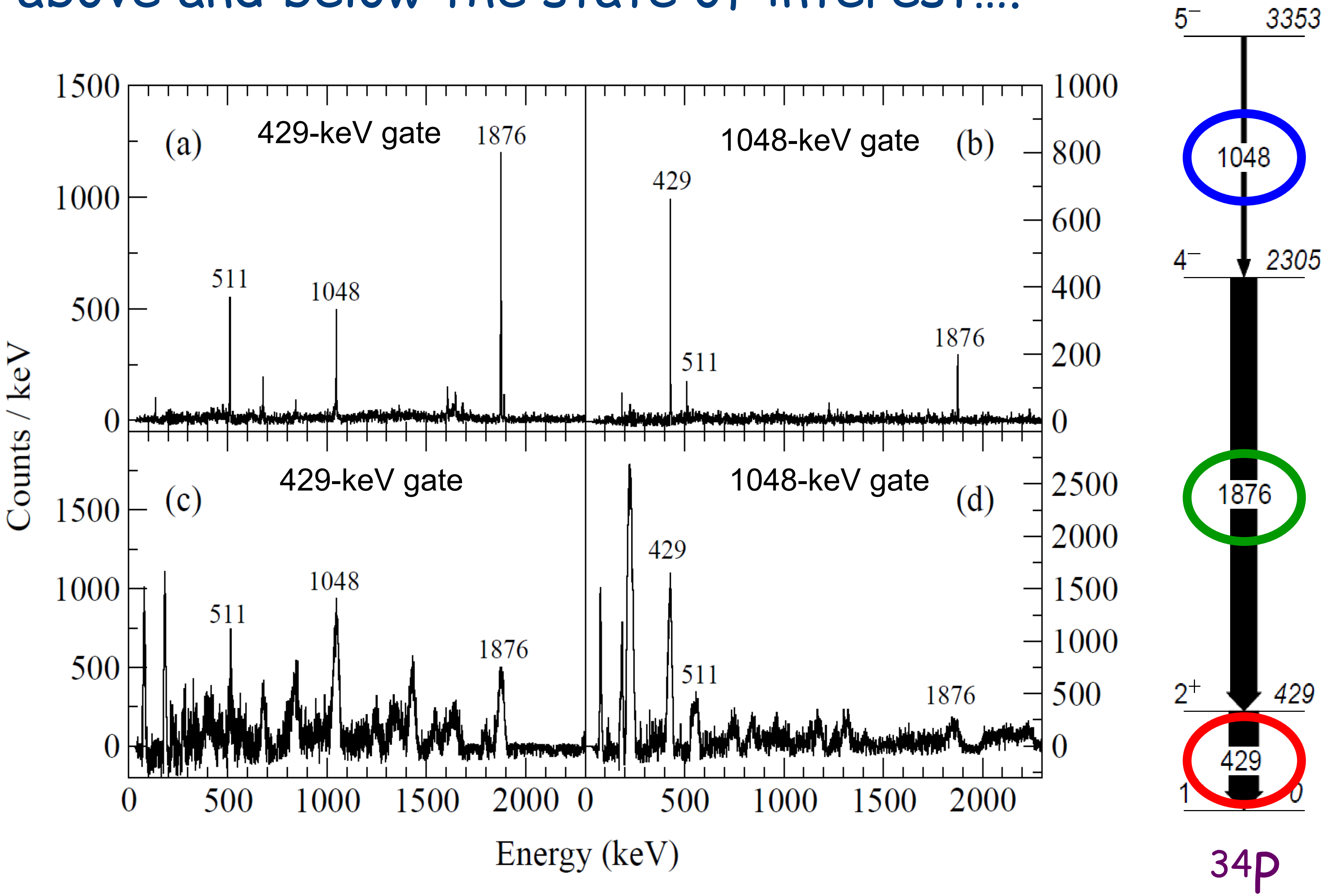

$LaBr_3$ – $LaBr_3$ Energy-gated time

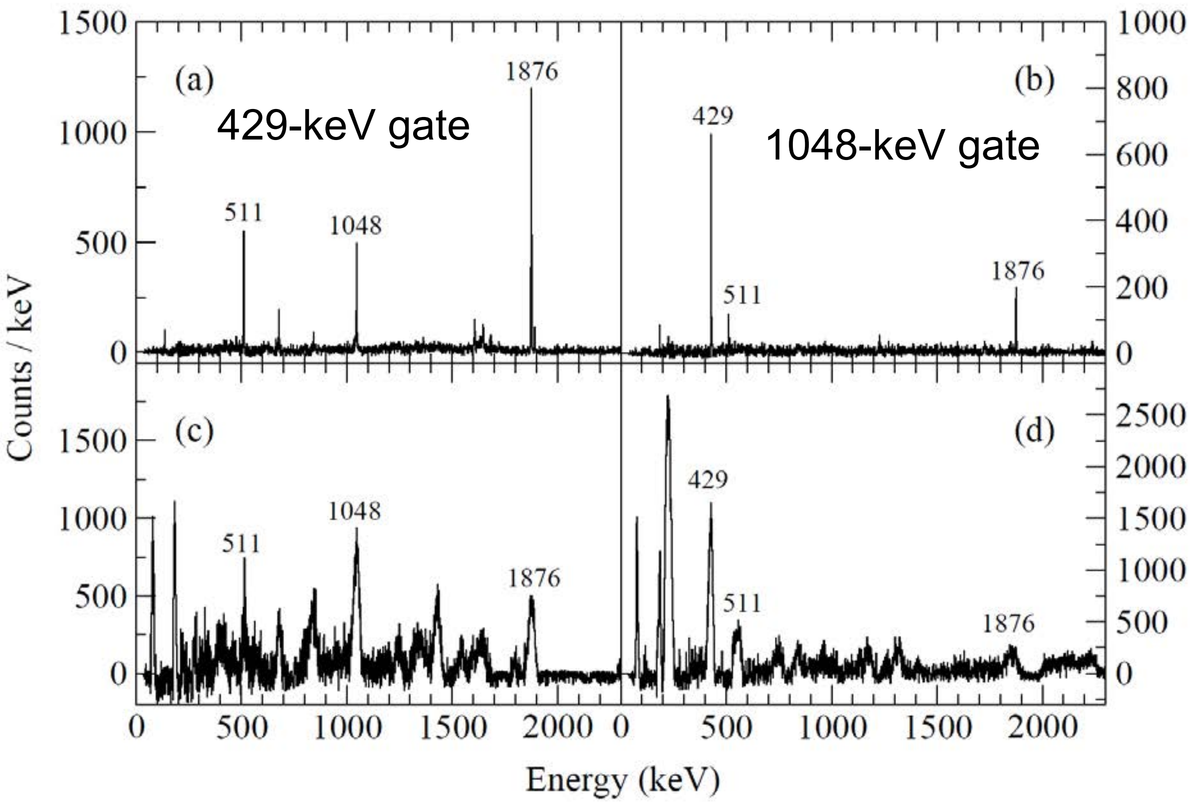

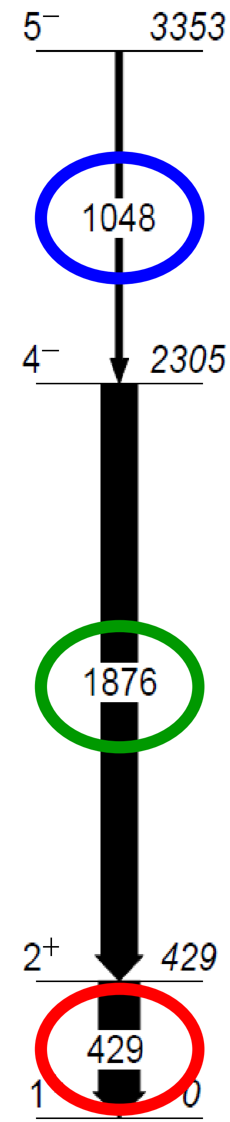

The 1876-429-keV time difference in ^{34}P should show prompt distribution as half-life of 2^+ is much shorter than prompt timing response.

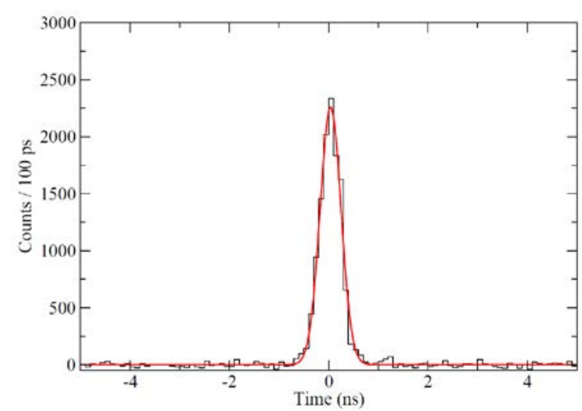

Measured FWHM = 470(10) ps

Result: $T_{1/2}$ ($I^{\pi}=4^{-}$) in ^{34}P= 2.0(1) ns

429 / 1048

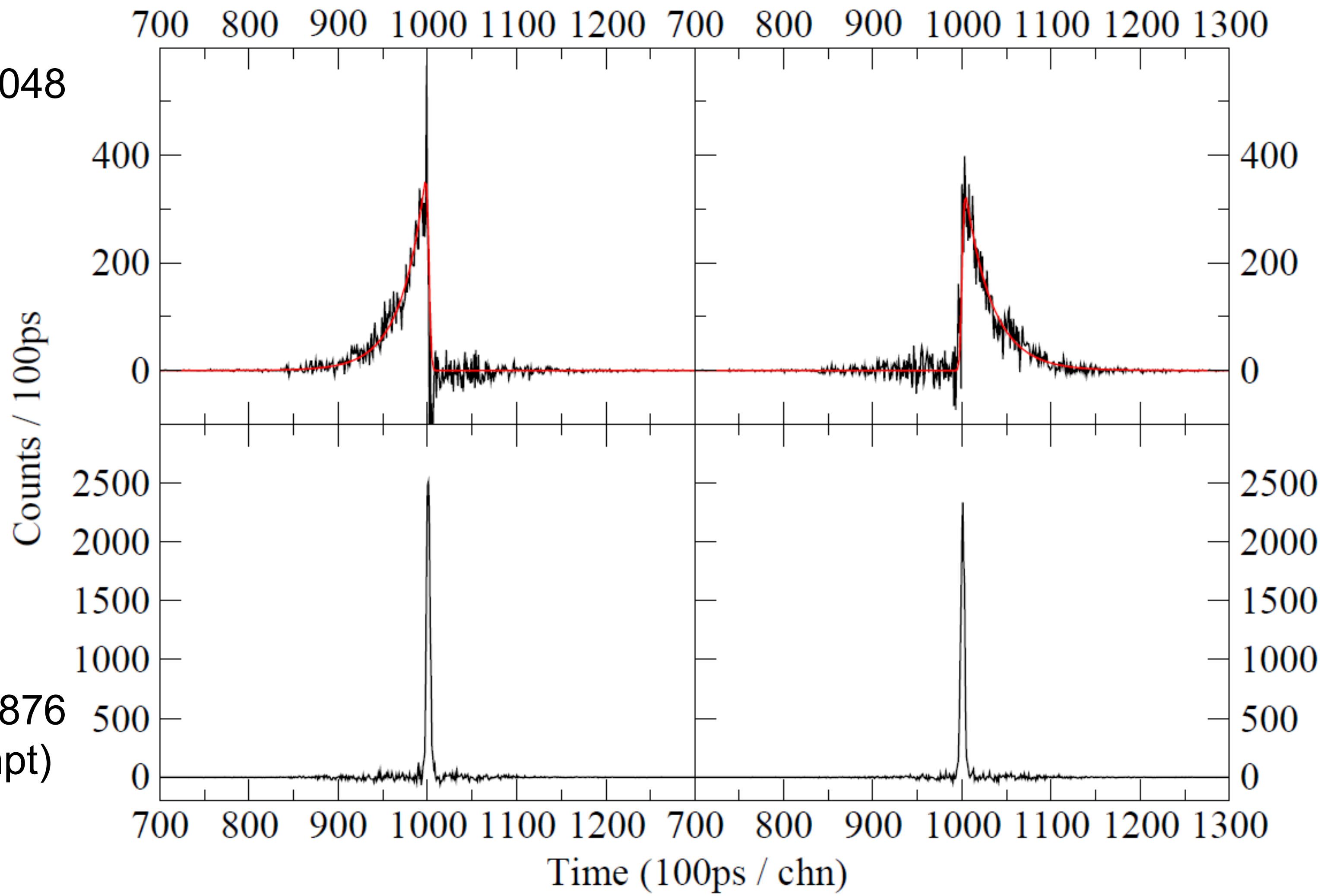

429 / 1876
(~prompt)

$T_{1/2}$ = 2.0(1)ns = 0.064(3) Wu for 1876 M2 in ^{34}P.

429 / 1048

429 / 1876 (~prompt)

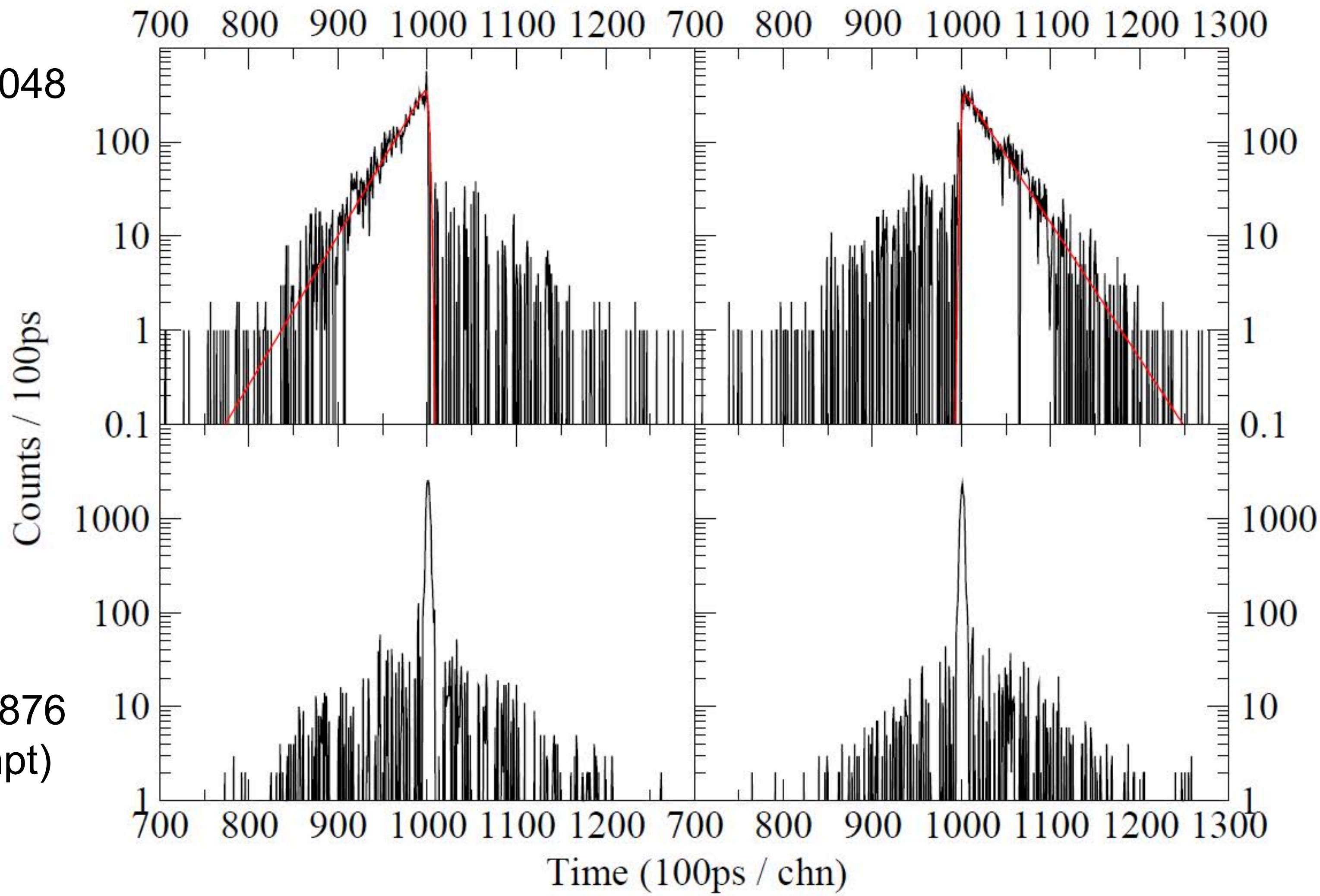

What about ‘faster’ transitions..
i.e. $< \sim 10$ ps ?

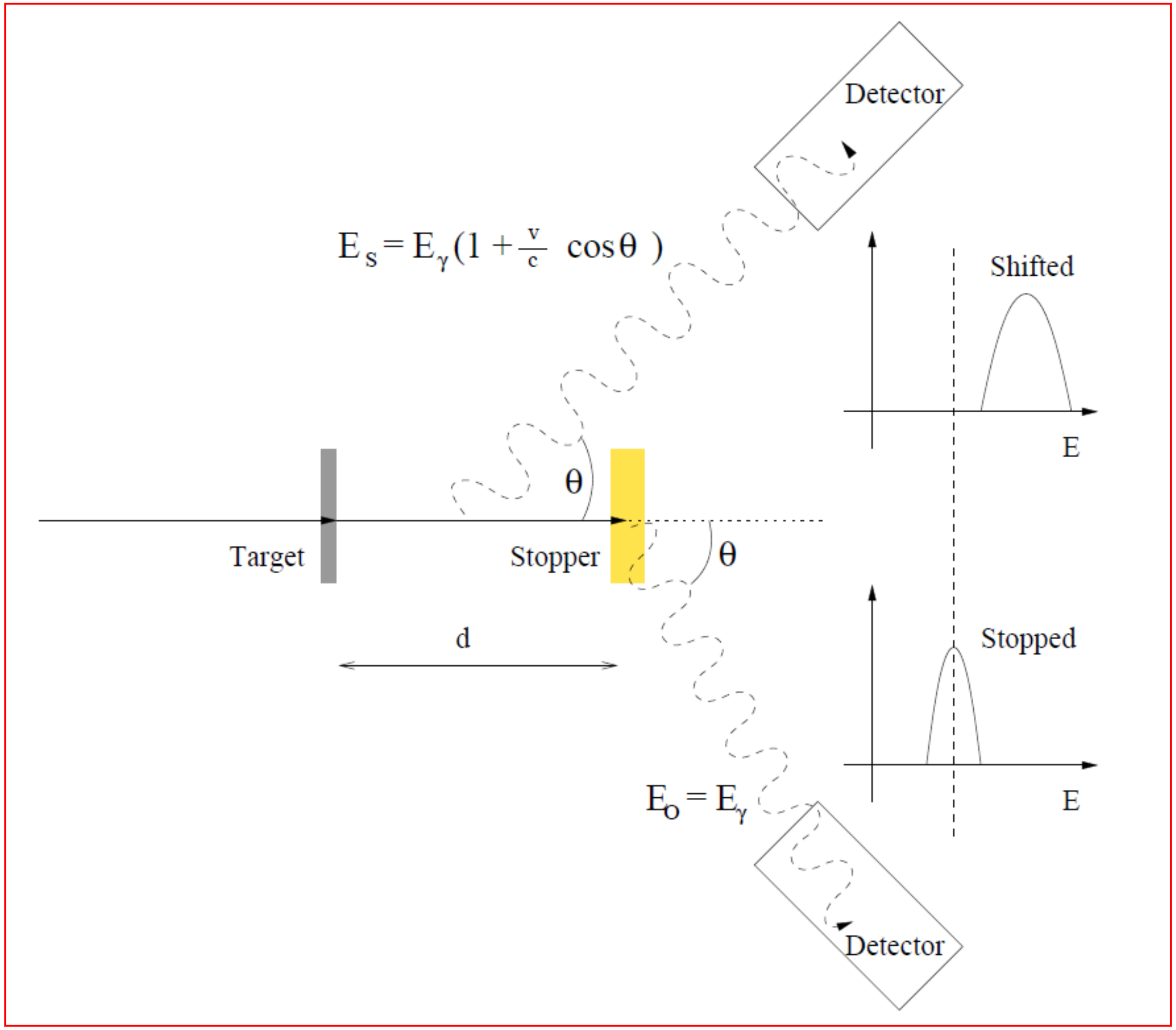

$$
\begin{aligned}
E_0 &= E_0 \\
E_S &= E_0\left(\frac{\sqrt{1-\beta^2}}{1-\beta\cos\theta}\right)
\end{aligned}
$$

$$E_S \approx E_0(1+\beta\cos\theta)$$

$$
\begin{aligned}
I_0 &= N_0 \exp\left(\frac{-d}{v\tau}\right) \\
I_S &= N_0\left(1-\exp\left(\frac{-d}{v\tau}\right)\right)
\end{aligned}
$$

$$
\begin{aligned}
R &= \frac{I_0}{I_0+I_S} = \exp\left(\frac{-d}{v\tau}\right) \\
\tau &= \frac{-d}{v\ln(R)}
\end{aligned}
$$

$$B(E2) = \frac{1}{1.225\times 10^9 E_\gamma^5 \tau(1+\alpha)},$$

$$
\boxed{
\begin{aligned}
B(E2) &= \frac{5}{16\pi} e^2 Q_t^2 |\langle J_i K 20 | J_f K\rangle|^2, \\
Q_t &\approx \frac{3}{\sqrt{5\pi}} Z R_0^2 \beta_2 (1+0.16\beta_2),
\end{aligned}
}
$$

PHYSICAL REVIEW C **76**, 064302 (2007)

Intrinsic state lifetimes in ^{103}Pd and ^{106,107}Cd

S. F. Ashley,[1,2,*] P. H. Regan,[1] K. Andgren,[1,3] E. A. McCutchan,[2] N. V. Zamfir,[2,4,5] L. Amon,[2,6] R. B. Cakirli,[2,6] R. F. Casten,[2] R. M. Clark,[7] W. Gelletly,[1] G. Gürdal,[2,5] K. L. Keyes,[8] D. A. Meyer,[2,9] M. N. Erduran,[6] A. Papenberg,[8] N. Pietralla,[10,11] C. Plettner,[2] G. Rainovski,[10,12] R. V. Ribas,[13] N. J. Thomas,[1,2] J. Vinson,[2] D. D. Warner,[14] V. Werner,[2] E. Williams,[2] H. L. Liu,[15] and F. R. Xu[15]

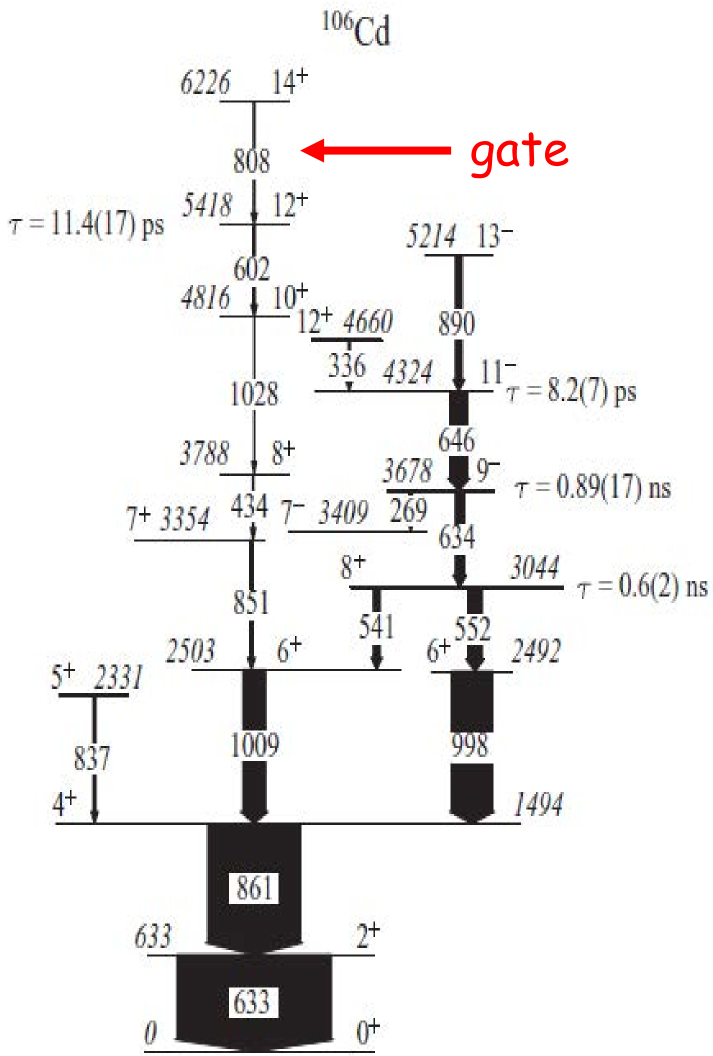

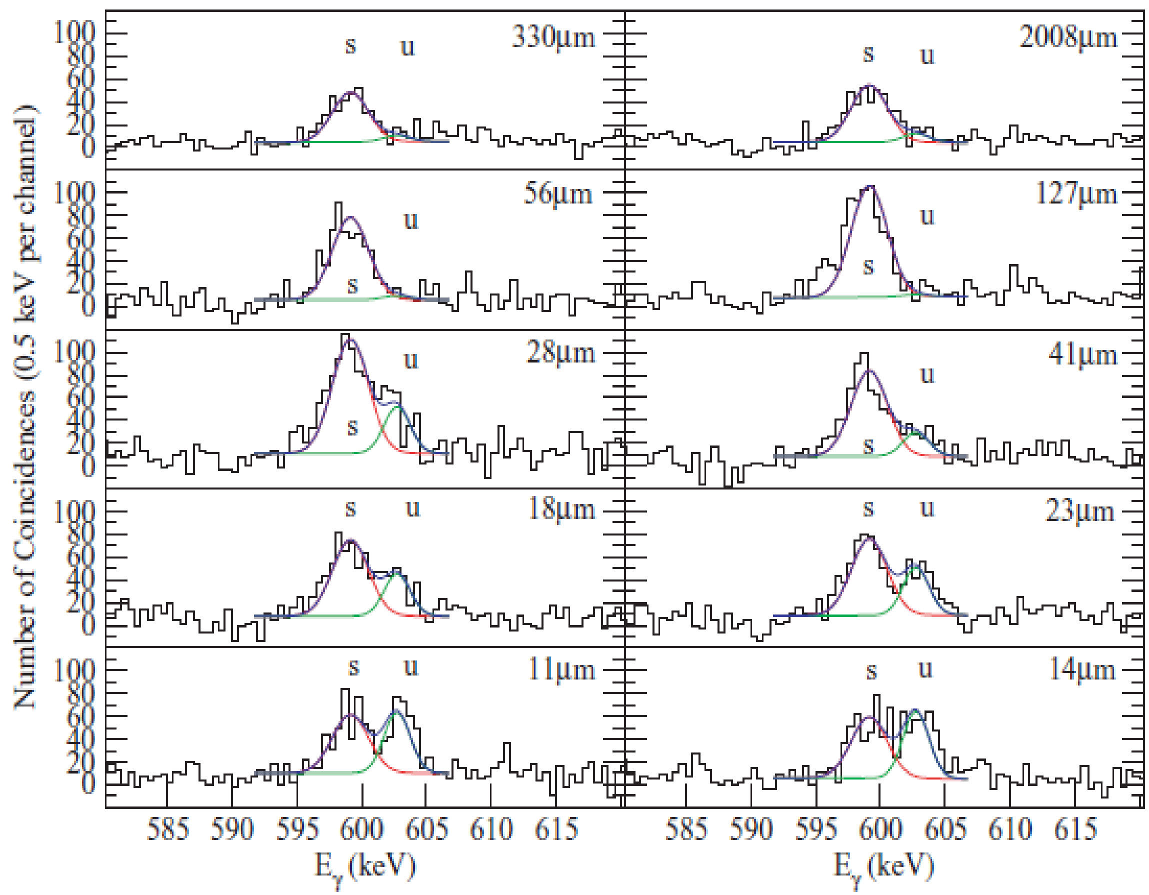

PHYSICAL REVIEW C **76**, 064302 (2007)

Intrinsic state lifetimes in ^{103}Pd and ^{106,107}Cd

S. F. Ashley,[1,2,*] P. H. Regan,[1] K. Andgren,[1,3] E. A. McCutchan,[2] N. V. Zamfir,[2,4,5] L. Amon,[2,6] R. B. Cakirli,[2,6] R. F. Casten,[2] R. M. Clark,[7] W. Gelletly,[1] G. Gürdal,[2,5] K. L. Keyes,[8] D. A. Meyer,[2,9] M. N. Erduran,[6] A. Papenberg,[8] N. Pietralla,[10,11] C. Plettner,[2] G. Rainovski,[10,12] R. V. Ribas,[13] N. J. Thomas,[1,2] J. Vinson,[2] D. D. Warner,[14] V. Werner,[2] E. Williams,[2] H. L. Liu,[15] and F. R. Xu[15]

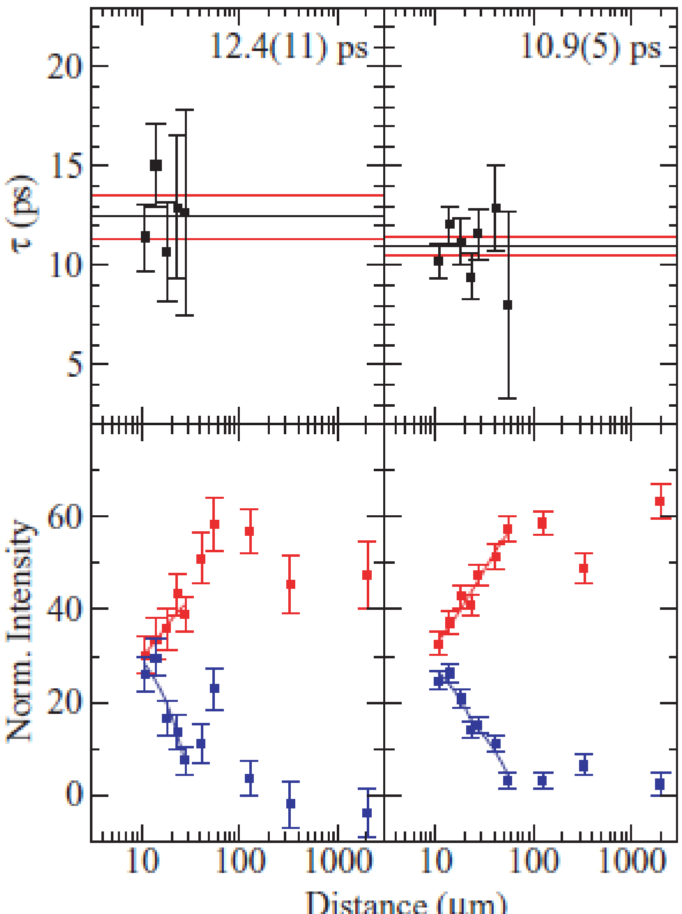

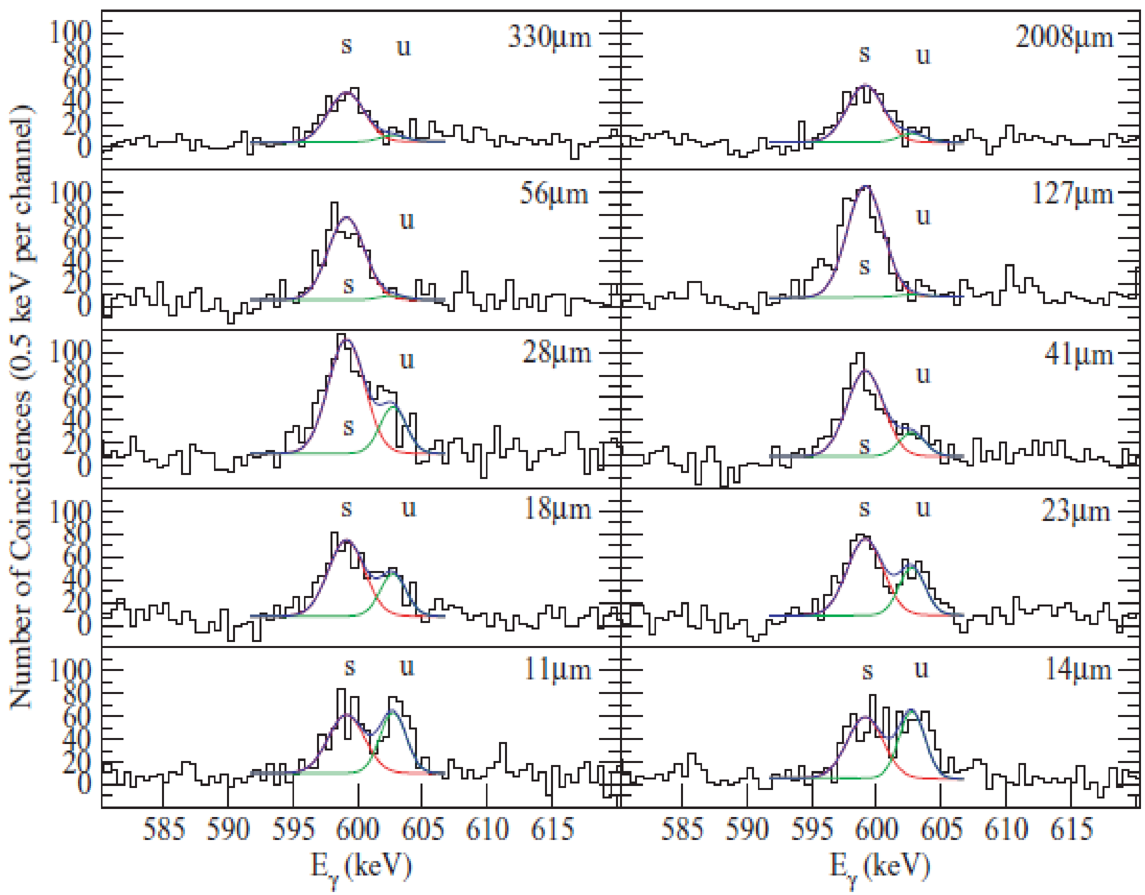

$$\tau = \frac{I_U}{v \frac{dI_s}{dx}}$$

If the lifetime to be measured is so short that all of the states decay in flight, the RDM reaches a limit.

To measure even shorter half-lives (<1ps).
In this case, make the 'gap' distance zero !! i.e., have nucleus slow to do stop in a backing.

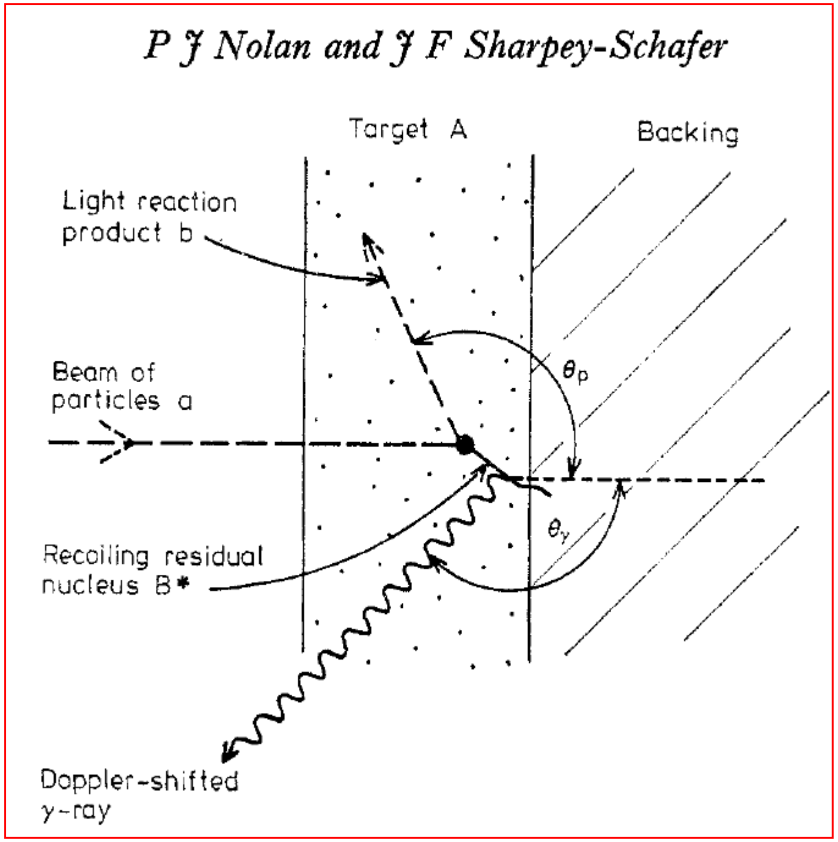

We can use the quantity
$F(\tau) = (v_s / v_{max})$.

$E_s(v,\theta) = E_0(1+{}^{v}/_{c} \cos(\theta))$ (for $v/c<0.05$)

Measuring the centroid energy of the Doppler shifted line gives the **average** value for the quantity E_s (and this v) when transition was emitted.

The ratio of vs divided by the maximum possible recoil velocity (at t=0) is the quantity, $F(\tau)$ = fractional Doppler shift.

In the rotational model,

$$\frac{1}{\tau} = 1.223 E_\gamma^5 \frac{5}{16} Q_o^2 | < J_i K 20 | J_f K > |^2$$

where the CG coefficient is given by,

$$< J_i K 20 | J_f K > = \sqrt{\frac{3(J-K)(J-K-1)(J+K)(J+K-1)}{(2J-2)(2J-1)J(2J+1)}}$$

Thus, measuring τ and knowing the transition energy, we can obtain a value for Q_0

$$Q_0 = \frac{3}{\sqrt{5\pi}} Z R^2 \beta_2 \left(1 + \frac{1}{8}\sqrt{\frac{5}{\pi}}\beta_2 \ldots\right)$$

VOLUME 59, NUMBER 19 PHYSICAL REVIEW LETTERS 9 NOVEMBER 1987

Intrinsic Quadrupole Moment of the Superdeformed Band in ^{152}Dy

M. A. Bentley, G. C. Ball,[a] H. W. Cranmer-Gordon, P. D. Forsyth, D. Howe, A. R. Mokhtar, J. D. Morrison, and J. F. Sharpey-Schafer
Oliver Lodge Laboratory, University of Liverpool, Liverpool L69 3BX, United Kingdom

P. J. Twin, B. Fant,[b] C. A. Kalfas,[c] A. H. Nelson, and J. Simpson
Science and Engineering Research Council, Daresbury Laboratory, Daresbury, Warrington WA4 4AD, United Kingdom

and

G. Sletten
Niels Bohr Institutet, DK-4000 Roskilde, Denmark

(Received 9 February 1987; revised manuscript received 3 June 1987)

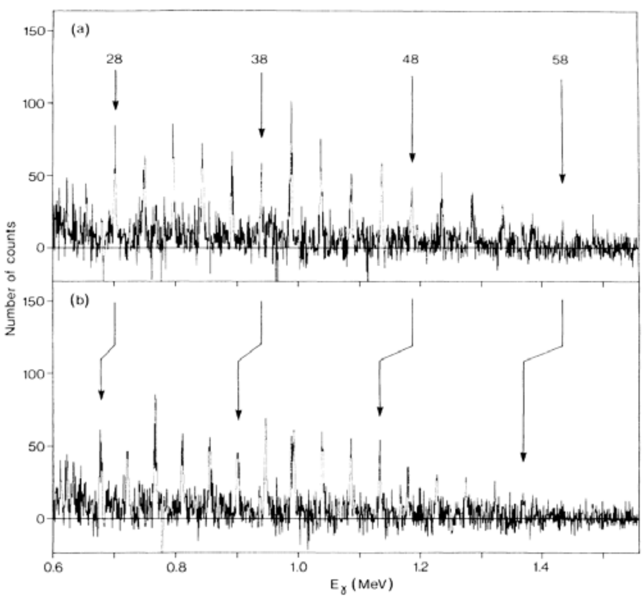

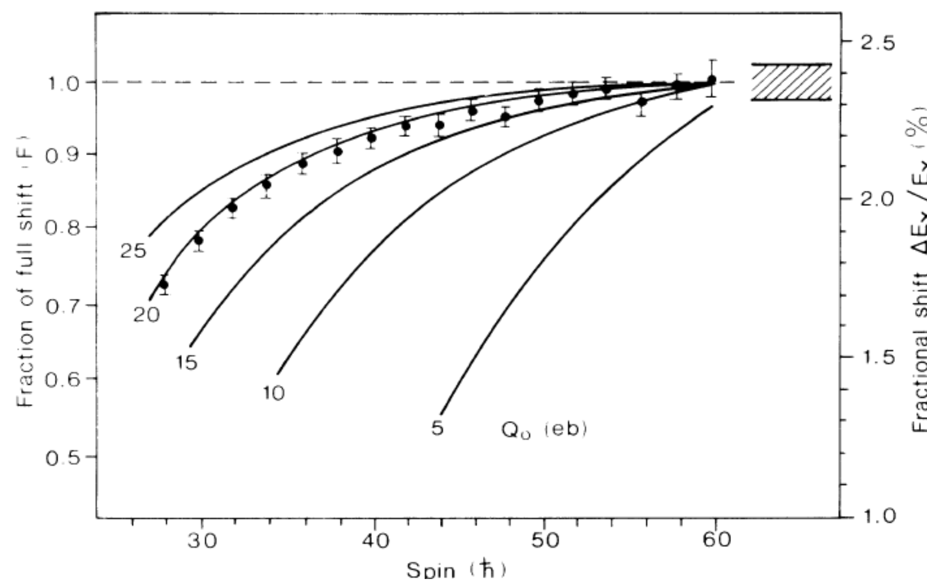

If we can assume a constant quadrupole moment for a rotational band (Qo), and we know the transition energies for the band, correcting for the feeding using the Bateman equations, we can construct 'theoretical' F(τ) curves for bands of fixed Q_0 values

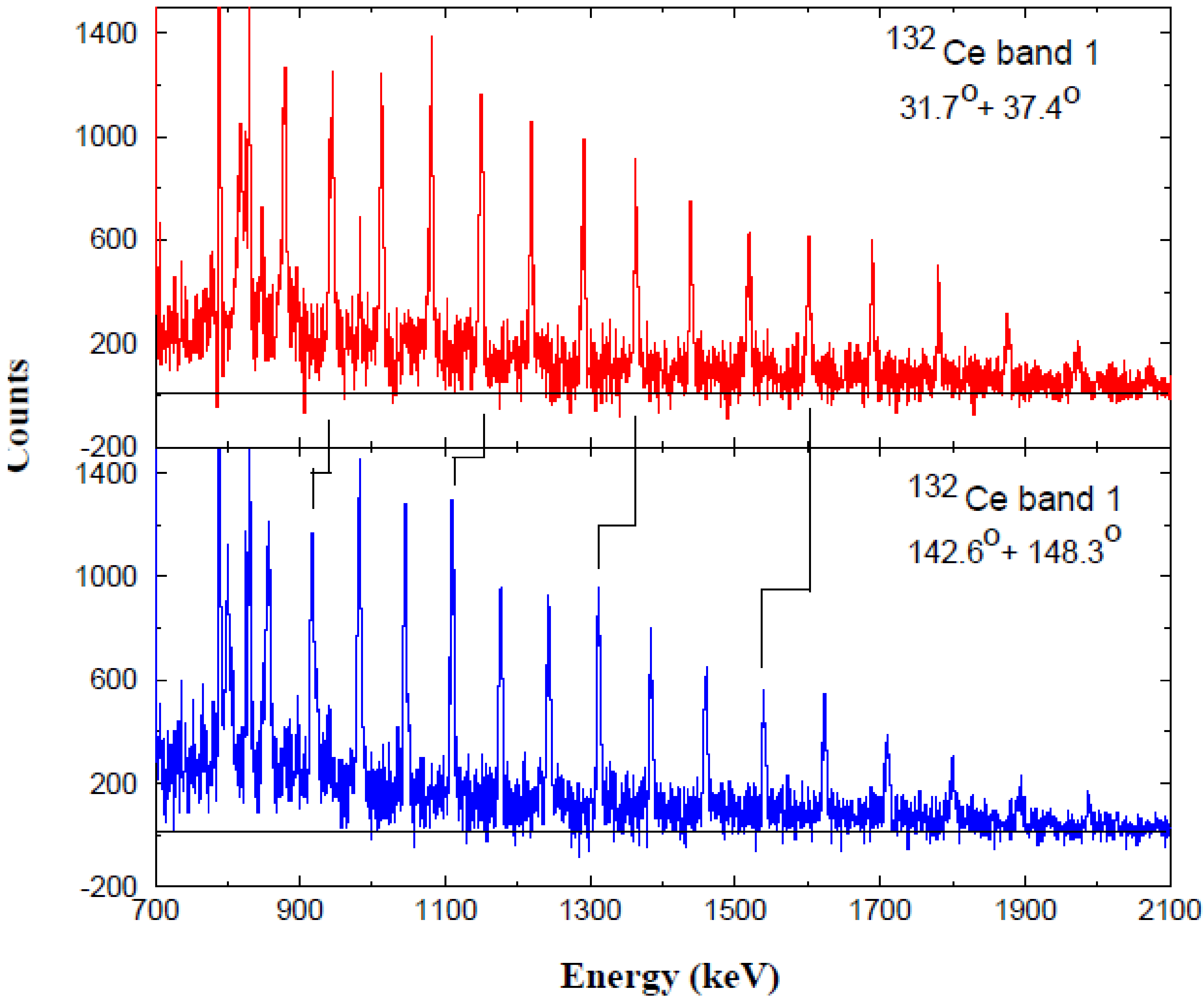

132 Ce band 1
31.7° + 37.4°
132 Ce band 1
142.6° + 148.3°
Counts
1400
1000
600
200
-200
700
900
1100
1300
1500
1700
1900
2100
Energy (keV)

Angular momentum coupling for multi-unpaired nucleons?

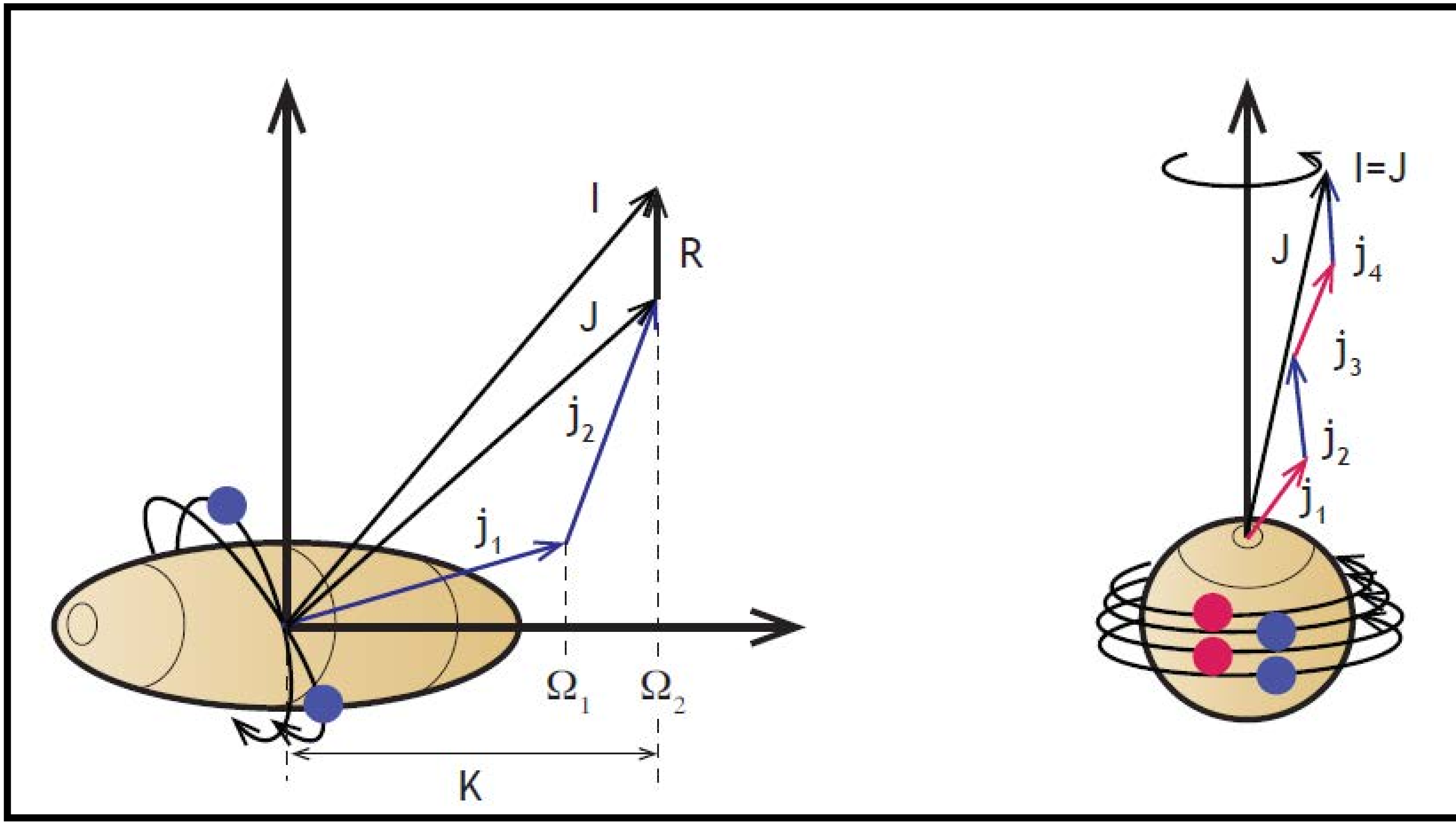

From DWK 2016

Unpaired Particles in Deformed Nuclei:

The Nilsson Model

Deformed Shell Model: The Nilsson Model

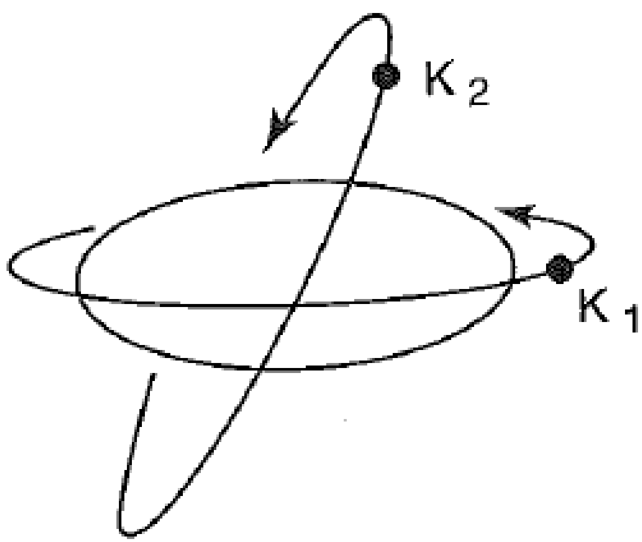

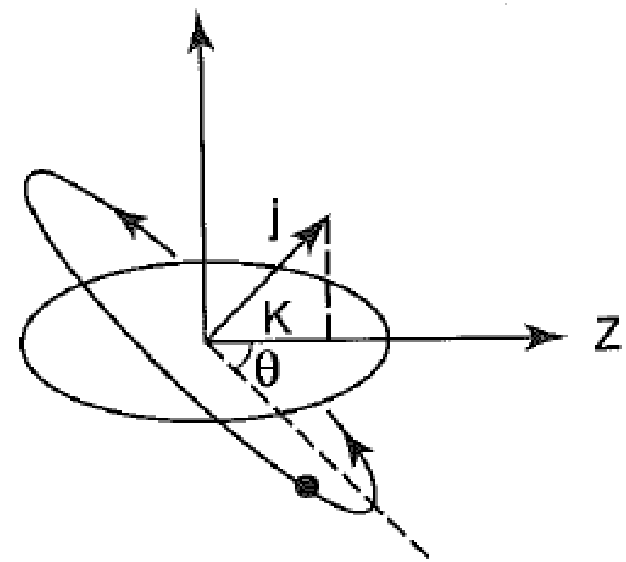

sin θ ~ K / j

$$H = \frac{\mathbf{p}^2}{2m} + \frac{1}{2} m \left[\omega_x^2 (x^2 + y^2) + \omega_z^2 z^2 \right] + C \mathbf{l} \bullet \mathbf{s} + D \mathbf{l}^2$$

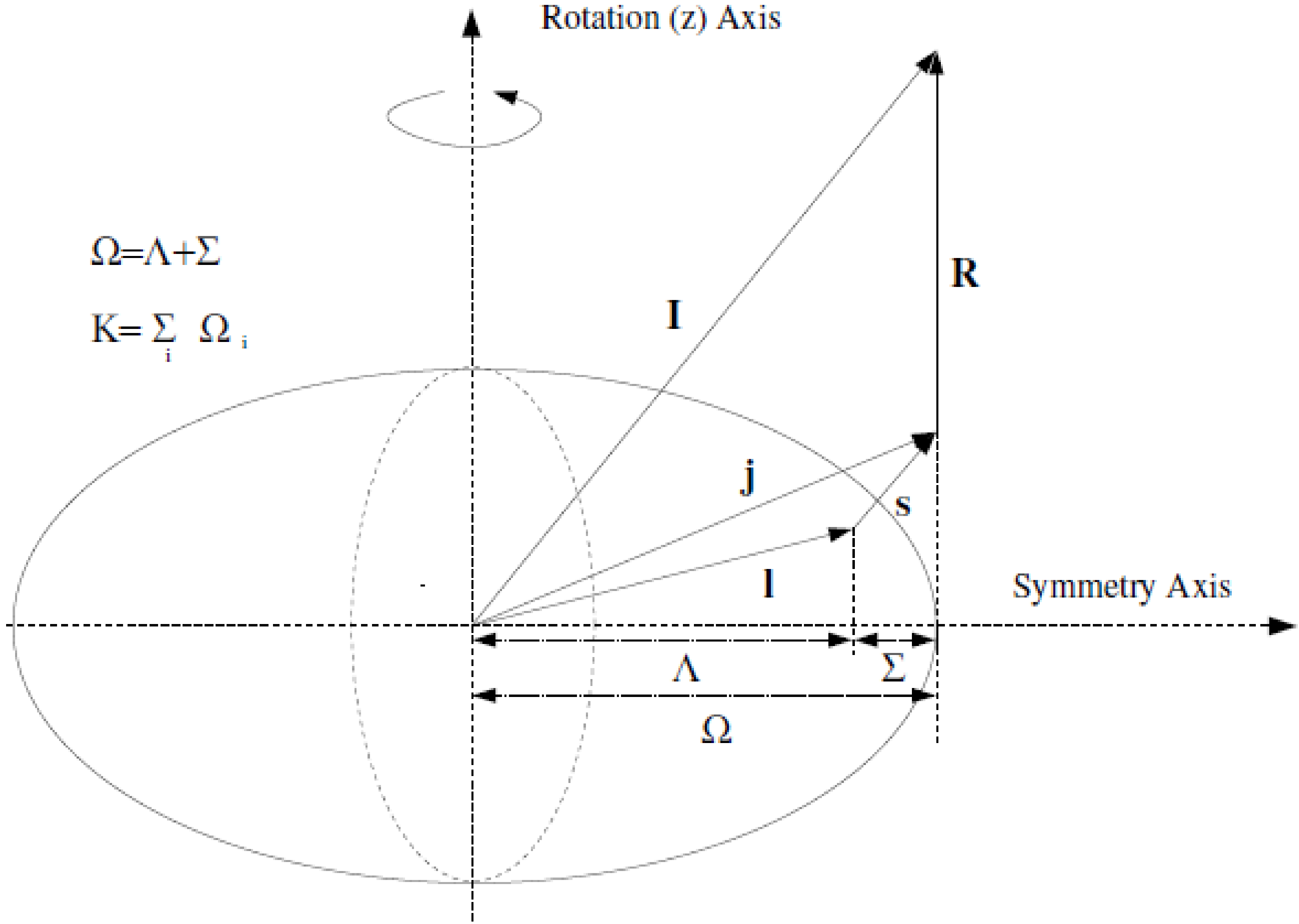

Rotation (z) Axis
Ω=Λ+Σ
K= Σ_i Ω_i
I
R
j
s
l
Symmetry Axis
Λ
Σ
Ω

Effect of Nuclear Deformation on K-isomers

Spherical, harmon. oscilator
$H = \hbar\omega + a\mathbf{l.l} + b\mathbf{l.s}$,
quantum numbers j^{π}, m_j

Nilsson scheme: Quadrupole deformed
3-D HO. where $\hbar\omega \rightarrow \hbar\omega_x + \hbar\omega_y + \hbar\omega_z$
axial symmetry means $\omega_x = \omega_y$
quantum numbers $[\mathbf{N}, \mathbf{n_x}, \mathbf{\Lambda}]\Omega^{\pi}$

> prolate β_2

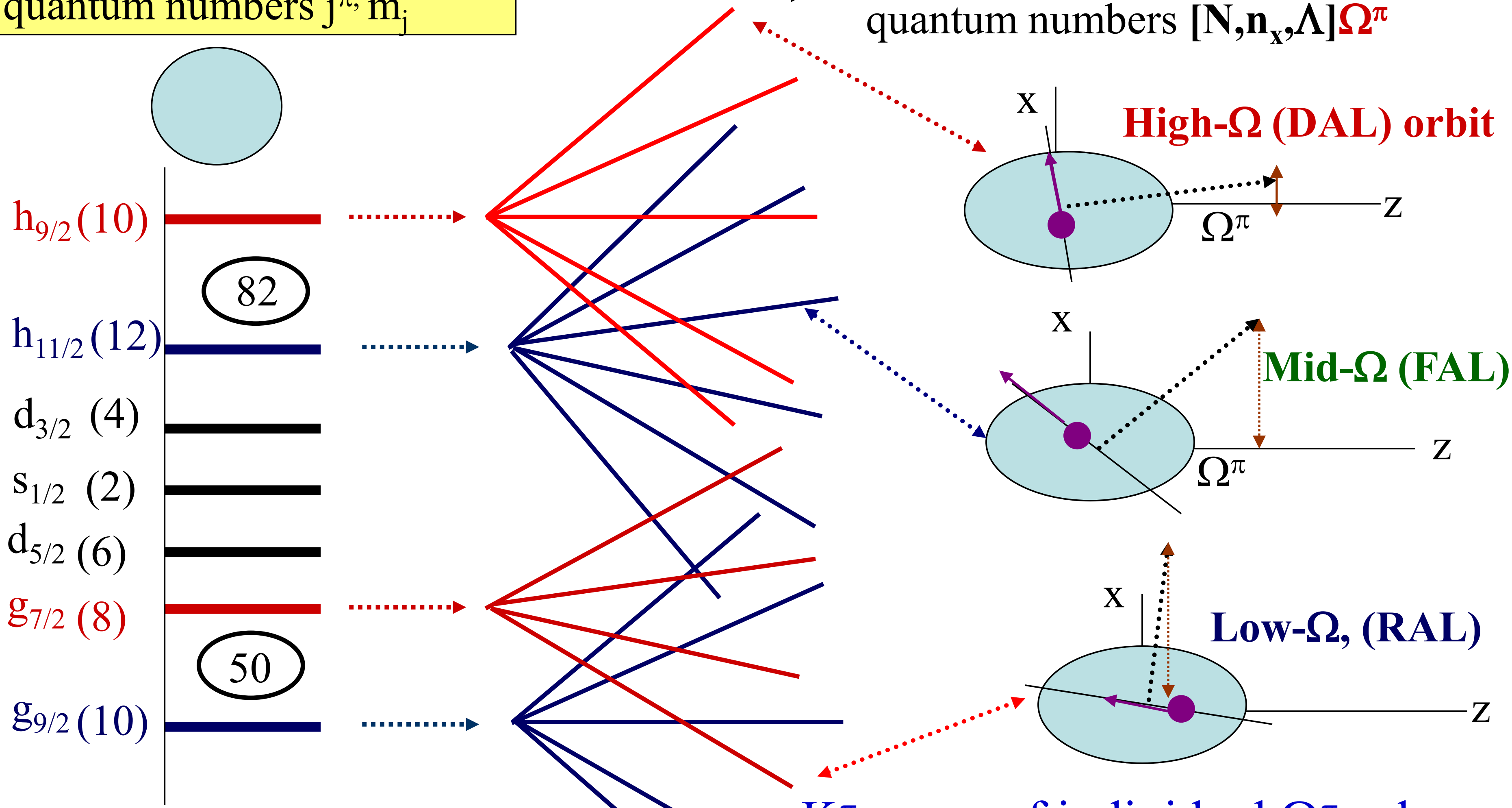

K^{π}= sum of individual Ω^{π} values.

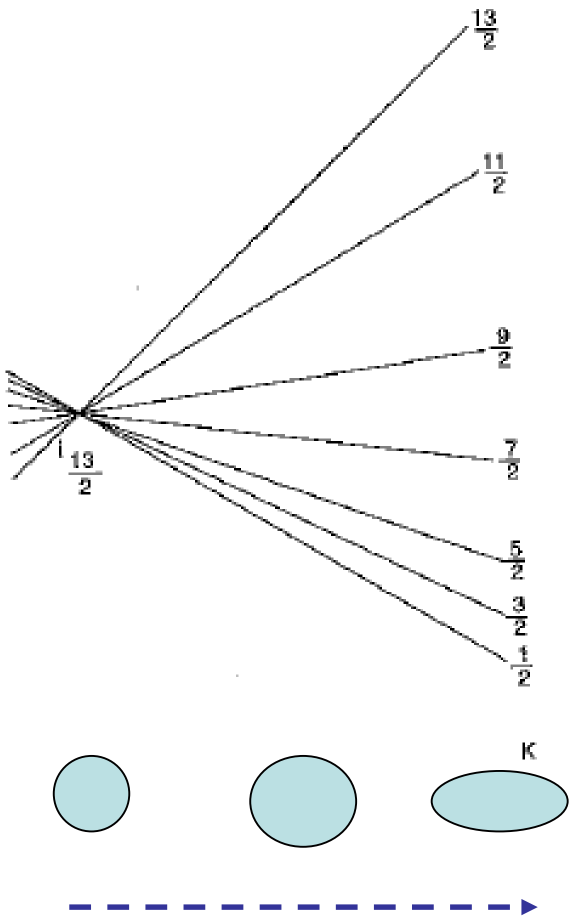

Increasing (prolate) deformation, bigger splitting.

High-Ω orbits, less Contact with main mass distribution.

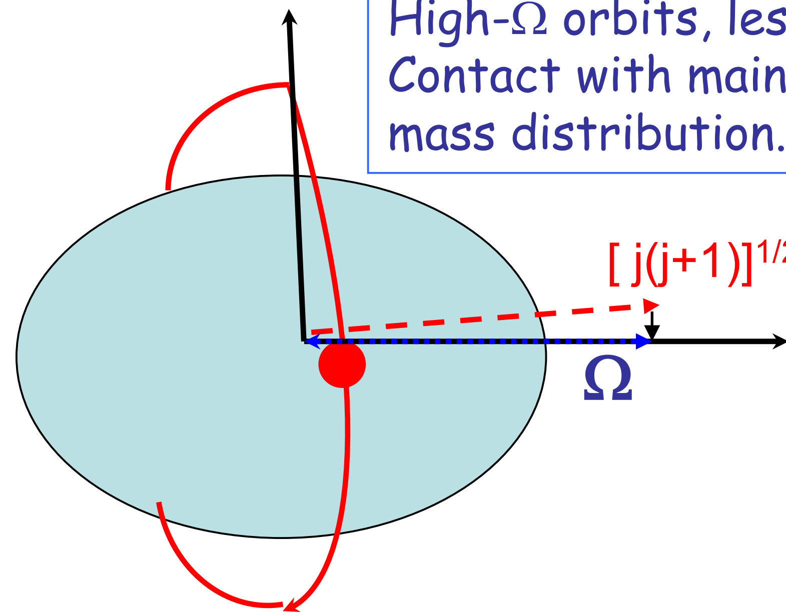

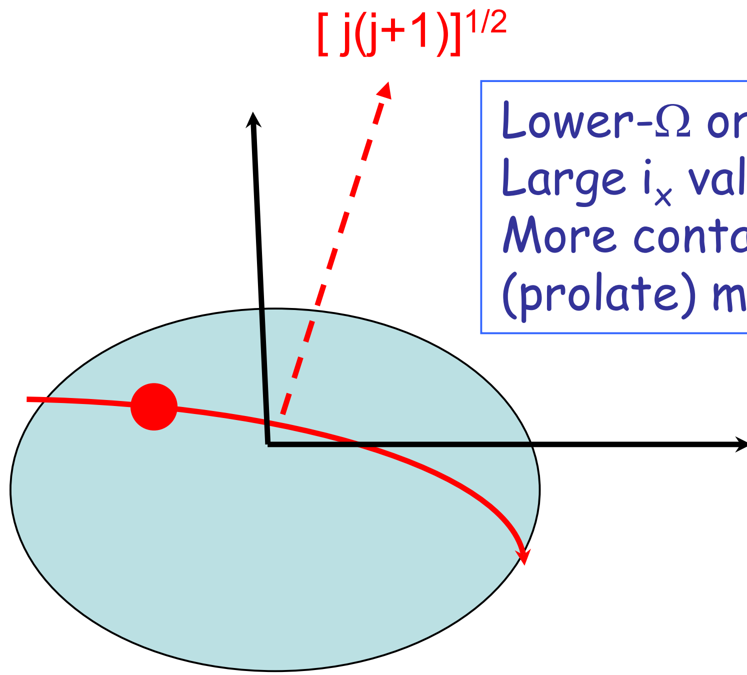

Lower-Ω orbits, have Large i_x values and More contact with main (prolate) mass distribution.

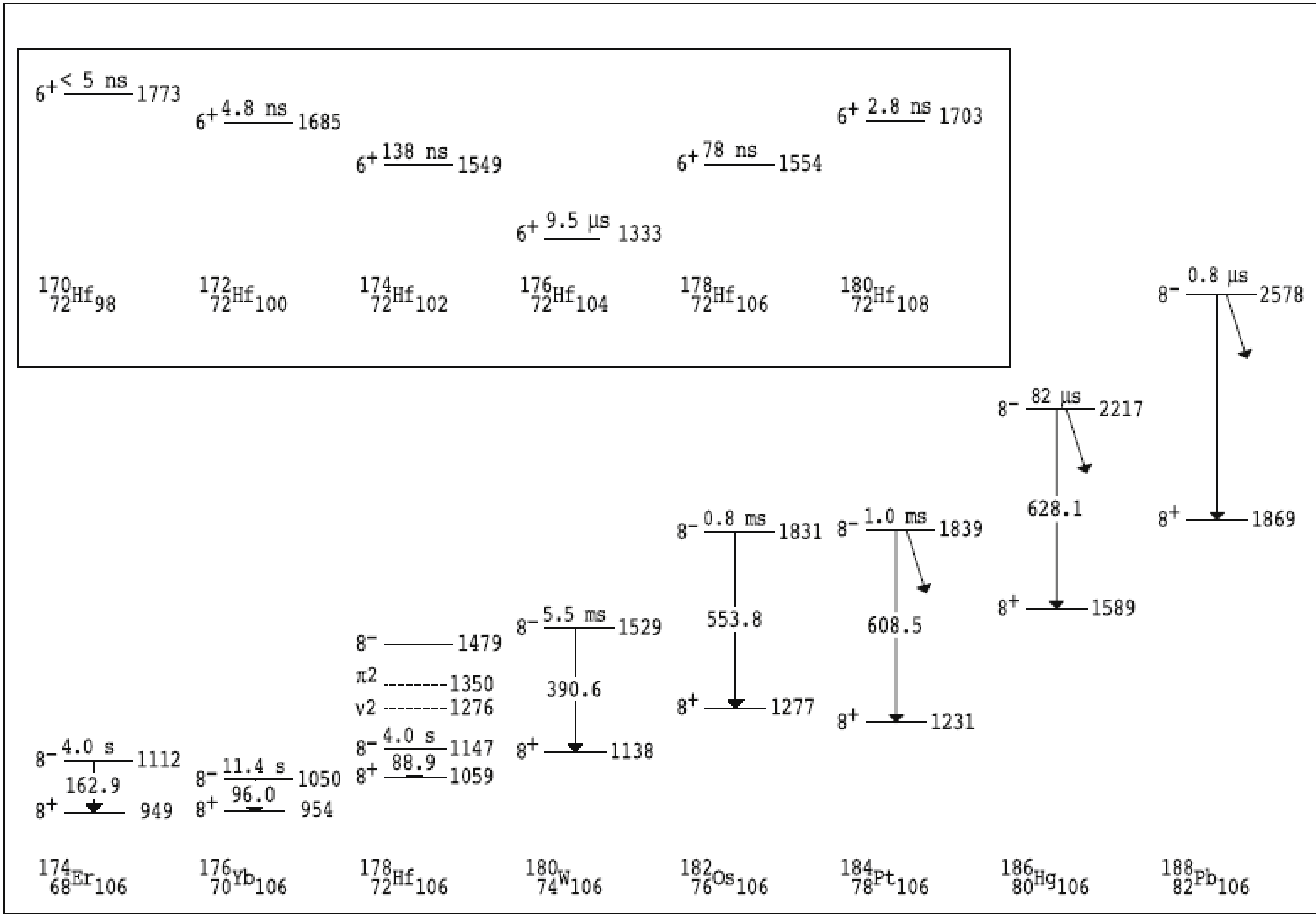

Fig. 4. Systematics of $K^\pi = 6^+$ isomers in the $Z = 72$ (Hf) isotopes and the $K^\pi = 8^-$ isomers in the $N = 106$ isotones.

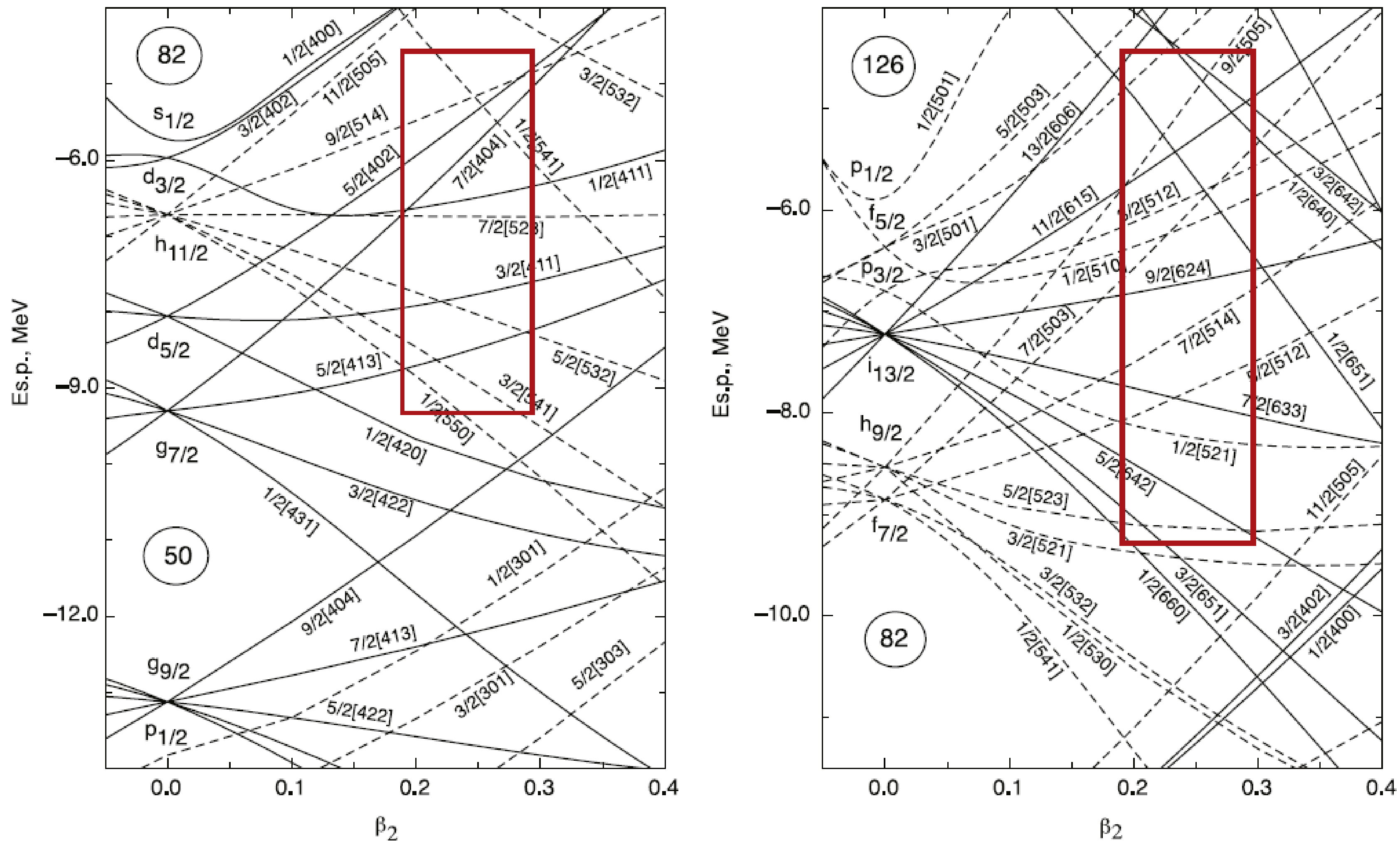

Nilsson levels for protons (left) and neutrons (right) in the $A \sim 170$–190 region. Boxes indicate the main orbitals of interest

From F.G.Kondev et al., ADNDT 103-104 (2015) p50-105

K isomers

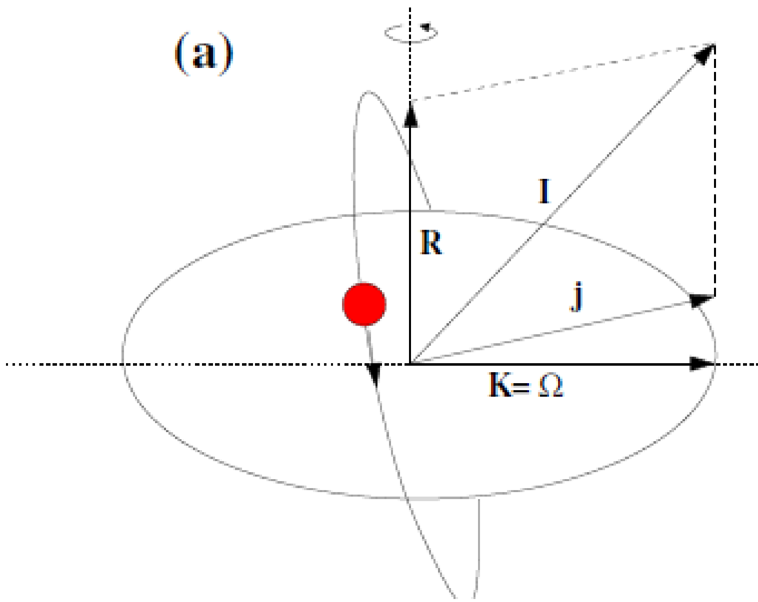

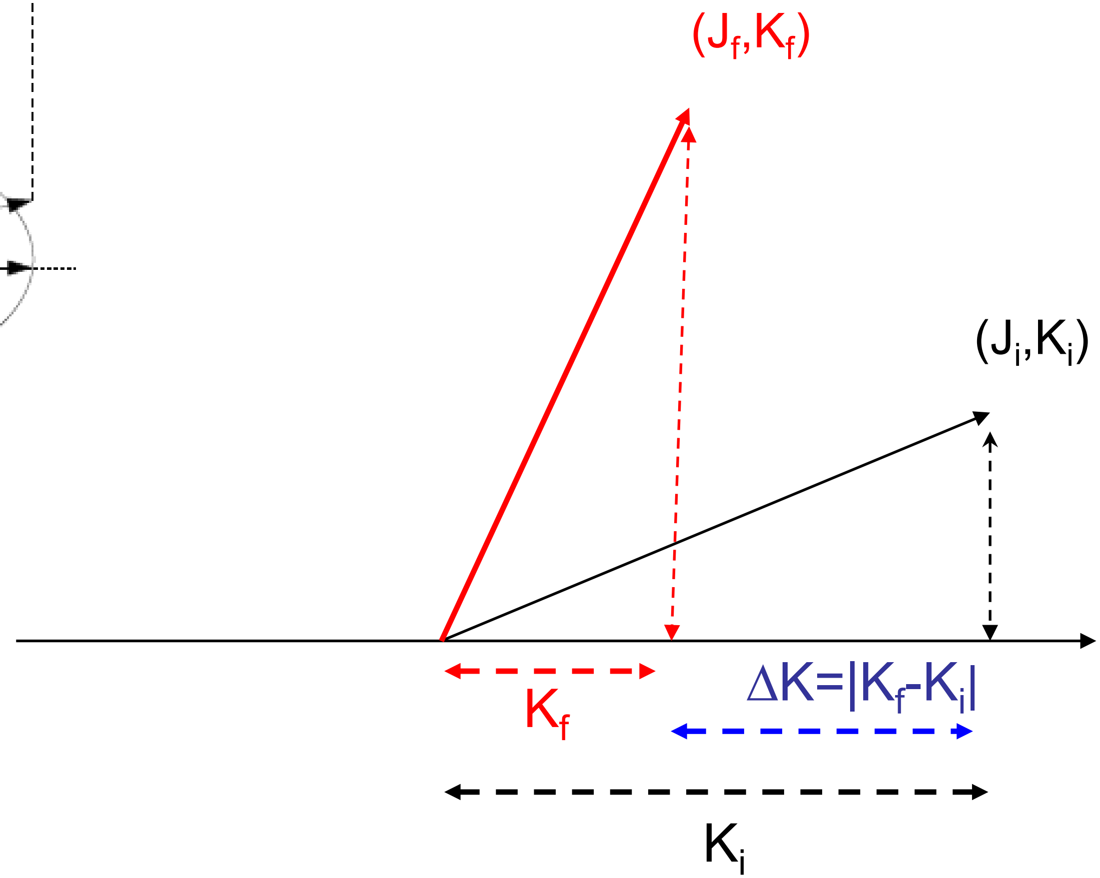

$$|K_i - K_f| = \Delta K \leq \lambda$$

$$\nu = \Delta K - \lambda$$

$$f_\nu = \left[\frac{T^\gamma_{1/2}}{T^W_{1/2}}\right]^{1/\nu}$$ = reduced hindrance for a K-isomeric decay transition.

K-isomers in deformed nuclei

In the strong-coupling limit, for orbitals where Ω is large, unpaired particles can sum their angular momentum projections on the nuclear axis if symmetry to give rise to 'high-K' states, such that the total spin/parity of the high-K Multi-particle state is give by:

$$J^{\pi} = K^{\pi} = \sum_i \Omega_i^{\Pi(\pi_i)}$$

These, high-K multi-quasi-particle states are expected to occur at excitations energies of:

$$E^* \approx \sum_k \sqrt{(\epsilon_k - \epsilon_F)^2 + \Delta^2}$$

where ε_k is the single-particle energy; ε_F is the Fermi energy and Δ is the pair gap (which can be obtained from odd-even mass differences)

M. Dasgupta et al. / Physics Letters B 328 (1994) 16–21

We can observe many 'high-K isomeric states' and 'strongly coupled rotational bands' built upon different combinations of deformed single- and multi-particle configurations in odd-A nuclei.

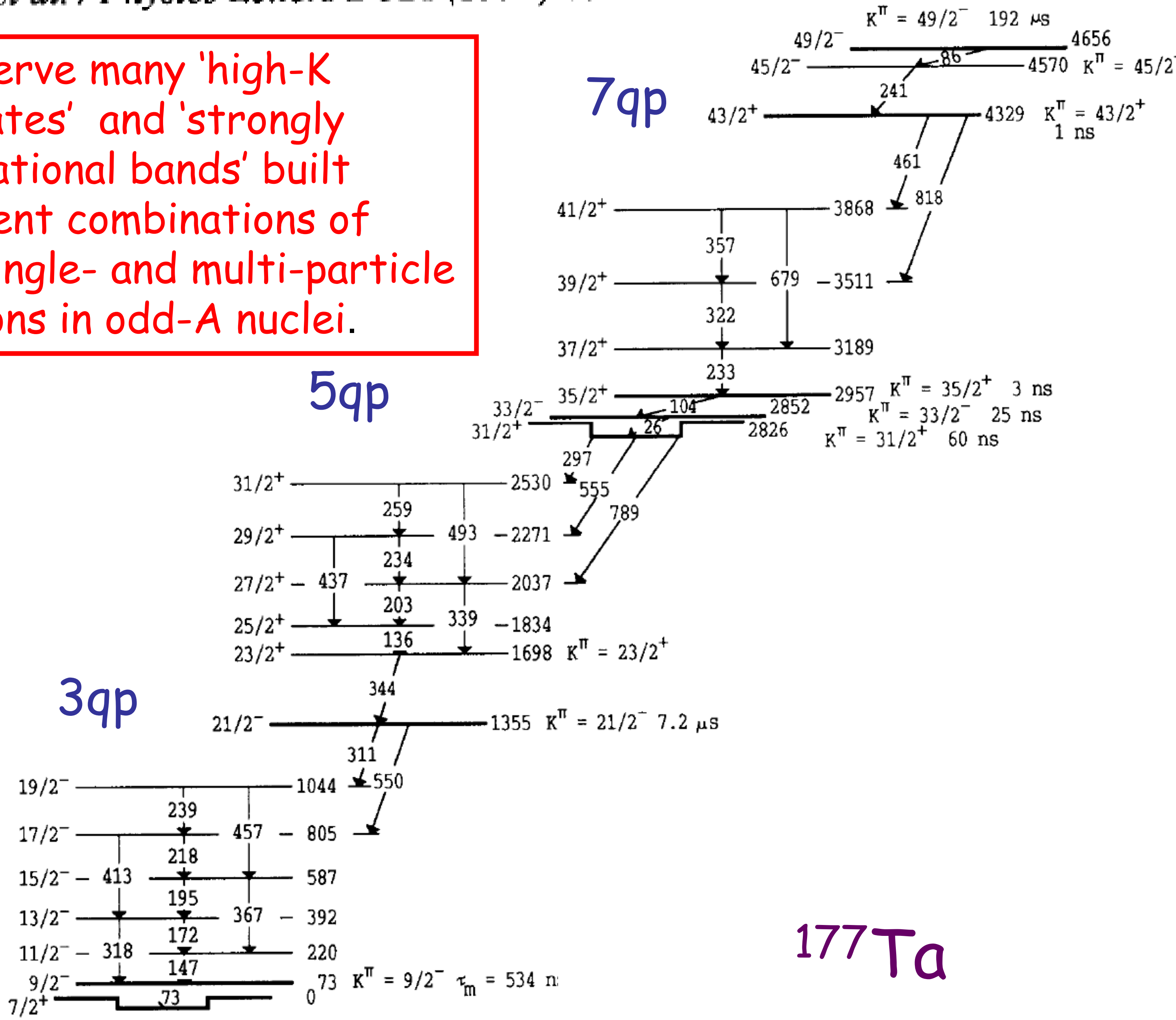

7qp

5qp

3qp

1qp

^{177}Ta

C.S.Purry et al., Nucl. Phys. A632 (1998) p229

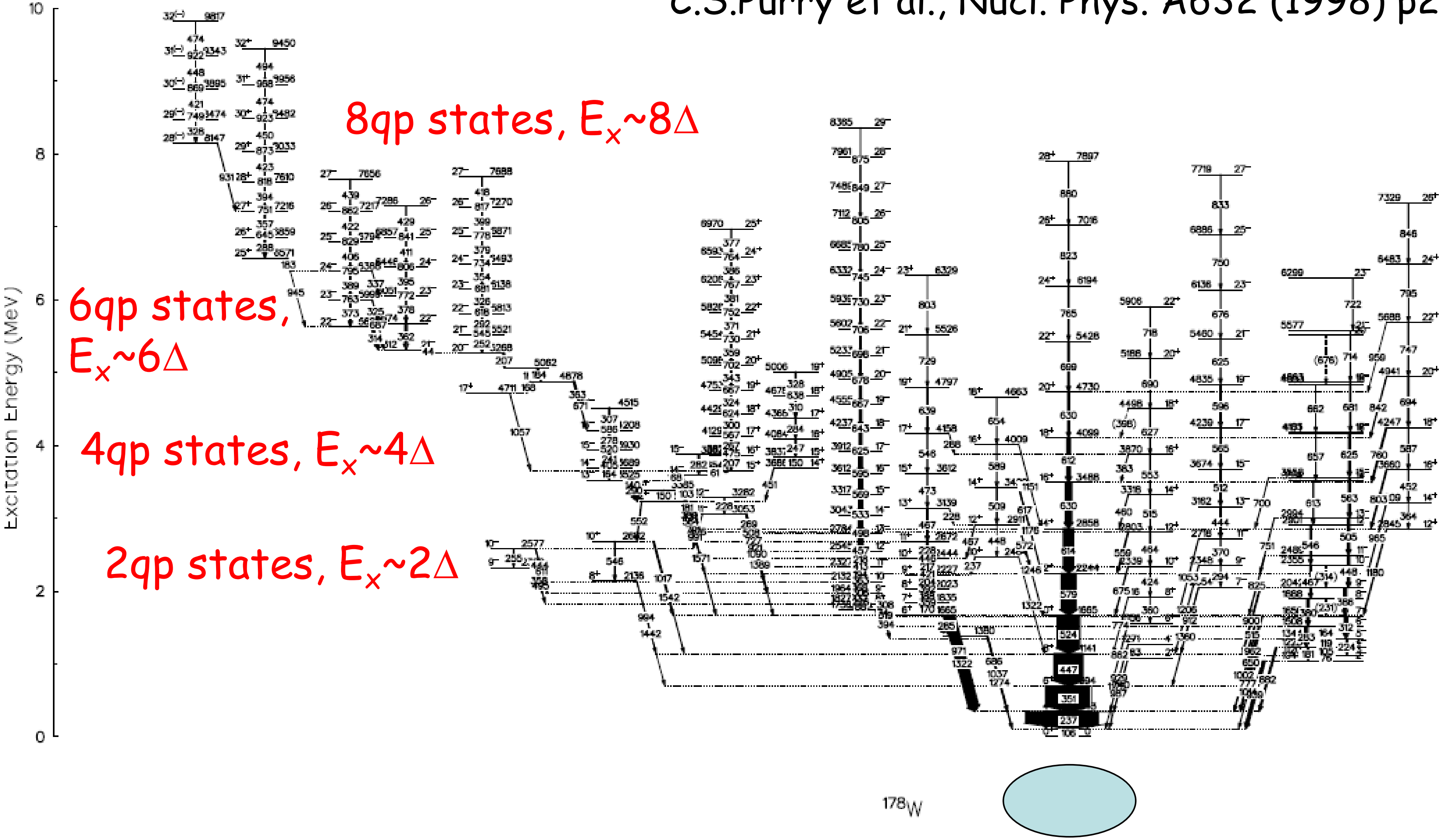

^{178}W: different and discrete 0, 2, 4, 6 and 8 quasi-particle band structures are all observed:
These are built on different underlying single-particle (Nilsson) orbital configurations.

'Forbiddenness' in K isomers

We can use single particle ('Weisskopf') estimates for transitions rates for a given multipolarity. (E_g (keV), $T_{1/2}$(s), Firestone and Shirley, *Table of Isotopes* (1996).

$$\text{Weisskopf Estimates for } T^{1/2} \quad A = 180,\ E_\gamma = 500\ \text{keV}$$

$$E1 \rightarrow T_W^{1/2} = 6.76\times10^{-6}\, E_\gamma^{-3} A^{-2/3} \rightarrow 1.6\times10^{-15}\, s$$

$$M1 \rightarrow T_W^{1/2} = 2.20\times10^{-5}\, E_\gamma^{-3} \rightarrow 1.8\times10^{-13}\, s$$

$$E2 \rightarrow T_W^{1/2} = 9.52\times10^{6}\, E_\gamma^{-5} A^{-4/3} \rightarrow 3.0\times10^{-10}\, s$$

$$M2 \rightarrow T_W^{1/2} = 3.10\times10^{7}\, E_\gamma^{-5} A^{-2/3} \rightarrow 3.1\times10^{-8}\, s$$

Hindrance (F) (removing dependence on multipolarity and E_γ) is defined by

$$F = \left(\frac{T^{\gamma}_{1/2}}{T^{W}_{1/2}}\right) = \text{ratio of expt. and Weisskopf trans. rates}$$

Reduced Hindrance (f_ν) gives an estimate for the 'goodness' of K- quantum number and validity of K-selection rule (= a measure of axial symmetry).

$$f_\nu = F^{1/\nu} = \left(\frac{T^{\gamma}_{1/2}}{T^{W}_{1/2}}\right)^{1/\nu}, \quad \nu = \Delta K - \lambda$$

$f_\nu \sim 100$ typical value for 'good' K isomer (see Lobner Phys. Lett. **B26** (1968) p279)

Smith, Walker et al., Phys. Rev. **C68** (2003) 031302

$K^{\pi} = 16^{+}$

$T_{1/2} = 31$ y

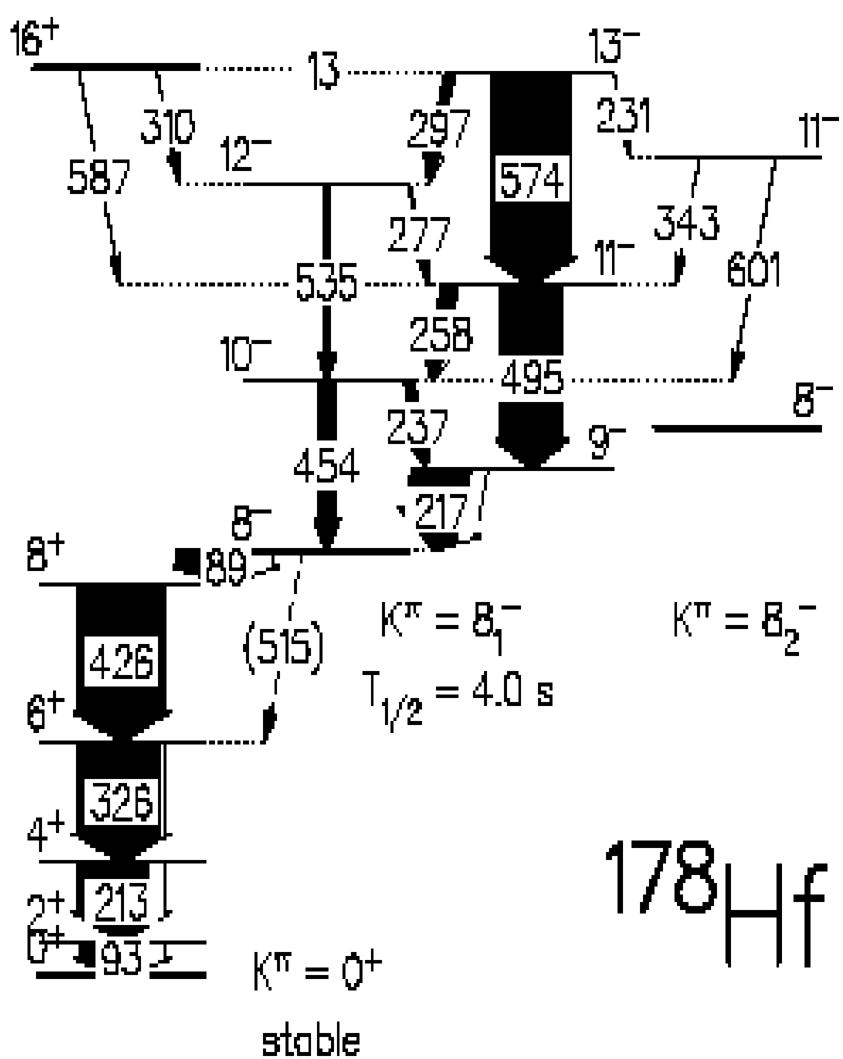

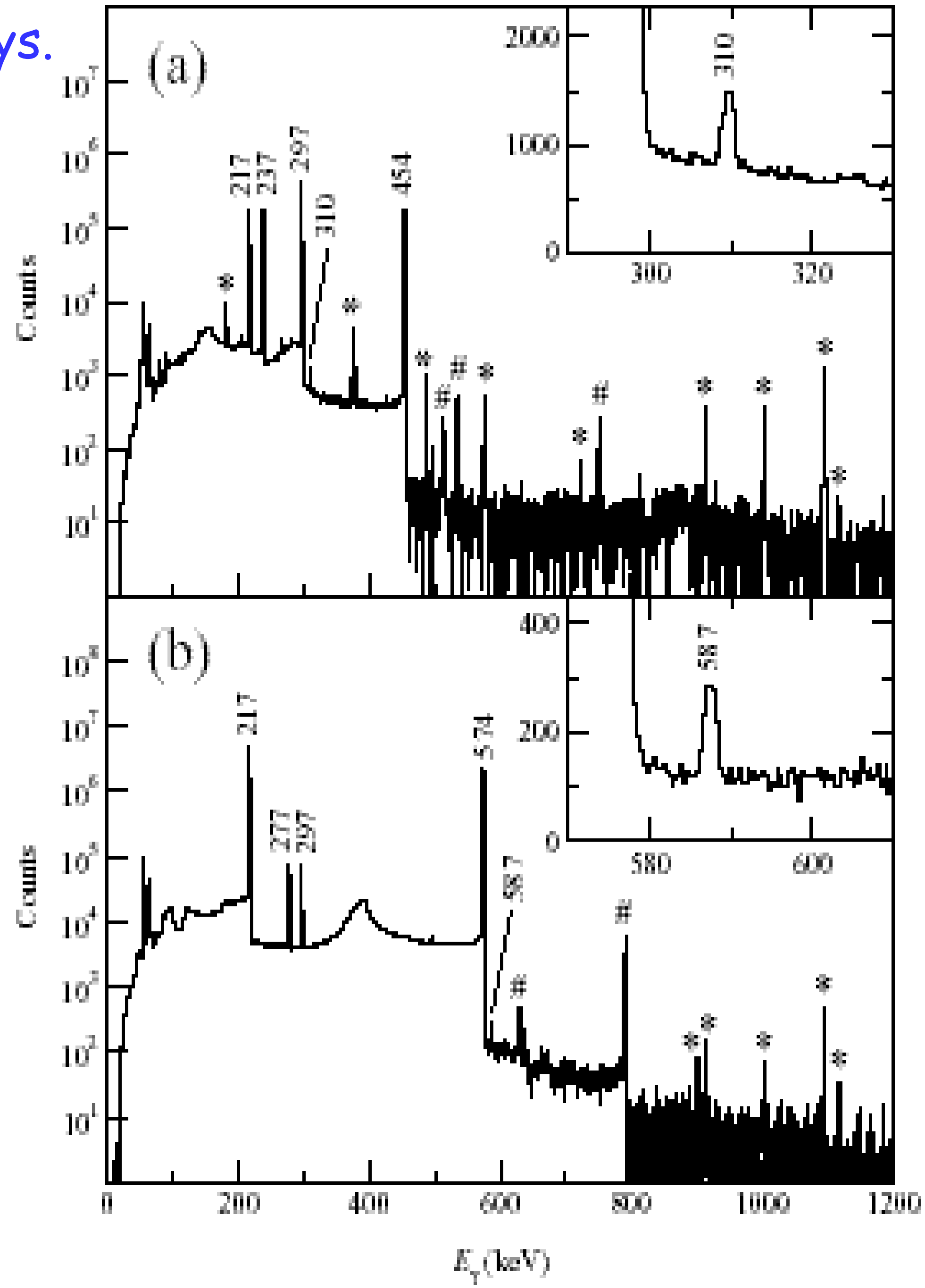

Smith, Walker et al., Phys. Rev. **C68** (2003) 031302